

# **DRAFT**

June, 2002

## **EVALUATION OF OBSERVATION-BASED METHODS FOR ANALYZING OZONE PRODUCTION AND OZONE-NOX-VOC SENSITIVITY**

by

Sanford Sillman  
Department of Atmospheric, Oceanic and Space Sciences  
University of Michigan  
Ann Arbor, Michigan 48109-2143

Purchase Order number 1D-5795-NTEX

Project Officer

Deborah Luecken

---

Atmospheric Research and Exposure Assessment Laboratory  
Research Triangle Park, NC 27711

NATIONAL EXPOSURE RESEARCH LABORATORY  
OFFICE OF RESEARCH AND DEVELOPMENT  
U.S. ENVIRONMENTAL PROTECTION AGENCY  
RESEARCH TRIANGLE PARK, NC 27711

**TABLE OF CONTENTS**

<u>Section</u>	<u>page</u>
Notation.	
Acknowledgements	
EXECUTIVE SUMMARY	
1. INTRODUCTION	
1.1 Overview	
1.2 Scope of this report	
1.3 The purpose of OBMs	
1.4 VOC versus NO <sub>x</sub> as the major source of uncertainty	
1.5 Background information on O <sub>3</sub> -NO <sub>x</sub> -VOC sensitivity	
2. SURVEY OF OBSERVATION-BASED METHODS	
2.1 Criteria for Evaluation	
2.2 Overview of OBM approaches and issues	
2.3 Evaluation of individual OBMs	
2.3.1 Secondary species as NO <sub>x</sub> -VOC indicators	
2.3.2 Smog production algorithms	
2.3.3 Constrained steady state – instantaneous chemistry based on measured NO <sub>x</sub> and VOC	
2.3.4 Observation-based model using measured NO <sub>x</sub> and VOC (Cardelino-Chameides)	
2.3.5. Direct analysis of measured NO <sub>x</sub> and VOC to estimate emissions	
2.3.6 Inverse modeling for NO <sub>x</sub> and VOC emissions	
2.3.7. Empirical ozone isopleths	
2.3.8 Other methods	
2.4 Supplemental topic: Receptor modeling	
2.5 Supplemental topic: Evaluating long term trends for ozone and related air pollutants	
2.6 Conclusions	
3. THEORETICAL EVALUATION	

### 3.1 NO<sub>x</sub>-VOC indicators

#### 3.1.1 Summary information

#### 3.1.2 Conclusions and recommendations

#### 3.1.3 Results from 3-d models

#### 3.1.4 Results from 0-d calculations and isopleth plots

#### 3.1.5 Contrary evidence

#### 3.1.6 Model correlations between indicator species

#### 3.1.7 Results from ambient measurements

#### 3.1.8. Model evaluations with measured indicator species: a method for regulatory use

#### 3.1.9 Results for O<sub>3</sub> versus PAN: possible impact of erroneous measurements

#### 3.1.10 Supplementary topic: Definition of O<sub>3</sub>-NO<sub>x</sub>-VOC sensitivity.

#### 3.1.11 Supplementary topic: Determining background values

#### 3.1.12 Supplementary topic: radical chemistry and O<sub>3</sub>-NO<sub>x</sub>-VOC sensitivity

### 3.2 SMOG PRODUCTION ALGORITHMS (EXTENT-OF-REACTION PARAMETERS)

#### 3.2.1 Summary information

#### 3.2.2 Conclusions and recommendations

#### 3.2.3 The smog production concept: results from smog chamber experiments

#### 3.2.4 Evaluation with 3-d models

#### 3.2.5 Contrary evidence

#### 3.2.6 Uncertainties associated with the theoretical basis

#### 3.2.7. Applications of smog production algorithms

#### 3.2.8 Evaluations with ambient measurements

### 3.3 CONSTRAINED STEADY STATE AND OTHER ANALYSES BASED ON AMBIENT VOC AND NO<sub>x</sub>

#### 3.3.1 Summary information

#### 3.3.2 Conclusions and recommendations

#### 3.3.3 Constrained steady state models

#### 3.3.4 Short formulas for NO<sub>x</sub>-VOC sensitivity

3.3.5 Integrating from instantaneous ozone production to ozone concentrations

3.3.6 Accuracy and completeness of NO<sub>x</sub> and VOC measurements

3.3.7 Methods for evaluating emission inventories from measurements

3.3.8 Inverse modeling

3.3.9 Other uncertainties

#### 4.0 PRACTICAL IMPLEMENTATION OF OBSERVATION-BASED METHODS

4.1 NO<sub>x</sub>-VOC indicators

4.1.1 Required measurements

4.1.2 Quality assurance of measurements

4.1.3 Interpretation of measurements

4.1.4 Evaluation of air quality models

4.1.5. Summary of proposed regulatory procedure

4.2 Constrained steady state models with measured NO<sub>x</sub> and VOC

4.2.1 Required measurements

4.2.2 Quality assurance of measurements

4.2.3 Interpretation of measurements

4.2.4 Evaluation of air quality models

4.2.5 Summary of proposed regulatory procedure

#### 5. RECOMMENDATIONS FOR FUTURE RESEARCH

5.1 NO<sub>x</sub>-VOC indicators

5.2 Constrained steady state/measured NO<sub>x</sub> and VOC

#### 6. REFERENCES

APPENDIX: ADDITIONAL RESULTS FOR NO<sub>x</sub>-VOC INDICATORS

## NOTATION

AQM	Three-dimensional Eulerian air quality model (e.g. UAM, RADM, etc.)
CB-IV	The Carbon Bond IV photochemical mechanism (Gery et al., 1989).
CSS	Constrained steady state model (Kleinman et al., 1997). This term is also used to refer to the observation-based model developed by Cardelino and Chameides (1995).
$H_x$ (radicals, odd hydrogen):	The sum of OH, HO <sub>2</sub> and RO <sub>2</sub> and RCO <sub>3</sub> radicals (analogous to CH <sub>3</sub> O <sub>2</sub> and CH <sub>3</sub> CO <sub>3</sub> ).
$k_{OH_i}$	Rate constant for the reaction of OH with an individual VOC (VOC <sub>i</sub> ).
$L_H$	Summed loss rate for NO <sub>x</sub> , including conversion to nitric acid and organic nitrates.
$L_N$	Summed rate of photochemical removal of NO <sub>x</sub> , also equal to the rate of production of NO <sub>z</sub> .
NO <sub>x</sub> (i)	Initial NO <sub>x</sub> concentration in smog chamber experiments
NO <sub>y</sub>	Total reactive nitrogen, including NO <sub>x</sub> , HNO <sub>3</sub> , NO <sub>3</sub> <sup>-</sup> and organic nitrates.
NO <sub>z</sub>	NO <sub>x</sub> reaction products, or NO <sub>y</sub> -NO <sub>x</sub> .
O <sub>3b</sub> , NO <sub>yb</sub> , etc:	Background (upwind) values of O <sub>3</sub> , NO <sub>y</sub> , etc.
OBM	Observation-based method for determining O <sub>3</sub> -NO <sub>x</sub> -VOC sensitivity. The observation-based model developed by Cardelino and Chameides (1995), sometimes referred to as OBM, is referred to here as CSS.
OPE <sub>N</sub>	Ozone production efficiency per NO <sub>x</sub> .
OPE <sub>R</sub>	Ozone production efficiency per primary radical production.
P <sub>O3</sub>	Rate of production of ozone.
P <sub>HNO3</sub>	Rate of production of nitric acid.
P <sub>orgN</sub>	Rate of production of organic nitrates (including PAN).
P <sub>perox</sub>	Rate of production of peroxides (including H <sub>2</sub> O <sub>2</sub> and organic peroxides).
ppb	parts per billion by volume
ppm	parts per million by volume
ppt	parts per trillion by volume
Q	Summed source of odd hydrogen radicals, including OH, HO <sub>2</sub> and RO <sub>2</sub> (referred to as Q in Kleinman et al., 1997), also referred to as S <sub>H</sub> .

RADM	Regional Acid Deposition Model and associated photochemical mechanism (Stockwell et al., 1990).
ROOH	Organic peroxides
rVOC	Reactivity-weighted sum of VOC, equal to $\sum_i k_{OH_i} VOC_i$
S <sub>H</sub>	Summed source of odd hydrogen radicals, including OH, HO <sub>2</sub> and RO <sub>2</sub> (referred to as Q in Kleinman et al., 1997).
S <sub>N</sub>	Summed source of NO <sub>x</sub> .
SP	Smog produced (in association with smog production algorithms)
SP <sub>max</sub>	Maximum potential smog production for a given precursor mixture (in association with smog production algorithms).
VOC	Summed volatile organic compounds
VOC <sub>i</sub>	Concentration of an individual VOC

## ACKNOWLEDGEMENTS

This work was supported by the Office of Research and Development of the U.S. Environmental Protection Agency under grant #F005300. Many of the results reported here were based on research supported by the Office of Research and Development of the U.S. Environmental Protection Agency under the Science To Improve Results (STAR) program, grant #R826765, and in association with the Southern Oxidant Study. Although the research described in this article has been funded by EPA, it has not been subjected to peer and administrative review by either agency, and therefore may not necessarily reflect the views of the agency, and no official endorsement should be inferred.

## ***EXECUTIVE SUMMARY***

*Observation-based methods* (OBMs) refer to techniques for using ambient measurements to evaluate the sensitivity of ozone to emissions of anthropogenic NO<sub>x</sub> and volatile organic compounds (VOC). As such, they represent part of a trend to link the predictions of air quality models more closely to ambient measurements. OBMs offer several advantages as a basis for establishing and evaluating regulatory policy. These include:

- Measurement-based evaluation of the accuracy of model predictions concerning the effectiveness of control strategies, especially with regard to the issue of NO<sub>x</sub> versus VOC controls.
- Evaluation of the accuracy of emission inventories, which represent a major source of uncertainty in air quality models.
- Evaluation of the effectiveness of previously implemented control strategies, and identification of the reasons for success or failure of existing regulatory policies – thus providing a basis for accountability for control policy.

The major OBMs require measurements for the following species: O<sub>3</sub>, total reactive nitrogen (NO<sub>y</sub>), NO<sub>x</sub>, and speciated VOC. Use of OBMs would require an extensive network of measurements for these species with high standards for accuracy. If implemented, OBMs would correct a long-standing tendency to evaluate air quality models based only on their ability to reproduce observed ozone. It has been recognized since at least 1991 that comparisons with measured ozone are not sufficient to insure the accuracy of control strategy predictions from air quality models (NRC, 1991). The OBMs can provide a much stronger measurement-based evaluation of model accuracy.

The main focus of OBMs has been the issue of NO<sub>x</sub> versus VOC controls for ozone, although the same techniques can provide insight for other ozone-related issues as well. O<sub>3</sub>-NO<sub>x</sub>-VOC sensitivity represents one of the largest uncertainties associated with the process of ozone formation, and is also a major uncertainty in terms of regulatory policy. It is generally known that for some conditions, the rate of ozone formation increases with increasing NO<sub>x</sub> and is largely insensitive to anthropogenic VOC, while for other conditions, ozone formation increases with increasing VOC and is insensitive (or negatively sensitive) to NO<sub>x</sub>. However, it is difficult to determine whether ozone in an individual location or during a specific event is primarily sensitive to NO<sub>x</sub> or VOC.

The  $\text{NO}_x$ -VOC issue is a major source of uncertainty associated with predictions for the effectiveness of control strategies for air pollutants.

OBFs were originally conceived as a replacement for the 3-dimensional Eulerian air quality models (AQMs), which are regularly used to establish and evaluate regulatory policy. The OBFs were intended to provide the same level of analysis as the AQMs, but would derive their initial concentration fields from ambient measurements rather than from emission inventories. It is now recognized that OBFs have their own uncertainties and limitations and are unlikely to provide a replacement for AQMs. However the OBFs are potentially very useful as a complement to AQMs. OBFs provide a link between AQMs and ambient measurements, which is often missing in regulatory studies, and provide a basis for evaluating the accuracy of model control strategy predictions. OBFs are also useful as stand-alone methods (if their limitations are properly recognized) because they can provide an analysis of trends over an entire season, and can identify event-to-event variations that might be overlooked by the AQMs.

Two OBFs are especially worthy of investigation: (i) the method of  $\text{NO}_x$ -VOC indicators, which uses total reactive nitrogen ( $\text{NO}_y$ ),  $\text{NO}_x$  reaction products ( $\text{NO}_z$ ), and nitric acid to derive inferences about  $\text{O}_3$ - $\text{NO}_x$ -VOC sensitivity; and (ii) constrained steady state calculations that use ambient VOC and  $\text{NO}_x$ . These two methods are complementary, in that they use different measurements to draw inferences about the same issue. The constrained steady state method can also be combined with other analytical tools (e.g. from Parrish et al., 1998) that use measured  $\text{NO}_x$  and VOC to evaluate the accuracy of emission inventories. Analyses that show consistent results from AQMs,  $\text{NO}_x$ -VOC indicators and measured  $\text{NO}_x$  and VOC are very likely to provide accurate predictions concerning  $\text{O}_3$ - $\text{NO}_x$ -VOC sensitivity.

$\text{NO}_x$ -VOC indicators are based on the theory that the ratios  $\text{O}_3/\text{NO}_y$ ,  $\text{O}_3/\text{NO}_z$  and  $\text{O}_3/\text{HNO}_3$ , and the equivalent species correlations between species, show different values depending on whether ozone is predominantly sensitive to  $\text{NO}_x$  or VOC. This approach is based on results from 3-d Eulerian air quality models, which generally show that high values of these ratios are associated with  $\text{NO}_x$ -sensitive chemistry and low values are associated with VOC-sensitive chemistry. Some contradictory results from models have been reported, but these can be corrected by adjusting the original indicator ratios to account for upwind conditions. The ratio of ozone production per  $\text{NO}_x$  removed (also referred to as ozone production efficiency per  $\text{NO}_x$ ) is also higher in model calculations for  $\text{NO}_x$ -sensitive conditions than for VOC-sensitive conditions. The ratio  $\text{H}_2\text{O}_2/\text{HNO}_3$  is strongly associated with  $\text{NO}_x$ -

VOC sensitivity, but this ratio is more difficult to use in practice because measured  $\text{H}_2\text{O}_2$  or total peroxides are usually not available.

There is strong evidence from both models and ambient measurements that indicator ratios show different values for  $\text{NO}_x$ -sensitive versus VOC-sensitive conditions. However, there is no strong evidence that indicator ratios are universally applicable for all ambient conditions. Therefore, ambient values of indicator ratios should be viewed as a broad indication of  $\text{NO}_x$ -VOC sensitivity patterns, rather than as a rigid “rule of thumb”. Indicator ratios are likely to be useful for identifying apparently different  $\text{NO}_x$ -VOC conditions between different locations or for different events. In addition, indicator ratios and species correlations are especially useful as a method for evaluating the accuracy of  $\text{NO}_x$ -VOC predictions from AQMs. When predicted correlations between  $\text{O}_3$  and  $\text{NO}_y$  and between similar species are compared with measured values, patterns often emerge that can be interpreted as evidence of bias in the AQM towards VOC-sensitive or  $\text{NO}_x$ -sensitive chemistry. These interpretations are likely to remain valid even if the stated connection between indicator ratios and  $\text{O}_3$ - $\text{NO}_x$ -VOC sensitivity is not precise.

Changes in the observed correlations between  $\text{O}_3$  and  $\text{NO}_y$  can also be used to identify the causes of changes in  $\text{O}_3$  over time, as a basis for evaluating the effectiveness of control strategies. The correlation between  $\text{O}_3$  and  $\text{NO}_y$  can also be used to identify changes in global background  $\text{O}_3$  and its impact on  $\text{O}_3$  in the U.S.

Constrained steady state calculations are based on the theory that  $\text{O}_3$ - $\text{NO}_x$ -VOC sensitivity is closely connected to ambient concentrations of VOC and  $\text{NO}_x$ . Ozone-precursor sensitivity is often not directly linked to  $\text{VOC}/\text{NO}_x$  ratios, because ozone is the result of photochemical production over several hours and along extended air mass trajectories. Photochemistry along these trajectories is affected by short-lived VOC species, including biogenic species, that may not be leave evidence as the air mass moves downwind. However, the instantaneous rate of ozone production shows a  $\text{NO}_x$ -VOC sensitivity pattern that is closely associated with ambient  $\text{NO}_x$  and VOC. The  $\text{NO}_x$ -VOC sensitivity for instantaneous ozone production is also loosely associated with the ratio of reactivity-weighted VOC (rVOC) to  $\text{NO}_x$ .

The constrained steady state models calculate instantaneous rates of ozone production as a function of ambient  $\text{NO}_x$  and VOC (and, if available, incident solar radiation). The version developed by Cardelino and Chameides (1995) also calculates the sum of instantaneous ozone production rates and summed sensitivity to  $\text{NO}_x$  and VOC, assuming that a series of measurement sites can be used to characterize photochemistry in an urban area. This

analysis of summed ozone production is likely to be closely related to  $O_3$ - $NO_x$ -VOC sensitivity, but results may vary depending on the exact location of measurement sites and transport patterns. As is the case for  $NO_x$ -VOC indicators, the constrained steady state calculations are useful for providing a general indication of  $O_3$ - $NO_x$ -VOC sensitivity in a specified region.

Measured  $NO_x$  and VOC can also be used directly to infer emission rates of  $NO_x$  and VOC and to evaluate emission inventories. This is important because emission inventories represent the largest uncertainty in air quality models and are often the major source of uncertainty in  $NO_x$ -VOC predictions from models. Parrish et al. (1998) described a series of correlations between individual VOC that can be used to infer emission rates. The same correlations can be used to evaluate the accuracy of VOC and  $NO_x$  in air quality models. As is the case for  $NO_x$ -VOC indicators, comparison of results from AQMs with measured  $NO_x$  and VOC can be used to identify biases in AQMs that affect  $NO_x$ -VOC predictions. The same analysis can also be used to identify changes in emissions of  $NO_x$  and VOC over time.

Smog production algorithms, which are widely used to evaluate  $O_3$ - $NO_x$ -VOC sensitivity in regulatory applications, are also evaluated in this document. Smog production algorithms also use measured total reactive nitrogen ( $NO_y$ ) to infer  $NO_x$ -VOC sensitivity, but (in contrast to the indicator method) the interpretation of measurements is based primarily on results from smog chamber experiments rather than from 3-d air quality models. The smog production algorithms are also based on the theory (derived from both smog chamber experiments and 0-d calculations) that VOC-sensitive conditions are associated with relatively fresh emissions and  $NO_x$ -sensitive conditions are associated with photochemically aged air in which most of the  $NO_x$  has reacted to form  $O_3$ . The smog production algorithms assume that in photochemically aged air the summed amount of ozone produced per  $NO_x$  (ozone production efficiency) has a constant value that is independent of VOC emissions. Evidence from both 0-d calculations and ambient measurements challenges this view. Results from 3-d models suggest that the smog production algorithms can identify locations with strongly VOC-sensitive chemistry, which are usually associated with unprocessed direct emissions. The smog production algorithms are less reliable for photochemically aged air, which usually has the highest  $O_3$  and which can have either  $NO_x$ -sensitive or VOC-sensitive conditions.

Use of OBMs (including indicator ratios, constrained steady state calculations and direct inferences from measured  $NO_x$  and VOC) depends critically on the availability and accuracy of measurements. The  $NO_x$ -VOC

indicators require a network of measured  $O_3$  and either  $NO_y$  or  $HNO_3$  (and, if possible,  $NO_x$ ) over a region that includes locations with the highest  $O_3$ . Constrained steady state and related methods require measurements of a relatively complete set of primary VOC, including short-lived and biogenic species, and also measured  $NO_x$ . These methods do not require as extensive a measurement network as the  $NO_x$ -VOC indicators do, but the measurements must be extensive enough to characterize VOC and  $NO_x$  throughout a metropolitan region and to include locations with high biogenic VOC. In both cases it is critically important that measurements meet standards of accuracy. Measurement techniques for  $NO_x$  and  $NO_y$  are both subject to characteristic errors that would compromise their use in evaluations of  $O_3$ - $NO_x$ -VOC sensitivity. Questions have also been raised about the accuracy of measured VOC, especially about measurements of highly reactive species. In general, it is preferable to base the OBMs with a relatively small number of highly accurate measurements, rather than an extensive network of measurements of questionable accuracy.

Because accuracy of measurements is a critical issue, analysis with an OBM should include evaluation of the pattern of measured data to identify possible sources of error. The species correlations associated with  $NO_x$ -VOC indicators and correlations among VOC used to evaluate emissions can also be used to identify possible errors in measured data sets and to identify other ambient conditions that would invalidate results from an OBM.

Finally, standard protocols should be developed for the use of OBMs in regulatory applications. These protocols would facilitate the interpretation of results from investigations in different locations and insure that quality assurance of measurements is included. Protocol for  $NO_x$ -VOC indicators should include display of arrays of measured correlations between  $O_3$  and  $NO_y$ , etc., in comparison with model patterns that would identify characteristic errors in measurements or other inconsistencies that would invalidate the method. Protocol for  $NO_x$ -VOC indicators should also include guidance for comparison between measured indicator correlations and results of an AQM, and development of standards that would define a successful model-measurement comparison. Protocol for constrained steady state should include display of measured correlations between individual VOC, following methods from Parrish et al. (1998) that would identify erroneous measurements or missing VOC. This would also provide an evaluation of the emission inventory to be used in an AQM. Protocol would also need to be established for situations in which analyses from OBMs and from standard air quality models gave contradictory results.

## ***SECTION 1. INTRODUCTION***

### **1.1 OVERVIEW**

*Observation-based methods* (OBMs) refer to a collection of techniques that have been developed for analyzing the ozone production process directly from ambient measurements. The OBMs have been proposed as methods that can be used in the development of control strategies for reducing the levels of ambient ozone during pollution events. Specifically, OBMs have been proposed as methods to evaluate the relative effectiveness of controls on volatile organic compounds (VOC) as opposed to controls on nitrogen oxides (NO<sub>x</sub>) as strategies for reducing ambient ozone.

Traditionally, analysis of ozone production and the development of control strategies have been based on 3-dimensional air quality models (AQMs). These AQMs include the following components: an inventory of anthropogenic and biogenic emissions; a representation of meteorology during the event or events of interest; a mechanism representing photochemical reactions believed to be important in ozone formation; and a simulation procedure within a 3-dimensional grid that represents the process of emissions, photochemical transformations, and transport.

The AQMs have a number of advantages as a basis for developing ozone policy. They provide an analysis of specific air pollution events that includes the most complete available knowledge of the ozone formation process. Computer simulations are by their nature flexible and can be adopted to represent conditions unique to individual locations. They also can be modified to reflect scientific advances. They are especially advantageous for the policy-making process because they can analyze the impact of specific emission sources (by location or by source type) and evaluate the impact of specific proposed policies on ambient ozone. No OBM can evaluate the impact of specific emission sources or control policies in this level of detail.

While the AQM's have been successful in providing specific answers to the problem of ozone control strategies, it has been more difficult to establish whether those answers are accurate. As computer models, AQMs are dependent on a range of inputs and assumptions concerning the process of ozone formation. These assumptions affect not just the model ability to successfully model the amount of ozone formed in the atmosphere, but also the

ability to predict the impact of control strategies. Specifically, results from AQM's depend on the accuracy of emission inventories, which have been regarded as very uncertain (e.g. Fujita et al., 1992; Geron et al., 1994).

Evaluation of the accuracy of predicted control strategies from AQMs has also been unsatisfactory. The performance of AQMs has been evaluated extensively versus ambient ozone, and statistical criteria have been established to define an acceptable level of performance (NRC, 1991). However, model accuracy for ozone by itself does not guarantee the accuracy of model predictions for the effectiveness of control strategies. It is frequently possible to generate alternative model scenarios for the same event, with similar O<sub>3</sub> but different predictions for the impacts of VOC and NO<sub>x</sub> controls on O<sub>3</sub> (e.g. Sillman et al., 1995; Pierce et al, 1998). Specific AQM applications have occasionally been evaluated against a more extensive array of ambient measurements (e.g. Jacobson et al., 1996) but it is difficult to establish whether control strategy predictions from AQMs are accurate.

Uncertainties associated with isoprene (C<sub>5</sub>H<sub>8</sub>), a biogenic VOC emitted primarily by deciduous trees, have been a major source of dissatisfaction with AQM's. It is now recognized that isoprene has a significant impact on ozone formation in many urban areas in the U.S. AQMs that include isoprene often give results for the effectiveness of NO<sub>x</sub>-based and VOC-based control strategies that are very different from AQMs without isoprene or with isoprene from different emission inventories (Pierce et al., 1998). The initial recommendations to develop observation-based approaches for ozone was motivated largely by the uncertainty associated with isoprene (Chameides et al., 1992). For many years AQMs were used without including biogenic VOCs, and errors resulting from these omissions were not identified by the evaluation procedures of AQM's. This might be counted as a failure of AQMs as an analytical tool.

OBMs offer several general advantages over AQMs for analyzing ozone. Unlike the AQMs, the proposed OBMs are usually not dependent on the accuracy of emission inventories. Since these inventories are believed to be the major source of uncertainty in AQMs, methods that do not require the use of these inventories may have significantly less uncertainty. OBMs are generally perceived as less dependent on model assumptions than AQMs. OBMs are also advantageous because they have a direct link to ambient measurements. Because they rely on measurements, OBM predictions are based on real-world conditions to a greater extent than AQMs. By relying on measurements, the OBMs also may provide stronger evidence in support of their control strategy predictions. Perhaps the most useful aspect of OBMs is their ability to compensate for the drawbacks of AQMs. When OBMs

are used in combination with standard AQMs, they provide a link between AQM predictions and ambient measurements that is often missing in the standard AQM analysis.

While OBMs offer advantages as an analytical tool, there are also major disadvantages and potential sources of error associated with OBMs. These sources of error are especially important because the disadvantages of OBMs are not known as widely as the sources of error in standard AQMs. Like AQMs, the OBMs are always dependent on a series of assumptions about the ozone formation process. Accuracy of measurements and the spatial representativeness of the measurement network are also potential errors for OBMs.

## **1.2 SCOPE OF THIS REPORT**

This report provides a critical evaluation of the various proposed OBMs, as part of an effort to develop guidance for the use of OBMs in air quality management. It includes OBMs that can be used to analyze ozone production during air pollution events in specific urban areas, usually in terms VOC-NO<sub>x</sub> sensitivity. The report also includes methods that use observations to evaluate and correct emission inventories. These methods are included only if they are useful for analyzing ozone production during individual events in specific locations.

A number of issues peripherally related to the process of ozone production are specifically excluded from this analysis. The development and evaluation of photochemical mechanisms (usually involving smog chamber or chemical kinetics experiments) is clearly observation-based, but this represents a separate issue and is not included in this report. The development of meteorological fields for use in air quality models is also excluded. Receptor modeling, analysis of ozone incremental reactivity for individual VOC and evaluation of ozone production efficiency per NO<sub>x</sub> are discussed briefly, but are mainly beyond the scope of this report. This report focuses exclusively on physical processes and does not consider economics or cost-benefit analysis.

Section 2 presents a survey of the various OBMs. It includes a description of each OBM, the rationale for its use, the extent of investigations designed to demonstrate its validity, and evaluates practical strengths and weaknesses of the method. Based on this survey, three or four of the most promising OBM techniques will be selected for more detailed investigation.

Sections 3 and 4 provide an in-depth investigation of the selected OBMs, including the theoretical basis, justification, and weaknesses of the method (Section 3) and the practical issues of implementation for air quality

management (Section 4). The latter includes a discussion of the issues that need to be resolved for the use of OBMs in combination with standard AQMs.

If OBM's are to be used widely as a tool for air quality management, protocol will need to be developed for interpreting specific applications. This should include evaluation of the quality of measurements that drive the OBM and tests for the validity of the OBM in the individual application. In addition, protocol must be developed to reconcile cases in which analysis based on OBMs disagree with the results of standard air quality models. These issues will be addressed discussed in Section 4.

### **1.3 THE PURPOSE OF OBMs**

Observations are routinely used throughout the atmospheric sciences, e.g. to evaluate atmospheric models and to derive inferences about various atmospheric processes. In this report the concept of observation-based methods is linked to one specific purpose: evaluation of whether ozone formation rates are sensitive primarily to VOC or to  $\text{NO}_x$ . Only OBMs that address this specific issue are included. Some OBMs that address some secondary issues that directly relate to the VOC-vs.- $\text{NO}_x$  issue (e.g. accuracy of emission inventories) are also included.

The VOC- $\text{NO}_x$  issue is the focus of OBMs because it represents the major source of uncertainty in the evaluation of control strategies for ozone (see next section). Predictions about control strategies are all subject to uncertainties based on model formulation, imprecise knowledge of ambient conditions and uncertain identification of atmospheric sources. The issue of VOC- $\text{NO}_x$  chemistry typically leads to uncertainties that are much larger than the other issues. Erroneous representation of VOC- $\text{NO}_x$  chemistry can lead models to predict that a particular strategy will be highly effective in lowering ambient ozone, when in fact the recommended strategy would have no impact on ambient ozone or would cause ozone to increase. This report evaluates OBMs that are designed specifically to reduce the uncertainty associated with VOC- $\text{NO}_x$  sensitivity.

This report includes some OBMs that are designed to address a secondary goal: the evaluation of the accuracy of emission inventories. Evaluation of emission inventories is included because this often represents the main source of uncertainty in VOC- $\text{NO}_x$  predictions from AQMs. Some of the proposed OBMs seek to duplicate the analysis of transport and photochemistry contained in standard AQM's, while eliminating the need for an emission inventory. Methods that seek to adjust emission inventories in AQMs based on observations are closely related to these OBMs, and are therefore included for comparison.

The concept of OBMs often includes methods that can be used to evaluate the accuracy of control strategy predictions from AQMs. This type of model evaluation should also be recognized as part of the purpose of OBMs. Methods of model evaluation are not included explicitly in this report, but are included the discussion of combined approaches with OBMs and AQMs (Section 4.)

The techniques of receptor modeling (Henry, 1984) should also be recognized as an observation-based approach with many similarities to the methods considered here. Receptor modeling also seeks to derive information about pollutants directly from observations. Typically, receptor techniques involve observation-based signals for specific pollutant sources. These techniques are included in the survey of observation-based approaches (Section 2) but have not been included in the in-depth analysis (Section 3 and 4) because they address a somewhat different issue.

Investigation of ozone trends and evaluation of the successes and/or failures of past regulatory policy have become an increasingly important component of air quality analyses. These investigations are also closely linked to observations and use observation-based approaches. Many of the OBMs proposed for use to evaluate O<sub>3</sub>-NO<sub>x</sub>-VOC sensitivity can also be used to evaluate and interpret ozone trends. Methods for analyzing ozone trends are discussed in the survey of OBMs (Section 2).

#### **1.4 UNCERTAINTY ASSOCIATED WITH VOC VERSUS NO<sub>x</sub> CONTROL PREDICTIONS**

The question of VOC versus NO<sub>x</sub> controls is only one of many policy-relevant issues relating to ozone formation. However, the uncertainties associated with NO<sub>x</sub>- versus VOC-sensitivity tend to be much larger than the uncertainties associated with other issues involving ozone. The large uncertainty justifies the focus of OBMs on this issue.

The impact of uncertain NO<sub>x</sub>-VOC sensitivity is illustrated in Figure 1.1. The figure shows how the predicted impact of control strategies varies in a series of model scenarios for two days in Atlanta (from Sillman et al., 1995, 1997). The scenarios include alternative cases with variations in anthropogenic emission rates, wind speeds and mixed layer height of up to 25%, and with two different biogenic emission inventories (BEIS1 and BEIS2). The figure shows the predicted impact of 35% reductions in anthropogenic VOC and NO<sub>x</sub> on peak O<sub>3</sub> in each model scenario. The impact of reduced NO<sub>x</sub> in VOC has been expressed as a fraction relative to excess ozone in the model scenario, where excess ozone represents the difference between peak O<sub>3</sub> and O<sub>3</sub> at the model boundary.

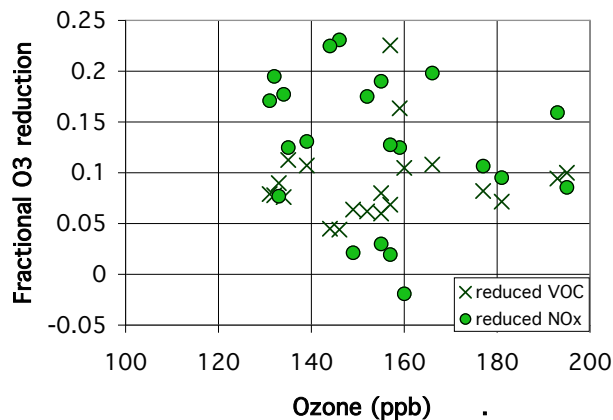
The figure shows the extent of uncertainty associated with control strategy predictions. On August 10 some model scenarios predict that reduced  $\text{NO}_x$  would be an effective strategy for reducing peak  $\text{O}_3$ , with predicted reduction in excess ozone as high as 23% for a 35% reduction in emissions. But other scenarios show predicted reductions in ozone of just 10%, and a few scenarios predict zero impact on peak  $\text{O}_3$ . Similarly, reduced VOC is predicted to be an effective control strategy in some scenarios, with predicted reductions in excess ozone also reaching 23% for a 35% reduction in emissions. But other scenarios show much predicted reductions as low as 4%.

Predicted peak  $\text{O}_3$  also varies among the scenarios (from 131 ppb to 195 ppb) but the variation in predicted peak  $\text{O}_3$  is much smaller (relative to its median value) than the variation in the predicted effectiveness of control strategies. The variation in peak  $\text{O}_3$  among the model scenarios is also not related to the uncertainty in control strategy predictions. Scenarios with similar peak  $\text{O}_3$  can give very different predictions concerning control strategies. The ability of a model to reproduce observed  $\text{O}_3$  does not demonstrate that the model control strategy predictions are accurate.

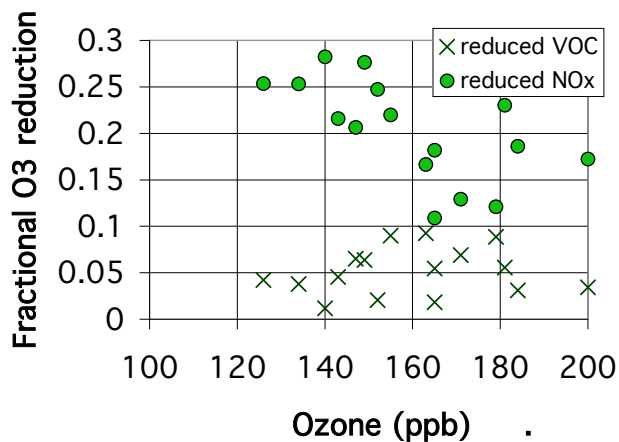
During the second event (August 11) there is less uncertainty in control strategy predictions. In this case the model scenarios all predict that reduced VOC would lead to reductions in peak  $\text{O}_3$  of 9% or less, while reduced  $\text{NO}_x$  would reduce  $\text{O}_3$  by an amount ranging from 9% to 28%.

The uncertain control strategy predictions are associated specifically with the question of  $\text{NO}_x$ -sensitive versus VOC-sensitive photochemistry. The divergence among the model scenarios on August 10 occurs because some model scenarios have predominantly  $\text{NO}_x$ -sensitive chemistry while others have predominantly VOC-sensitive chemistry. When the range of model scenarios includes both  $\text{NO}_x$ -sensitive and VOC-sensitive chemistry, then the control strategy predictions become very uncertain. By contrast, when model scenarios all include mainly  $\text{NO}_x$  sensitive chemistry, or when models include mainly VOC-sensitive chemistry, then the uncertainties are lower.

The purpose of the OBMs discussed here is to reduce this uncertainty.



(a) August 10, 1992



(b) August 11, 1992

**Figure 1.1.** Predicted reduction in peak O<sub>3</sub> resulting from 35% reductions in anthropogenic VOC emissions (crosses) and from 35% reductions in NO<sub>x</sub> (solid circles) in a series of model scenarios for Atlanta. The predicted reductions are shown as fractions relative to peak excess O<sub>3</sub>, defined as peak O<sub>3</sub> minus the model background O<sub>3</sub>. The model is described in Table 3.1.1. Scenarios are from Sillman et al. (1995, 1997).

## 1.5 BACKGROUND INFORMATION ON O<sub>3</sub>-NO<sub>x</sub>-VOC SENSITIVITY

The relationship between O<sub>3</sub>, NO<sub>x</sub>-and VOC is illustrated in isopleth plots, e.g. Figure 1.2, which shows ozone concentrations as a function of NO<sub>x</sub> and VOC emission rates. This particular plot is based on calculated photochemistry for a 3-day period. Similar patterns are found for single-day calculations and for calculations that relate instantaneous rates of ozone production to concentrations of NO<sub>x</sub> and VOC.

As shown in the figure, O<sub>3</sub> shows a nonlinear dependence on NO<sub>x</sub> and VOC. O<sub>3</sub> increases with increasing NO<sub>x</sub> when NO<sub>x</sub> concentrations are low and when VOC/NO<sub>x</sub> ratios are high. As NO<sub>x</sub> increases, O<sub>3</sub> eventually reaches a maximum and then decreases in response to further increases in NO<sub>x</sub>. This maximum value (the 'ridge line') is used to define two regions with different photochemistry and with different ozone precursor sensitivity. At high VOC/NO<sub>x</sub> ratios (below the 'ridge line' in Figure 1.5.1) ozone increases with increasing NO<sub>x</sub> and is relatively insensitive to increasing VOC. At low VOC/NO<sub>x</sub> ratios (above the 'ridge line') ozone increases with increasing VOC and decreases with increasing NO<sub>x</sub>. The split between these two regimes is the source of much uncertainty in control strategy predictions (see Section 1.4).

The split between NO<sub>x</sub>-sensitive and VOC-sensitive regimes is associated with the photochemistry of odd hydrogen radicals (OH, HO<sub>2</sub> and RO<sub>2</sub> radicals) that control the rate of ozone production. The chemistry of ozone production and radicals is described more fully in Section 3.1.12.

The split into NO<sub>x</sub>-sensitive and VOC-sensitive regimes also depends on the precise definition of the 'ridge line'. This can be defined as the location of maximum O<sub>3</sub> (or the maximum rate of ozone formation) relative to variation in NO<sub>x</sub> (NO<sub>x</sub> benefits versus disbenefits), or it can be defined as the location where identical percent reductions in NO<sub>x</sub> and VOC would cause the same reduction in O<sub>3</sub> (NO<sub>x</sub>-sensitive versus VOC-sensitive). This is discussed in Section 3.1.10.

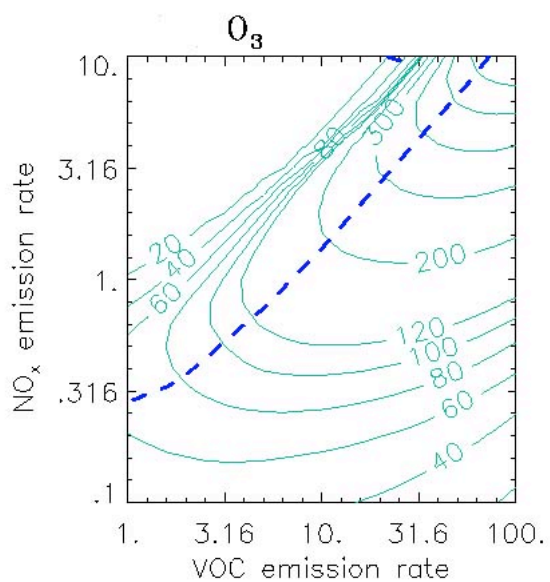


**Figure 1.2.** Ozone isopleths (ppb) as a function of the average emission rate for NO<sub>x</sub> and VOC ( $10^{12}$  molec.  $\text{cm}^{-2} \text{s}^{-1}$ ) in 0-d calculations. The isopleths (solid green lines) represent conditions during the afternoon following 3-day calculations with a constant emission rate, at the hour corresponding to maximum O<sub>3</sub>. The short blue dashed line represents the transition from VOC-sensitive to NO<sub>x</sub>-sensitive conditions.

## **SECTION 2: SURVEY OF OBSERVATION-BASED METHODS**

This section presents summary information about the approaches which have been proposed as OBM's and which are capable of either replacing or supplementing standard AQM's for evaluating the relative impact of NO<sub>x</sub> and VOC on ozone formation. This section also includes an evaluation of the strengths and weaknesses of each approach and selection of approaches for in-depth investigation.

In addition, this section presents a brief summary of two additional topics that are linked to observation-based methods: receptor modeling, which uses ambient measurements to identify emission sources of ambient species; and methods for evaluating of long-term trends for ozone and other species. Evaluation of trends is especially important as a basis for identifying whether past policies have been effective in reducing ambient concentrations and for identifying the reasons for the success or failures of those policies.

### **2.1 CRITERIA FOR EVALUATION**

Individual OBMs are discussed in terms of the following topics.

***Theoretical basis:*** This refers to the rationale offered for why the particular OBM works successfully. This is especially important for the OBMs that include simple rules for identifying whether ozone is primarily sensitive to NO<sub>x</sub> or to VOC. The rules should be explainable in terms of ozone chemistry, rather than just a technique that appears to work empirically.

***Method of justification:*** OBMs typically must offer some type of test (in terms of model calculations or experiments) to demonstrate that the information provided by the OBM is correct.

***Range of applications:*** The range of apparently successful applications (consistent with the claims of the method) will be presented here. In order to justify use, an OBM should be tested and applied successfully in many different locations, preferably by several independent investigators. These tests should include applications that test the validity of the method, as well as tests that just apply the method.

***Contrary evidence:*** Applications that generate apparently contrary results are presented here.

***Is it universal?*** In order to be used successfully, an OBM must be widely applicable in locations and situations of interest for air quality management. Tests for the validity of an OBM should be sufficiently broad to demonstrate that the concept works successfully in a range of conditions, rather than just in a small number of events or

locations. Limitation on the applicability of an OBM does not in itself prevent use of the OBM in air quality management. However, the limitations of the OBM must be well understood, and it must be demonstrated that the OBM is broadly applicable for the range of locations for which it is proposed.

***Other sources of error:*** The most likely causes of error in individual applications are discussed here. This includes situations in which the method might not return a useful answer as well as situations in which the OBM might lead to erroneous conclusions. The potential errors of OBMs are especially important in comparison to the sources of error in standard AQMs.

***Ease of use:*** In order to be used successfully in air quality applications, an OBM must be able to yield useful answers for a reasonable amount of effort. Some levels of analysis may be useful as part of research efforts but require a level of analysis that is beyond the scope of most investigations for air quality management. In addition, the measurements required by an OBM must be available or potentially obtainable with a reasonable effort.

In this context, it may be necessary to caution against "rules of thumb" that are too simplistic.

***Availability and accuracy of measurements:*** The required measurements must be either available from an existing network or must involve equipment that is available and might be implemented with reasonable effort. These measurements also must meet standards of accuracy.

***Can the method be evaluated or modified in individual applications?*** Some OBMs consist of a single procedure that would be applied for individual locations, with results that must be accepted on a "take-it-or-leave-it" basis. It is a major advantage if an OBM also includes methods to evaluate the individual applications and identify errors (e.g. erroneous measurements, conditions that invalidate the OBM for the specific applications, etc.) Existing OBMs rarely include this type of evaluation. The possibility for developing such an evaluation is important to consider in selecting OBMs for wider use.

***Synthesis with Eulerian models:*** It is advantageous if an OBM can be applied in a way that complements the use of standard AQMs.

**Format for evaluation:** The following section includes an overview of each method and discussion of the performance of the method in relation to each of the above topics. Results for each topic will be presented based on the available information on the OBM in published literature. Modifications or opinions offered by the author of this report will be labeled as "*comments*". In addition, the label "*controversial issue*" is used to identify issues or

recommendations by the author that relate to central policy choices or to issues where disagreement is expected.

The presentation of each OBM is followed by a summary recommendation that describes the major advantages and disadvantages of the approach and recommends possible further development.

## **2.2 OVERVIEW OF OBM APPROACHES AND ISSUES.**

The following categories are useful for understanding the range of options among OBMs.

**Primary species, secondary species, or radicals:** Virtually all OBMs for ozone production rely on measurements of chemically active species (e.g. as opposed to meteorological variables). Based on the choice of measurements, three general approaches can be identified. Several methods rely on measurements of directly emitted ozone precursors, usually speciated VOC and  $\text{NO}_x$ . A second grouping involves measurements of long-lived secondary species (e.g. reactive nitrogen) that are produced concurrently with the production of ozone. A third grouping is based on direct or indirect measurement of short-lived radical species (e.g.  $\text{HO}_2$ ).

These three approaches also imply different strategies of analysis. Analysis based on primary species typically provides information about the ozone production that will occur in the future as the measured precursor species move downwind. Analysis based on secondary species provides information about the ozone production that has already occurred upwind at the time of measurement. These two approaches are largely complementary in that they can provide information on the same issue (impact of VOC versus  $\text{NO}_x$ ) using different evidence. They also require different measurement strategies. Primary species need to be measured near major emission sources and in regions with high ozone production; whereas secondary species need to be measured downwind in locations with the highest ambient ozone. Analysis based on radical species only provides information about instantaneous ozone production.

**Models versus smog chambers:** A major distinction between OBMs concerns the method used to obtain the interpretation of measurements used in the OBM and to prove its validity. Some methods (e.g. Sillman, 1995) use 3-d Eulerian photochemical models (similar to standard AQMs) to identify measurements and interpretations that can be used as an OBM. Others (e.g. Blanchard et al., 1999) use smog chamber experiments to interpret measurements.

**Instantaneous production versus ozone concentrations:** Elevated ozone usually is the result of combined photochemistry and transport over a time period of several hours or more (often including time periods greater than

one day). The relation between ozone concentrations and its precursors is complicated by the mix of fresh and aged emissions and changing photochemistry as an air mass travels downwind from emission source regions. Some OBMs seek to identify the impact of upwind VOC and NO<sub>x</sub> precursor emissions on the total ozone concentration, while others seek to identify the impact of local emissions on the instantaneous rate of ozone production.

It is important to recognize that the instantaneous dependence of ozone photochemistry on NO<sub>x</sub> and VOC is often very different from the sensitivity of ozone concentrations to upwind NO<sub>x</sub> and VOC. It is generally easier and more reliable to derive information about the factors that control the instantaneous rate of ozone production than it is to derive information about the total impact on ozone as emissions from a source move downwind. However, information about instantaneous chemistry is more difficult to interpret in the context of policy.

**Definition of NO<sub>x</sub>-VOC sensitivity:** The OBMs included in this survey are all intended to aid in evaluating the relative impact of NO<sub>x</sub> and VOC on ozone formation. Results of these OBMs often depend on how terms such as "NO<sub>x</sub>-sensitive" and "VOC-sensitive" are defined. A summary of various alternative definitions is presented here.

*NO<sub>x</sub>-sensitive versus VOC-sensitive:* The term "NO<sub>x</sub>-sensitive" will be used to describe a situation if a given reduction in NO<sub>x</sub> emissions is expected to cause a significant decrease in O<sub>3</sub>, and if O<sub>3</sub> with reduced NO<sub>x</sub> emissions is also expected to be significantly lower than O<sub>3</sub> with an equivalent reduction (as a percent of total emissions) of anthropogenic VOC.

Similarly, the term "VOC-sensitive" will be used if a given reduction in anthropogenic VOC emissions is expected to cause a significant decrease in O<sub>3</sub> and is expected to result in significantly lower O<sub>3</sub> than an equivalent reduction (in proportion to total emissions) of anthropogenic NO<sub>x</sub>.

In this definition, "significant" is an ambiguous term that depends on the individual situation. Here, it is assumed that "significant" refers to the physical context of the situation and not the policy context. Typically, OBMs can provide information on how the expected decrease in O<sub>3</sub> resulting from reduced NO<sub>x</sub> compares to the expected decrease in O<sub>3</sub> from an equivalent reduction in VOC. They do not provide information on whether these reductions are significant in terms of policy.

The above definition can be used in reference to ozone concentrations or to instantaneous production rates.

*NO<sub>x</sub> benefits versus disbenefits:* An alternative way to define control predictions is to define situations based on whether reductions in NO<sub>x</sub> emissions would lead to a decrease in O<sub>3</sub> (NO<sub>x</sub> benefits) or an increase in O<sub>3</sub> (NO<sub>x</sub> disbenefits). This distinction is often important in terms of policy.

This definition is different from the definition of NO<sub>x</sub>-sensitive and VOC-sensitive given above in that many VOC-sensitive situations still have predicted small benefits rather than disbenefits from NO<sub>x</sub> controls. Tonnesen and Dennis (2000b) discussed the difference between the two definitions in detail.

*VOC benefits versus zero impact:* Lu and Chang (1998) and Kirchner et al. (2000) both made an additional distinction between locations in which reduced anthropogenic VOC has a negligibly small impact on ozone, as opposed to locations in which reduced anthropogenic VOC causes some reduction in ozone. In their definition, situations in which reduced VOC would cause a nonzero ozone reduction would be regarded as sensitive to both NO<sub>x</sub> and VOC, even if reduced NO<sub>x</sub> had a much larger impact than the equivalent percent reduction in VOC.

*NO<sub>x</sub> titration without VOC benefits:* In situations in the vicinity of very large NO<sub>x</sub> emissions sources, it frequently is predicted that ozone would increase in response to reduced NO<sub>x</sub> emissions, but would be virtually unaffected by reduced VOC. This situation occurs only when the rate of photochemical formation of ozone (via NO-to-NO<sub>2</sub> conversions) is negligibly small. Ozone would decrease in response to NO emissions because NO removes O<sub>x</sub> through the reaction



The process also occurs at night, when there is no significant photochemical production of O<sub>3</sub>.

In some analyses, a distinction is made between situations dominated by NO<sub>x</sub> titration (in which VOC emissions have little effect) and situations with standard VOC-sensitive or NO<sub>x</sub> saturated chemistry, in which ozone increases with increasing VOC.

*Extent of NO<sub>x</sub> and VOC reductions:* The relative impact of reduced NO<sub>x</sub> and VOC is often very different for large reductions (as a percent of total emissions) as opposed to small reductions. In general, NO<sub>x</sub> controls appear more advantageous relative to VOC when very large percent reductions are considered, while VOC controls appear more advantageous relative to NO<sub>x</sub> if relatively small changes are made. It is quite common for a location to be

"VOC-sensitive" with respect to emission reductions of 25% and "NO<sub>x</sub>-sensitive" with respect to emission reductions of 75% (Roselle and Schere, 1995).

*Definitions used in this study:* Unless otherwise stated, this study will use the terms "NO<sub>x</sub>-sensitive" to refer to situations in which significantly greater reduction in O<sub>3</sub> is expected from reduced NO<sub>x</sub> relative to an equivalent percent reduction in VOC, and "VOC-sensitive" for the opposite. Some subsections will refer to studies that define sensitivity in terms of NO<sub>x</sub> benefits versus disbenefits. These will be referred to as "NO<sub>x</sub>-sensitive" versus "NO<sub>x</sub>-saturated". Some sections will also use NO<sub>x</sub> titration as an additional classification. Unless otherwise specified, these terms will all be used with reference to emission reductions in anthropogenic NO<sub>x</sub> and VOC of 25%-50%.

## **2.3 EVALUATION OF INDIVIDUAL OBM<sub>s</sub>**

### **2.3.1. Secondary species as NO<sub>x</sub>-VOC indicators**

*Overview:* NO<sub>x</sub>-VOC indicators refers to a series of species and species ratios, usually involving reactive nitrogen, that are believed to be linked to O<sub>3</sub>-NO<sub>x</sub>-VOC sensitivity. The method is based on the concept that when ozone concentrations are sensitive primarily to NO<sub>x</sub> rather than VOC, measured values of these indicator ratios are high. When ozone concentrations are sensitive primarily to VOC rather than NO<sub>x</sub>, measured values of the indicator ratios are low.

The indicator ratios are associated with NO<sub>x</sub>-VOC sensitivity only at the exact time and place of measurement. Measured values at one location and during a single event do not provide any information about NO<sub>x</sub>-VOC sensitivity at a different location or at the same location during a different event. Consequently, the method can be used only when there is an extensive network of measurements that includes the region where peak O<sub>3</sub> occurs.

The original work on this concept (Sillman, 1995) identified two major classes of ratios that were likely to serve as NO<sub>x</sub>-VOC indicators: (i) O<sub>3</sub>/NO<sub>y</sub> (where NO<sub>y</sub> represents total reactive nitrogen) and the closely related ratios O<sub>y</sub>/(NO<sub>y</sub>-NO<sub>x</sub>) and O<sub>3</sub>/HNO<sub>3</sub>; and (ii) H<sub>2</sub>O<sub>2</sub>/HNO<sub>3</sub> and a series of similar ratios involving peroxides and reactive nitrogen. Subsequent researchers identified slightly different variations. Other proposed indicator ratios (NO<sub>y</sub>, HCHO/NO<sub>y</sub>, and O<sub>3</sub>/NO<sub>x</sub>) were subsequently found to have major flaws.

The concept of indicator ratios was originally developed by Milford et al. (1994), Sillman (1995) and Sillman et al. (1995, 1997, 1998, 2001a, 2001b) and subsequently analyzed by Tonnesen and Dennis (1998), Lu and Chang

(1998), Chock et al. (1999), Vogel et al., 1999, and Martilli et al., 2001. Tonnesen and Dennis (1998) extended the concept and investigated various alternative indicator ratios (see additional results in Section 2.3.3).

**Theoretical basis:** The main indicator ratios ( $O_3/NO_y$  and  $H_2O_2/HNO_3$ ) were both justified in terms of radical chemistry. Instantaneous ozone chemistry is sensitive to  $NO_x$  when the rate of conversion of radicals to peroxides exceeds the rate of conversion to  $HNO_3$ , or (alternatively) when the rate of production of radicals exceeds the rate of removal of  $NO_x$ . Based on this radical chemistry,  $NO_x$ -sensitive conditions should be associated with high values of  $O_3/NO_y$  and  $H_2O_2/HNO_3$ .

**Comment:** The ratio  $O_3/NO_y$  can also be interpreted as ratio of ozone production to  $NO_x$  removal, or ozone production efficiency per  $NO_x$  (Trainer et al., 1993). This ozone production efficiency is higher in  $NO_x$ -sensitive conditions based on either the radical chemistry above or the higher  $VOC/NO_x$  ratios associated with  $NO_x$ -sensitive conditions. The ratio  $O_3/NO_y$  also is affected by photochemical age (see discussion of smog production algorithms in Section 2.3.2 below).

**Method of justification:** The  $NO_x$ -VOC indicators are identified from 3-d Eulerian simulations, including standard AQMs. Initial model scenarios are repeated with 25%-50% reductions in domain-wide emissions of anthropogenic VOC and of  $NO_x$  in order to obtain the predicted response to VOC and  $NO_x$  controls. These control predictions are correlated with the value of the proposed indicator ratios in the model base case. The test simulations include perturbed scenarios with changed base case emissions and meteorology in order to insure that the apparent relationship between  $NO_x$ -VOC sensitivity and indicator ratios is not dependent on model assumptions.

**Range of applications:** Tests for the validity of the indicator method require the use of 3-d Eulerian models, although measurement-based applications can provide supporting evidence by showing whether measured species are consistent with the range of model predictions. Applications with model-based tests of validity include the following locations: the northeast corridor and Lake Michigan airsheds (Sillman, 1995); Atlanta\* (Sillman et al., 1995); New York and Los Angeles\* (Sillman et al., 1997); Nashville\* (Sillman et al., 1998); the eastern U.S. (Tonnesen et al., 2000a); Switzerland (Staffelbach et al., 1997, Dommen et al., 1999) Milan, Italy\* (Martilli et al., 2001, Hammer et al., 2001); and Paris, France\* (Sillman et al., 2001). Many of these applications (identified by asterisks) included measurements and model-measurement comparisons for the relevant species. Tests that generated contrary evidence are listed below. The tests included several different photochemical mechanisms:

Sillman's mechanism based on Lurmann et al. (1986); CB4 (Gery et al., 1989), and mechanisms based on EMEP in Europe.

**Contrary evidence:** Model-based investigations of the San Joaquin valley (Lu and Chang, 1998) and in Los Angeles (Chock et al., 1999) both generated results for  $\text{NO}_x$ -VOC indicators that differed substantially from the results reported by Sillman, above. Blanchard and Stoeckenius (2001) also reported contradictory results in a review that included the above model applications. Both sets of contrary results used CB-4 chemistry. West et al. (2000) found contrary results from a model-based investigation in Mexico City. Blanchard et al. (2001) reported that the method was successful qualitatively, but that indicator values varied with individual applications. Results from Paris, France (Sillman et al., 2001) also identify situations where measurements may not be of sufficient accuracy.

**Is it universal?** It is uncertain whether the original  $\text{NO}_x$ -VOC indicators are broadly applicable or if their use varies from location to location.  $\text{NO}_x$ -VOC indicators were originally presented as a concept that would be universally valid. Consistent results were obtained for many different locations and model types. However, the contrary results for San Joaquin and Los Angeles suggest that the  $\text{NO}_x$ -VOC indicators may show significant variation among different locations. It is likely that a modified version of the indicator formula would be valid even in these cases, but it is unclear whether a modified formula would have universal validity or if it would need to be adjusted for each location.

The  $\text{NO}_x$ -VOC indicators can only be used during a prescribed range of conditions: afternoon (between 1 pm and sunset) during relatively sunny days and without rain.

**Other sources of error:**  $\text{NO}_x$ -VOC indicators would return misleading results in situations where  $\text{HNO}_3$  were removed from the ambient atmosphere (by deposition or by conversion to aerosol nitrate) much more rapidly than currently represented in AQMs. Similarly misleading results would occur if measured  $\text{NO}_y$  did not include  $\text{HNO}_3$ . Measured ( $\text{NO}_y$ - $\text{HNO}_3$ ) apparently cannot be used evaluating  $\text{NO}_x$ -VOC sensitivity.

**Ease of use:** The  $\text{NO}_x$ -VOC indicators require an extensive network of measurements and care to insure measurement accuracy. If measurements are available, the method itself consists of a simple "rule of thumb" that identifies  $\text{NO}_x$ -sensitive and VOC-sensitive regions. A thorough application of the method would include testing with an AQM and evaluation of measured species correlation patterns in comparison with model results. This

evaluation would require the development of detailed protocols, but would probably be no more difficult than existing evaluation of AQM results versus measured  $O_3$ . Some additional interpretation is also needed if the  $NO_x$ -VOC indicators are used to evaluate 8-hour average  $O_3$ .

**Availability and accuracy of measurements:** Among the proposed indicator ratios, only  $O_3/NO_y$  (and possibly  $O_3/(NO_y-NO_x)$  and  $O_3/HNO_3$ ) can be considered for widespread regulatory use. The  $NO_x$ -VOC indicators involving peroxides appear to be more accurate, but peroxides require a research-grade measurement.  $O_3$ ,  $NO_x$  and  $NO_y$  can be measured using commercially available instruments.

The EPA PAMs network currently measures  $NO_y$  at a small number of sites in the northeast. These are all rural sites and are less likely to have unusually high  $O_3$ . Widespread application of the indicator method would be possible only if this network were expanded. In addition, there are issues of measurement accuracy. The indicator method requires measured  $NO_y$  with uncertainties less than 20% (preferably less than 10%).  $NO_y$  measurements are subject to error if  $HNO_3$  is lost in the measurement inlet tube. Such an error would render the measurement invalid for use as a  $NO_x$ -VOC indicator.

**Can the method be evaluated or modified in individual applications?** Because  $NO_x$ -VOC indicators are generated by AQMs, routine application of AQMs in the regulatory process can also be used to evaluate and modify the  $NO_x$ -VOC indicators for specific locations and events. It is more difficult to evaluate measurements associated with applications of the indicator method.

**Synthesis with Eulerian models:**  $NO_x$ -VOC indicators can be used to evaluate the accuracy of individual AQM applications, in the same way that measured  $O_3$  has been used in the past. Because  $NO_x$ -VOC indicators are closely associated with Eulerian AQMs, there are various ways in which AQMs and indicator measurements can be used in combination. In cases where measured indicator ratios are consistent with results of a regulatory AQM, they provide a stronger basis for confidence in the AQM than would be provided by measured  $O_3$  alone. However, it is unclear how to respond in a case where major differences appeared between the AQM and measured indicator ratios.

**Overall evaluation:** Indicator ratios have a number of advantages for regulatory use as an OBM. They have been applied and tested very widely. There has been more contrary evidence for the  $NO_x$ -VOC indicators than for other methods, but this may be due to the fact that indicators have been tested more extensively than other methods.

The simplest indicator ratio ( $O_3/NO_y$ ) can be used with commercially available instrumentation, and the method can be evaluated and updated separately even in regulatory applications. The most promising use of indicator ratios would be to evaluate the accuracy of individual applications of Eulerian AQMs. Use of measured indicator ratios to evaluate AQMs would probably remain valid even if it were found that the indicator ratios failed as a stand-alone method to evaluate ozone control strategies.

Case studies with  $NO_x$ -VOC indicators have given mixed results. In some instances the  $NO_x$ -VOC indicators seemed to provide clear evidence for  $NO_x$ -sensitive or VOC-sensitive conditions, but in other cases the indicator values were uncertain. Interpretation of  $NO_x$ -VOC indicators must account for the sources of error discussed above.

If  $NO_x$ -VOC indicators were used in regulatory applications, protocol would need to be developed for situations in which results from indicators and results from AQMs disagreed. In some cases AQMs may predict  $NO_x$ -sensitive conditions while measured indicator ratios suggest VOC-sensitive conditions, or vice versa. It would then be necessary either to correct the regulatory AQM or to reject the evidence from indicators.

There are important opportunities for synthesis between  $NO_x$ -VOC indicators and smog production algorithms, described in Section 2.3.2.

### **2.3.2. Smog production (extent-of-reaction) algorithms**

**Overview:** Smog production algorithms are methods of evaluating  $O_3$ - $NO_x$ -VOC sensitivity based on ambient measurement of a few species, primarily reactive nitrogen. The distinctive feature of smog production algorithms (as opposed to the  $NO_x$ -VOC indicators discussed in Section 2.3.1) is that they were initially derived based on smog chamber experiments rather than 3-d Eulerian models. The smog production algorithms are also based on a specific rationale: the belief that VOC-sensitive conditions are associated with relatively fresh emissions and that  $NO_x$ -sensitive conditions are associated with aged air in which ozone producing reactions have been run to completion. The smog production algorithms all use measurements to infer the maximum smog production for the given amount of ozone precursors ( $SP_{max}$ ) in comparison with actual smog production (SP). The ratio ( $SP/SP_{max}$ ) is referred to as the extent of reaction, and high values are associated with  $NO_x$ -sensitive conditions. The extent of reaction is obtained from formulas based on measured  $O_3$ , NO, and either  $NO_x$  and  $NO_y$ . The main formulas use variants of the ratios  $O_3/NO_y$ ,  $O_3/NO_x$  and  $NO_x/NO_y$ , each measured in locations with high  $O_3$ .

As with the  $\text{NO}_x$ -VOC indicators, the smog production algorithms provide information on  $\text{O}_3$ - $\text{NO}_x$ -VOC sensitivity only at the exact time and place of measurement.

The smog production concept was originated by Graham Johnson (1984, 1989) and subsequently extended and modified by Hess et al. (1992), Olszyna et al. (1994), T. Chang et al. (1997, 1998) and Blanchard et al. (1999, 2000, 2001). The extensions have included modifications based on additional smog chamber experiments and 0-d model calculations, tests with 3-d Eulerian models, and limited confirmation of the theory based on ambient data. Smog production algorithms have been used to diagnose  $\text{O}_3$ - $\text{NO}_x$ -VOC sensitivity extensively in the U.S. (in the New York-Connecticut-Massachusetts and Baltimore-Washington corridors, Atlanta, Houston and other cities in Texas, Chicago, Los Angeles and the San Joaquin Valley) and in Australia (Melbourne).

***Theoretical basis:*** As described above, the smog production algorithms are based on the concept that VOC-sensitive conditions occur when precursor emissions are relatively fresh and have not reacted to completion, and that  $\text{NO}_x$ -sensitive conditions occur when precursors have reacted to completion. This "extent of reaction" refers to the extent of reaction of  $\text{NO}_x$ .  $\text{NO}_x$ -sensitive conditions occur when most of the emitted  $\text{NO}_x$  has already been processed and converted to product species.

***Comment:*** The notion that VOC-sensitive conditions are associated with relatively unprocessed emissions and  $\text{NO}_x$ -sensitive conditions are associated with aged air is often true, but it is not always true. There is extensive evidence from smog chambers (e.g. Blanchard et al., 1999), 0-d and 3-d model calculations (Milford et al., 1994, Blanchard et al., 1999) and some ambient measurements (Olszyna et al., 1994) to support this concept. However there is also contrary evidence from 3-d models (Sillman and He, 2001). In addition, the theoretical basis assumes that maximum smog production ( $\text{SP}_{\text{max}}$ ) is a simple function of the initial  $\text{NO}_x$  concentration. Recent evidence from power plants (Ryerson et al., 1998, 2001) suggests that plumes with different amounts of biogenic VOC produce different amounts of ozone, even after all the  $\text{NO}_x$  has reacted away.

The finding that VOC-sensitive chemistry has low ozone production per  $\text{NO}_x$  and that  $\text{NO}_x$ -sensitive chemistry has high ozone production per  $\text{NO}_x$  may provide a stronger justification for the smog chamber algorithms. The smog production formulas based on  $\text{O}_3/\text{NO}_y$  have values that reflect the rate of ozone production per  $\text{NO}_x$  as well as extent of reaction.

**Method of justification:** The smog production algorithms were derived from experiments in outdoor smog chambers at CSIRO (Australia), University of North Carolina and University of California, Riverside and from 0-d or box model calculations (Blanchard et al., 1999). Both the smog chamber and 0-d calculations represented an initial high concentration of ozone precursors followed by photochemical reaction without additional emissions (or, occasionally, with a second single burst of emissions). Sensitivity to  $\text{NO}_x$  and VOC was inferred by comparing experiments or calculations with changes in initial  $\text{NO}_x$  and VOC concentrations. Results of 3-d models were also used to test the accuracy of the smog production algorithms.

**Range of applications:** Smog production algorithms have been used very widely to diagnose  $\text{O}_3$ - $\text{NO}_x$ -VOC sensitivity in urban areas (e.g. T. Chang and Suzio, 1995, 1996; Blanchard, 2001), but most of these cases have simply been applications of the smog production formula rather than evaluations of its validity. The validity of the smog production algorithms is based on the range of smog chamber experiments, and includes experiments by three groups (CSIRO, University of North Carolina and University of California, Riverside). The validity of smog production algorithms has also been established by 0-d model calculations with two photochemical mechanisms: CB-4 and Lurmann et al., 1987. Evaluation of the smog production algorithms based on 3-d models has been performed for episodes in southern California, the San Joaquin Valley, Texas (near Houston), Lake Michigan and the northeast corridor (T. Chang et al., 1997; Blanchard et al., 2001). The 3-d model tests were done with the Urban Airshed Model (UAM-IV and UAM-V) and San Joaquin Air Quality Model (SAQM), both with CB-4 chemistry. In addition, ambient measurements in rural Tennessee were used to identify the pattern of ozone production versus extent of reaction (Olszyna et al., 1994). This measurement-based investigation found a pattern similar to that observed in smog chamber experiments.

**Contrary evidence:** Sillman (1999) and Sillman and He (2001) found that the smog production formulas based on the ratio  $\text{NO}_x/\text{NO}_y$  do not correlate well with  $\text{NO}_x$ -VOC sensitivity in 3-d models (for the northeast corridor and Lake Michigan regions). The poor correlation was found in regional-scale models that included transport over 500 km or more, rather than a single city. The accuracy of smog production formulas based on  $\text{NO}_x/\text{NO}_y$  has never been demonstrated in a 3-d model.

Blanchard et al. (2001) and Sillman and He (2001) also reported somewhat ambiguous results from 3-d simulations for algorithms based on the ratio  $O_3/NO_y$ . Blanchard (2000) identified uncertainties based on measurements of  $NO_x$  from commercial instruments.

***Is it universal?*** The smog chamber experiments suggest that the smog production algorithms are at least qualitatively valid for a wide range of conditions. Results from 3-d models reported by Blanchard et al. (2001) suggest that the exact transition from  $NO_x$ -sensitive to VOC-sensitive conditions may vary in different locations. Blanchard et al. (2001) found that there is a large range of values with uncertain  $NO_x$ -VOC sensitivity, and only extreme values of the smog production parameter can be definitely correlated with  $NO_x$ -sensitive or VOC-sensitive conditions everywhere. The smog production formula based on  $O_3/NO_y$  may be less subject to variation than the indicator ratios used by Sillman (1995) because they are not affected by background conditions.

As was the case with  $NO_x$ -VOC indicators (Section 2.3.1), the smog production algorithms cannot be used if most of the  $NO_y$  associated with ozone production has been removed by deposition. This prevents the use of smog production algorithms at night or in events with precipitation.

***Other sources of error:*** Smog production algorithms based on measured  $NO_y$  are subject to error based on the uncertain rate of removal of  $NO_y$  from the ambient atmosphere. There are also possible errors in  $NO_y$  measurements. Smog algorithms that use  $NO_x$  instead of  $NO_y$  are less subject to uncertainty due to deposition. However the smog production algorithm based on  $NO_x$  has not been tested in 3-d models.

***Ease of use:*** Smog production algorithms require measured  $O_3$ , NO and either  $NO_x$  or  $NO_y$ . As with the  $NO_x$ -VOC indicators, these measurements must be extensive enough to characterize the entire area of peak  $O_3$ . If measurements of sufficient accuracy are available, application of the smog production algorithms is straightforward. The smog production formula generates a measurement-based index that identifies  $NO_x$ -sensitive and VOC-sensitive locations.

***Availability and accuracy of measurements:***  $O_3$  and  $NO_x$  measurements are both widely available through the PAMs network, although there is some question about the accuracy of  $NO_x$  measured by commercial instruments (Winer et al., 1974, Logan, 1989). Blanchard (2001) included sensitivity to measurement error in applications of smog production algorithms.  $NO_y$  is less readily available, but instruments to measure  $NO_y$  are commercially available. The same concerns about accuracy associated with  $NO_x$ -VOC indicators (above) apply here.

***Can the method be evaluated or modified in individual applications?*** The smog production algorithms represent a universal formula based on smog chambers and cannot be modified for individual applications. The method also does not include a way to evaluate the accuracy of measurements used in individual applications, although Blanchard (2001) included analysis of sensitivity to measurement uncertainties in their applications. The accuracy of smog production algorithms can be evaluated in individual applications if an AQM is used.

***Synthesis with Eulerian models:*** Smog production algorithms were developed independently from Eulerian AQMs, and there are no immediately obvious ways to develop a synthesis. However, smog production algorithms can probably be extended for use as a tool to evaluate the accuracy of AQM scenarios. Combined use of AQMs and smog algorithms can be done in the same way as combined use of AQMs and  $\text{NO}_x$ -VOC indicators. It is unclear how to respond when AQMs and smog production algorithms lead to opposite conclusions in terms of control strategies.

***Overall evaluation:*** Smog production algorithms are currently the most widely used OBM, especially in regulatory applications. Research on the method has included many investigators and involved limited evaluation with 3-d model calculations and some analysis of ambient data in addition to the extensive smog chamber experiments. It can be incorporated easily into existing regulatory evaluations and can be used with measurements currently available from the PAMs network.

Its major drawback is vagueness about uncertainties when the method is applied to ambient conditions. In most applications the method has been used as a plug-in formula, used to provide answers with relatively little investigation of its accuracy. The rate of removal of  $\text{NO}_y$ , a critical parameter and source of uncertainty, is not included in the algorithms and is instead left for users to estimate. There is also no clear guidance for identifying background  $\text{O}_3$ , which is an important parameter in most of the smog algorithms. The method could be improved if it were combined with a broader analysis of ambient measurements and with comparisons between measurements and model results.

Of the three types of smog production algorithms, the algorithm based on  $\text{O}_3$  and  $\text{NO}_y$  appears to be the most accurate. The method based on  $\text{NO}_x$  and  $\text{NO}_y$  was found to give poor results when tested in 3-d air quality models (Sillman, 2000; Sillman and He., 2001). The method based on  $\text{O}_3$  and  $\text{NO}_x$  also appears to give ambiguous results when tested in air quality models.

The smog production algorithms closely resemble some of the NO<sub>x</sub>-VOC indicator formulations. Some of the problems associated with smog production algorithms might be addressed based on results from investigations of the indicator formulas, while some of the problems associated with indicators might be addressed by using results from the smog production algorithms. A combination of the two methods might be useful.

**Controversial issue – models versus smog chamber results:** The major issue for smog production algorithms concerns the level of confidence in smog chamber experiments as a basis for developing an OBM. By contrast, NO<sub>x</sub>-VOC indicators were developed based on 3-d Eulerian models. Reliance on 3-d models has several advantages. Indicators derived from models can be evaluated and modified for individual situations based on results from AQMs. Indicators can also be used to provide a broader evaluation of the accuracy of AQMs, and these evaluations can also expose flaws in the indicator formula or in the accuracy of individual measurements. The models used to derive indicators include a more detailed representation of the geographic pattern of emissions and include multiday transport. Smog chambers, by contrast, represent a single emission source followed by chemical evolution without added emissions. Such conditions rarely occur in the ambient atmosphere.

Here, it will be assumed that smog production algorithms are valid only when they can be shown to perform successfully in 3-d models.

### **2.3.3. Constrained steady state (CSS): Instantaneous chemistry based on measured NO<sub>x</sub> and VOC**

**Overview:** The constrained steady state method (CSS) is presented here as a combination of two similar methods that have been developed independently: one by Kleinman et al. (1997, 2000, 2001) and the other by Tonnesen and Dennis (2000b). Kirchner et al. (2001) also proposed a similar method. Although no intercomparison has been made, the methods appear to use the same species and the same strategy. The observation-based model developed by Cardelino and Chameides (1995, 2001) is also closely related but is discussed separately (see section 2.3.4).

Both methods seek to evaluate the instantaneous rate of production of O<sub>3</sub> and how it depends on NO<sub>x</sub> and VOC. Both methods are based on the use of measured primary species (NO<sub>x</sub> and VOC). Both methods derive a relation for NO<sub>x</sub>-VOC sensitivity in terms of radical budgets. Both also derive indicators for instantaneous NO<sub>x</sub>-VOC sensitivity in terms of a reactivity-weighted sum of VOC and NO<sub>x</sub>. Tonnesen and Dennis derive a formula with the form  $\sum_i k_i \text{VOC}_i / (\sum_i k_i \text{VOC}_i + k_n \text{NO}_2)$ , where VOC<sub>i</sub> and NO<sub>2</sub> represent measured quantities. An

equivalent formula based on a simple ratio of summed reactivity-weighted VOC to  $\text{NO}_x$  could also be developed. A formula based on the ratio of reactivity-weighted VOC to  $\text{NO}_x$  was also proposed informally by Chameides et al. (1992). Kleinman et al. derive a more complex formula involving VOC,  $\text{NO}_x$  and the total radical source (calculated or inferred from measured VOC). Tonnesen et al. also derive an indicator based on summed organic peroxy radicals ( $\text{RO}_2$ ), but this is not immediately useful for regulatory applications due to the scarcity of measurements.

Kleinman et al. also use a series of 0-d calculations ('constrained steady state') driven by measurements, which can be used to derive the  $\text{NO}_x$ -VOC dependence of the instantaneous rate of ozone production. This type of steady-state calculation is frequently used to evaluate ozone production in the remote troposphere (e.g. Ridley et al., 1992, see also Jaegle et al, 1998, 2001). Kleinman et al. represent the only attempt to do a similar analysis in polluted locations.

**Theoretical basis:** Kleinman et al. and Tonnesen and Dennis both derive their analyses based on radical chemistry.  $\text{NO}_x$ -sensitive chemistry is associated with conditions in which formation of peroxides represents the dominant sink for the family of radicals (including OH,  $\text{HO}_2$  and  $\text{RO}_2$ ), while VOC-sensitive chemistry is associated with conditions in which formation of nitric acid represents the dominant sink for radicals. The link between instantaneous  $\text{NO}_x$ -VOC sensitivity and reactivity-weighted VOC and  $\text{NO}_x$  is derived from radical chemistry.

**Comment:** This is similar to the rationale proposed for  $\text{NO}_x$ -VOC indicators. Since it involves instantaneous chemistry rather than the more complex chemistry and transport that affect ozone concentrations, it is more likely to be universally true.

**Method of justification:** Kleinman et al. justify their methods through a series of steady-state calculations, which represent instantaneous chemistry. Tonnesen and Dennis used trajectory model calculations (OZIPR, familiar as part of the EKMA modeling approach) and results of a 3-d AQM. Because this method focuses on instantaneous photochemical production, the 3-d model results were used largely to provide a series of photochemical calculations for a range of conditions. Kleinman et al. and Tonnesen and Dennis both used RADM2 chemistry (Stockwell et al., 1990). Kleinman et al. incorporated the mechanism of Paulson and Seinfeld (1992) for isoprene.

**Range of applications:** Kleinman et al. applied their method (including both 0-d model calculations and measurements) to cases in Phoenix, AZ and New York City. Tonnesen and Dennis presented model results only, using an EKMA model for Atlanta and a RADM simulation for the northeastern U.S.

**Contrary evidence:** None.

**Is it universal?** The instantaneous chemistry formulas have been developed based on a small number of cases and only one photochemical mechanism (RADM2). However, there is reason to believe that a variation of the method with universal validity can be developed. Constrained steady state calculations have been used very widely to evaluate instantaneous photochemistry in the remote troposphere. These calculations are equivalent to 3-d AQMs in terms of being universally applicable, and are less sensitive to model parameters or assumptions than the AQMs. The abbreviated formulas as functions of measured VOC and  $\text{NO}_x$  were presented by Kleinman et al. and Tonnesen and Dennis as universal derivations from radical chemistry. Due to the complex nature of VOC chemistry, much more extensive testing and analysis is needed to establish whether the formulas have universal validity.

**Other sources of error:** All variants of the instantaneous chemistry formula rely on measured VOC and  $\text{NO}_x$ , and are subject to errors common to all methods that depend on these measurements:

- Surface ozone concentrations result from photochemical production throughout the daytime convective mixed layer, which typically extends to a height of 1000-2000 meters. VOC and  $\text{NO}_x$  concentrations vary significantly with height, and surface measurements (which are most commonly available) do not reflect this variation. This is especially true for biogenic VOC.
- Measured VOC and  $\text{NO}_x$  at the surface are often affected by emission sources in the immediate vicinity of the monitor, and may therefore not be representative of average conditions in the area.
- Concern has been expressed that measured VOC from the EPA PAMs network may underestimate the amount of alkenes and other highly reactive VOC (Parrish et al., 1998, 2000). If these species are underrepresented, the method will return biased results.
- Concern has been expressed that measured  $\text{NO}_x$  using commercially available instruments represents the sum of  $\text{NO}_x$  and various  $\text{NO}_x$  reaction products (Winer et al., 1974, Logan, 1989, Blanchard, 2001). This

would compromise the use of the method. In addition, Cardelino and Chameides (2000) found that measured NO may not be of sufficient accuracy to distinguish NO<sub>x</sub>-sensitive from VOC-sensitive chemistry.

***Ease of use:*** Because these formulas represent instantaneous photochemistry only, they require considerable interpretation in order to be used in regulatory applications. The major regulatory concern is the relation between ozone concentrations and precursor emissions. Currently there is no clear method available for using the formulas for instantaneous chemistry to address regulatory concerns.

The formula developed by Tonnesen and Dennis represents a one-step calculation and can be made easily from measured VOC and NO<sub>x</sub>. The formula developed by Kleinman et al. requires more effort. The steady-state model used by Kleinman et al. has the same level of complexity as traditional 0-d or box models. This is considerably simpler than the current generation of 3-d AQMs. Such a model could be easily developed for regulatory use (especially if linked to the format of available measurements), but an easy-to-use version is not currently available.

***Availability and accuracy of measurements:*** The methods that are most likely to be of practical use would require complete sets of measured VOC and NO<sub>x</sub> at locations spread throughout the area of interest. Because the calculations are only valid for the exact time and place of measurements, the network would need to be extensive. Kleinman et al. present an alternative formula that does not need complete measurement of VOC. However, the alternative would require measured formaldehyde (HCHO) and would probably require other aldehydes and alkenes (as radical sources) as well. This is likely to be just as difficult as complete primary VOC.

Primary VOC and NO<sub>x</sub> measurements are generally available through the EPA PAMs network. Concern about the accuracy of these measurements is discussed above (see *sources of error*).

***Can the method be evaluated or modified in individual applications?*** The constrained steady state calculation is a universal calculation and would not be modified in individual applications. It might be possible to modify the instantaneous formulas for individual applications, using results from individual AQMs (in effect duplicating the work of Tonnesen and Dennis), though this would be laborious.

***Synthesis with Eulerian models:*** The VOC-NO<sub>x</sub> formula developed by Tonnesen and Dennis could be used as a basis for evaluating the accuracy of AQM applications. Given that this formula is related to NO<sub>x</sub>-VOC chemistry, it could be expanded into a general evaluation of the accuracy of AQM representation. This would remain true even if it were found that the formula was imprecise as a NO<sub>x</sub>-VOC indicator. The VOC-NO<sub>x</sub> formula is also useful

because it relates to emissions in an AQM, and might be used to as a basis for generating a modified AQM scenario. The steady state calculation developed by Kleinman et al. could be used similarly, although it does not have a direct connection to emissions in AQMs.

**Overall evaluation:** Of the various proposed OBMs proposed for evaluating  $\text{NO}_x$ -VOC sensitivity, the instantaneous formulas are the most strongly grounded in scientific principles and have the strongest claim to universal validity. The CSS calculation in particular is widely used in investigations of tropospheric chemistry and is likely limited only through the extent and accuracy of the available measurements. The concept of  $\text{NO}_x$ -VOC sensitivity developed by Kleinman et al. is also being used in research projects that evaluate the accuracy of current representations of ozone photochemistry (Thornton et al. 2002) However, the instantaneous formulas do not represent the complete process of photochemistry and transport that causes elevated ozone. In many ways the higher degree of scientific validity occurs because they omit the processes that are most difficult to analyze.

The instantaneous formula based on VOC and  $\text{NO}_x$  is especially interesting because measured VOC and  $\text{NO}_x$  have often have been used as a diagnostic tool for ozone. Throughout the 1980's it was thought that  $\text{O}_3$ - $\text{NO}_x$ -VOC sensitivity could be evaluated based on the ratio of VOC to  $\text{NO}_x$  measured in an urban center during the early morning. This morning VOC/ $\text{NO}_x$  ratio was subject to many errors as a basis for determining  $\text{NO}_x$ -VOC sensitivity: it did not account for reactivity of individual VOC; it did not account for biogenics; and it did not account for the transport process. However, a formula based on reactivity-weighted VOC and  $\text{NO}_x$  may be generally applicable as a way to evaluate instantaneous photochemistry. With this understanding, measured VOC and  $\text{NO}_x$  might be used more appropriately in the regulatory process.

The formula for instantaneous  $\text{O}_3$ - $\text{NO}_x$ -VOC sensitivity based on measured VOC needs to be tested with other photochemical mechanisms and for a wider range of conditions. It should also be compared with the analysis of ozone formation potential (e.g. Carter et al., 1994, 1995).

The question of the vertical distribution of individual VOCs and the possibility of influence from sources in the immediate vicinity of measurement sites are likely to be the greatest challenge for this method.

The observation-based model of Cardelino and Chameides (Section 2.3.4 below) is closely related to this method.

#### **2.3.4. Observation-based model using $\text{NO}_x$ and VOC (Cardelino-Chameides)**

**Overview:** The observation-based model developed by Cardelino and Chameides (1995, 2000) was developed directly in response to the perceived deficiencies of AQMs and the need for observation-based methods. It was originally described as a model calculation that would duplicate many features of AQMs ('emission-based models') but would use ambient measurements in place of emission inventories to determine concentrations of primary pollutants.

The observation-based model consists of a series of 0-d or box model calculations constrained by measured  $O_3$ ,  $NO_x$  and VOC. These calculations are similar to the constrained steady state (CSS) calculations developed by Kleinman et al. (above), but they also include the impact of vertical diffusion. Overall impact of emitted  $NO_x$  and VOC on  $O_3$  is assessed by repeating the calculation with reduced  $NO_x$  and VOC, following a methodology similar to the studies of relative incremental reactivity by Carter et al. (1994, 1995). The overall impact of  $NO_x$  and VOC within a metropolitan area is assessed by a sum of relative incremental reactivities (weighted by ozone production rates) for each hour during the period of ozone production and for each measurement site.

The observation-based model grew out of work by Chameides et al. (1992), which is discussed in connection with  $NO_x$ -VOC isopleths, below.

**Theoretical basis:** The method consists of model calculations rather than a formula or rule of thumb. No specific rationale is needed in this case. The major theoretical issue concerns whether the factors controlling ozone concentrations (including transport over a wide range of conditions) can be adequately represented by a series of 0-d calculations, which represent conditions at discrete times and locations.

**Method of justification:** The OBM calculations are viewed as having universal validity by themselves, equivalent to 3-d Eulerian AQMs. In addition, the calculations have been compared with results from AQMs for a series of scenarios in Atlanta.

**Range of applications:** The only complete analysis based on a network of measurements throughout an urban area was done for Atlanta. This analysis also included extensive comparisons with an Eulerian AQM. Other applications were developed for individual measurement sites in Washington D.C., New York and Texas. Although limited to a single measurement site, these studies included several days at each site. They also included cross-comparisons between measured individual VOC species as a form of quality assurance.

**Contrary evidence:** None. However, Cardelino and Chameides (2000) questioned whether the available measurements were of sufficient accuracy.

**Is it universal?** The 0-d calculations used in the OBM are likely to have universal validity. However it is uncertain whether the sum of 0-d calculations over all measurement sites within a metropolitan area would accurately represent  $O_3$ - $NO_x$ -VOC sensitivity in the area. Accuracy may depend on the location of measurement sites. In addition, the method only represents average  $O_3$ - $NO_x$ -VOC sensitivity throughout the area. It may not be able to identify the conditions associated with high ozone in specific locations.

**Other sources of error:** The OBM is subject to the same uncertainties as the constrained steady state method, discussed above. Measured VOC and  $NO_x$  may represent surface conditions only rather than average conditions throughout the convective mixed layer. They may be affected by emission sources in the immediate vicinity of the measurement site. Concern has been expressed whether measured VOC and NO is sufficiently accurate. Cardelino and Chameides (2000) reported that  $NO_x$ -sensitive conditions are generally associated with NO concentrations below 0.9 ppb, and VOC-sensitive conditions are associated with higher NO. Commercially available measurement instruments may not be accurate enough to measure such low values of NO.

**Ease of use:** The OBM requires model calculations and a data base of measured VOC and  $NO_x$ . The calculation is much simpler than current AQMs. Its level of difficulty would be equivalent to 0-d or box models or to the old OZIPR (EKMA) method. It also would not add much difficulty to the general task of analyzing measured VOC and  $NO_x$ .

**Availability and accuracy of measurements:** The method requires a complete set of measured primary VOC and  $NO_x$ . These are currently available from the PAMs network, although these may not be sufficiently accurate (see *sources of error*).

**Can the method be evaluated or modified in individual applications?** The OBM calculation is a universal calculation and would not be modified in individual applications.

**Synthesis with Eulerian models:** There is no immediately obvious synthesis with Eulerian models. One possible approach would be to repeat the OBM calculations using simulated ambient concentrations from an AQM and comparing with results from OBM calculations driven by ambient measurements. This comparison could be

used as an evaluation of possible bias in  $\text{NO}_x$ -VOC predictions from the AQM. However, the same result might be obtained by comparing measured VOC and  $\text{NO}_x$  with the AQM directly.

**Overall evaluation:** The OBM is very similar to the CSS approach described above. As with CSS, the OBM accurately represents the  $\text{NO}_x$ -VOC dependence associated with instantaneous rates of photochemical production. It is less clear whether the sum of OBM calculations over all hours and all sites would adequately characterize ozone chemistry throughout a metropolitan area. This is especially true because  $\text{O}_3$ - $\text{NO}_x$ -VOC chemistry changes as air moves from downtown towards a downwind region.

One possible use of the OBM would be to monitor day-to-day changes in ozone chemistry, during cases where extensive measurements are available. The OBM could be used to evaluate day-to-day changes more easily than standard AQMs, which are usually exercised for a few episodes. The OBM might also be used to monitor year-to-year changes.

The OBM will be analyzed in detail below in combination with the CSS methods.

### **2.3.5. Direct analysis of measured $\text{NO}_x$ and VOC to estimate emissions**

**Overview:** This refers to a series of investigations that have used measured cross-correlations between species in order to make inferences about emission rates. Many of these investigations have occurred in rural areas, but some have also occurred in urban locations. Investigations of this type include correlations between CO and  $\text{NO}_y$  (e.g. Parrish et al., 1991), between individual VOC species and  $\text{NO}_y$  (Goldan et al., 1995, 1997, Harley et al., 1997) and between various individual VOC (Goldan et al., 1995, 1997, McKeen and Liu, 1993, McKeen et al., 1996). Buhr et al. (1992) derived emission estimates from principal component analysis (PCA) and other statistical methods. Many of these studies are summarized in Trainer et al. (2000) and Parrish et al. (1998, 2000). Goldstein and Schade (2000) also used species correlations to identify the relative impacts of anthropogenic and biogenic emissions.

These studies have generally been individual research efforts and have never been developed as a formalized method for use in regulatory applications.

**Theoretical basis:** Because emission of many anthropogenic species comes from the same location (e.g. urban versus rural), observation of these species should show correlations that reflect emission ratios. McKeen et al. (1996) developed an adjustment to account for photochemical loss of individual VOC in aged air masses.

**Method of justification:** In some studies of the remote troposphere, species correlations have been compared with results from models with known emission inventories (Chin et al., 1994, McKeen et al., 1996).

**Range of applications:** Species correlations have been investigated in Boulder, CO (Parrish et al., 1991, Goldan et al., 1995, 1997), Nashville, TN (Goldan et al., 2001), Los Angeles (Lurmann and Main, 1992), and at rural sites in the eastern U.S. (Buhr et al., 1992, 1995), and at sites in the remote troposphere.

**Contrary evidence:** None.

**Is it universal?** The method is likely to have universal validity, but results may depend on local conditions.

**Other sources of error:** This method is subject to the same uncertainties as other approaches that rely on measured primary VOC and NO<sub>x</sub> (see constrained steady state method, Sections 2.3.3 and 2.3.4). VOC, NO<sub>x</sub> and especially isoprene are affected by the assumed rate of vertical mixing in the AQM, and this is not corrected when emission rates are inferred from measured values. Measured VOC and NO<sub>x</sub> may be affected by emission sources in the immediate vicinity of the measurement site. Concern has been expressed whether measured VOC and NO is sufficiently accurate.

Unlike other methods based on measured NO<sub>x</sub> and VOC, analysis based on species correlations includes methods for identifying erroneous measurements.

**Ease of use:** Investigations of species correlations have usually been associated with research-grade efforts and have lengthy requirements in terms of data processing and quality assurance. In addition, there are currently no established procedures for doing this type of analysis. Each individual investigation has represented a unique effort. If this method were developed for use in regulatory applications, a standard procedure would need to be developed. However, it is likely that a procedure could be developed that could be used in regulatory applications without much difficulty.

**Availability and accuracy of measurements:** The method requires a complete set of measured primary VOC and NO<sub>x</sub>. These are currently available from the PAMs network, although these may not be sufficiently accurate.

**Can the method be evaluated or modified in individual applications?** Different statistical techniques and adjustments photochemical removal have been developed for different locations. However, the methods used should be regarded as useful.

**Synthesis with Eulerian models:** Information derived from species correlations would be used to update emission inventories in Eulerian AQMs, which would then be used in regulatory applications.

**Overall evaluation:** Evaluation and modification of emission inventories includes a wide range of measurement-based studies. The presentation here is based on a few well-documented studies and is not complete. These types of evaluation also can include a range of receptor modeling approaches (see Henry, 1994). The topic is beyond the scope of this report, which focuses more narrowly on OBMs for ozone production and ozone chemistry. They relate to the OBMs largely because emission inventories represent a major uncertainty for analyses of ozone production. Species correlations would also use the same measurements (ambient VOC and NO<sub>x</sub>, available through the PAMs network) as some of the other OBMs.

The advantages of this approach is that it includes methods to evaluate the accuracy of measured VOC, and it can also be used to identify other errors that affect interpretation of measured VOC and NO<sub>x</sub> (e.g. impact on on-site emissions). In addition, this method generates a natural correction to Eulerian AQMs, by identifying emission rates based on measurements. Based on these two advantages, it is useful to include these methods in combination with the constrained steady state approach (Sections 2.3.3 and 2.3.4).

If updates of emissions based on measurements were to be used in regulatory modeling, a formal procedure would need to be established for deriving the updated emission fields and for quality assurance of the measured data and the analysis.

### **2.3.6. Inverse modeling for emissions**

**Overview:** Inverse modeling (M. Chang et al., 1996, 1997, Mendoza-Dominguez and Russell, 2000, 2001) refers to a process by which emission inventories are adjusted based on a comparison between results from an Eulerian AQM and measured values. The ensemble of measured values is compared with model concentrations of directly emitted species. Emission inventories are then adjusted to generate a model scenario with the closest possible agreement with measurements.

Unlike other methods considered here, inverse modeling does not provide a direct estimate of NO<sub>x</sub>-VOC sensitivity. Instead, it generates an AQM scenario based on measurements, which can then be used to generate control strategy predictions. It is included here because it responds to the overall strategy of OBMs, which seeks to generate ozone control strategy predictions that are closely linked with atmospheric measurements. The strategy of

inverse modeling is also comparable with goals of the original OBM developed by Cardelino and Chameides (1995). As with the original OBM, inverse modeling seeks to generate model calculations in which observations are used in place of emission inventories to obtain concentrations of directly emitted species.

***Theoretical basis:*** Because the method is based on model calculations, no specific rationale is needed or provided.

***Method of justification:*** The method was tested by generating "pseudo-observations" from an Eulerian AQM with a known emission inventory, and then applying inverse methods to a separate AQM to see if the original emission inventory could be created. In some cases the "pseudo-observations" were modified based on random perturbations.

***Range of applications:*** The method has only been used for ozone in Atlanta, and the Atlanta case included tests for the validity of the method. The method has also been used to analyze aerosols in a model for the eastern U.S. (Mendoza-Dominguez et al., 2001)

***Contrary evidence:*** None.

***Is it universal?*** The method is likely to have universal validity.

***Other sources of error:*** The inverse modeling approach is subject to the same uncertainties as other approaches that rely on measured primary VOC and NO<sub>x</sub> (see constrained steady state method, above). VOC, NO<sub>x</sub> and especially isoprene are affected by the assumed rate of vertical mixing in the AQM, and this is not corrected by the inverse modeling. Measured VOC and NO<sub>x</sub> may be affected by emission sources in the immediate vicinity of the measurement site. Concern has been expressed whether measured VOC and NO is sufficiently accurate.

To some extent, the uncertainty associated with vertical mixing can be identified and corrected in individual applications. Erroneous model vertical mixing would lead to a simultaneous adjustment of emissions of all species, and would compromise the ability of the model to reproduce observed O<sub>3</sub>. This possibility can be corrected within the inverse modeling procedure. The interaction between vertical mixing and concentrations of biogenic species is more difficult to correct.

***Ease of use:*** Inverse modeling requires repeated exercise of an AQM in order to update emission fields. This may be burdensome for regulatory applications.

**Availability and accuracy of measurements:** The method requires a complete set of measured primary VOC and  $\text{NO}_x$ . These are currently available from the PAMs network, although these may not be sufficiently accurate.

**Can the method be evaluated or modified in individual applications?** Inverse modeling is a universal calculation and does not need to be modified in individual applications.

**Synthesis with Eulerian models:** Inverse modeling is directly connected with AQMs. Unlike other OBMs, it generates an alternative AQM scenario with a closer fit to measurements, which can then be used to evaluate control strategies.

**Overall evaluation:** Inverse modeling has many advantages over the other methods based on measured  $\text{NO}_x$  and VOC. Whereas the other methods result only in a general indication of control strategies, inverse modeling generates a complete AQM scenario that can be used to evaluate policy. In effect, it combines the advantages of the direct OBMs based on  $\text{NO}_x$  and VOC and standard Eulerian AQMs.

The inverse modeling procedure also poses a direct question to users: do the measurement-based results inspire enough confidence to justify changing the emission inventory? Inverse modeling provides a basis for answering this question because the resulting change in inventory values can be rated against the uncertainties associated with the inventories. Results of inverse modeling would also generate a data base that can be evaluated for day-to-day consistency. Errors resulting from inaccurate measurements or model formulation (e.g. erroneous vertical mixing) are also more likely to be identified by examining the resulting changes in emission inventories from the inverse model. These errors are more difficult to identify in the other OBMs that use measured  $\text{NO}_x$  and VOC.

The major disadvantage of the inverse modeling procedure is that it is unusually difficult and may require a level of effort that is beyond the usual regulatory activity. The method also does not provide an assessment of the range of uncertainty in the derived emission inventory.

This method should also be compared with less formal methods for evaluating emission inventories, discussed above (Section 2.3.5).

### **2.3.7. Empirical ozone isopleths**

**Overview:** The concept of empirical ozone isopleths involves simultaneous measurement of  $\text{O}_3$ , VOC and either  $\text{NO}_x$  or  $\text{NO}_y$  over an extended time period. The array of measurements is then used to generate ozone isopleths as a function of measured  $\text{NO}_x$  and VOC. The shape of the isopleth curve should show how  $\text{O}_3$  varies in

response to changes in  $\text{NO}_x$  and VOC concentrations. The change in  $\text{O}_3$  in response to changed emissions might be inferred from this pattern.

Chameides et al. (1992) originated approach by comparing measured values of  $\text{O}_3$ ,  $\text{NO}_x$  and summed propene-equivalent carbon at various urban and rural sites in the U.S. These were used to derive general insights about the nature of ozone in urban areas. Thielmann et al. (2001b) applied the method to a single urban area (Milan, Italy).

In a loosely related study, Buhr et al. (1995) used statistical cluster analysis on measurements to identify periods with high VOC and with high  $\text{NO}_x$  and to identify  $\text{O}_3$  associated with high VOC and  $\text{NO}_x$ , as a way of evaluating the sensitivity of  $\text{O}_3$  to  $\text{NO}_x$  and VOC.

**Theoretical basis:** There is no formal rationale for the method. In effect, it assumes that day-to-day and hour-to-hour variations in the observed pattern of  $\text{O}_3$ , VOC and  $\text{NO}_x$ , and variations from place to place, can also be used to make inferences about the relation between  $\text{O}_3$  and precursor emissions.

**Method of justification:** No analytical justification is offered. The correlations between measured  $\text{O}_3$ , VOC and  $\text{NO}_x$  are offered as independent evidence.

**Range of applications:** Chameides et al. (1992) used the method to compare measurements at rural sites in the U.S. with urban measurements in Los Angeles. Buhr et al. (1995) used the measurement to analyze conditions for a rural site in Alabama. Thielmann et al. (2001b) presented the most extensive data and used it to evaluate the urban plume in Milan, Italy.

**Contrary evidence:** None.

**Is it universal?** The method only yields clear results if applied to a region with large variations in  $\text{NO}_x$  and VOC. Frequently in urban areas  $\text{NO}_x$  and VOC are correlated and vary simultaneously with each other. In this case, no signal for how  $\text{O}_3$  varies with  $\text{NO}_x$  as opposed to VOC can be detected.

**Other sources of error:** It is not always clear whether the directly observed variations of  $\text{O}_3$  with  $\text{NO}_x$  and VOC can be used to infer causal relations between  $\text{O}_3$  and precursors, or whether these are coincidental relationships that have other causes.  $\text{O}_3$ ,  $\text{NO}_x$  and VOC both show diurnal variations that are independent of the ozone-precursor relationship. Biogenic VOC shows a diurnal variation that differs from anthropogenic VOC and  $\text{NO}_x$ , and biogenic VOC varies with temperature.  $\text{O}_3$  in relation to biogenic VOC may reflect these coincidental variations rather than causal factors. In general,  $\text{O}_3$  is formed in urban plumes as air moves downwind and  $\text{NO}_x$  is

photochemically removed. This process may result in an anticorrelation between  $O_3$  and  $NO_x$ , which also does not imply causality. Reactivity-weighted VOC varies in response to local emissions (especially for biogenic VOC), and this variation may be only coincidentally related to  $O_3$ .

**Ease of use:** The method requires an extensive data set of  $O_3$ ,  $NO_x$  and VOC. The required statistical analysis may be comparable to the demands of an Eulerian AQM.

**Availability and accuracy of measurements:** The method requires a complete set of measured primary VOC and  $NO_x$ . These are currently available from the PAMs network.

**Can the method be evaluated or modified in individual applications?** Each application represents an individual effort to obtain information from measurements.

**Synthesis with Eulerian models:** There is no obvious synthesis.

**Overall evaluation:** This method is speculative and not suited to regulatory application at present. Chameides et al., Buhr et al. and Thielmann et al. were all able to obtain significant results, but these often were related to specific circumstances of their studies. The study by Buhr et al. in particular was successful because it covered an area that was impacted by two distinctly different emission sources, one with high VOC and the other with high  $NO_x$ . This type of separation of VOC and  $NO_x$  emission sources is not common. This should be regarded as a research tool rather than a tool for general application.

### 2.3.8. Other methods

A brief summary of other methods is presented here.

**Photochemical steady state calculations:** These calculations are used to infer the instantaneous rate of ozone production, based on measured  $O_3$ , NO,  $NO_2$  and the measured photolysis rate of  $NO_2$ . The rate of ozone production is calculated as the difference between the rates of photolysis of  $NO_2$  and reaction of  $O_3$  with NO. This calculation is commonly used to identify the rate of ozone production in rural areas (R e.g. Ridley et al.). It is unlikely to have direct use for evaluating ozone-precursor relationships. The constrained steady state model described above represents an adaptation of this method to investigate ozone-precursor relationships.

**Ozone production efficiency (OPE):** OPE represents the rate of production of ozone per  $NO_x$ , and is usually expressed as the ratio of ozone production to loss of  $NO_x$ . This parameter is used widely to estimate the amount of ozone produced photochemically in the global troposphere (Liu et al., 1987 Lin et al., 1988). It is often inferred

from the measured correlation between  $O_3$  and  $NO_y$ - $NO_x$  (also known as  $NO_2$ ) (Trainer et al., 1993). Ozone production efficiency has also been inferred from correlations between  $O_3$  and CO (e.g. Chin et al., 1994). It has been especially useful as a basis for evaluating the impact of emissions from large power plants (Gillani et al., 1996; Ryerson et al., 1998, 2001). Analyses of ozone production efficiency are likely to be useful to regulators as a basis for evaluating the relative impact of urban emissions and power plant emissions.

***Separating anthropogenic and biogenic VOC - PPN/MPAN:*** Roberts et al. (1998) used statistical regression between three organic nitrates (PAN, PPN and MPAN) in order to separate the influence of biogenic and anthropogenic VOC on ozone formation. These products include species created photochemically only from anthropogenic emissions (PPN) and only from biogenic emissions (MPAN). This is unlikely to be useful in regulatory studies, but may be important in identifying the relative impact of anthropogenic and biogenic species.

#### **2.4 SUPPLEMENTAL TOPIC: RECEPTOR MODELING**

Receptor modeling (Henry et al., 1984, 1992; Hopke, 1985; Kim and Henry, 2000; Watson et al., 2000) refers to a series of techniques that are used to evaluate the relative contribution of various emission sources to ambient concentrations at a given site (a “receptor”). Most of these techniques are based on interpretations of ambient measurements, and are can therefore be regarded as observation-based methods.

Receptor modeling is most commonly used to identify sources of ambient aerosols (e.g. Kim and Henry, 2000) and VOC (e.g. Watson et al. 2000) based on measurements that identify a large number of chemical components (e.g. aerosol chemical composition or concentrations of individual VOC). Typically, this analysis identifies the contribution of emission source categories (e.g. gasoline exhaust, coal-fired industry) that generate emissions with a distinct chemical signature. The ambient measurements are analyzed based on their chemical composition to identify the relative contribution of these source types. In the most common receptor-based method, chemical mass balance, it is assumed that emission profiles from each of the various source types is known. The relative contribution of each source type to ambient conditions at the receptor is calculated based on apportionment of the measured receptor profile to the known source profiles, usually based on least-squares fits. Other receptor-based methods use multivariate statistics (principal component analysis, factor analysis, or multivariate regression) to identify the chemical signature of source types that contribute to ambient concentrations, based solely on measured concentrations.

A separate approach, also referred to as a receptor-based method, seeks to identify geographic source regions that contribute to measured ambient concentrations (e.g. Cheng et al., 1993). Typically these methods are based on a known geographical distribution of emission sources and use back-trajectory calculations to identify the relative contribution of each source to ambient conditions.

Receptor modeling has been widely used in environmental analyses, and EPA has developed protocols for the application of various methods (e.g. see summary in Watson et al., 2001). Receptor models are generally dependent on certain assumptions and have specific limitations on their use. It is assumed that the composition of source emissions are constant with time, that all sources that contribute to ambient concentrations at the receptor are identified, and that the sources are sufficiently different in terms of their chemical signatures so that source contributions may be easily distinguished in the receptor measurement. When source profiles are similar (collinear), then large uncertainties appear in the source apportionment. It is usually necessary neglect photochemical removal of the measured species or aerosol composition and assume that the measured species are nonreactive, although some methods have been proposed that allow the use of receptor modeling techniques for reactive hydrocarbons (Lin and Milford, 1994). The attempt by Lin and Milford (1994) to account for photochemical aging while using receptor techniques to analyze VOC might be compared to the methods for interpreting measurements of photochemically aged VOC discussed in Sections 2.3.5 and 3.3.7.

Receptor modeling is of limited use for analyzing sources of ambient ozone because receptor techniques generally cannot account for the complex chemistry of ozone formation. The major use of receptor modeling in association with ozone is to identify the emission sources of ambient VOC. However, this source apportionment cannot account for the relative impact of VOC sources on ozone formation, because it does not account for the different impact of individual VOC species. Assessment of the role of individual VOC in the ozone formation process is generally done by the method of incremental reactivity (e.g. Carter et al., 1994, 1995) rather than by receptor methods. Receptor methods have also been used to identify emission sources of ambient  $\text{NO}_x$  and  $\text{NO}_y$  (Stehr et al., 2000). This type of analysis is potentially most useful in studies of regional transport of ozone, where it might be used to identify the relative impact of coal-fired power plants as opposed to other  $\text{NO}_x$  emission sources.

Receptor modeling cannot be used to evaluate the relative impact of  $\text{NO}_x$  and VOC on ozone formation. Most receptor modeling approaches (including carbon mass balance and trajectory analysis) require that each source is

associated with a distinct, measurable chemical signature at the receptor cite. No such signature exists for identifying NO<sub>x</sub>-sensitive versus VOC-sensitive conditions for ozone. The central challenge for OBM's associated with ozone formation is to identify such a signature. More generally, all receptor modeling techniques are based on the assumption of a clear causal link between emission patterns at the source and observed patterns at the receptor, and cannot represent complex chemical interactions. It is unlikely that receptor modeling could identify observed patterns that could be linked to NO<sub>x</sub>-sensitive versus VOC-sensitive conditions.

Buhr et al. (1992) did succeed in deriving information about NO<sub>x</sub>-VOC sensitivity at a site in Alabama using principal component analysis (PCA), but this was an exceptional case. The Alabama site was affected by plumes from two different emission sources: a coal-fired power plant with high NO<sub>x</sub> emissions and little VOC, and a paper mill with relatively high anthropogenic VOC and little NO<sub>x</sub>. The statistical analysis was thus able to distinguish conditions associated with high VOC from conditions associated with high NO<sub>x</sub>. At most locations there would be no such signal to distinguish the impact of NO<sub>x</sub> from that of VOC.

Some of the techniques of receptor modeling (especially the multivariate statistical techniques) can be used to evaluate long term trends in the concentration of ozone and precursor species (see next section).

## **2.5 SUPPLEMENTAL TOPIC: EVALUATING LONG-TERM TRENDS FOR OZONE AND RELATED AIR POLLUTANTS**

Determining the changes in ambient concentrations of ozone and its precursors over time represents one of the major tasks associated with environmental control. Evaluation of long term trends is necessary to evaluate whether past attempts to control ozone have been successful and to identify reasons for the success or failure of those efforts. Thus, evaluation of trends for ozone and its precursors can be viewed as a way to provide accountability to the current structure of control strategies. Evaluation of long term trends is also important in order to identify trends that may cause harm in the future. This is especially important because recent evidence suggests that background ozone in the U.S. and western Europe may be increasing as a result of a general increase in emissions worldwide (Lefohn et al., 1998; Jacob et al., 1999; Yienger et al., 2000; Collins et al., 2000; Wild and Akimoto, 2001; Li et al., 2001; Fiore et al., 2002).

Evaluation of trends for ozone poses methodological problems because ozone shows a complex and nonlinear dependence on meteorology. As with most pollutants, ambient ozone is dependent on rates of dispersion and on

regional and continental-scale transport patterns. However ozone is also dependent on temperature and on sunlight. Year-to-year variation in ambient ozone is often due primarily to changes in the frequency of occurrence of meteorological conditions conducive to ozone formation, especially in the eastern U.S. Evaluation of trends for ozone must filter out these meteorological influences. In addition, policy analysts are usually interested in the most extreme events. Trends associated with these extreme events are difficult to evaluate in a statistically robust manner.

The relation between ozone and various meteorological parameters has been analyzed using multivariate linear regression (Clark and Karl, 1992), although this type of analysis is difficult due to the nonlinear nature of the relation between ozone and meteorological variables such as temperature. Multivariate linear regression has also been used to evaluate long-term trends in ozone while at the same time filtering out the effect of year-to-year changes in temperature (Fiore et al., 1998; Kubler et al., 2001). Regression approaches are especially useful because they can be used to distinguish statistically significant trends from random variations, although they are again limited by the required assumption of nonlinearity. Long-term trends have also been evaluated for  $\text{NO}_x$  (Fenger, 1999, Butler et al., 2001, Bowen et al., 2001) and  $\text{SO}_2$  (Fenger, 1999).

One potential gap in the analysis of ozone trends is the inability to establish a link between the observed trends in ozone and trends in precursor emissions. Trends in precursor ambient concentrations have been difficult to determine because until relatively recently, there were no routine measurement of ozone precursors (NARSTO, 2000). The EPA PAMS network is intended to remedy this.

A network of ambient  $\text{NO}_y$  may be especially useful as a basis for monitoring the impact on ozone of proposed reductions in  $\text{NO}_x$  emissions (especially from power plants) at the regional scale. Because  $\text{NO}_x$  is relatively short-lived,  $\text{NO}_y$  provides a stronger basis for monitoring the impact of reduced emissions on ambient concentrations. A strong correlation between  $\text{O}_3$  and  $\text{NO}_y$  is observed in rural areas (e.g. Trainer et al., 1993) and this correlation can be used to monitor the impact of emissions reductions on regional transport of  $\text{O}_3$ . The correlation between  $\text{O}_3$  and  $\text{NO}_y$  can also be used to determine levels of background  $\text{O}_3$  in the U.S. (e.g. Trainer et al., 1993) and identify possible changes due to increasing emissions outside the U.S. A joint evaluation of ambient ozone and  $\text{NO}_x$  is a central feature of one of the proposed OBM's for evaluating  $\text{O}_3$ - $\text{NO}_x$ -VOC sensitivity (see Sections 2.3.1 and 3.1.6).

Establishment of a network of measured  $\text{NO}_y$  and expansion of this approach may be very useful in evaluating ozone trends and establishing possible causes for these trends.

Measured VOC, which would be used to establish trends in VOC emissions, are also used by OBM's to evaluate  $\text{NO}_x$ -VOC sensitivity (see Sections 2.3.3, 2.3.4, 2.3.5, 2.3.6 and 3.3). OBM's that are based on evaluation of emission rates for VOC (Sections 2.3.5, 2.3.6 and 3.3.7) are also closely related to efforts to establish trends in emission of VOC based on ambient measurements. Development of measurement networks associated with these OBMs and application of the OBM's should therefore contribute to efforts to establish trends for ozone and precursors, and evaluate the effectiveness of past ozone control strategies.

## 2.6 CONCLUSIONS

Of the various OBMs for use in evaluating  $\text{O}_3$ - $\text{NO}_x$ -VOC sensitivity, three stand out as being the most widely used:  $\text{NO}_x$ -VOC indicators, smog production algorithms and constrained steady state models based on observed  $\text{NO}_x$  and VOC. Each of these methods have been developed and applied for several locations. In addition, there is a close resemblance between the constrained steady state model developed by Kleinman et al. (1997) and the observation-based model developed by Cardelino and Chameides. These similar methods might effectively be combined, and results from one can be interpreted as evidence in support of the other. Each of these methods is potentially useful for regulatory studies.

Assuming that measurements are readily available, analysis based on these methods could be combined with the standard AQM-based analysis with minimal effort. One potential use of either method is to investigate how  $\text{O}_3$ - $\text{NO}_x$ -VOC sensitivity varies among different events. If measurements are available, evaluation of day-to-day variation is easier using the OBMs than using Eulerian AQMs.

In addition to direct use of OBMs, it is useful to consider methods for evaluating and updating emission inventories based on measured  $\text{NO}_x$  and VOC. These methods include both direct analysis of ambient measurements (including evaluation of measurement data accuracy) and formal inverse modeling to update emission fields in an AQM. Direct analysis of measured  $\text{NO}_x$  and VOC is especially useful in combination with the constrained steady state approach because it includes methods for evaluating the accuracy of measured VOC and identifying either erroneous measurements or situations in which the CSS approach would not be valid.

A synthesis of OBMs with Eulerian AQM's is only possible if alternative AQM scenarios with updated emissions are included. Inverse modeling and other methods to evaluate the accuracy of emission inventories may need to be considered in this context.

The subsequent section contains in-depth analysis of the three most widely used methods: NO<sub>x</sub>-VOC indicators, smog production algorithms, and constrained steady state. The constrained steady state approach will be discussed in combination with direct analysis of measured NO<sub>x</sub> and VOC, which can significantly improve the constrained steady state method. The analysis of each methods will include (i) the OBM itself; (ii) methods to evaluate the accuracy of measurements and identify conditions in which the OBM is inappropriate; and (iii) approaches that combine the OBM with results from standard air quality models.

### **SECTION 3. THEORETICAL EVALUATION**

In this section, a detailed evaluation will be presented of three observation-based methods: (1) secondary species as  $\text{NO}_x$ -VOC indicators (based on Sillman, 1995 and subsequent analyses); (2) smog production/extent of reaction parameters (based on Blanchard et al., 1999, and preceding and subsequent analyses); and (3) constrained steady-state calculations driven by observed  $\text{NO}_x$  and VOC (Kleinman et al., 1997, and subsequent analyses) in combination with the observation-based model developed by Cardelino and Chameides (1995, 2000). The constrained steady state method includes related material developed by Tonnesen and Dennis (2000a) and Kirchner et al. (2001). In addition, proposed methods to derive information about emissions from measured  $\text{NO}_x$  and VOC (direct interpretation of measurements and inverse modeling to match emissions and measurements in AQMs) will be included in Section 3.3.

#### **3.1 $\text{NO}_x$ - VOC INDICATORS**

##### **3.1.1. Summary information**

- *NO<sub>x</sub>-VOC indicators* refers to a series of species ratios, usually involving reactive nitrogen and peroxides, that were initially proposed by Sillman (1995) as indicators for  $\text{NO}_x$ -sensitive versus VOC-sensitive ambient conditions.
- The  $\text{NO}_x$ -VOC indicators were developed based on 3-d photochemical models. The identified indicator ratios show different values when models predict  $\text{NO}_x$ -sensitive versus VOC-sensitive conditions.
- The proposed indicator ratios are:  $\text{O}_3/\text{NO}_y$  (where  $\text{NO}_y$  represents total reactive nitrogen);  $\text{O}_3/\text{NO}_z$  (where  $\text{NO}_z$  represents the sum of  $\text{NO}_x$  reaction products, or  $\text{NO}_y$ - $\text{NO}_x$ );  $\text{O}_3/(\text{HNO}_3+\text{NO}_3^-)$ ;  $\text{H}_2\text{O}_2/\text{HNO}_3$ , and several other ratios involving peroxides. High values of these ratios (above a certain transition value) represent  $\text{NO}_x$ -sensitive conditions, and low values represent VOC-sensitive conditions.
- Ratios involving peroxides show a stronger and more certain connection to  $\text{NO}_x$ -VOC sensitivity, but measured peroxides are rarely available in a regulatory context. Measured  $\text{O}_3$ ,  $\text{NO}_x$  and  $\text{NO}_y$  (and, to a lesser extent,  $\text{HNO}_3$ ) are more likely to be widely available for regulatory use.
- The theoretical basis derives from the view that the amount of ozone produced per  $\text{NO}_x$  removed (ozone production efficiency) is higher for  $\text{NO}_x$ -sensitive conditions than for VOC-sensitive conditions.

- Indicator ratios have been tested in a series of 3-d photochemical models for individual events, including models with changed anthropogenic and biogenic emissions. Generally consistent results have been found in models for the northeastern U.S., Lake Michigan, Atlanta, Nashville, Los Angeles, Milan, and Paris. These tests included scenarios with UAM-IV, RADM, the model developed by Sillman, and two European models and included CB-IV, RADM, and modified Lurmann et al. (1986) chemical mechanisms.
- Contradictory results from 3-d models were reported by Lu and Chang (1998) for the San Joaquin valley and by Chock et al. (1999) for Los Angeles. In the case of Lu and Chang, the contradictory results are apparently related to the impact of model boundary conditions and are correctable. Improved results are obtained if the original indicator ratios are modified to account for background (rural) values immediately upwind of an urban area.
- A broadly useful approach is to examine the predicted correlations between species ( $O_3$  versus  $NO_y$ , etc.) rather than just the indicator ratios. Models predict a different range of values for  $O_3$  versus  $NO_y$  in VOC-sensitive conditions as opposed to  $NO_x$ -sensitive conditions. These ranges of values can be used to interpret measured data sets. This approach is advantageous because errors that would invalidate the use of indicator ratios often are readily apparent in comparisons between predicted and observed correlations.
- Measured correlations between indicator species have been consistent with predictions from 3-d models, and suggest that measured values of these species are different for  $NO_x$ -sensitive versus VOC-sensitive conditions. However, evaluations of measured data sets do not demonstrate that indicator ratios are universally valid, and cannot prove whether the  $NO_x$ -VOC transition values assigned to indicator ratios are correct.
- Indicator ratios involving  $NO_y$  and  $NO_z$  are only valid if they are based on accurate, unbiased ambient measurements of  $NO_y$ . In some cases, measured  $NO_y$  may not include ambient  $HNO_3$ . Measurements that do not include  $HNO_3$  in the  $NO_y$  sum cannot be used as  $NO_x$ -VOC indicators.
- Indicator ratios based on  $O_3/NO_y$  appear to be somewhat more reliable than  $O_3/NO_z$ , because they include the impact of photochemical aging (represented by  $NO_x/NO_y$ ) as well as the relative rates of production of ozone and  $NO_x$  reaction products. Both of these factors affect  $NO_x$ -VOC sensitivity. However,  $O_3/NO_z$  or  $O_3/HNO_3$  also have advantages in that they generate a stronger correlation pattern (which can be tested against measurements) and because measurements of these ratios are unaffected by on-site emissions.

- Indicator ratios are only valid in measurements made during the afternoon hours (as opposed to morning or nighttime), and indicator ratios are not valid during precipitation events.
- The rate of dry deposition of  $\text{HNO}_3$  and possible conversion to  $\text{NO}_3^-$  also represent uncertainties for indicator ratios.

### **3.1.2. Conclusions and recommendations**

- There is strong evidence that indicator ratios and related species correlations are linked to  $\text{NO}_x$ -VOC sensitivity in general. However, there is no strong evidence that ratio values identified as representing the transition from VOC- to  $\text{NO}_x$ -sensitive chemistry are exactly right, or that these transition values do not vary with different conditions.
- In using indicators, it is preferable to use the predicted correlation patterns for  $\text{O}_3$  versus  $\text{NO}_y$ ,  $\text{O}_3$  versus  $\text{NO}_z$ , etc., rather than the simple indicator ratios. Correlations (as opposed to ratios) are useful because they provide an evaluation of the measured data rather than a simple rule of thumb for  $\text{NO}_x$ - versus VOC-sensitive conditions. Evaluation of measured species correlations can also identify situations in which the indicator ratios are not valid.
- Indicators are potentially useful for providing a general overview of  $\text{NO}_x$ -VOC trends in a data set. They can identify likely variations in  $\text{NO}_x$ -VOC sensitivity from day to day and between different locations. These should be interpreted as suggestions, rather than as proofs.
- The strongest and most certain use of indicator correlations is to provide part of a model-measurement evaluation. Because indicator species are usually correlated with  $\text{NO}_x$ -VOC sensitivity in models, models should be required to demonstrate satisfactory performance in comparison with measured values of these species. Such a demonstration could potentially be included in the regulatory process.
- If indicator ratios are to be used in the regulatory process, critical attention must be given to the accuracy of measurements.

### **3.1.3. Results from 3-d models**

#### ***3.1.3c. The original indicator ratios***

The original indicator ratios ( $O_3/NO_y$ ,  $O_3/NO_z$ ,  $O_3/HNO_3$ ,  $H_2O_2/HNO_3$  and other peroxide ratios) were justified based on results of 3-d photochemical models for ozone, as illustrated in Figure 3.1.1. The figure is based on results from an initial model scenario, an equivalent scenarios with a 35% reduction in anthropogenic VOC emissions, and equivalent runs with a 35% reduction in anthropogenic  $NO_x$  emissions. Different cases used reductions of 25% or 50% rather than 35%, but always the same percent reduction for  $NO_x$  and VOC. The figure then shows three values: the size of the ozone reduction predicted from reduced VOC at each model location for a specified time of day; the size of the ozone reduction predicted from reduced  $NO_x$  (where negative values would represent a predicted increase in  $O_3$ ); and the value of the indicator ratio in the initial model scenario at the same time and location. Figure 3.1.1 includes results from four separate scenarios, representing four different locations and including two different photochemical mechanisms (see Table 3.1.1 for a complete description).

Typically, models show some locations with a strongly  $NO_x$ -sensitive response to emission reductions and other locations with a strongly VOC-sensitive response. In the cases shown in Figure 3.1.1, the  $NO_x$ -sensitive responses are primarily associated with high values of the indicator ratio  $O_3/NO_y$ , and VOC-sensitive responses are primarily associated with low values. There is also a clearly identifiable value associated with mixed  $NO_x$ -VOC sensitivity and the transition from  $NO_x$ -sensitive to VOC-sensitive values.

Results have been published from a series of models for different locations and with different photochemical mechanisms (see Table 3.1). Except as noted in Section 3.1.5 below, these models gave consistent results.  $NO_x$ -sensitive conditions were associated with high values of the proposed indicator ratios, VOC sensitive conditions were associated with low values, and the transition from  $NO_x$ -sensitive to VOC-sensitive conditions occurred at close to the same value. Transition values reported by Sillman et al. (1998) are:  $O_3/NO_y=6-8$ ;  $O_3/NO_z=8-10$ ; and  $O_3/NO_3=10-16$ .

Based on the consistency of results among many models, it was suggested that: (i) measured values of indicator ratios that were associated with  $NO_x$ -sensitive or VOC-sensitive conditions in the models could be taken as evidence that ambient conditions were  $NO_x$ -sensitive or VOC-sensitive, respectively; and (ii) a comparison between model and measured values for indicator ratios should be an essential part of model evaluation.

The proposed indicator ratios were interpreted to apply only to the exact time and place of the measurements, and would not preclude a different  $NO_x$ -VOC response at a different time of day or at a different location. The proposed

ratios also only applied during the afternoon hours. At nighttime the indicator ratios were heavily influenced by dry deposition within the nocturnal boundary layer. During morning and noon, indicator ratios showed a different  $\text{NO}_x$ -VOC transition than during the afternoon.

In order to facilitate comparisons between models, a numerical summary was developed that would identify the essential features of the correlation in Figure 3.1.1. The summary form allowed a comparison between model results based on brief summary data. This is described in the Appendix, along with more complete model results.

Based on the availability of measurements, the subsequent discussion will focus on the ratios  $\text{O}_3/\text{NO}_y$ ,  $\text{O}_3/\text{NO}_z$ , and to a lesser extent,  $\text{O}_3/\text{NO}_3$ . Results based on peroxides generally show a stronger and more consistent correlation with  $\text{NO}_x$ -VOC sensitivity in models, and measured peroxides also allow a test for consistency (see Section 3.1.7). However, measured peroxides are unlikely to be available for regulatory use. Inclusion of  $\text{HNO}_3$  in measurement networks has been proposed (McClenny et al., 2000) but intercomparisons of  $\text{HNO}_3$  measurements have shown significant discrepancies between individual instruments (Parrish et al., 2000). Errors are also possible with measured  $\text{NO}_y$  (see further discussion in Section 3.1.9), but measurement intercomparisons have shown good agreement between different instruments and inclusion of  $\text{NO}_y$  in measurement networks has been recommended.

**Table 3.1.1****3-d simulations used in this study**

Asterisks (\*) denote models included in Figure 3.1.1, 3.1.2, etc.. A pound sign (#) identifies models that generated contrary results, which are discussed in Section 3.1.5.

Location	Model	Photochemistry	Model Domain	Comparison w/ measurements	Reference
Nashville*	Sillman et al., 1998	modified Lurmann et al., 1986	5x5 km urban; upwind domains incl eastern U.S	O <sub>3</sub> , NO <sub>y</sub> , peroxides	Sillman et al., 1998
Lake Michigan*	Sillman et al., 1993	modified Lurmann et al., 1986	20x20 km in region; upwind domains includes eastern U.S	O <sub>3</sub>	Sillman, 1995
Northeast corridor*	Sillman et al., 1993	modified Lurmann et al.,	20x20 km in region; upwind domains includes eastern U.S	O <sub>3</sub>	Sillman, 1995
Atlanta	UAM-IV, Morris and Myers, 1990	CB4 (Gery et al., 1989)	5x5 km urban	O <sub>3</sub> , NO <sub>y</sub> , isoprene, HCHO, other VOC	Sillman et al., 1997
San Joaquin* (Sillman)	MAQSIP (Odman and Ingram, 1996)	CB4 (Gery et al., 1989)	12x12 km; domain includes all central California	O <sub>3</sub>	Sillman et al., 2001
San Joaquin# (Lu and Chang)	SAQM, Chang et al., 1997	CB4 (Gery et al., 1989)	12x12 km; domain includes all central California	O <sub>3</sub>	Lu and Chang, 1998
Los Angeles* (Godowitch)	UAM-IV, Morris and Myers, 1990	CB4 (Gery et al., 1989)	5x5 km urban	O <sub>3</sub> , NO <sub>y</sub> , NO <sub>z</sub>	Godowitch et al. 1994; Sillman et al., 1997
Los Angeles# (Chock)	UAM-IV, Morris and Myers, 1990	CB4 (Gery et al., 1989)	5x5 km urban	O <sub>3</sub>	Chock et al., 1999

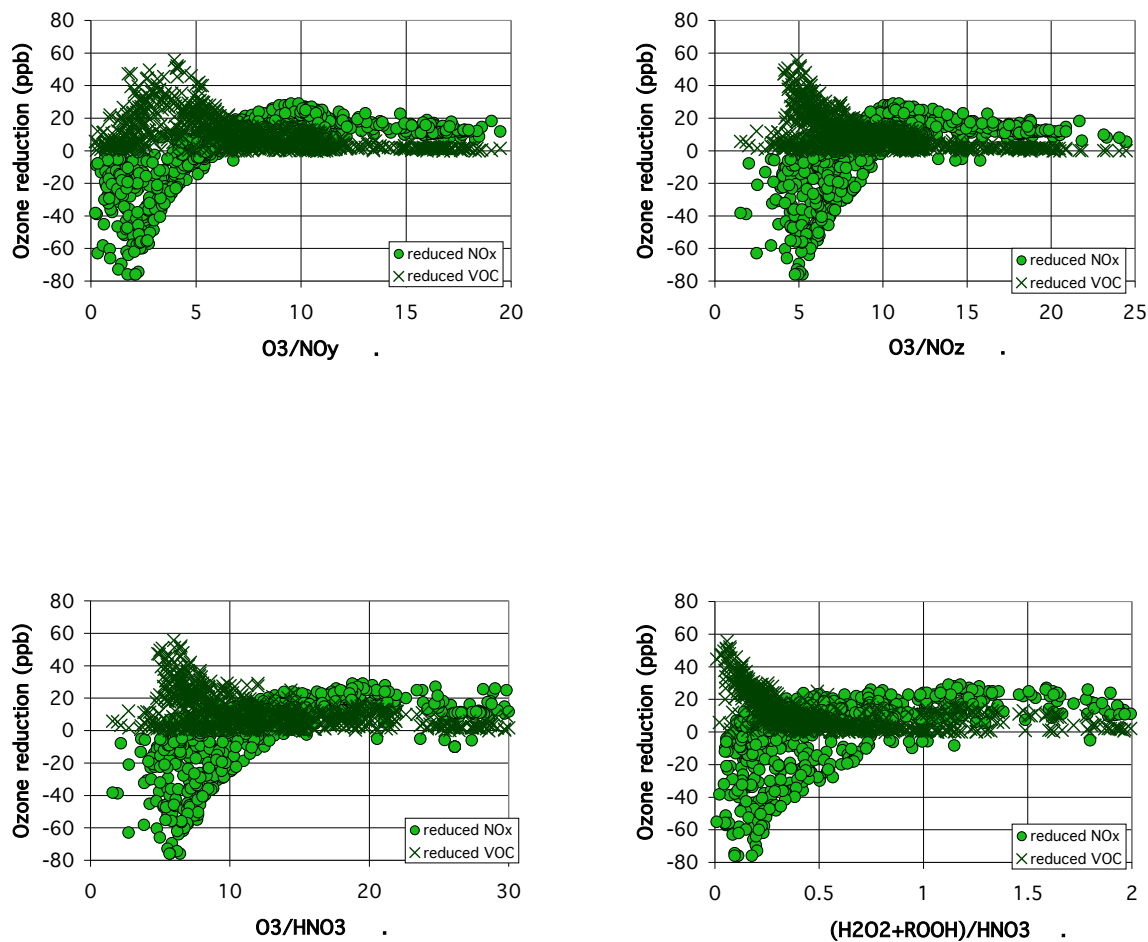


**Figure 3.1.1.** Predicted reductions in ozone in response to a percent reduction in emissions of anthropogenic VOC (crosses), and predicted reductions in response to the same percent reduction in emissions of anthropogenic  $NO_x$  (green circles), plotted versus model values for proposed indicator ratios:  $O_3/NO_y$ ,  $O_3/NO_z$ ,  $O_3/HNO_3$ , and  $(H_2O_2+ROOH)/HNO_3$ . Results are shown for four separate model scenarios (Lake Michigan, northeast, Nashville, and Los Angeles-Godowitch version, from Table 3.1.1). Percent reductions are either 25% or 35% in individual scenarios.

### **3.1.3b. Modification based on background values**

The original indicator ratios were developed based on regional-scale models with boundary conditions that were representative of the clean troposphere (40 ppb O<sub>3</sub>, NO<sub>y</sub> less than 1 ppb). This analysis did account for situations in which elevated O<sub>3</sub> (and, to a lesser extent elevated reactive nitrogen) was transported into an urban region from upwind. Contrary evidence emerged (see Section 3.1.5) in two cases where indicator ratios were tested in models that included different boundary conditions.

The impact of upwind transport into a city or region can be accounted by modifying the form of the original indicator ratios to subtract the background conditions. The modified ratios would be:  $(O_3 - O_{3b}) / (NO_y - NO_{yb})$ ,  $(O_3 - O_{3b}) / (NO_z - NO_{zb})$  and  $(O_3 - O_{3b}) / (HNO_3 - HNO_{3b})$ , where O<sub>3b</sub>, NO<sub>yb</sub>, NO<sub>zb</sub> and HNO<sub>3b</sub> represent background values. Tonnesen and Dennis (2000b) used the ratio (O<sub>3</sub>-40)/HNO<sub>3</sub>, which is equivalent to these modified ratios for their model (with background O<sub>3</sub> equal to 40 ppb and zero background HNO<sub>3</sub>). The equivalent cannot be done for ratios involving peroxides. Indicators of these form have some similarity to the smog production (extent of reaction) parameters (see Section 3.2). This form is also more consistent with results obtained from 0-d calculations of ozone isopleths (see Section 3.1.4).

As shown in Figure 3.1.2, models give generally consistent results for the modified ratios. The transition values are obviously different from the transition values for the original indicator ratios. Transition values reported by Sillman and He (2002) are:  $(O_3 - O_{3b}) / (NO_y - NO_{yb}) = 4-6$ ;  $(O_3 - O_{3b}) / (NO_z - NO_{zb}) = 5-7$ ; and  $(O_3 - O_{3b}) / (HNO_3 - HNO_{3b}) = 8-10$ . More complete results and identification of the transition values is discussed in the Appendix. Results from the model for San Joaquin from Lu and Chang (1998) is broadly consistent with this transition value.

A critical uncertainty for indicator ratios with this form is the need to define background concentrations. This is discussed below in Section 3.1.11 (supplemental topic).

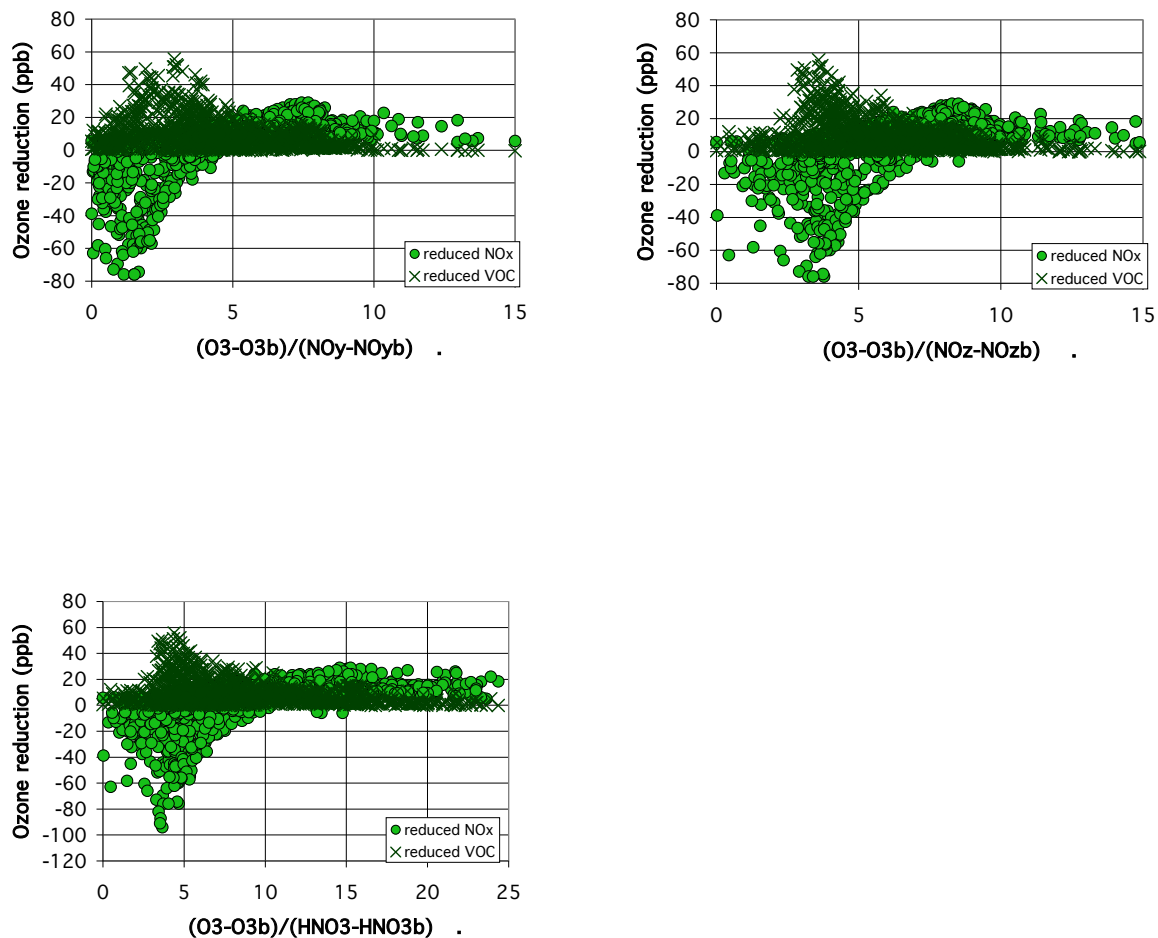


**Figure 3.1.2.** Predicted reductions in ozone in response to a percent reduction in emissions of anthropogenic VOC (crosses), and predicted reductions in response to the same percent reduction in emissions of anthropogenic  $NO_x$  (green circles), plotted versus model values for proposed indicator ratios:  $(O_3-O_{3b})/(NO_y-NO_{yb})$ ,  $(O_3-O_{3b})/(NO_z-NO_{zb})$ , and  $(O_3-O_{3b})/(HNO_3-HNO_{3b})$ . Results are shown for five separate model scenarios (see Table 3.1.1). Percent reductions are either 25% or 35% in individual scenarios.

### 3.1.4. Results from 0-d calculations and isopleth plots

Tonnesen and Dennis (2000b), Kirchner et al. (2001) and Sillman and He (2002) used 0-d calculations (box models) to generate standard ozone isopleths versus  $\text{NO}_x$  and VOC emissions. These isopleths illustrate the pattern of behavior of  $\text{O}_3$  as a function of  $\text{NO}_x$  and VOC, including the split into  $\text{NO}_x$ -sensitive and VOC-sensitive regimes (see Section 1.4). These isopleth diagrams can be used to identify the range of validity of  $\text{NO}_x$ -VOC indicators.

Figure 3.1.3 shows comparisons between ozone isopleths and isopleths for various indicator ratios:  $\text{O}_3/\text{NO}_z$ ,  $(\text{O}_3-\text{O}_{3b})/(\text{NO}_z-\text{NO}_{zb})$  and  $(\text{O}_3-\text{O}_{3b})/(\text{HNO}_3-\text{HNO}_{3b})$ , and summed peroxides/ $\text{HNO}_3$ . As shown in the figure, the ratio peroxides/ $\text{NO}_z$  shows an excellent correlation with the  $\text{NO}_x$ -VOC sensitivity transition. The isopleth for peroxide/ $\text{NO}_z$  equal to 0.4 directly parallels the  $\text{NO}_x$ -VOC transition line, and higher and lower values are associated with  $\text{NO}_x$ -sensitive and VOC-sensitive conditions respectively. The results for  $\text{O}_3/\text{HNO}_3$  and  $\text{O}_3/\text{NO}_z$  are worse. High values of these ratios are generally associated with  $\text{NO}_x$ -sensitive conditions and low values with VOC-sensitive conditions, but the ratio isopleths are not parallel to the  $\text{NO}_x$ -VOC transition line. A much better correlation is obtained when background  $\text{O}_3$  is subtracted from the ratios. Isopleths for  $(\text{O}_3-\text{O}_{3b})/(\text{NO}_z-\text{NO}_{zb})$  and  $(\text{O}_3-\text{O}_{3b})/(\text{HNO}_3-\text{HNO}_{3b})$  are correlated closely with the  $\text{NO}_x$ -VOC transition line. Significantly, the ratio  $(\text{O}_3-\text{O}_{3b})/(\text{NO}_z-\text{NO}_{zb})$  is correlated with  $\text{NO}_x$ -VOC sensitivity only for ozone below 200 ppb. When ozone is greater than 200 ppb the correlation becomes much worse, possibly because organic nitrates become a dominant component of  $\text{NO}_z$  rather than  $\text{HNO}_3$ .

The above results are from calculations for 3-day time periods by Sillman et al. (2002), using a modified form of the mechanism of Lurmann et al. (1986) with updated rate constants. Analogous results for a less extensive range of conditions were published by Tonnesen and Dennis (2000b). Although the calculations by Tonnesen and Dennis were for a shorter time period (9 hours) and used a different photochemical mechanism (RADM, Stockwell et al., 1990), the results for  $\text{O}_3/\text{HNO}_3$  and  $\text{O}_3/\text{NO}_z$  along the  $\text{NO}_x$ -VOC sensitivity transition were similar (see Figure 3.1.4.)

The reason for the close correlation between these ratios and  $\text{NO}_x$ -VOC sensitivity is discussed in terms of chemistry in Section 3.1.12 below.

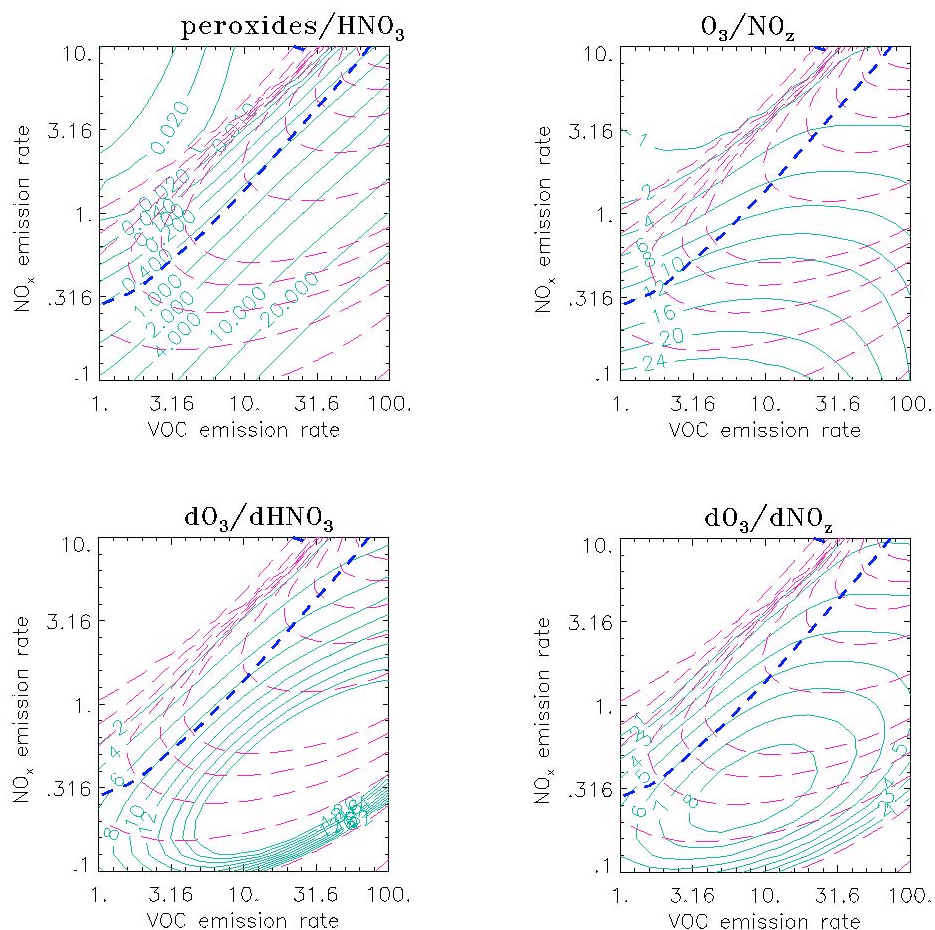


**Figure 3.1.3.** Isopleths as a function of the average emission rate for  $\text{NO}_x$  and VOC ( $10^{12}$  molec.  $\text{cm}^{-2} \text{s}^{-1}$ ) in 0-d calculations. The isopleths represent conditions during the afternoon following 3-day calculations, at the hour corresponding to maximum  $\text{O}_3$ . Isopleths are shown for (a)  $(\text{H}_2\text{O}_2 + \text{ROOH})/\text{HNO}_3$ ; (b)  $\text{O}_3/\text{NO}_z$ ; (c)  $(\text{O}_3 - \text{O}_{3b})/(\text{HNO}_3 - \text{HNO}_{3b})$ ; and (d)  $(\text{O}_3 - \text{O}_{3b})/(\text{NO}_z - \text{NO}_{zb})$ . Isopleths are shown as solid green lines. Isopleths for  $\text{O}_3$  in ppb (red dashed lines) are superimposed on the other isopleth plots (see also Figure 1.2). The short blue dashed line represents the transition from VOC-sensitive to  $\text{NO}_x$ -sensitive conditions. From Sillman and He (2002).

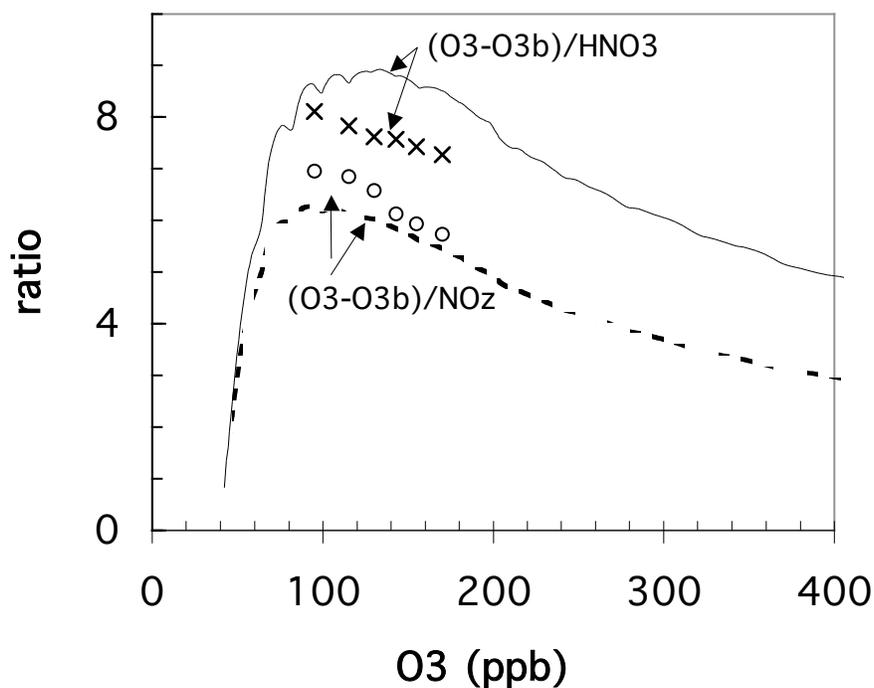


**Figure 3.1.4.** Comparison of the values of  $(O_3-O_{3b})/(NO_z-NO_{zb})$  and  $(O_3-O_{3b})/(HNO_3-HNO_{3b})$  along the  $NO_x$ -VOC sensitivity transition in isopleth plots based on 0-d calculations. The lines show values along the sensitivity transition from 3-day calculations by Sillman and He (2002), shown in Figure 3.1.3. The points show values along the sensitivity transition from 12-hour calculations by Tonnesen and Dennis (2000b).

### 3.1.5. Contrary evidence

Lu and Chang (1998) and Chock et al. (1999) both published results from 3-d models that sharply contradicted the original indicator findings. Lu and Chang reported results from a model for the San Joaquin valley (see Table 3.1.1) that included VOC-sensitive conditions for values of  $O_3/NO_z$  as high as 25. Lu and Chang used a definition of the terms “ $NO_x$ -sensitive” and “VOC-sensitive” that differed from the definition used by Sillman (1995) (see Section 3.1.10), but even when the original definition from Sillman (1995) is used, it is apparent that the model results from Lu and Chang differ from others. The range of values of  $O_3/NO_z$  is 15-30 in the model reported by Lu

and Chang (see Figure 3.1.5), as opposed to 5-20 in the models reported previously (Figure 3.1.1). Using Sillman's definition, the  $\text{NO}_x$ -VOC transition occurs for  $\text{O}_3/\text{NO}_z$  equal to 17-20 in the model reported by Lu and Chang, as opposed to 8-11 in the models shown in Figure 3.1.1.

Chock et al. (1999) also reported contrary results for indicator ratios in a model for Los Angeles (Figure 3.1.3). As shown in the figure, VOC-sensitive conditions are found for much higher values of  $\text{O}_3/\text{NO}_y$  (up to 12) and  $\text{O}_3/\text{NO}_z$  (up to 20) than in other models, including another model for Los Angeles.

Blanchard and Stoeckenius (2001) compared results from several models (including the original models from Sillman, 1995 and the model reported by Lu and Chang, 1998). They found that the transition point from  $\text{NO}_x$ - to VOC-sensitive conditions varied considerably in models for different cities.

The contrary results reported by Lu and Chang are due primarily to different boundary conditions, and can be corrected by using indicator ratios with the form  $(\text{O}_3 - \text{O}_{3b})/(\text{NO}_z - \text{NO}_{zb})$ . In the model by Lu and Chang, the San Joaquin valley was apparently affected by inflow of air from the model boundary with 75 ppb  $\text{O}_3$  and less than 1 ppb  $\text{NO}_z$ . This had a significant effect on model results (Sillman et al., 2001). Figure 3.1.5 shows results from the model by Lu and Chang using the ratio  $(\text{O}_3 - \text{O}_{3b})/(\text{NO}_z - \text{NO}_{zb})$ , with background conditions defined for the San Joaquin valley as described in Section 3.1.10. The ratio does not correlate with  $\text{NO}_x$ -VOC sensitivity as strongly as in most of the other models, but the approximate range of ratio values (3-7 for VOC-sensitive locations, 5-15 for  $\text{NO}_x$ -sensitive locations) is comparable to the range of VOC-sensitive values (3-6) and  $\text{NO}_x$ -sensitive values (5-15) in other models. The model by Lu and Chang also showed correlation patterns for  $\text{O}_3$  versus  $\text{NO}_z$  that differed substantially from other models (see Section 3.1.6). The difference in correlation patterns might be used to identify anomalous results.

Results from the model for Los Angeles reported by Chock et al. still show contradictory results, even for the ratios  $(\text{O}_3 - \text{O}_{3b})/(\text{NO}_y - \text{NO}_{yb})$ . There is no apparent reason for the contrary results, although the model used by Chock et al. also included varying boundary conditions (from 40 ppb to 80 ppb  $\text{O}_3$ ).

Chock et al. (1999) also suggested that plots of the geographical distribution of indicator values and predicted  $\text{NO}_x$ -sensitive and VOC-sensitive locations would identify inadequacies in indicator ratios that were not visible in the more direct plots of predicted impact of reduced  $\text{NO}_x$  and VOC versus indicator values. However, as shown in Figure 3.1.6, the geographical distribution of indicator values and  $\text{NO}_x$ -VOC sensitivity regions suggests the same

indicator behavior as can be seen in the standard indicator plots, and in the numerical representation in the Appendix.

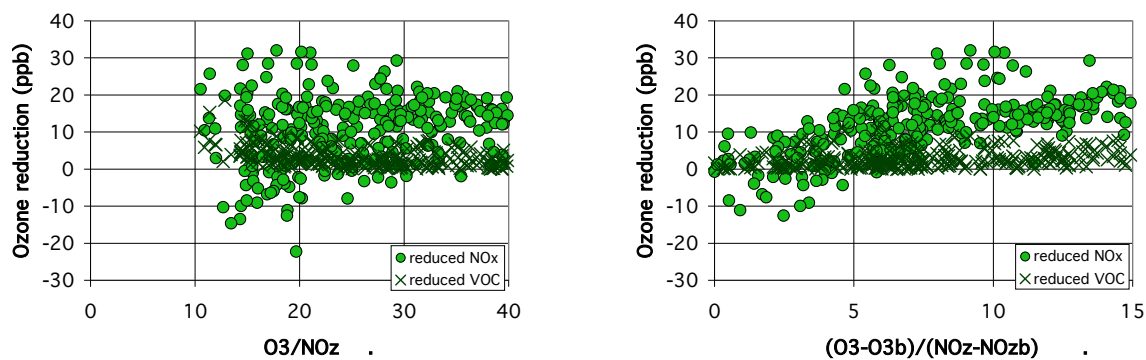


**Figure 3.1.5.** Contrary evidence from Lu and Chang (1998): Predicted reductions in ozone in response to a 50% reduction in emissions of anthropogenic VOC (crosses), and predicted reductions in response to the same percent reduction in emissions of anthropogenic  $\text{NO}_x$  (green circles), plotted versus model values for indicator ratios. Results are shown for  $\text{O}_3/\text{NO}_z$  and  $(\text{O}_3-\text{O}_{3b})/(\text{NO}_z-\text{NO}_{zb})$  from the model for San Joaquin reported by Lu and Chang (1998).

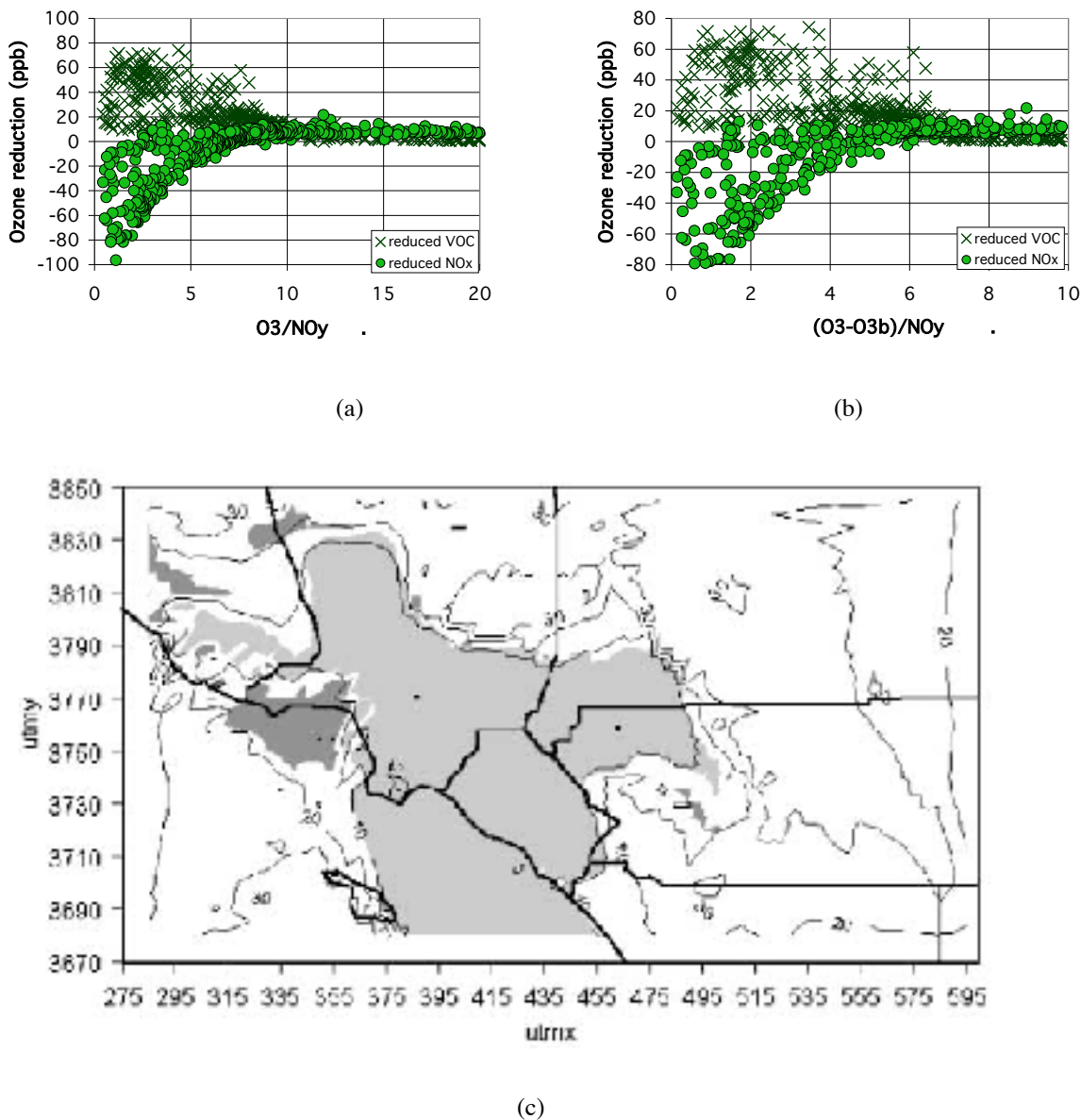


**Figure 3.1.6** . Contrary evidence from Chock et al. (1999): Predicted reductions in ozone in response to a percent reduction in emissions of anthropogenic VOC (crosses), and predicted reductions in response to the same percent reduction in emissions of anthropogenic  $NO_x$  (green circles), plotted versus model values for indicator ratios: contrary evidence. Results are shown for  $O_3/NO_y$  and  $(O_3-O_{3b})/(NO_y-NO_{yb})$ . Geographical contours for  $O_3/NO_y$  in Los Angeles, with shadings to show VOC-sensitive (light gray) and  $NO_x$ -sensitive locations (dark gray) from Winkler and Chock (2001) are also shown.

### 3.1.6. Model correlations between indicator species

An alternative way to use the indicator concept is to focus on the predicted correlation between species rather than just the indicator ratios. This approach is illustrated in Figure 3.1.7.

Figure 3.1.7 shows the composite correlation between  $O_3$  and  $NO_y$  and between  $O_3$  and  $NO_z$  from five separate model scenarios (listed in Table 3.1.1). The correlation has been sorted based on predicted  $NO_x$ -VOC sensitivity at each model location into four categories:  $NO_x$ -sensitive, VOC-sensitive, mixed, and locations dominated by  $NO_x$  titration.\* Precise definitions are given below in Section 3.1.10.

As shown in the figure,  $NO_x$ -sensitive and VOC-sensitive locations are associated with different ranges of values in the correlation plots for  $O_3$  versus  $NO_y$  and  $O_3$  versus  $NO_z$ .  $NO_x$ -sensitive locations all show a fairly tight correlation between  $O_3$  and  $NO_y$ , etc. VOC-sensitive locations are associated with a broader range of  $O_3$  versus  $NO_y$  and  $NO_z$ , but the range of VOC-sensitive values always have lower  $O_3$  for a given value of  $NO_y$  or  $NO_z$  than the  $NO_x$ -sensitive locations. Mixed locations occupy an intermediate region between the  $NO_x$ -sensitive and VOC-sensitive locations. Locations dominated by  $NO_x$  titration all have very low  $O_3/NO_y$ . The correlation pattern for individual model scenarios, shown in Figure 3.1.8, is often quite different from the composite pattern.

Figure 3.1.7 is useful because it provides a basis for evaluating whether an individual set of measurements is consistent with the indicator approach. The indicator ratios are valid for an individual set of measurements only if the measured correlations are consistent with the correlation patterns predicted for either  $NO_x$ -sensitive or VOC-sensitive locations. If a range of measured values for  $O_3$  versus  $NO_y$  and  $O_3$  versus  $NO_z$  differs from the values shown in Figure 3.1.7, it suggests a flaw that would invalidate the indicator approach for the individual data set.

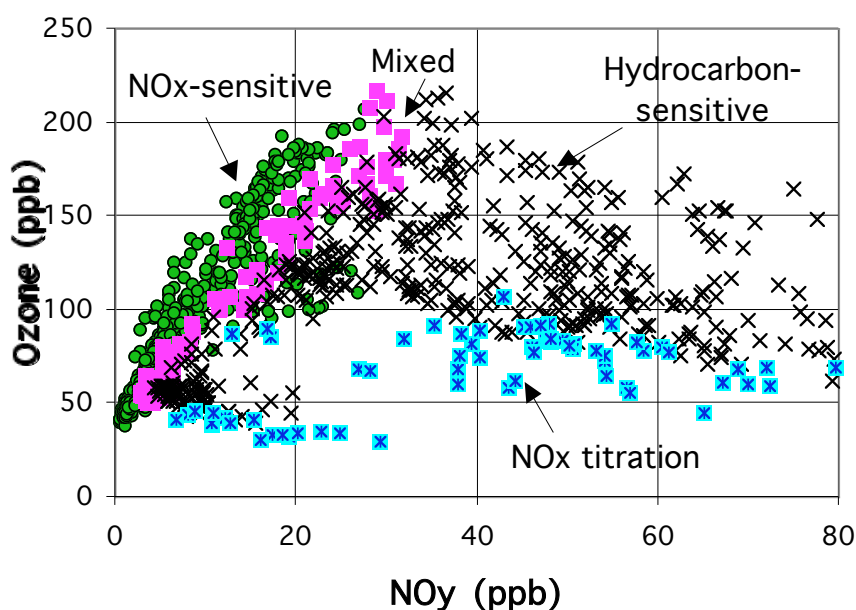
---

\*  $NO_x$  titration is used here to describe strongly  $NO_x$ -saturated locations in which  $O_3$  is predicted to increase in response to reduced  $NO_x$  emissions and to be unaffected by changes in VOC. typically, these conditions are found only in the immediate vicinity of large  $NO_x$  emission sources, and have  $O_3$  lower than the regional background. As shown in Figure 3.1.7, locations with  $NO_x$  titration all have very low  $O_3/NO_y$ . They sometimes are 'exceptions' to the indicator correlations, especially for  $H_2O_2/HNO_3$ . In a pure  $NO_x$  titration process, there is no production of  $O_3$  or of any secondary species.

This type of evaluation will identify many situations in which indicator ratios are not valid, due to either erroneous measurements or to real-world conditions that are inconsistent with the indicator ratios.

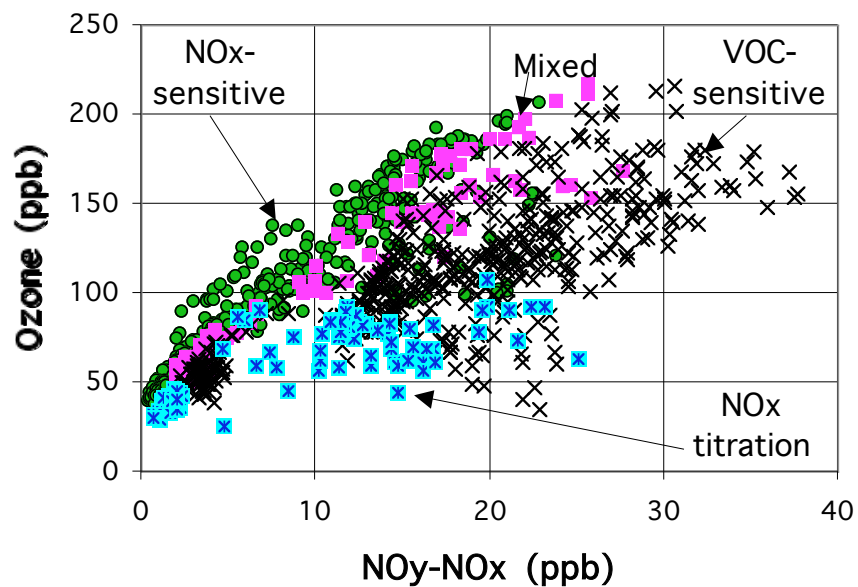
In the case study for San Joaquin reported by Lu and Chang (1998), the model correlations between  $O_3$  and  $NO_z$  differ substantially from the composite predictions of other model scenarios. As shown in Figure 3.1.8, the model results for San Joaquin show much higher  $O_3$  for a given level of  $NO_y$  and  $NO_z$  relative to the other model scenarios shown in Figure 3.1.7 and 3.1.8. The contradictory results for indicator ratios reported by Lu and Chang are also associated with the difference in the  $O_3$ - $NO_z$  correlation pattern. By examining measured correlations in comparison with Figures 3.1.7 and 3.1.8, it is possible to evaluate whether a set of measurements is consistent with the original indicator predictions (Figure 3.1.7) or the contradictory results reported by Lu and Chang (3.1.8).

Equivalent results for measurements are shown in Section 3.1.7.



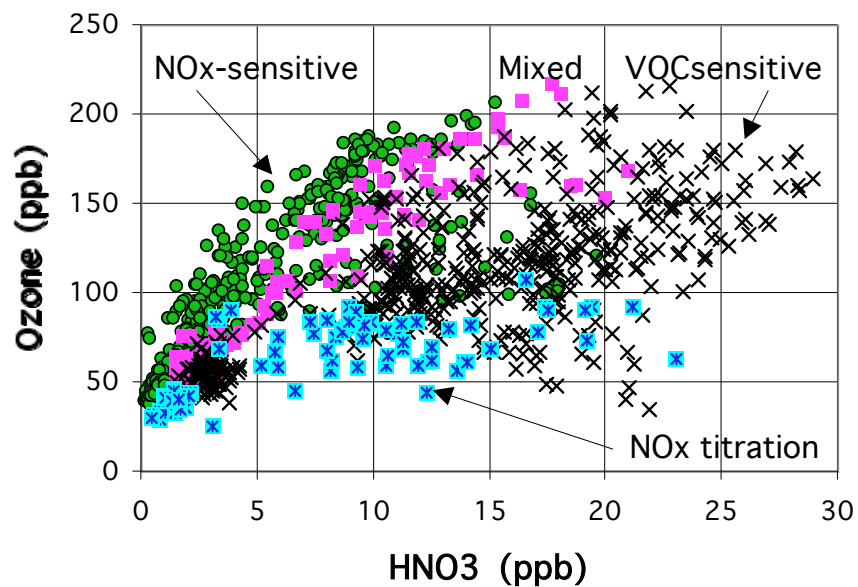
(a)

**Figure 3.1.7.** Correlations for (a)  $O_3$  vs.  $NO_y$ , (b)  $O_3$  vs.  $NO_z$ , (c)  $O_3$  vs.  $HNO_3$ , and (d) total peroxides vs.  $HNO_3$  (all in ppb) from the 3-d simulations listed in Table 3.1.1. Each location is classified as  $NO_x$ -sensitive (green circles), VOC-sensitive (crosses), mixed or with near-zero sensitivity (lavender squares), and dominated by  $NO_x$  titration (blue asterisks) based on definitions in the text. From Sillman and He (2002).



(b)

**Figure 3.1.7.** Correlations for (a) O<sub>3</sub> vs. NO<sub>y</sub>, (b) O<sub>3</sub> vs. NO<sub>z</sub>, (c) O<sub>3</sub> vs. HNO<sub>3</sub>, and (d) total peroxides vs. HNO<sub>3</sub> (all in ppb) from the 3-d simulations listed in Table 3.1.1. Each location is classified as NO<sub>x</sub>-sensitive (green circles), VOC-sensitive (crosses), mixed or with near-zero sensitivity (lavender squares), and dominated by NO<sub>x</sub> titration (blue asterisks) based on definitions in the text. From Sillman and He (2002).



(c)

**Figure 3.1.7.** Correlations for (a) O<sub>3</sub> vs. NO<sub>y</sub>, (b) O<sub>3</sub> vs. NO<sub>z</sub>, (c) O<sub>3</sub> vs. HNO<sub>3</sub>, and (d) total peroxides vs. HNO<sub>3</sub> (all in ppb) from the 3-d simulations listed in Table 3.1.1. Each location is classified as NO<sub>x</sub>-sensitive (green circles), VOC-sensitive (crosses), mixed or with near-zero sensitivity (lavender squares), and dominated by NO<sub>x</sub> titration (blue asterisks) based on definitions in the text. From Sillman and He (2002).

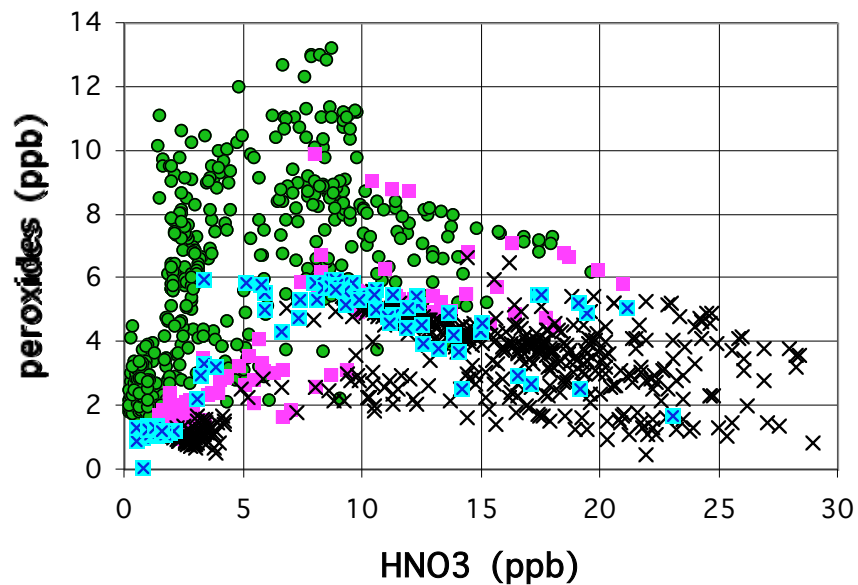


**Figure 3.1.7** . Correlations for (a)  $O_3$  vs.  $NO_y$ , (b)  $O_3$  vs.  $NO_z$ , (c)  $O_3$  vs.  $HNO_3$ , and (d) total peroxides vs.  $HNO_3$  (all in ppb) from the 3-d simulations listed in Table 3.1.1. Each location is classified as  $NO_x$ -sensitive (green circles), VOC-sensitive (crosses), mixed or with near-zero sensitivity (lavender squares), and dominated by  $NO_x$  titration (blue asterisks) based on definitions in the text. From Sillman and He (2002).

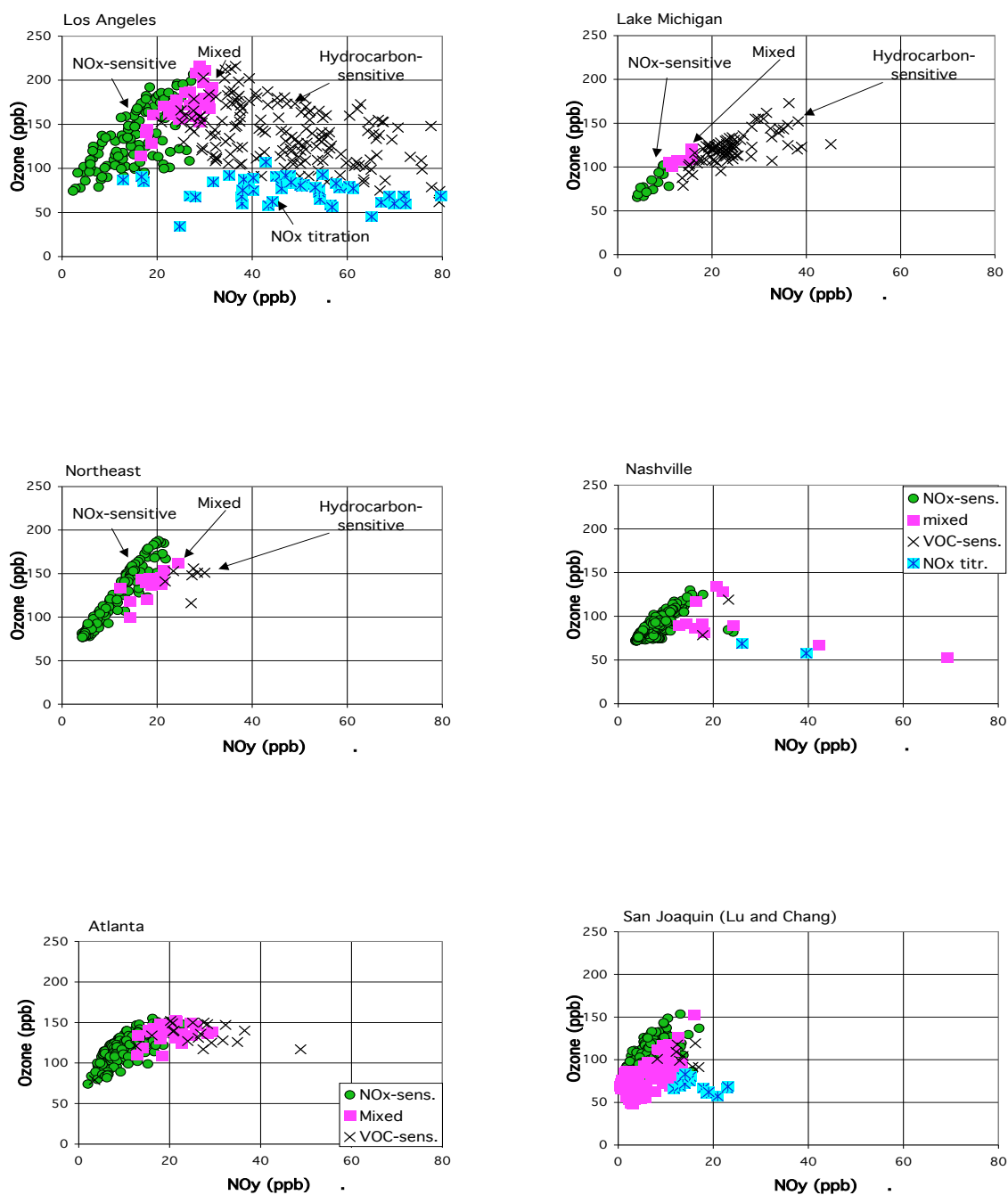


**Figure 3.1.8.** Correlations for O<sub>3</sub> vs. NO<sub>y</sub> in ppb from individual 3-d simulations listed in Table 3.1.1. Each location is classified as NO<sub>x</sub>-sensitive (green circles), VOC-sensitive (crosses), mixed or with near-zero sensitivity (lavender squares), and dominated by NO<sub>x</sub> titration (blue asterisks) based on definitions in the text. Models are (a) Los Angeles (Godowitch), (b) Lake Michigan, (c) northeast corridor, (d) Nashville, (e) Atlanta, and (f) San Joaquin (Lu and Chang).

### 3.1.7. Results from ambient measurements

Figure 3.1.9 shows correlations between measured  $O_3$  and  $NO_y$  and between  $O_3$  and  $NO_y$  during events in four metropolitan areas: Atlanta (August 10, 1992); Nashville (July 15, 1995); Paris (July 17, 1999); and Los Angeles (August 27, 1988).

These correlation patterns show substantial differences between urban areas, which might be interpreted as evidence of different  $NO_x$ -VOC sensitivity. Comparing with Figure 3.1.6, these patterns would be interpreted as suggestive of  $NO_x$ -sensitive conditions in Atlanta, mixed sensitivity in Nashville and Paris, and strongly VOC-sensitive conditions in Los Angeles.

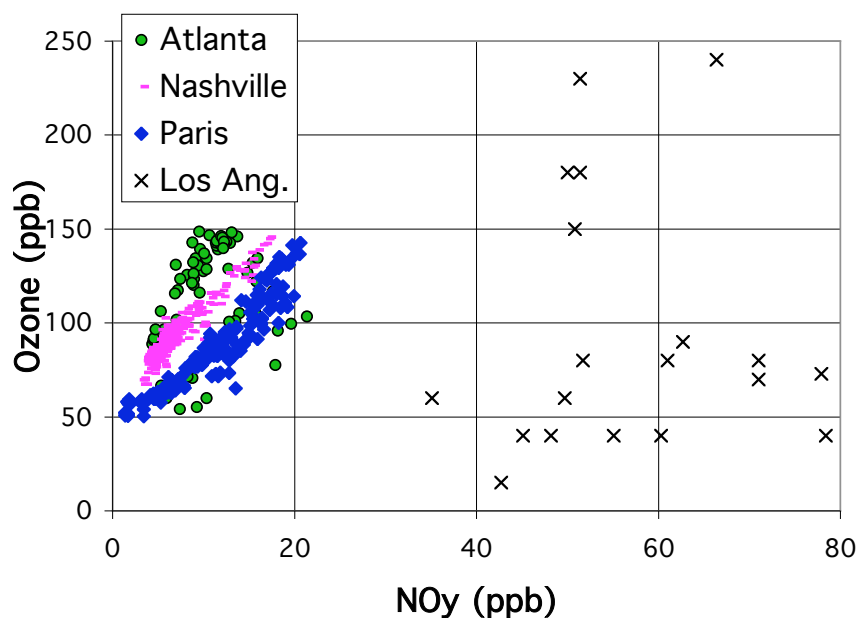
Correlation patterns of  $O_3$  versus  $NO_z$  in rural areas also show variations, which have been interpreted as representative of differences between  $NO_x$ -sensitive and VOC-sensitive conditions (Jacob et al., 1995; Hirsh et al., 1996). However, since rural areas usually have  $NO_x$ -sensitive chemistry, correlations among these species from research-grade measurements in rural areas provide an important test for the accuracy of the predicted correlation patterns shown in Figure 3.1.7 and Figure 3.1.8.

Figure 3.1.10 shows results from research-grade field measurements in rural areas in the eastern and southern U.S. These correlations (between  $O_3$  and  $NO_y$  and between  $O_x$  and  $NO_z$ ) are consistent with the model correlation for  $NO_x$ -sensitive conditions.

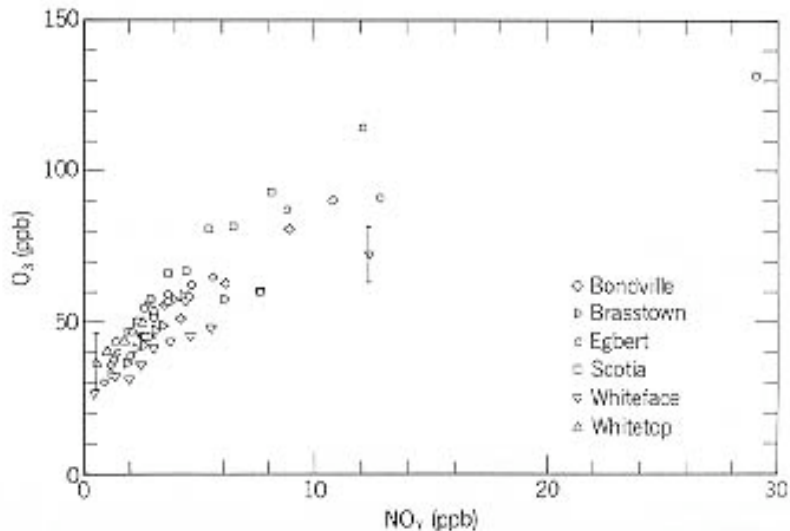
More detailed information can be obtained in cases where measured  $H_2O_2$  or total peroxides are available. As shown in Figure 3.1.11, 3-d models and measurements both predict a strong correlation between  $O_3$  and the sum ( $2H_2O_2+NO_z$ ). This correlation represents an important evaluation of the indicator approach because the species involved are all major components of the indicator ratios.

The correlation between  $O_3$  and ( $2H_2O_2+NO_z$ ) is important because discrepancies between model and measured correlations would suggest errors that would invalidate the indicator method. Unlike the proposed indicator ratios,  $O_3$  and ( $2H_2O_2+NO_z$ ) show a similar linear correlation in both  $NO_x$ -sensitive and VOC-sensitive locations. This means that any discrepancy between model and measured correlations suggests errors that are unrelated to predicted  $NO_x$ -VOC sensitivity. These errors would cast doubt on the relation between indicator ratios and  $NO_x$ -VOC sensitivity as predicted by models. Alternatively, a good agreement between models and measurements for  $O_3$

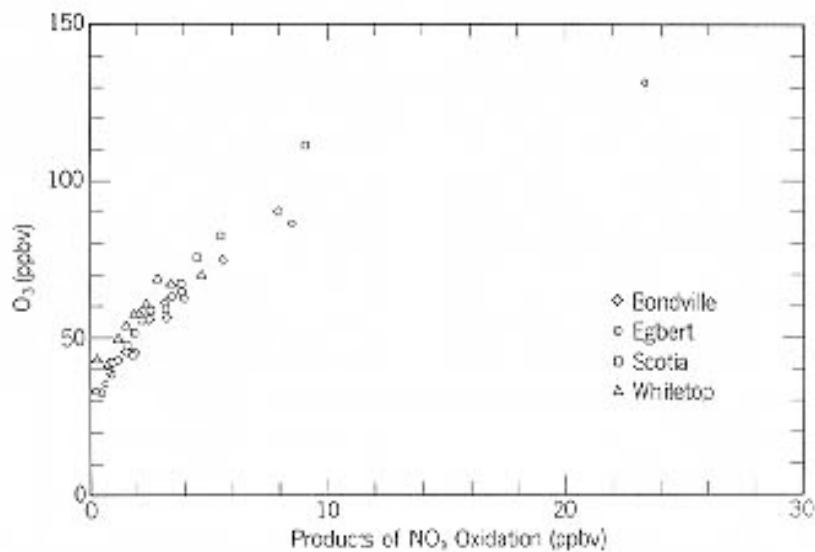
versus  $(2\text{H}_2\text{O}_2 + \text{NO}_z)$  can provide evidence that many uncertain features of the model (ozone production efficiencies, dry deposition rates, etc.) are consistent with measured values.



**Figure 3.1.9.** Measured correlation between O<sub>3</sub> and NO<sub>z</sub> in Atlanta (green circles), Nashville (pink dashes), Paris (blue diamonds) and Los Angeles (crosses) for the events of August 10, 1992 (Atlanta); July 13, 1995 (Nashville); July 17, 1999 (Paris); and August 28, 1987 (Los Angeles), from measurements reported by Sillman et al. (1995, 1997, 1998, 2002).

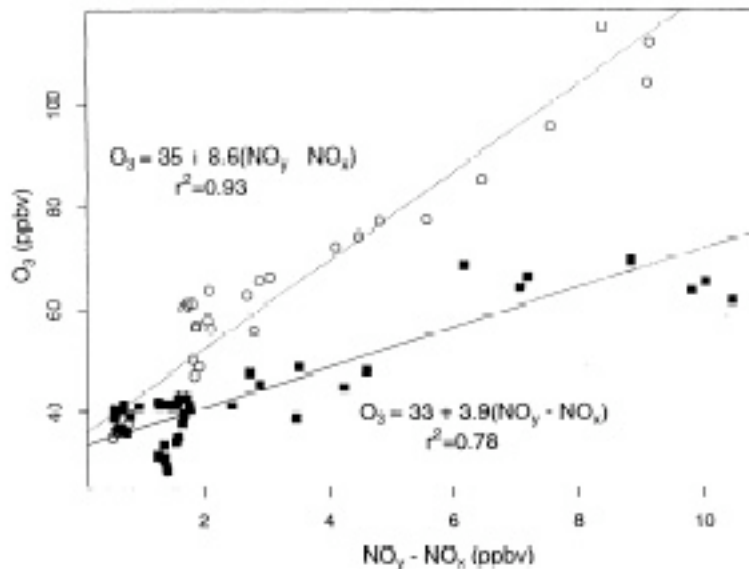


(a)  $O_3$  versus  $NO_y$  at six rural sites (Trainer et al., 1993)

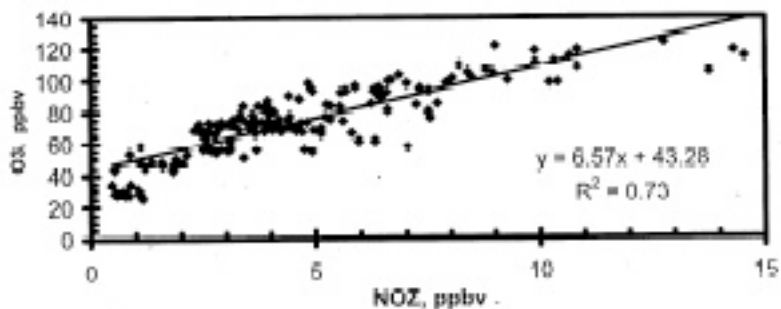


(b)  $O_3$  versus  $NO_2$  at six rural sites (Trainer et al., 1993)

**Figure 3.1.10.** Measured  $O_3$  versus  $NO_y$ ,  $O_3$  versus  $NO_2$  and  $O_3$  versus PAN. The figures show (a)  $O_3$  versus  $NO_y$  at six rural sites in the eastern U.S. (Trainer et al., 1993); (b)  $O_3$  versus  $NO_2$  at six rural sites in the U.S. (Trainer et al., 1993); (c)  $O_3$  versus  $NO_2$  for two week-long time periods at a rural site in Massachusetts with different correlation patterns (Hirsch et al., 1996); (d)  $O_3$  versus  $NO_2$  at rural sites in Tennessee (Olszyna et al., 1998); and (e)  $O_3$  versus PAN at rural sites in Tennessee (Roberts et al., 1998).



(c)  $O_3$  versus  $NO_z$  in rural Massachusetts (Hirsch et al., 1996)



(d)  $O_3$  versus  $NO_z$  at a site in Tennessee (Olszyna et al., 1998)

**Figure 3.1.10** . Measured  $O_3$  versus  $NO_y$ ,  $O_3$  versus  $NO_z$  and  $O_3$  versus PAN. The figures show (a)  $O_3$  versus  $NO_y$  at six rural sites in the eastern U.S. (Trainer et al., 1993); (b)  $O_3$  versus  $NO_z$  at six rural sites in the U.S. (Trainer et al., 1993); (c)  $O_3$  versus  $NO_z$  for two week-long time periods at a rural site in Massachusetts with different correlation patterns (Hirsch et al., 1996); (d)  $O_3$  versus  $NO_z$  at rural sites in Tennessee (Olszyna et al., 1998); and (e)  $O_3$  versus PAN at rural sites in Tennessee (Roberts et al., 1998).

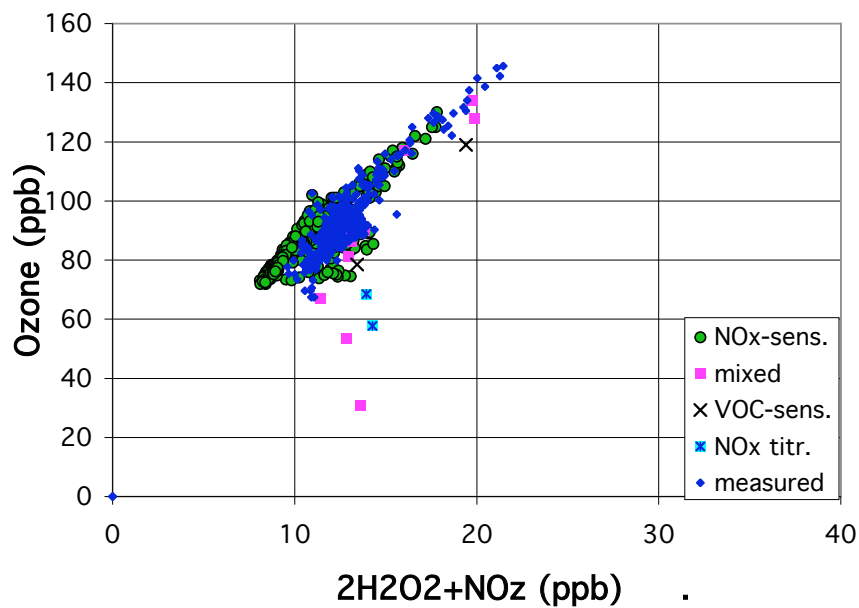


**Figure 3.1.11.** Measured correlation between O<sub>3</sub> and the sum 2H<sub>2</sub>O<sub>2</sub>+NO<sub>z</sub> (ppb) in Nashville (blue diamonds), compared with model results. Each model location is classified as NO<sub>x</sub>-sensitive (green circles), VOC-sensitive (crosses), mixed or with near-zero sensitivity (lavender squares), and dominated by NO<sub>x</sub> titration (blue asterisks) based on definitions in the text. The model and measurements are from Sillman et al. (1998).

### 3.1.8. Model evaluations with measured indicator species: a method for regulatory use

The most promising use of the indicator concept involves the use of measured species identified as  $\text{NO}_x$ -VOC indicators to evaluate results from 3-d models.

Evaluations of model performance using measured indicator species have been reported for Atlanta, Nashville, Los Angeles and Paris (Sillman et al., 1995, 1997, 1998, 2002b). In each of these evaluations, measured correlations between  $\text{O}_3$  and  $\text{NO}_y$  and between  $\text{O}_3$  and  $\text{NO}_z$  were compared with predicted correlations from a series of model scenarios. The model scenarios included cases with  $\text{NO}_x$  and VOC emissions modified from the initial rates derived from emission inventories and with modified wind speeds and mixing heights. Due to the modified emissions, the model scenarios also included cases with different  $\text{NO}_x$ -VOC predictions (see Figure 1.2 and Section 1.4 above). These scenarios provide a test to see whether the model-measurement evaluation can distinguish between alternatives with different control predictions.

Figure 3.1.12 shows four model-measurement comparisons that illustrate different types of results. In the case for Atlanta (Figure 3.1.12a), model  $\text{O}_3$  versus  $\text{NO}_y$  shows a correlation that largely agrees with measured correlation, but only when the model predicts  $\text{NO}_x$ -sensitive conditions. When the model predicts VOC-sensitive conditions, especially for high ozone, the model  $\text{O}_x$  and  $\text{NO}_y$  differ from the measured correlation. The model values of the ratio  $\text{O}_3/\text{NO}_y$  associated with VOC-sensitive conditions are also much lower than measured values. This pattern strongly suggests that the model (which used the BEIS1 inventory) was biased in its  $\text{NO}_x$ -VOC control predictions and overestimated the benefits of reduced VOC.

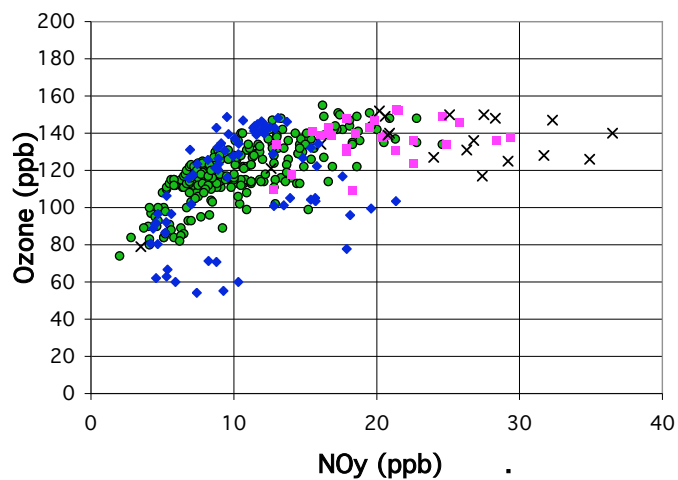
In the case for Los Angeles (Figure 3.1.12b) the model  $\text{O}_3$  versus  $\text{NO}_z$  agrees with the measured correlation only when the model predicts VOC-sensitive conditions. When the model predicts  $\text{NO}_x$ -sensitive conditions it has  $\text{O}_3$  and  $\text{NO}_z$  that is higher than measured values. There is some uncertainty here because the highest measured  $\text{O}_3$  is not that far removed from the model  $\text{NO}_x$  sensitive region. However, the general comparison suggests that the model (which had VOC emissions much higher than inventory values) overestimated the possible benefits of reduced  $\text{NO}_x$ .

In the case for Nashville (Figure 3.1.12c) there is a good agreement between model and measured  $\text{O}_3$  and  $\text{NO}_y$ , suggesting that the model provides an unbiased estimate of the impacts of reduced  $\text{NO}_x$  and VOC emissions.

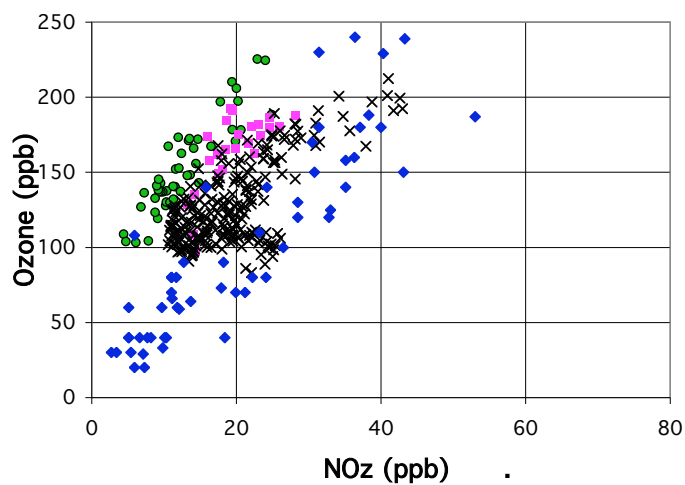
In the case for Paris (Figure 3.1.12d) there is a disagreement between models and measurements throughout the model domain. This disagreement is not related to model  $\text{NO}_x$ -VOC predictions. The same disagreement appears for both  $\text{NO}_x$ -sensitive and VOC-sensitive conditions. In this case, the measured  $\text{O}_3$  versus  $\text{NO}_z$  cannot be interpreted as evidence concerning  $\text{NO}_x$ -VOC sensitivity. The cause of the model-measurement discrepancy is unknown, but there is a high likelihood that the cause (e.g. rapid deposition of  $\text{HNO}_3$ , conversion to unmeasured aerosol nitrate, erroneous measurements, etc.) would invalidate the use of measured values as  $\text{NO}_x$ -VOC indicators.

These comparisons have been chosen to illustrate the different patterns that appear and do not represent a complete analysis of either city.

If indicator ratios are to be used for regulatory purposes, protocols are needed to distinguish between the three types of model-measurement comparison shown here.

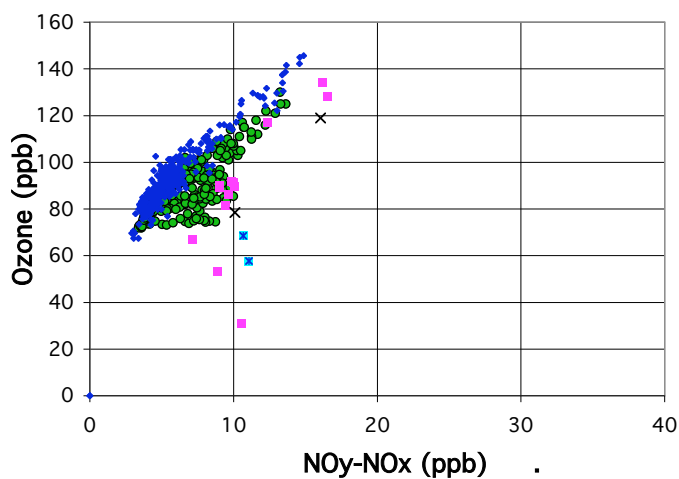


(a) Atlanta, August 10, 1992

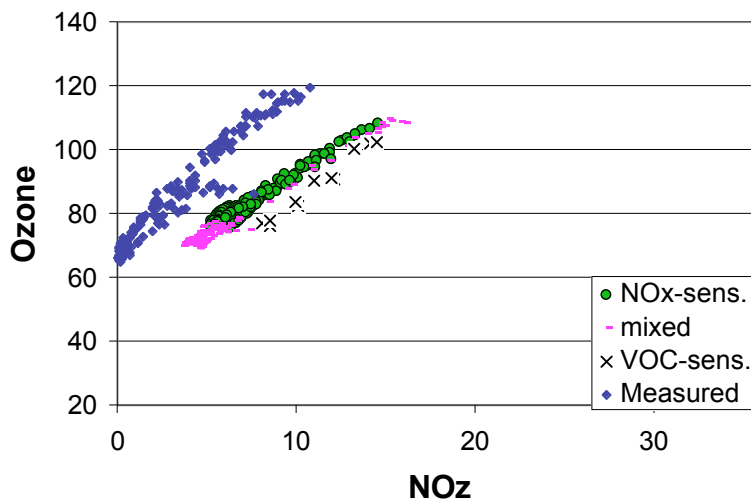


(b) Los Angeles, August 27, 1987

**Figure 3.1.12.** Measured correlation between  $O_3$  and  $NO_y$  and between  $O_3$  and  $NO_z$  (ppb) (blue diamonds), compared with model results. Each model location is classified as  $NO_x$ -sensitive (green circles), VOC-sensitive (crosses), mixed or with near-zero sensitivity (lavender squares), and dominated by  $NO_x$  titration (blue asterisks) based on definitions in the text. Cases are shown for (a) Atlanta, (b) Los Angeles, (c) Nashville, and (d) Paris, from Sillman et al. (1995, 1997, 1998, 2002).



(c) Nashville, July 13, 1995



(d) Paris, July 18, 1999

**Figure 3.1.12.** Measured correlation between  $O_3$  and  $NO_y$  and between  $O_3$  and  $NO_z$  (ppb) (blue diamonds), compared with model results. Each model location is classified as  $NO_x$ -sensitive (green circles), VOC-sensitive (crosses), mixed or with near-zero sensitivity (lavender squares), and dominated by  $NO_x$  titration (blue asterisks) based on definitions in the text. Cases are shown for (a) Atlanta, (b) Los Angeles, (c) Nashville, and (d) Paris, from Sillman et al. (1995, 1997, 1998, 2002).

### 3.1.9. Results for O<sub>3</sub> versus PAN: possible impact of erroneous measurements

A major issue for NO<sub>x</sub>-VOC indicators concerns the accuracy of available measurements.

Measured NO<sub>y</sub> and NO<sub>z</sub> can only be used in indicator ratios and correlations if the measurements include HNO<sub>3</sub>. The information in these ratios that relates to NO<sub>x</sub>-VOC sensitivity is contained primarily in HNO<sub>3</sub>. The other components of NO<sub>z</sub>, including PAN and other organic nitrate, are not related to O<sub>3</sub>-NO<sub>x</sub>-VOC sensitivity. Ratios such as O<sub>3</sub>/PAN are not correlated with NO<sub>x</sub>-VOC sensitivity in models (Tonnesen and Dennis, 2000b).

This issue is important because HNO<sub>3</sub> is sometimes lost along the inlet tubes when NO<sub>y</sub> is measured (Parrish et al., 2000; McClenny et al., 2000). If HNO<sub>3</sub> were missing from measured NO<sub>y</sub>, then the remaining measurement (NO<sub>x</sub>+organic nitrates) could not be used to evaluate NO<sub>x</sub>-VOC sensitivity.

NO<sub>x</sub> measurements that use chemiluminescence also sometimes respond to PAN in addition to NO<sub>x</sub> (Logan, 1989), McClenny, 2000). This would affect the accuracy of NO<sub>z</sub>, which is measured as the difference between NO<sub>y</sub> and NO<sub>x</sub>.

McClenny (2000) recommended changes in the PAMS network that would insure the accuracy of measured NO<sub>y</sub> and NO<sub>x</sub>. Williams et al. (1998) also reported good results from an intercomparison of NO<sub>y</sub> instruments. However it is also important to evaluate individual measurement sets to determine whether these types of errors occur. Luke et al. (1998) reported incidences of apparent errors in individual measurements of NO<sub>y</sub>.

Figure 3.1.13 shows the correlation between O<sub>3</sub> and organic nitrates (defined as NO<sub>y</sub>-NO<sub>x</sub>-HNO<sub>3</sub>) for the five models shown in figure 3.1.7. In this figure a very similar correlation pattern is shown for both NO<sub>x</sub>-sensitive and VOC-sensitive locations.

The correlation between O<sub>3</sub> and organic nitrates is also distinctly different from the predicted correlation for O<sub>x</sub> versus NO<sub>z</sub> in Figure 3.1.7. Thus, comparison of measured O<sub>3</sub> versus NO<sub>z</sub> with the predicted correlation for O<sub>3</sub> versus organic nitrates can be used as a diagnostic test for this type of measurement error.

The model correlation between O<sub>3</sub> and organic nitrates is generally consistent with ambient measurements of O<sub>3</sub> versus PAN (Figure 3.1.14).

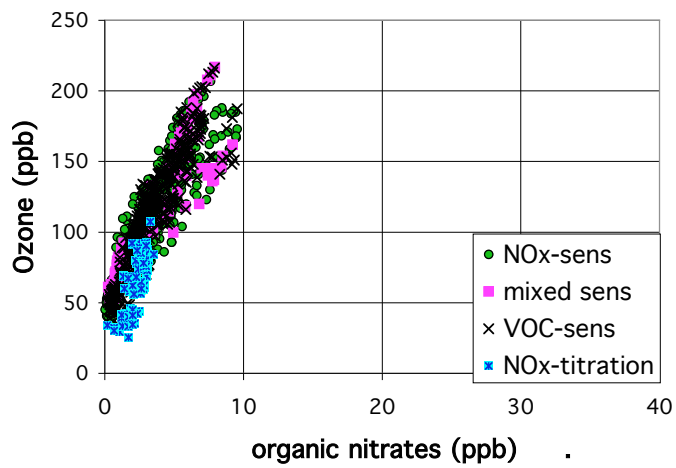


**Figure 3.1.13.** Correlations for organic nitrates (defined as  $\text{NO}_y\text{-NO}_x\text{-HNO}_3$ , in ppb) from the 3-d simulations listed in Table 3.1.1. Each location is classified as  $\text{NO}_x$ -sensitive (green circles), VOC-sensitive (crosses), mixed or with near-zero sensitivity (lavender squares), and dominated by  $\text{NO}_x$  titration (blue asterisks) based on definitions in the text.

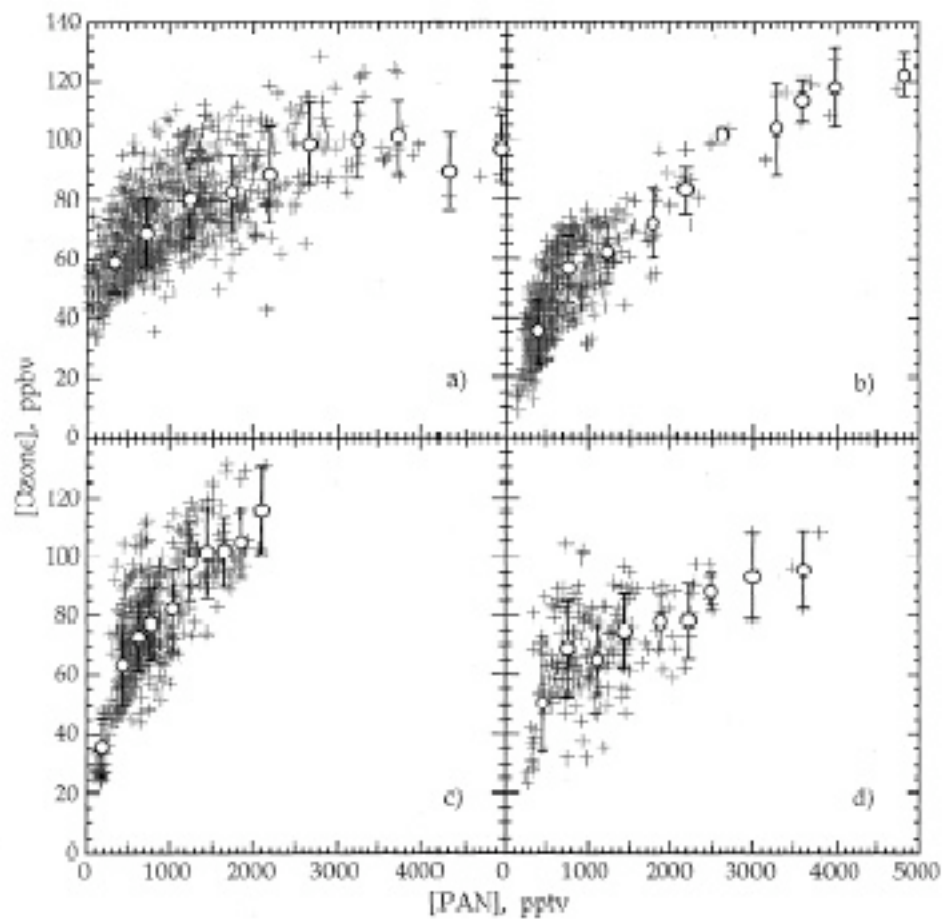


**Figure 3.1.14.** Measured  $O_3$  (ppb) versus PAN (ppt) at in Tennessee, including (a) aircraft measurements, and (b, c and d) suburban sites near Nashville (Roberts et al., 1998).

### 3.1.10. Supplemental topic: Defining O<sub>3</sub>-NO<sub>x</sub>-VOC sensitivity

As described in Section 2.2, there are two standard ways to define O<sub>3</sub>-NO<sub>x</sub>-VOC sensitivity: relative impact of reduced NO<sub>x</sub> versus reduced VOC; and NO<sub>x</sub> benefits versus disbenefits. The results reported by Sillman were all based on the first definition. Tonnesen and Dennis (2001b) reported results for both definitions and found small but significant differences in the indicator transition values. Typically, transition values were 15% lower for NO<sub>x</sub> benefits versus disbenefits than for the relative impact of NO<sub>x</sub> versus VOC. In each case, NO<sub>x</sub>-VOC sensitivity was defined relative to changes in emissions of anthropogenic NO<sub>x</sub> and VOC ranging from 25% to 50%. A different response to changed NO<sub>x</sub> and VOC can be expected if much higher percent reductions were used (Schere and Roselle, 1995).

The correlation plots (Figures 3.1.7, etc.) all used the following definition of sensitivity, applied to specific model locations relative to predicted changes in O<sub>3</sub> at the same time and location in model scenarios with reduced NO<sub>x</sub> and VOC:

*NO<sub>x</sub>-sensitive:* O<sub>3</sub> in model scenarios with reduced NO<sub>x</sub> is lower than O<sub>3</sub> in the base case by at least 5 ppb, and lower than in model scenarios with the same percent reduction in VOC by at least 5 ppb.

*VOC-sensitive:* O<sub>3</sub> in the scenario with reduced VOC is lower than O<sub>3</sub> in both the base case and in the scenario with reduced NO<sub>x</sub> by at least 5 ppb.

*Mixed:* The scenarios with reduced NO<sub>x</sub> and reduced VOC have O<sub>3</sub> within 5 ppb of each other, and both have O<sub>3</sub> lower than in the base case by at least 5 ppb.

*NO<sub>x</sub>-titration:* O<sub>3</sub> in the scenario with reduced NO<sub>x</sub> is larger than O<sub>3</sub> in the base case by at least 5 ppb, and O<sub>3</sub> in the simulation with reduced VOC is not lower by 5 ppb or more relative to the base case.

All other locations are viewed as insensitive to NO<sub>x</sub> and VOC in the context of the model domain. These typically represent locations with O<sub>3</sub> dominated by transport from outside the model boundary rather than calculated photochemical production.

The locations dominated by NO<sub>x</sub>-titration are usually near large sources of NO. These locations typically have relatively low O<sub>3</sub>, and O<sub>3</sub> has been affected primarily by the reaction O<sub>3</sub>+NO → NO<sub>2</sub> in the presence of directly emitted NO rather than by ozone production chemistry. These locations always have very low O<sub>3</sub>/NO<sub>y</sub> and O<sub>3</sub>/NO<sub>x</sub>, and are therefore easy to identify.

### ***3.1.11. Supplemental topic: Determining background values***

Background concentrations represent an important uncertainty for indicator ratios such as  $(O_3 - O_{3b}) / (NO_y - NO_{yb})$ . Background concentrations in models can be identified based on boundary conditions, but for ambient conditions the background is less clear. In evaluating model results it is necessary to determine background concentrations in a way that is directly comparable to the background that can be determined from a measured data set.

Sillman and He (2002) adopted the following procedure for boundary conditions. They assumed that modeling was to be done for a metropolitan area with a network of surface measurements (including the surrounding rural area). They defined background concentrations as equal to the value at the measurement site that reported minimum  $NO_y$ , using measurements at the same hour (in the afternoon) as the  $O_3$  they intended to analyze. Although somewhat arbitrary, this definition would allow background concentrations to be determined from surface measurements alone and avoided the need to make assumptions about the upwind origin of air. The equivalent background concentration from model scenarios was found by identifying the model surface grid with minimum  $NO_y$  within the metropolitan area.

An additional problem with model interpretation concerned the interpretation of model sensitivity predictions in when the background concentrations determined in this way were different from the model boundary conditions. For example, in an examined case for Atlanta (using the model listed in Table 3.1.1), the model boundary  $O_3$  was 55 ppb and the background  $O_3$  determined by the above method was 74 ppb. In this case, the background  $O_3$  already included significant  $O_3$  production and the model sensitivity runs included changed background  $O_3$ . In this case, consistent results were found only if the predicted impact of reduced  $NO_x$  and VOC at the background location were subtracted from the predicted impact of reduced  $NO_x$  and VOC elsewhere in the model domain. With sensitivity adjusted in this way, model correlations between indicator ratios and  $NO_x$ -VOC sensitivity were identical with the derived background concentrations as they would be with background concentrations set equal to the model boundary values.

Olszyna et al. (1994) determined background  $O_3$  in connection with smog production algorithms (Section 3.2) by extrapolating the observed linear correlation of  $O_3$  with  $NO_z$  to find the  $O_3$  that would be associated with zero  $NO_z$ .

This method may not be applicable in many urban cases, because the correlation between  $O_3$  and  $NO_z$  is not always linear.

In regional-scale analyses, model background conditions are often set based on typical conditions in the clean troposphere outside the borders of the U.S. (including conditions over the Atlantic and Pacific Oceans and sparsely populated parts of Canada). In these cases there may be no appropriate measurements to identify the regional background, but background conditions may be reasonably assumed to be equal to the model background. Conditions in the clean troposphere in summer are typically 30-40 ppb  $O_3$ , 0.1 ppb  $NO_x$  or lower, and less than 1 ppb  $NO_y$ , with little day-to-day variation. (Logan, 1988; Carroll et al., 1990; Chin et al., 1994).

### 3.1.12. Supplemental topic: Radical chemistry and $O_3$ - $NO_3$ -VOC sensitivity

The relation between the ratio  $O_3/NO_z$  and  $NO_x$ -VOC sensitivity can be understood intuitively in terms of the well-known relationship between  $NO_x$ -VOC sensitivity and VOC/ $NO_x$  ratios. The main reactions associated with ozone formation are summarized in Table 3.1.2. The ozone production sequence is initiated by reaction of various VOC and CO with OH (R1 in Table 3.1.2). The resulting  $RO_2$  and  $HO_2$  radicals go on to react with NO (R2 and R3), and the resulting  $NO_2$  photolyzes to produce ozone. Because the reaction of VOC with OH is the rate-limiting step for the sequence it is possible to regard the rate of ozone production as proportional to the summed rate of VOC+OH (R1). This rate may be compared to the rate of formation of nitric acid ( $NO_2$ +OH, R10). Comparing the rates of reactions R1 and R10, it is possible to express the ratio of the rate of ozone production to that of nitric acid as follows:

$$\frac{P_{O_3}}{P_{HNO_3}} = \frac{\sum_i k_{OH_i}[VOC_i]}{k_{OHn}[NO_2]} \quad (3.1.1)$$

where  $VOC_i$  represents individual VOC species and  $k_{OH_i}$  represents the rate constant for the reaction of the individual VOC with OH. The ratio on the right side of Equation 3.1.1 is the familiar ratio of reactivity-weighted VOC (abbreviated rVOC) to  $NO_x$ , normalized relative to the rate constant for the reaction of  $NO_2$  with OH ( $k_{OHn}$ ). As will be discussed in Section 3.3, the ratio of reactivity-weighted VOC to  $NO_x$  is closely associated with the  $NO_x$ -VOC sensitivity of instantaneous ozone production.

The ratios  $O_3/NO_x$  and  $O_3/HNO_3$  could therefore be regarded as surrogates for the sum of the ratio of reactivity-weighted VOC to  $NO_x$  over time.

Photochemical uncertainties include the following: variations in the rate of ozone production per VOC+OH reaction for individual VOC and for different photochemical mechanisms; rates of formation of organic nitrates (which affect  $O_3/NO_x$ ); impact of nighttime formation of  $HNO_3$  via aerosol reactions; and the deposition rate of  $HNO_3$ .

Sillman (1995), Kleinman et al. (1997) and Tonnesen and Dennis (2000a) presented more detailed analyses of the chemistry of  $O_3$ - $NO_x$ -VOC sensitivity, based on the chemistry of odd hydrogen radicals. A summary is presented here. The odd hydrogen radicals include OH,  $HO_2$  and  $RO_2$  (including  $CH_3O_2$ ,  $CH_3CO_3$ , and analogous radicals). The chemistry of these species has a large influence on the ozone formation process.

Tonnesen and Dennis (2001) presented the cycle of odd hydrogen in terms of three stages: **chain initiation**, or radical sources (abbreviated as  $S_H$  in publications by Sillman et al. and as Q in the work of Kleinman et al.); **chain propagation**, or interconversion among OH,  $HO_2$  and  $RO_2$ ; and **chain termination**, or radical sinks. Chain initiation occurs through the photolysis of ozone (R5), photolysis of HCHO and other secondary VOC (R6), and reaction of alkenes with  $O_3$  (R7). Chain propagation occurs through reactions of CO and VOC with OH (R1) and reactions of  $HO_2$  and  $RO_2$  with NO (R2 and R3), each of which is part of the ozone formation sequence. Chain termination occurs through three processes: formation of peroxides (R8 and R9); formation of nitric acid (R10); and formation of PAN and other organic nitrates (R11).

It is easy to show that ozone formation will have  $NO_x$ -sensitive characteristics whenever peroxides represent the dominant odd hydrogen sink and VOC-sensitive characteristics whenever nitric acid represents the dominant sink. Because odd hydrogen radicals are short-lived, the sources and sinks must be in steady state:

$$S_H = 2P_{perox} + P_{HNO_3} + P_{orgN} \quad (3.1.2)$$

If peroxides represent the dominant sink, then the concentration of  $HO_2$  and  $RO_2$  (controlled by  $S_H$  and the quadratic loss rates through R8 and R9) is largely independent of  $NO_x$  and VOC, and the ozone formation rate (via  $HO_2+NO$  and  $RO_2+NO$ , R2 and R3) increases with increasing  $NO_x$ . If nitric acid represents the dominant sink, then OH (controlled by  $S_H$  and removal through  $OH+NO_2$ , R10) decreases with increasing  $NO_x$  and the ozone

formation rate (roughly proportional to VOC+OH, R1) increases with increasing VOC. Sillman (1995) and Kleinman et al. (1997) both found that the transition between NO<sub>x</sub>-sensitive and VOC-sensitive chemistry occurs when formation of peroxides and nitric acid are equal as odd hydrogen sinks ( $P_{perox}/P_{HNO_3}=0.5$ ). The transition between NO<sub>x</sub>-sensitive and NO<sub>x</sub>-saturated conditions (defined as NO<sub>x</sub> benefits versus disbenefits) occurs at a lower ratio ( $(P_{perox}/P_{HNO_3})\approx 0.3$ ). Figure 3.1.3 shows how the NO<sub>x</sub>-VOC transition in 0-d calculations is closely matched to the concentration ratio [peroxides]/[HNO<sub>3</sub>].

The controlling ratio  $P_{perox}/P_{HNO_3}$  can also be expressed (through Equation 3-1) in a different form:

$$2 \frac{P_{perox}}{P_{HNO_3}} = 1 \square \frac{S_H \square P_{orgN}}{P_{HNO_3}} \quad (3.1.3a)$$

If net production of organic nitrates is ignored, then this ratio becomes

$$2 \frac{P_{perox}}{P_{HNO_3}} = 1 \square \frac{S_H}{L_N} \quad (3.1.3b)$$

where  $L_N$  represents the removal rate for NO<sub>x</sub>.

The ratio  $S_H/L_N$  is used as the basis for the constrained steady state method developed by Kleinman et al. (1997) (see Section 3.3). Kleinman et al. expressed this ratio in reciprocal form as  $L_N/Q$ , where Q represents the radical source. Here, the transition between NO<sub>x</sub>-sensitive and VOC-sensitive conditions would occur at  $S_H/L_N=2$  (see Sillman et al., 2002). Results from Kleinman et al. (1997, 2000, 2001) and Sillman and He (2002) suggests that the NO<sub>x</sub>-VOC sensitivity of instantaneous ozone production rates is consistently related to this parameter. This provides a useful basis for understanding the photochemical factors associated with NO<sub>x</sub>-VOC sensitivity. The radical source ( $S_H$  or Q) is associated with sunlight, increases with VOC, and increases with the amount of time available for photochemical processing. The loss rate for NO<sub>x</sub> ( $L_N$ ) depends largely on the amount of NO<sub>x</sub> available.

The ambient ratio O<sub>3</sub>/NO<sub>z</sub> can be interpreted in these terms as a sum over time of the instantaneous chemical production ratio  $S_H/L_N$ . The major uncertainty in this interpretation is how O<sub>3</sub> is related to  $S_H$ . O<sub>3</sub> is related to  $S_x$  in part because photolysis of O<sub>3</sub> (reaction R5) is a direct source of radicals and in part because the source of radicals from hydrocarbons (R6 and R7) are associated with reaction sequences R1 and R2 which also lead directly to ozone

formation. Since photolysis of  $O_3$  is usually an important source of odd hydrogen, the relation between  $O_3$  and  $S_H$  should also vary depending on the extent of photochemical aging.

In the original 3-d models by Sillman (1995) it was found that the  $NO_x$ -VOC transition occurs at a lower value of  $O_3/NO_z$  early in the day, possibly due to the influence of photochemical aging. The ratio  $O_3/NO_z$  performs somewhat better as a  $NO_x$ -VOC indicator because it represents a ratio of reaction products ( $O_3/NO_z$ ) modified by a ratio related to photochemical aging ( $NO_z/NO_y$ ).

Table 3.1.2

## Chemical reactions relevant to ozone formation and odd hydrogen radicals

**Ozone formation sequence:**

- R1.  $\text{VOC} + \text{OH} \rightarrow \text{RO}_2$   
 R1a.  $\text{CO} + \text{OH} \rightarrow \text{HO}_2$   
 R2.  $\text{RO}_2 + \text{NO} \rightarrow \text{NO}_2 + \text{HO}_2 + \text{intermediate VOC}$   
 R3.  $\text{HO}_2 + \text{NO} \rightarrow \text{OH} + \text{NO}_2$   
 R4.  $\text{NO}_2 + h\nu \xrightarrow{\text{O}_2} \text{NO} + \text{O}_3$

**Sources of odd hydrogen radicals (chain initiation):**

- R5.  $\text{O}_3 + h\nu \xrightarrow{\text{H}_2\text{O}} 2\text{OH}$   
 R6.  $\text{HCHO} + h\nu \rightarrow 2\text{HO}_2 + \text{CO}$   
 R6a. other aldehydes +  $h\nu \rightarrow \text{HO}_2, \text{RO}_2, \text{RCO}_3$   
 R7. Olefin +  $\text{O}_3 \rightarrow \text{OH}, \text{HO}_2, \text{intermediate VOC}$

**Sinks for odd hydrogen (chain termination):**

- R8.  $\text{HO}_2 + \text{HO}_2 \rightarrow \text{H}_2\text{O}_2$   
 R9.  $\text{HO}_2 + \text{RO}_2 \rightarrow \text{ROOH}$   
 R10.  $\text{OH} + \text{NO}_2 \rightarrow \text{HNO}_3$   
 R11.  $\text{CH}_3\text{CO}_3 + \text{NO}_2 \rightarrow \text{PAN (net formation)}$

## 3.2 SMOG PRODUCTION ALGORITHMS (EXTENT OF REACTION PARAMETERS)

### 3.2.1. Summary information

- *Smog production algorithms* (also known as extent-of-reaction parameters) refers to a series of parameters developed by Johnson (1984), Hess et al. (1992a, b and c), Chang et al. (1997) and Blanchard et al. (1999, 2000) to analyze O<sub>3</sub>-NO<sub>x</sub>-VOC sensitivity. The parameters all involve measured O<sub>3</sub>, NO<sub>x</sub> and/or NO<sub>y</sub>.
- The distinctive feature of smog production algorithms (as opposed to NO<sub>x</sub>-VOC indicators) is that the smog algorithms are derived from smog chamber experiments, whereas the NO<sub>x</sub>-VOC indicators discussed in Section 3.1 (often involving the same species) were derived from 3-d photochemical models.
- The smog production algorithms are based on the concept that the rate of ozone production in fresh emissions is always VOC-sensitive, and that conditions become NO<sub>x</sub>-sensitive when the initial NO<sub>x</sub> concentration of the air mass has reacted away. VOC-sensitive versus NO<sub>x</sub>-sensitive conditions can be diagnosed through parameters that represent the extent of reaction.
- The parameter  $(1-\text{NO}_x/\text{NO}_y)$  has been widely used by researchers to represent extent of reaction or photochemical aging (e.g. Trainer et al., 1993; Olszyna et al., 1994). Here, the term “smog production algorithms” will be used to refer to the specific theory that extent of reaction may be used to identify NO<sub>x</sub>-VOC sensitivity.
- Several forms of smog production algorithms have been developed. The major alternatives are based on the ratios  $(\text{O}_3-\text{O}_{3b})/\text{NO}_y$ ,  $\text{NO}_x/\text{NO}_y$  and  $(\text{O}_3-\text{O}_{3b})/\text{NO}_x$ .
- The smog production algorithms were developed from chamber experiments that represent an initial large concentration of VOC and NO<sub>x</sub>, followed by photochemical evolution without additional emissions. It is unclear whether the relationships derived from these experiments are applicable to ambient conditions, which have a complex pattern of continuous anthropogenic and biogenic emissions.
- The smog algorithms have been widely used to evaluate NO<sub>x</sub>-VOC chemistry in the U.S., and have included evaluations of data over several years rather than just for individual events. These evaluations have consisted primarily of deriving the measured smog production parameters and interpreting them as evidence for NO<sub>x</sub>-VOC sensitivity. There has been very little interpretation of measured data to determine the viability of the method.

- Evaluation of smog production parameters in comparison with  $\text{NO}_x$ -VOC predictions in 3-d models has yielded mixed results. The smog production parameters based on  $(\text{O}_3-\text{O}_{3b})/\text{NO}_y$  are generally correlated with  $\text{NO}_x$ -VOC sensitivity in models. Parameters based on  $\text{NO}_x/\text{NO}_y$  and  $(\text{O}_3-\text{O}_{3b})/\text{NO}_x$  show a much worse correlation.
- The smog production parameters recommended by Chang et al. (1997) and Blanchard et al. (1999) have the form  $(\text{O}_3-\text{O}_{3b})/\text{NO}_y^\alpha$  where the exponent  $\alpha$  is 0.5 or 0.67. Model results suggest that simpler ratio,  $(\text{O}_3-\text{O}_{3b})/\text{NO}_y$ , is correlated more closely with  $\text{NO}_x$ -VOC sensitivity.
- Smog production algorithms assume zero deposition. A rough calculation is added to represent deposition.

### 3.2.2. Conclusions and recommendations

- Smog production algorithms appear to give meaningful results primarily in situations with strongly VOC-sensitive chemistry. They are less successful at distinguishing moderately VOC-sensitive conditions from  $\text{NO}_x$ -sensitive conditions.
- Smog production algorithms based on measured  $\text{NO}_x/\text{NO}_y$  or  $\text{O}_3/\text{NO}_x$  are unreliable and should not be used.
- The conclusions given in Section 3.1.2 for  $\text{NO}_x$ -VOC indicators also generally apply for smog production algorithms. Smog production algorithms require accurate measurement of  $\text{NO}_y$ ; they should be developed in the form of predicted species correlations rather than just used as a “rule of thumb”; and their use should be expanded to include a measurement-based evaluation of model predictions.

### 3.2.3. The smog production concept: results from smog chambers

The smog production concept, originally developed by Johnson (1984) and originally presented in scientific literature by Hess et al. (1992a, 1992b, 1992c) was based on a series of observations in smog chamber experiments. In these experiments it was found that the amount of smog produced (SP, defined as  $(\text{O}_3-\text{NO})-(\text{O}_3-\text{NO})_{\text{background}}$ ) increased linearly with time, where time elapsed was measured as the integrated sum of incident sunlight (expressed as  $\int j_{\text{NO}_2} dt$ , where  $j_{\text{NO}_2}$  represents the  $\text{NO}_x$  photolysis rate). The amount of smog produced in the experiments increased linearly up to the point where all the initial  $\text{NO}_x$  had reacted away. After that the amount of smog produced remained constant. Johnson and Hess et al. found that the final (maximum) amount of smog produced depended entirely on the initial amount of  $\text{NO}_x$  in the experiment and was independent of VOC. They also found that the rate of smog production during the initial phase depended on the amount of VOC.

Johnson interpreted as evidence that  $\text{NO}_x$ -VOC chemistry could be analyzed in terms of the extent of reaction of ambient  $\text{NO}_x$ . As a mixture of freshly emitted  $\text{NO}_x$  and VOC began producing ozone, the rate of ozone formation was limited by the availability of sunlight, expressed as the time integrated sum of  $j_{\text{NO}_2}$ . This “light-limited” regime corresponds to VOC-sensitive or  $\text{NO}_x$ -saturated conditions. After the initial  $\text{NO}_x$  has reacted to the point where the remaining  $\text{NO}_x$  is very low the mixture reaches the  $\text{NO}_x$ -limited regime, and additional smog formation is possible only if more  $\text{NO}_x$  is added.  $\text{NO}_x$ -sensitive conditions thus correspond to a situation in which the available  $\text{NO}_x$  has reacted to completion (high extent of reaction), whereas VOC-sensitive conditions correspond to situations in which the  $\text{NO}_x$  has not yet reacted completely (low extent of reaction).

In subsequent experiments it was found that additional injection of either VOC or  $\text{NO}_x$  produced results that were consistent with this analysis of light-limited and  $\text{NO}_x$ -limited regimes. A subsequent injection of  $\text{NO}_x$  would not affect the rate of smog production, but would allow smog formation to continue to a higher final total amount. A subsequent injection of VOC would cause the rate of smog production to increase, but it would not increase the final amount of smog, and would not cause a further increase if the initial  $\text{NO}_x$  had been reacted to completion. These experiments are illustrated in Figure 3.2.1. As shown in the figure, these patterns were reproduced in calculations using the CB-IV photochemical mechanism. Similar patterns were also found in 0-d calculations (Blanchard et al., 1999).

Based on these results, it was proposed that ozone chemistry could be evaluated in terms of an extent-of-reaction parameter, defined as:

$$Extent = \frac{SP}{SP_{\max}} \quad (3.2.1)$$

where  $SP_{\max}$  represents the maximum possible smog production if all the available  $\text{NO}_x$  were processed.  $SP_x$  was viewed as a function of the initial  $\text{NO}_x$  ( $\text{NO}_x(i)$ ) available in the air mass, which would be approximated from measurements. The subsequent smog production algorithms were all based on this form.

Johnson’s original algorithm used ambient  $\text{NO}_y$  to represent  $SP_{\max}$ . The resulting extent parameter from Johnson (1990) was

$$ExtentJ = \frac{O_3 - O_{3b} - NO + 0.9NO_y}{4.09NO_y} \quad (3.2.2)$$

This extent parameter has an obvious similarity to the indicator ratio  $(O_3 - O_{3b}) / (NO_y - NO_{yb})$ , developed much later by Sillman (1995). The ratio 4.09 represents the rate of ozone production per  $NO_x$ , assuming that all  $NO_x$  has reacted to completion. The implied result is that ozone production efficiency per  $NO_x$  always has a constant value (4.09) after the emitted  $NO_x$  has reacted completely.

Chang et al. (1997) and Blanchard et al. (1999, 2000) both generated modified forms of the original extent parameter. Blanchard et al. found that the final amount of ozone produced in smog chamber experiments ( $SP_{max}$ ) was not an exact linear function of initial  $NO_x$  ( $NO_x(i)$ ) and that  $SP_{max}$  is better represented by  $[NO_x(i)]^\square$ , with  $\square$  estimated at 0.5 by Chang and 0.67 by Blanchard, rather than by  $[NO_x(i)]$ . The correlation between  $SP_{max}$  and  $NO_x(i)$  reported by Blanchard is shown in Figure 3.2.2. Blanchard et al. also generated extent formulas based on  $NO_x/NO_y$ , and  $O_3/NO_x$ , in addition to a modified version of the original formula based on  $O_3/NO_y$ . The extent parameters proposed by Blanchard et al. (1999) were as follows. The parameter based on  $O_3/NO_y$  used the following format:

$$ExtentB1 = \frac{O_3 + D[O_3] - O_{3b} - NO + 0.95NO_x(i)}{19(NO_x(i))^{0.67}} \quad (3.2.3a)$$

where  $NO_x(i)$  is determined from ambient  $NO_y$ :

$$NO_x(i) = NO_y + D[NO_y] \quad (3.2.3b)$$

here, all species concentrations refer to ambient measurements at the location for which  $O_x$ - $NO_x$ -VOC sensitivity is being investigated. As was the case for  $NO_x$ -VOC indicators, the smog production formulas provide evidence about  $NO_x$ -VOC sensitivity of ozone concentrations (not instantaneous production rates), only at the exact time and place of the measured values.  $D[O_3]$  and  $D[NO_y]$  represent estimates for loss of  $O_3$  and  $NO_y$  through deposition as the air mass has traveled from the emission source to the measurement site. Deposition is not included in any of the smog production formulas. Blanchard et al. recommend that deposition rates be calculated for a time interval beginning at sunrise and ending at the (afternoon) hour (t) being evaluated, as follows:

$$D[O_3] = \frac{36 \int_{t=0600}^t v_d(\Delta) O_3(\Delta)}{z(t)} \quad (3.2.4a)$$

where  $v_d(\Delta)$  represents the time-varying deposition velocity in  $\text{cm s}^{-1}$  and  $z(t)$  represents the mixing height (m) at the hour being evaluated. They recommend that deposition velocity be approximated using a formula for diurnal variation:

$$v_d(t) = N + A \sin \frac{2\Delta(t - 0600)}{2800} \quad (3.2.4b)$$

with the above formula applied for daylight hours only, and the minimum diurnal deposition velocity (N) used at night. Deposition of  $\text{NO}_y$  would be determined in similar fashion. They recommend using  $N=0.2 \text{ cm s}^{-1}$  and  $A=0.3 \text{ cm s}^{-1}$  for both  $\text{O}_3$  and  $\text{NO}_y$ .

The smog production algorithm based on  $\text{NO}_x/\text{NO}_y$  is:

$$\text{ExtentB2} = \left[ \frac{\text{NO}_x}{\text{NO}_x(i)} \right]^{0.67} \quad (3.2.5)$$

where  $\text{NO}_x(i)$  is determined from measured  $\text{NO}_y$  as in Equation 3.2.3b.

The smog production algorithm based on  $\text{O}_3/\text{NO}_x$ , referred to here as ExtentB3, uses Equation 3.2.3a with the following determination of  $\text{NO}_x(i)$ :

$$\text{NO}_x(i) = \text{NO}_x + 296.3[2X + 1]^3 \quad (3.2.6)$$

where

$$X = \cos \left[ \frac{1}{3} \{ 4\Delta + \cos^{-1}(C) \} \right] \quad (3.2.7a)$$

$$C = 1 - (0.00177632)\Delta \quad (\text{for } -1 \leq C \leq 1) \quad (3.2.7b)$$

$$\Delta = O_3 + D[O_3] - O_{3b} - \text{NO} + 0.95\text{NO}_x \quad (3.2.7c)$$

Chang et al. (1997) used a different formula, also based on  $O_3/NO_y$  and similar to the first extent formula from Blanchard et al.

$$ExtentC = \frac{1.1O_3 \square O_{3b} \square NO + 1.29NO_y}{34.04NO_y^{0.5} + 1.29NO_y} \quad (3.2.8)$$

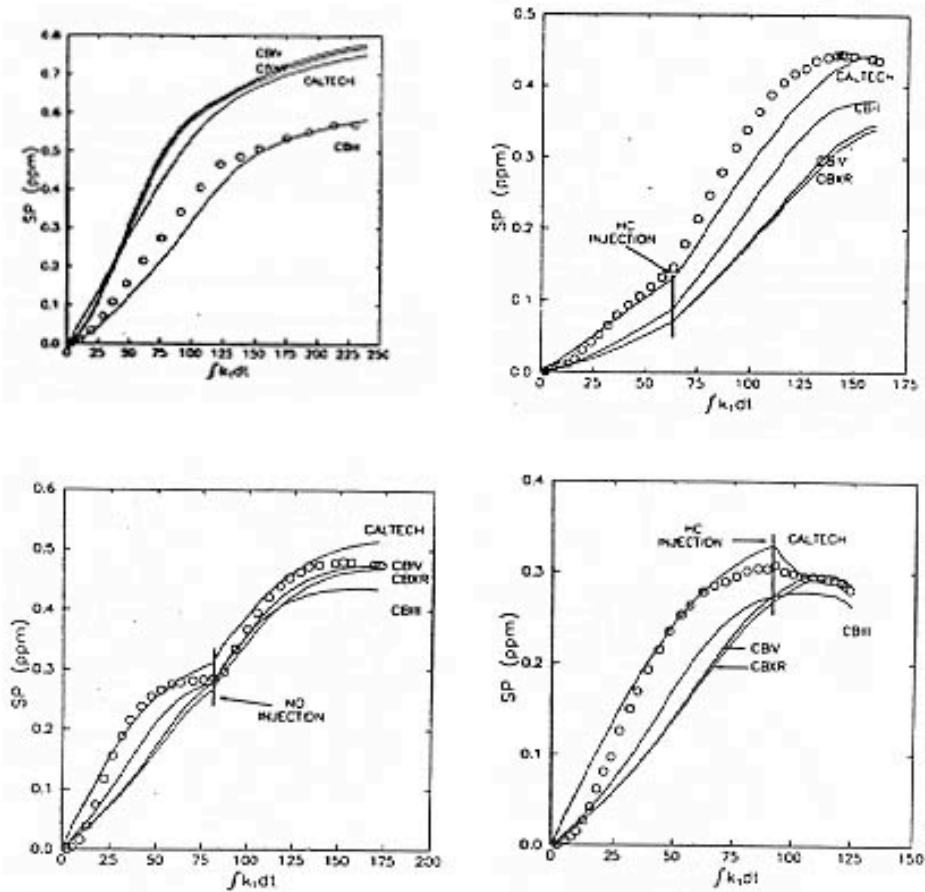


**Figure 3.2.1.** Results of smog chamber experiments associated with the smog production algorithms. The circles show smog produced (defined as  $(O_3-NO)-(O_3-NO)_{\text{background}}$ ), in ppm versus summed incident sunlight ( $\int j_{NO_2} dt$ ) in smog chamber experiments. Solid lines show equivalent calculations with photochemical mechanisms. The smog chambers all begin with a fixed amount of VOC and NO. Experiments include the impact of injected additional VOC and NO. From Hesse et al. (1992c).

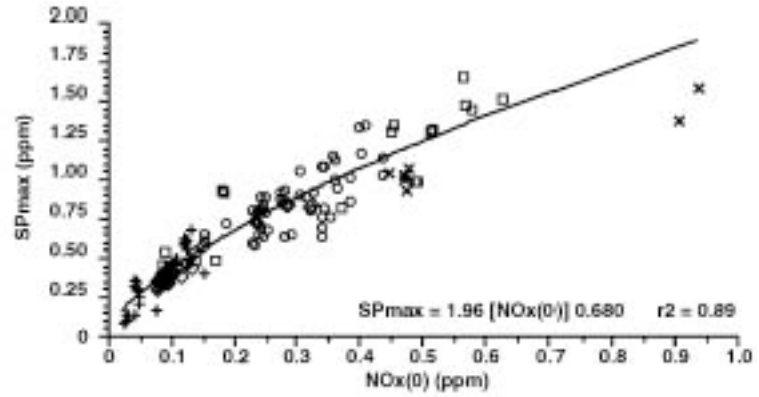


**Figure 3.2.2.**  $SP_{max}$  versus initial  $NO_x$  concentration (in ppm) from UNC, SAPRC and CSIRO smog chamber experiments. The regression line (solid line) is shown converted into concentration units. From Blanchard et al. (1999).

### 3.2.4. Evaluations with 3-d models

Chang et al. (1997), Tonnesen and Dennis (2000b) and Blanchard and Stoeckenius (2001) all presented evaluations of the smog production formulas against 3-d model predictions. These evaluations generally followed the same format as used by Sillman (1995) for  $\text{NO}_x$ -VOC indicators. Models were run for an initial scenario, an equivalent scenario with reduced anthropogenic VOC throughout the model domain (typically by 25%-50%), and an equivalent scenario with reduced anthropogenic  $\text{NO}_x$  by the same percent. The predicted reduction in  $\text{O}_3$  at a specific hour in the afternoon (corresponding to maximum or near-maximum  $\text{O}_3$ ) in the scenarios with reduced VOC and reduced  $\text{NO}_x$  was compared with the value of the extent parameter in the initial scenario at the same time and location. The extent parameters were calculated from predicted species concentrations in the model scenario and represent a potentially measurable quantity. The model evaluations generally used extent parameters based on  $\text{O}_3/\text{NO}_y$  from Chang et al. (1997) (Equation 3.2.8) or Blanchard et al. (1999) (Equation 3.2.3). Blanchard et al. (1999) also reported some results for the extent parameter based on  $\text{NO}_x/\text{NO}_y$  (Equation 3.2.5). Results for the parameters based on  $\text{NO}_x/\text{NO}_y$  and  $\text{O}_3/\text{NO}_y$  are also discussed as contrary evidence in Section 3.2.5.

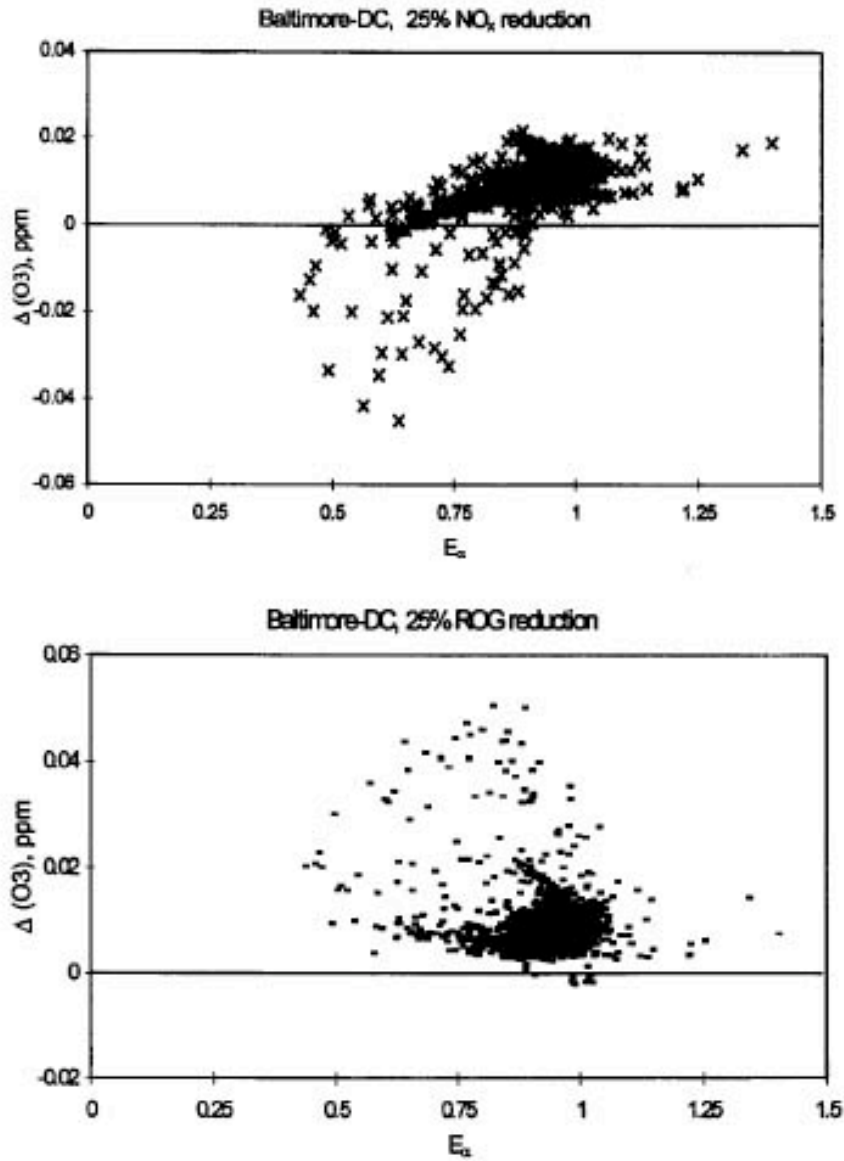
The general conclusion of the model-based studies is that an extent parameter below 0.6 is reliably associated with VOC-sensitive conditions, and an extent parameter of 0.9 or above is reliably associated with  $\text{NO}_x$ -sensitive conditions.  $\text{NO}_x$ -VOC sensitivity was variable for extent parameters between 0.6 and 0.9. The low (VOC-sensitive) extent parameters are generally associated with urban centers in models. Extent parameters above 0.9 generally occurred in rural areas with relatively low  $\text{O}_3$  and little sensitivity to VOC or  $\text{NO}_x$ . Blanchard and Stoeckenius (2001) regarded extent parameters above 0.8 as representing  $\text{NO}_x$ -sensitive conditions.

Chang et al. (1997) reported results for UAM-IV simulations (with CB-IV photochemistry) of events in Baltimore and Los Angeles (Figure 3.2.3). Tonnesen and Dennis (2000b) reported results from RADM simulations (with chemistry from Stockwell et al. 1990) of two events in New York (Figure 3.2.4). These results both used the extent parameter from Chock et al. (1997).

Blanchard and Stoeckenius (2001) reported results from simulations using different versions of UAM or the similar CAMx model for Los Angeles, Lake Michigan and southeast Texas, from simulations for the San Joaquin valley using SAQM (Lu and Chang, 1998), and from simulations for Lake Michigan and the northeast corridor from

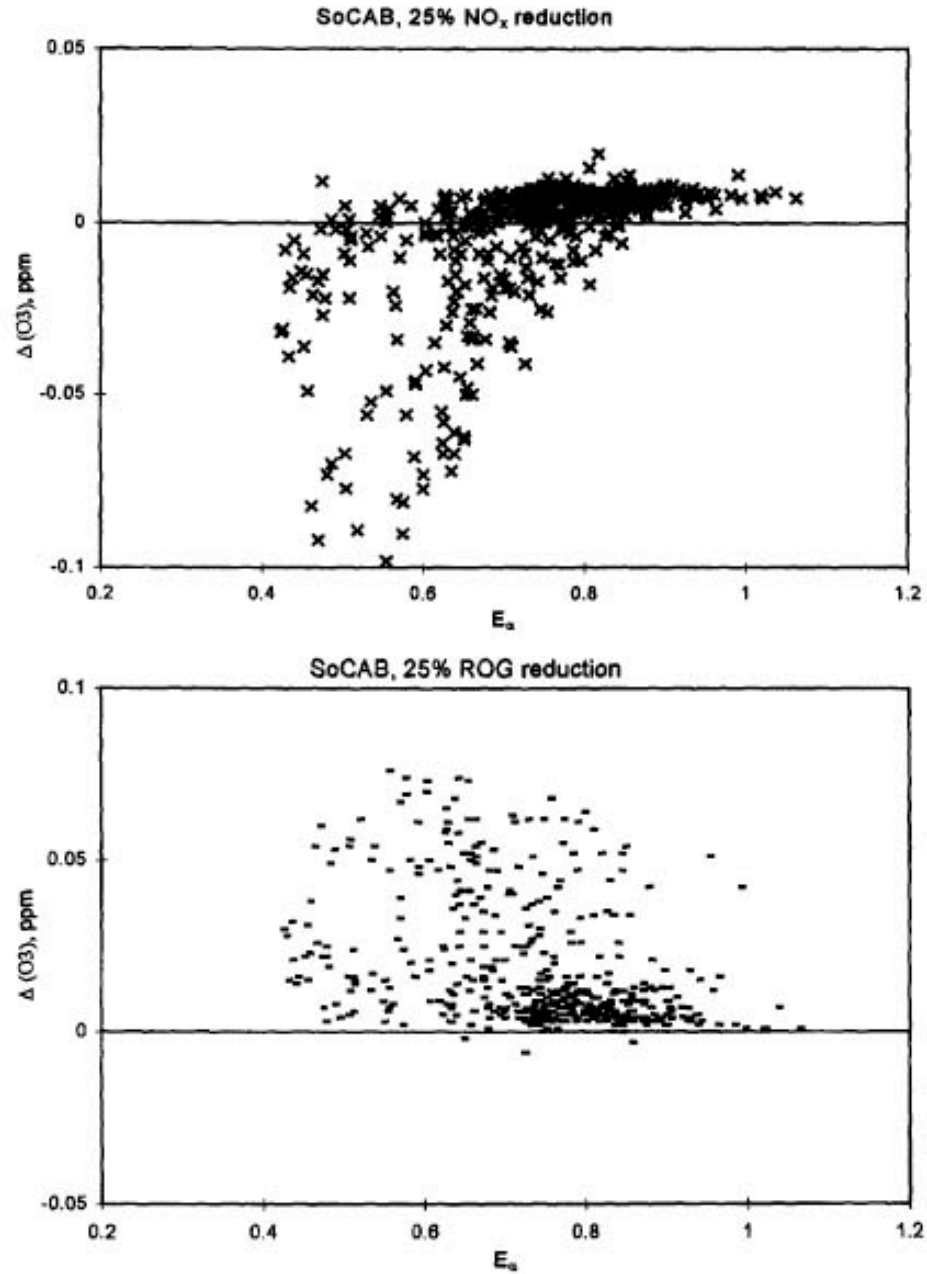
Sillman et al. (1993). These simulations all used versions of the CB-IV mechanism, except for the simulations from Sillman et al. (1993) which used a modified form of Lurmann et al. 1986. Results are shown in Figure 3.2.5.

Blanchard and Stoeckenius did a similar analysis of the indicator ratios  $O_3/NO_y$  and  $O_3/NO_z$ . They concluded that both the extent parameter and  $O_3/NO_y$  and  $O_3/NO_z$  could reliably separate  $NO_x$ -sensitive and VOC-sensitive locations, but only for relatively extreme values (extent below 0.6 or above 0.8,  $O_3/NO_y$  below 4 or above 8, and  $O_3/NO_z$  below 5 or above 10). Blanchard and Stoeckenius also reported cases of erroneous or ambivalent results, primarily for  $O_3/NO_y$  and  $O_3/NO_z$  but also for extent parameters, due to scenarios with different boundary conditions (see Section 3.1.5). Tonnesen and Dennis, by contrast, reported that the other indicator ratios generated a sharper separation of  $NO_x$ -sensitive and VOC-sensitive locations in their model than the extent parameter.



(a) Baltimore

**Figure 3.2.3.** Predicted reduction in O<sub>3</sub> resulting from a 25% reduction in anthropogenic VOC (X's) and from a 25% reduction in NO<sub>x</sub> (dashes), plotted against a version of the extent parameter (similar to Equation 3.2.3) from simulations using UAM-IV for Baltimore and Los Angeles. From Chang et al. (1997).



(b) Los Angeles

**Figure 3.2.3.** Predicted reduction in O<sub>3</sub> resulting from a 25% reduction in anthropogenic VOC (X's) and from a 25% reduction in NO<sub>x</sub> (dashes), plotted against a version of the extent parameter (similar to Equation 3.2.3) from simulations using UAM-IV for Baltimore and Los Angeles. From Chang et al. (1997).

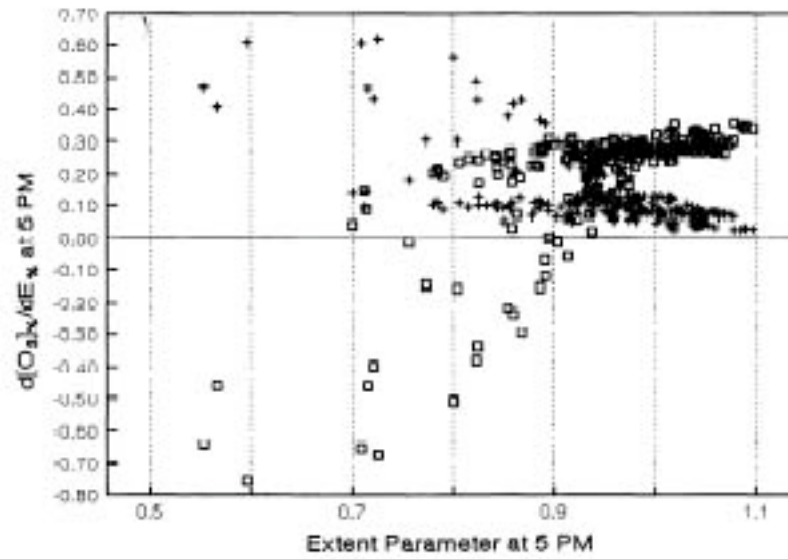


**Figure 3.2.4.** Predicted reduction in  $\text{O}_3$  resulting from a 30% change in anthropogenic VOC (+'s) (from +15% to -15% relative to base case emission rates) and from an equivalent 30% change in  $\text{NO}_x$  (squares), plotted against the version of the extent parameter used by Chang et al. (1997) (similar to Equation 3.2.3) from simulations using RADM for New York City. From Tonnesen and Dennis (2000b).

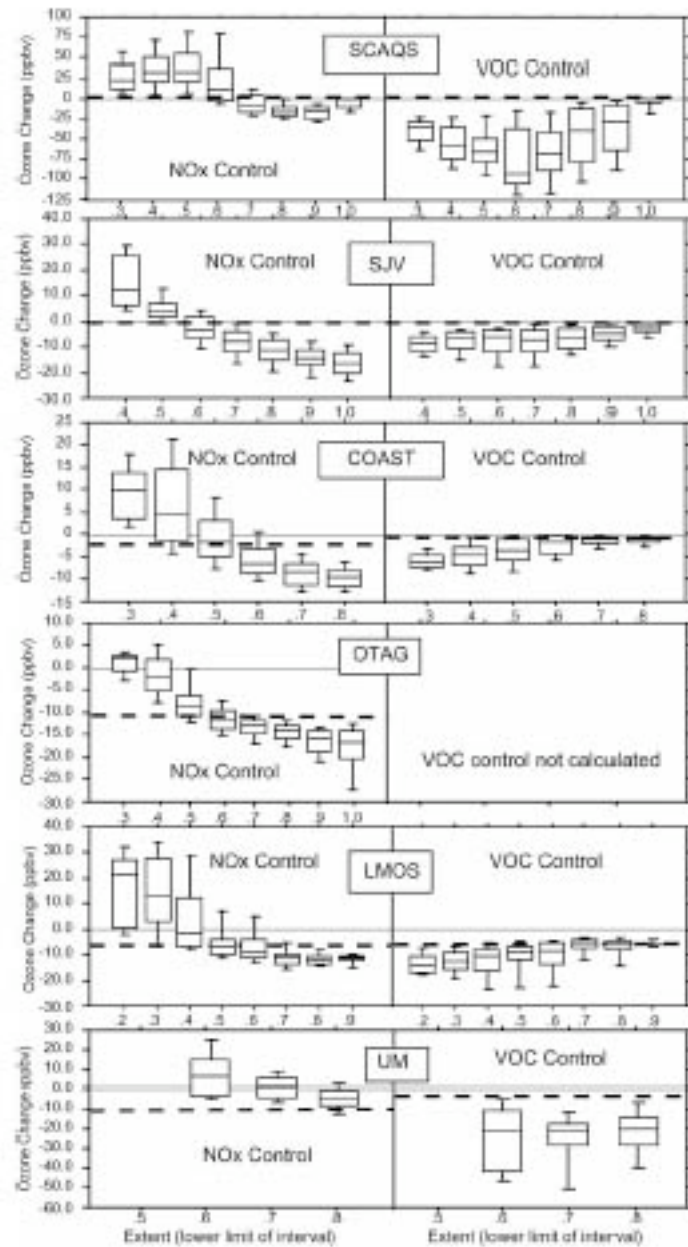


**Figure 3.2.5.** Statistical summary of predicted response of peak ozone to a change in emissions of either  $\text{NO}_x$  or VOC emissions versus extent of reaction parameter (Equation 3.2.3) in the model base case. The statistical summaries are presented as box plots, which show the 10<sup>th</sup>, 25<sup>th</sup>, 50<sup>th</sup>, 75<sup>th</sup> and 90<sup>th</sup> percentile response for all grid cells having  $\text{O}_3$  above 80 ppb and extent within 0.1-unit intervals (labeled using the lower limit of each interval). The dashed line shows the control response at the upwind model boundary. In contrast to the other figures in this report, positive responses represent an increase in  $\text{O}_3$  in response to reduced emissions. Negative responses represent a reduction in  $\text{O}_3$  in response to reduced emissions. From Blanchard and Stoeckenius (2001).

### 3.2.5. Contrary evidence

Sillman and He (2002) reported results from the five simulations shown in Table 3.1.1. These results included all three versions of the extent parameter proposed by Blanchard et al. (1999). They found a correctible flaw in the extent parameter based on  $O_3/NO_y$  and fundamental problems in the extent parameters based on  $NO_x/NO_x$  and  $O_3/NO_x$ . Results are shown in Figures 3.2.6 and 3.2.7.

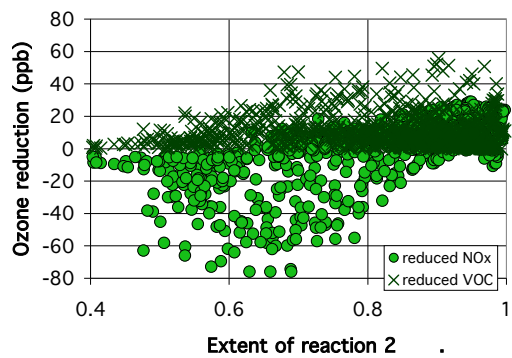
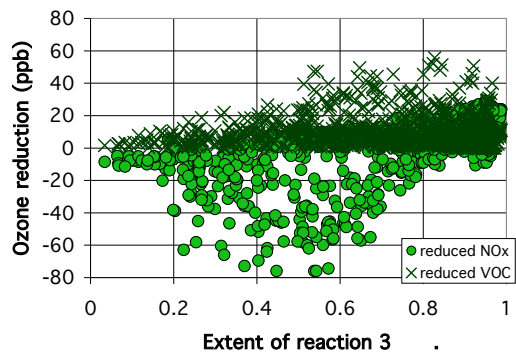
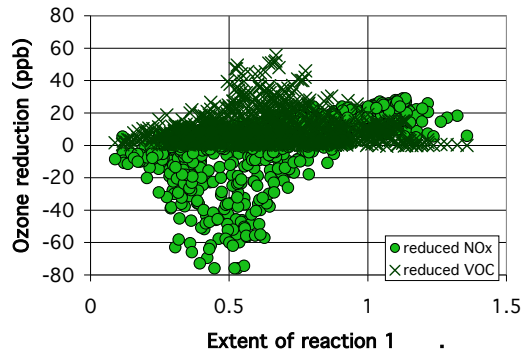
As shown in Figure 3.2.6,  $NO_x$ -sensitive locations are generally associated with high values of the first extent parameter (above 0.9) and VOC-sensitive locations are associated with low values (below 0.6). However there is also considerable overlap between  $NO_x$ -sensitive and VOC-sensitive parameter values. Strongly VOC-sensitive locations have extent parameters as high as 0.9, and strongly  $NO_x$ -sensitive locations include extent parameters as low as 0.6. This result is not dissimilar to the model-based results reported in Figures 3.2.3, 3.2.4 and 3.2.5 but is given a different emphasis. There is significantly less overlap between  $NO_x$ -sensitive and VOC-sensitive locations if the ratio  $(O_3-O_{3b})/(NO_y-NO_{yb})$  were used instead of the extent parameter (see Figure 3.1.2). This ratio, discussed as a  $NO_x$ -VOC indicator in Section 3.1.3b, is actually very similar to the original extent parameter (equation 3.2.2) proposed by Johnson.

Figure 3.2.7 shows the same results in the form of extent parameters plotted versus  $O_3$ . The locations in this plot have been classified as  $NO_x$ -sensitive, mixed or VOC-sensitive as was done above in Figure 3.1.7, using definitions described in Section 3.1.10. Here, it appears that the extent parameter can consistently separate  $NO_x$ -sensitive and VOC-sensitive locations, but that the transition between  $NO_x$ -sensitive and VOC-sensitive locations changes between regions of low and high ozone. Locations with  $O_3$  between 80 and 120 ppb fit the description given by Blanchard and Stoeckenius, with VOC-sensitive conditions corresponding to extent below 0.6 and  $NO_x$ -sensitive conditions corresponding to extent above 0.8. For  $O_3$  above 130 ppb, locations with extent equal to 0.8 or below are almost all VOC-sensitive, locations with extent above 0.95 (including many locations with extent greater than 1) are  $NO_x$ -sensitive. By contrast, the ratio  $(O_3-O_{3b})/(NO_y-NO_{yb})$  shows a consistent pattern for both low and high  $O_3$ , with VOC-sensitive conditions corresponding to  $(O_3-O_{3b})/(NO_y-NO_{yb})$  below 4 and  $NO_x$ -sensitive conditions corresponding to  $(O_3-O_{3b})/(NO_y-NO_{yb})$  above 6.

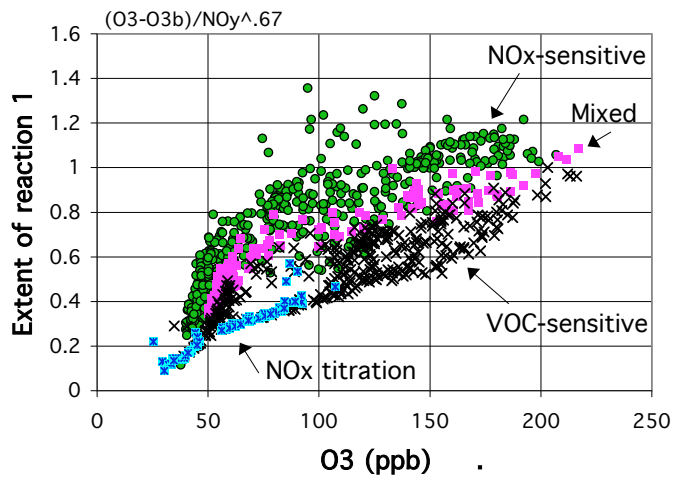
This comparison suggests that the modified form proposed by Chang et al. and Blanchard et al. (involving  $O_3/NO_y$  rather than  $O_3/NO_x$ ) may be a mistake for ambient conditions. Isopleth plots for  $(O_3-O_{3b})/(NO_z-NO_{zb})$  based on a 0-d model and constant emissions (Figure 3.1.3, Section 3.1.4) are also consistent with this result.

Results obtained with the extent parameters based on  $NO_x/NO_y$  and  $O_3/NO_x$ , also shown in Figures 3.2.6 and 3.2.7, show a much weaker correlation with  $NO_x$ -VOC sensitivity. For the extent parameter based on  $NO_x/NO_y$ , parameter values below 0.6 are consistently associated with  $NO_x$  disbenefits. Locations with the highest values also include the strongest predicted  $NO_x$  benefits. However, parameter values above 0.7 include both  $NO_x$ -sensitive and VOC-sensitive locations, and strongly VOC-sensitive locations can be found with extent parameters as high as 0.98. The poor results are associated largely with the model for Lake Michigan reported by Sillman et al. (1993). In this model a strongly VOC-sensitive plume from the Chicago area is transported across Lake Michigan and remains VOC-sensitive even after most of its  $NO_x$  has reacted away. However, the other models also include strongly VOC-sensitive locations with extent close to 0.9. The extent parameter based on  $O_3/NO_x$  also shows ambiguous results. As in the case of  $NO_x/NO_y$ , contrary results occur because ozone can retain VOC-sensitive characteristics even after most of its  $NO_x$  has reacted away.

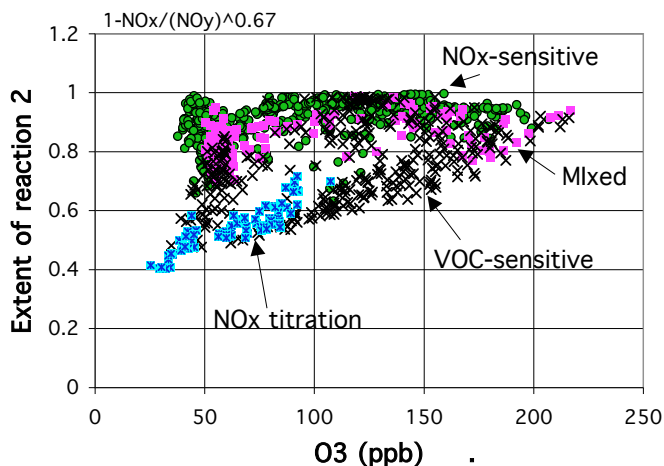
Calculations with the 0-d model described in Section 3.1.4 also provide contrary evidence concerning the extent parameter based on  $NO_x/NO_y$ . As shown in isopleth plots (Figure 3.2.8), a high value of  $NO_x/NO_y$  (corresponding to a low extent parameter) is associated with strongly  $NO_x$ -saturated conditions. However, low values of  $NO_x/NO_y$  are associated with either  $NO_x$ -sensitive or VOC-sensitive conditions. The isopleth pattern for  $(O_3-O_{3b})/NO_z$ , shown above in Figure 3.1.4, correlates more closely with  $NO_x$ -VOC sensitivity. These isopleth plots are based on calculations with continuous emissions. By contrast, the smog chamber experiments used to derive the extent parameters were all based on an initial high concentration of  $NO_x$  and VOC.



**Figure 3.2.6.** Predicted reductions in ozone in response to a percent reduction in emissions of anthropogenic VOC (crosses), and predicted reductions in response to the same percent reduction in emissions of anthropogenic  $\text{NO}_x$  (green circles), plotted versus model values for three extent parameters (B1, B2 and B3, defined in Equations 3.2.3, 3.2.5 and 3.2.8), for the five model scenarios from Table 3.1.1. Percent reductions are either 25% or 35% in individual scenarios. Based on results shown in Sillman and He (2002).

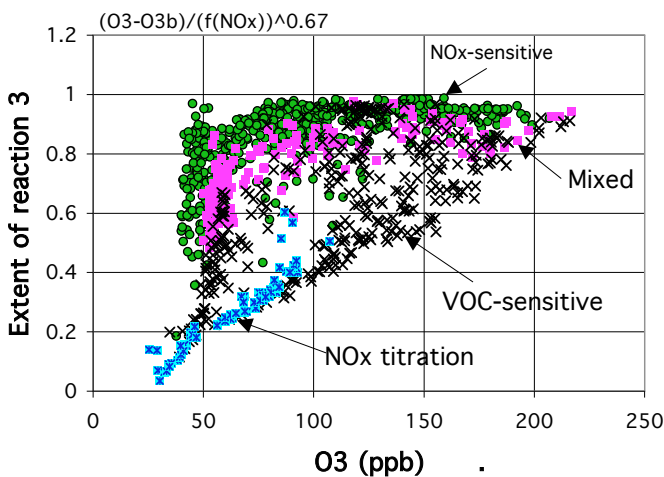


(a) ExtentB1 (Equation 3.2.3).

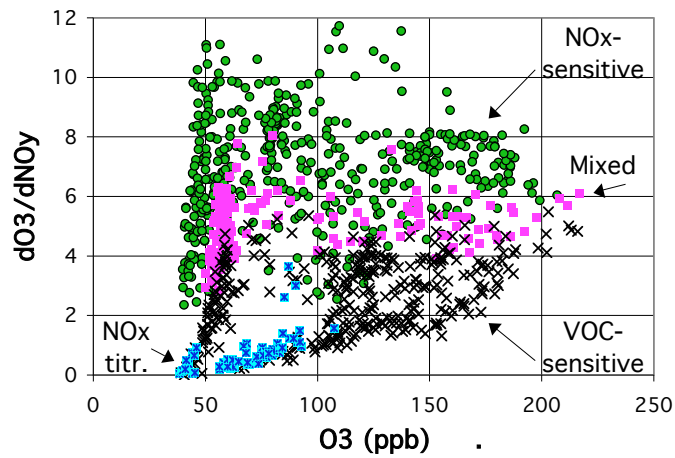


(b) ExtentB2 (Equation 3.2.5).

**Figure 3.2.7.** Extent of reaction versus O<sub>3</sub> for five model scenarios listed in Table 3.1.1. Each location is classified as NO<sub>x</sub>-sensitive (green circles), VOC-sensitive (crosses), mixed or with near-zero sensitivity (lavender squares), and dominated by NO<sub>x</sub> titration (blue asterisks) based on definitions in the text. Results are shown for the three extent parameters (B1, B2 and B3, defined in Equations 3.2.3, 3.2.5 and 3.2.8). Results for the ratio  $(O_3 - O_{3b}) / (NO_y - NO_{yb})$  are shown for comparison. From Sillman and He (2002).



(c) ExtentB3 (Equation 3.2.8).

(d)  $(O_3 - O_{3b}) / (NO_y - NO_{yb})$ 

**Figure 3.2.7.** Extent of reaction versus  $O_3$  for five model scenarios listed in Table 3.1.1. Each location is classified as NO<sub>x</sub>-sensitive (green circles), VOC-sensitive (crosses), mixed or with near-zero sensitivity (lavender squares), and dominated by NO<sub>x</sub> titration (blue asterisks) based on definitions in the text. Results are shown for the three extent parameters (B1, B2 and B3, defined in Equations 3.2.3, 3.2.5 and 3.2.8). Results for the ratio  $(O_3 - O_{3b}) / (NO_y - NO_{yb})$  are shown for comparison. From Sillman and He (2002).

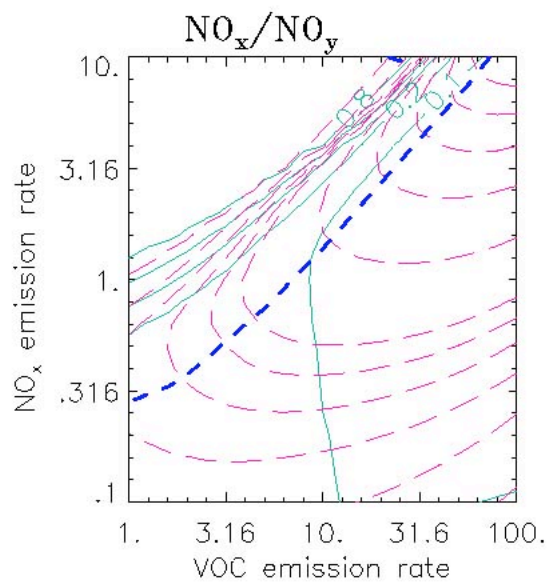


**Figure 3.2.8.** Isopleths for  $\text{NO}_x/\text{NO}_y$  as a function of the average emission rate for  $\text{NO}_x$  and VOC ( $10^{12}$  molec.  $\text{cm}^{-2} \text{s}^{-1}$ ) in 0-d calculations. The isopleths represent conditions during the afternoon following 3-day calculations, at the hour corresponding to maximum  $\text{O}_3$ . Isopleths are shown as solid green lines. Isopleths for  $\text{O}_3$  in ppb (red dashed lines) are superimposed (see also Figure 1.2 and Figure 3.1.4). The short blue dashed line represents the transition from VOC-sensitive to  $\text{NO}_x$ -sensitive conditions. From Sillman and He (2002).

### 3.2.6. Uncertainties associated with the theoretical basis

One problem with the extent parameters is the lack of a theoretical justification that would provide a causal link between extent parameters and  $\text{NO}_x$ -VOC sensitivity.

It is generally known that locations near urban centers and other large emission sources are often VOC-sensitive, while downwind locations are often  $\text{NO}_x$ -sensitive (Milford et al., 1989; 1994). It is also known that plumes from urban areas and power plants tend to change from  $\text{NO}_x$ -saturated to  $\text{NO}_x$ -sensitive as they move downwind (Milford et al., 1994; Gillani et al., 1996). This trend has been attributed to the more rapid removal of  $\text{NO}_x$  relative to VOC as a plume moves downwind, causing its  $\text{VOC}/\text{NO}_x$  ratio to increase. The trend is also due to the presence of biogenic VOC in rural areas. However, there is no reason why the transition from VOC-sensitive to  $\text{NO}_x$ -sensitive conditions should be associated with a certain extent of reaction.

Ozone isopleth plots generally show that air with a high ratio of VOC to  $\text{NO}_x$  should have  $\text{NO}_x$ -sensitive chemistry, regardless of whether the air consists of fresh or aged emissions. In theory,  $\text{NO}_x$ -sensitive chemistry is possible even with an extent parameter near zero, if emissions consist of strongly reactive VOC and a high  $\text{VOC}/\text{NO}_x$  ratio. No such conditions have appeared in either the smog chamber experiments or in the model results, but these may be based more on the specific conditions in the tests.

The extent parameters are all based on the assumption that cumulative ozone production per  $\text{NO}_x$  reaches a specified value in aged air, after most of the emitted  $\text{NO}_x$  has reacted away, and that the final ozone production per  $\text{NO}_x$  is unaffected by the amount of VOC. Ryerson et al. (2001) reported that ozone production per  $\text{NO}_x$  varies by a factor of 3 among plumes from power plants and with urban areas, even after the plume  $\text{NO}_x$  content has largely reacted away. Figure 3.2.9 compares measured  $\text{O}_3$  versus  $\text{NO}_z$  in two power plant plumes, both with similar reactive nitrogen content but with different amounts of biogenic VOC. Extent of reaction was similar in both plumes ( $\text{NO}_x/\text{NO}_y=0.2$ , and ExtentB2 parameter from equation 3.2.5 equal to 0.86), but ozone produced and ozone production per  $\text{NO}_x$  (shown as ozone per  $\text{NO}_z$ ) was much higher in the plume with high biogenic VOC. The different ozone content in these two plumes contradicts the theoretical basis of the extent of reaction parameters.

In this context, the smog production algorithms based on the ratio  $\text{O}_3/\text{NO}_y$  can be viewed as representing both extent of reaction ( $1-\text{NO}_x/\text{NO}_y$ ) and the rate of ozone production per  $\text{NO}_x$  ( $\text{O}_3/\text{NO}_z$ ). As described in Section 3.1.12, the rate of ozone production per  $\text{NO}_x$  (also known as ozone production efficiency) is associated with  $\text{NO}_x$ -

sensitive versus VOC-sensitive chemistry. The smog algorithm based on  $\text{NO}_x/\text{NO}_y$  is only associated with extent of reaction, and not with the rate of ozone production per  $\text{NO}_x$ . This may explain its poor performance in models.

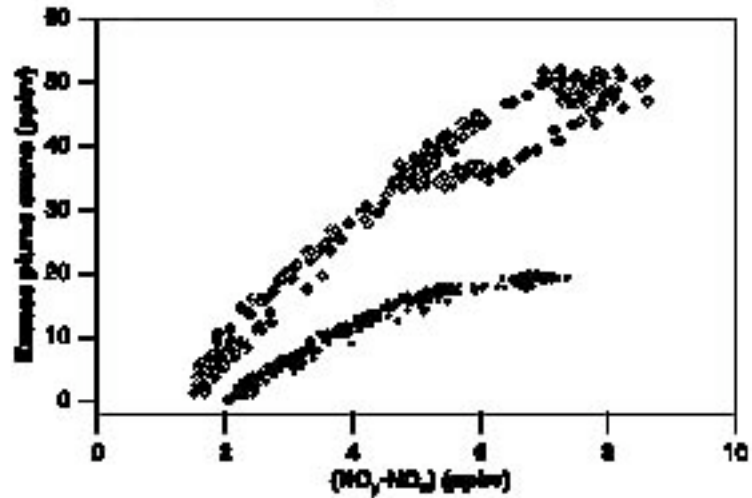


**Figure 3.2.9.** Measured  $\text{O}_3$  versus  $\text{NO}_z$  in aircraft transects downwind of two power plant plumes: Thomas Hill (dots) and Johnsonville (circles). These power plants have similar rates of  $\text{NO}_x$  emissions, and 80% of the original  $\text{NO}_x$  had been oxidized in each transect. Johnsonville, with higher input from biogenic VOC, had higher  $\text{O}_3$ . From Ryerson et al. (2001).

### 3.2.7. Applications of the smog production algorithms

The smog production algorithms have been used widely to interpret measurements in many urban areas in the U.S. Blanchard (2001) described applications in six regions in the U.S.: the northeast corridor, southern Lake Michigan, Atlanta, Texas (including Houston and Dallas), central California and southern California. These applications often included measurements for extended time periods, including several years, and provide a broad characterization of inferred  $\text{NO}_x$ -VOC sensitivity in urban areas. Blanchard et al. (1999) described applications to southern California and Lake Michigan in greater detail. Chang and Suzio (1996) also describe applications of the method during episodes in New York and the surrounding region, Washington D.C., Atlanta and Houston. Applications of the method have also been made in Melbourne, Australia and Auckland, New Zealand.

Figures 3.2.10 and 3.2.11 show results of the applications to southern Lake Michigan and Los Angeles. As shown here, the method characteristically shows VOC-sensitive conditions in urban centers and mixed or  $\text{NO}_x$ -sensitive conditions in rural areas.

In the broad application by Blanchard (2001), approximately half of the measured values represented VOC-sensitive conditions (extent below 0.6) and half represented mixed conditions (extent between 0.6 and 0.9). Values corresponding to  $\text{NO}_x$ -sensitive conditions (extent above 0.9) were measured approximately 10% of the time and these measurements generally occurred in rural locations. These results are summarized in Table 3.2.1.

In general, applications of the method have consisted primarily of calculating the values of the smog production parameter and presenting the interpretation in terms of  $\text{NO}_x$ -VOC sensitivity. Comparatively little analysis of ambient measurements has been done that might evaluate the accuracy of the measurements or whether the method is applicable to local conditions. No comparisons have been made between ambient measurements of smog production parameters and results of 3-d photochemical models.

Evaluations of the viability of the method based on ambient measurements and results from models that might be used to evaluate measurements are described in the next section (Section 3.2.8).

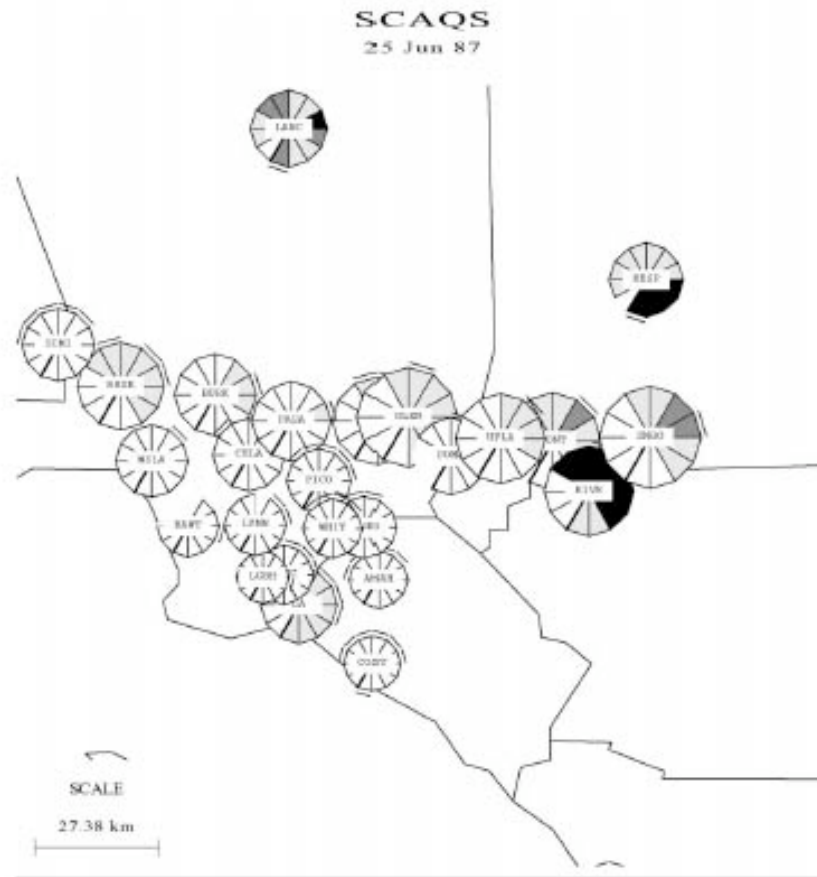


**Figure 3.2.10.** Application of smog chamber algorithms to southern California. The size of the circles are proportional to peak  $O_3$  at each site. White shadings in each circle represent percent of the time (over a period from 7am to 6pm) with extent below 0.6; gray shadings represent extent between 0.6 and 0.9, and black shadings represent extent greater than 0.9. From Blanchard et al., 1999.

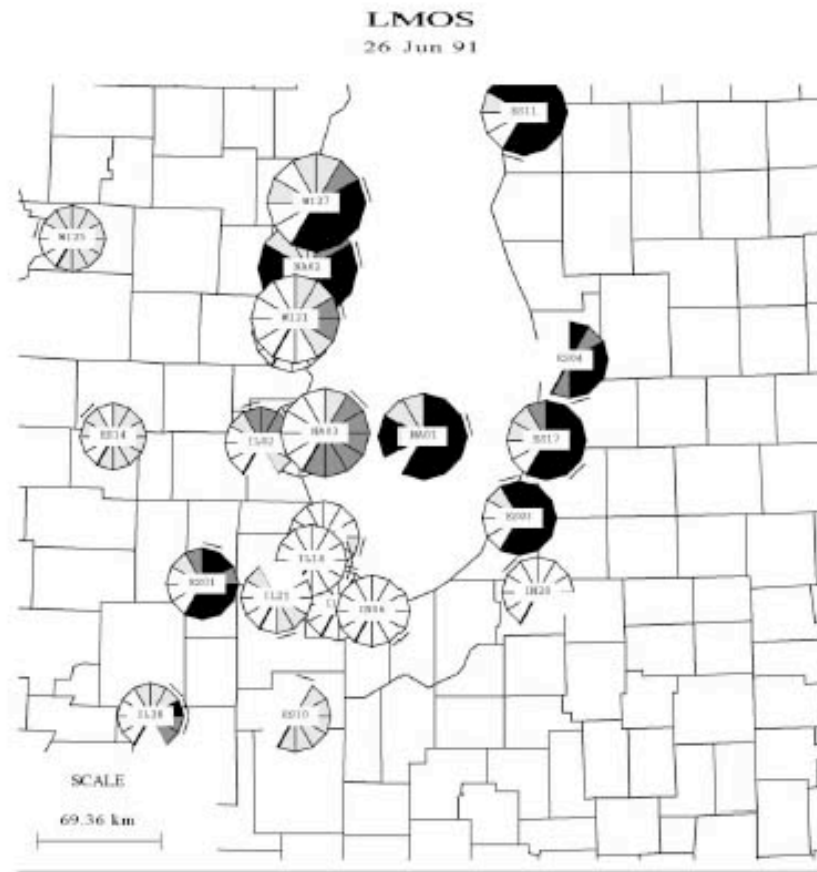


**Figure 3.2.11.** Application of smog chamber algorithms to Lake Michigan. The size of the circles are proportional to peak O<sub>3</sub> at each site. White shadings in each circle represent percent of the time (over a period from 7am to 6pm) with extent below 0.6; gray shadings represent extent between 0.6 and 0.9, and black shadings represent extent greater than 0.9. From Blanchard et al., 1999.

**Table 3.2.1****Measured extent of reaction parameters**

Summary of measured extent-of-reaction parameters at locations in the U.S. over a ten-year period. Extent was calculated from measured O<sub>3</sub> and NO<sub>x</sub> from EPA monitors. The table shows the frequency of occurrence of extent values below 0.6 (“VOC-sensitive”), between 0.6 and 0.9 (“transitional”), and above 0.9 (“NO<sub>x</sub>-sensitive”) for all monitors during hours when ozone concentrations were greater than 80 ppbv, along with the total number of at each site.

Domain	Years	Total Hours	Extent of Reaction (percent of hours)		
			VOC-limited Extent < 0.6	Transitional 0.6#Extent<0.9	NO <sub>x</sub> -limited Extent ≥ 0.9
<b>Central California</b>					
San Francisco Bay Area	1991-98	4269	81.3	18.1	0.6
Sacramento Valley	1994-97	4133	38.4	43.6	18.0
San Joaquin Valley	1994-97	36293	32.4	60.2	7.5
<b>Southern California</b>					
South Central Co	1994-97	11826	42.8	47.8	9.4
South Coast	1994-97	65416	74.4	24.6	1.0
Mojave	1994-97	15991	32.9	56.0	11.1
Salton Sea	1994-97	2844	32.6	54.6	12.8
San Diego	1994-97	6655	80.6	18.9	0.4

<b>Texas</b>					
<b>Houston</b>	1994-99*	2979	41.9	43.5	14.6
Beaumont-Port A	1994-99*	509	21.6	56.4	22.0
Dallas-Fort Wort	1994-99*	1777	39.6	48.0	12.4
El Paso	1994-99*	337	74.2	21.1	4.7
<b>Lake Michigan</b>					
	1991	492	13.8	40.7	45.5
	1994-98	2271	38.9	42.3	18.8
<b>Northeast and Mid-Atlantic</b>					
<b>Connecticut</b>	1994-99	1482	50.1	40.1	9.7
Washington, DC	1994-99	1692	51.7	38.4	10.0
Delaware	1995-99	416	53.8	40.9	5.3
Maine	1995-99	368	8.7	52.2	39.1
<b>Maryland</b>	1994-99	610	37.5	53.3	9.2
Massachusetts	1995-99	1783	30.0	56.1	13.9
New Jersey	1995-99	1551	16.7	56.8	26.5
<b>New York</b>	1995-99	1071	72.5	26.3	1.0

North Carolina	1995-99	3567	39.4	56.0	4.6
Pennsylvania	1995-99	1381	51.4	42.9	5.6
Rhode Island	1995-99	162	25.3	45.1	29.6
Virginia	1994-99	513	52.2	31.0	16.8
<b>Atlanta</b>					
1 upwind, 3 central, 2 downwind sites	1990	736	54.1	39.7	6.3
3 downwind sites	1994-99	3148	13.3	48.7	38.0

\* 1999 is a partial year

### 3.2.8. Evaluations with ambient measurements.

Blanchard and Stoeckenius (2001) reported correlation plots from a series of 3-d models, comparing model values of SP and  $SP_{\max}$  (derived from species concentrations in the model) as a function of model  $NO_y$ . Typically, these plots showed a broad range of the SP parameter. The parameter  $SP_{\max}$  is closely correlated with  $NO_x$  and represents an effective maximum value for the range of SP. These correlations, shown in Figure 3.2.12, may also provide a basis for evaluating an ambient data set. The correlation plot of SP versus  $NO_y$  shows the same type of scatter predicted for  $O_3$  versus  $NO_y$  (see Figure 3.1.7), which also might provide a basis for evaluating ambient data.

Blanchard (2001) also analyzed ambient measurements from five cities in order to identify the impact of uncertainty associated with measurements. The smog parameters were derived from measured  $O_3$  and  $NO_x$ , where  $NO_x$  was measured using commercial chemiluminescent instruments. These measurements generally represent the sum of true  $NO_x$  plus uncertain percentages of organic nitrates and  $HNO_3$ . Blanchard derived smog production parameters from this data in two ways, by interpreting the measurements as  $NO_x$  and applying Equation 3.2.6 or by interpreting the measurements as  $NO_y$  and applying equation 3.2.3. A comparison between the two alternative parameters (Figure 3.2.13) showed relatively little difference for values below 0.6 (corresponding to VOC-sensitive conditions). Large differences occurred for values above 0.6, which included the majority of the data set. When measurements are interpreted as  $NO_x$ , the extent values are almost all below 0.9. If interpreted as  $NO_y$ , extent values would be as high as 2.

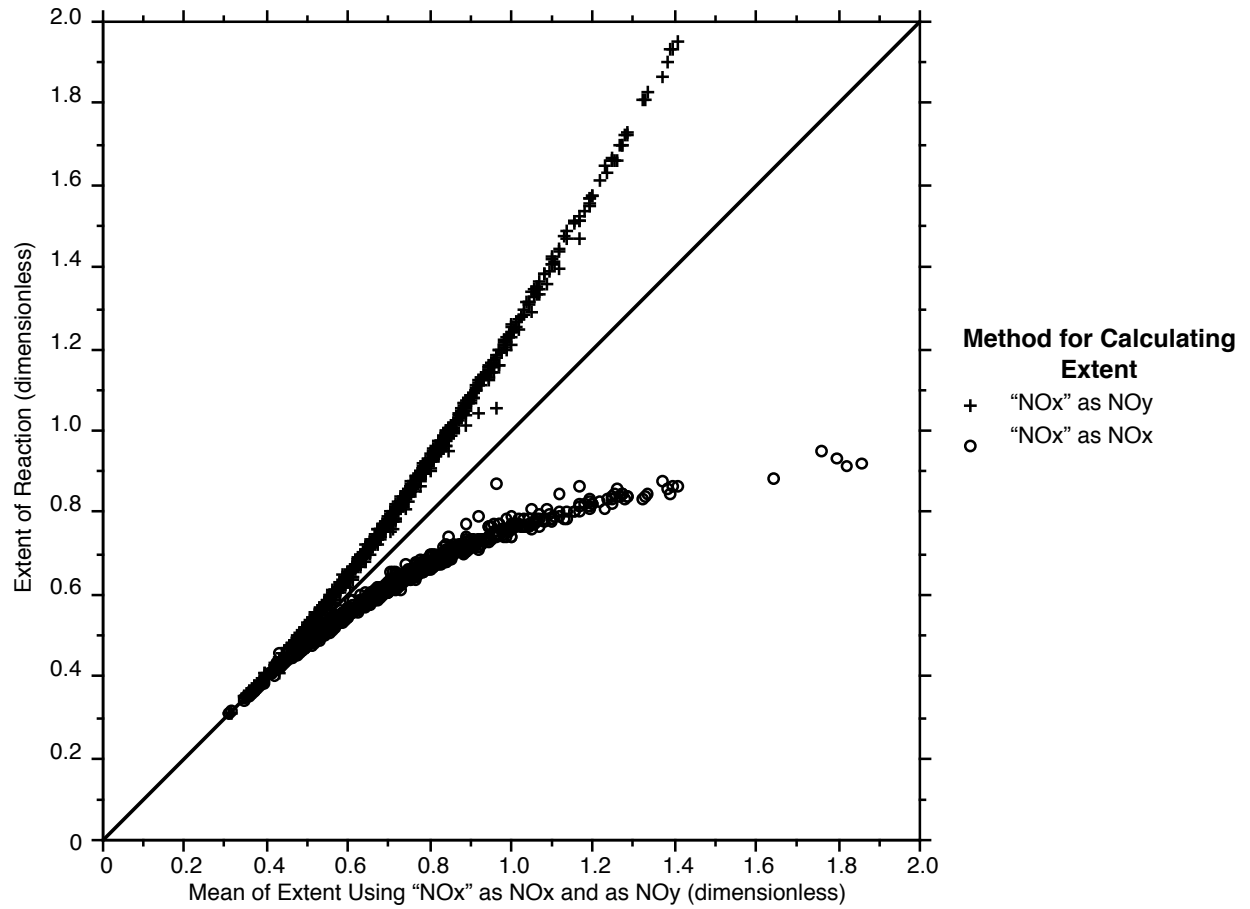


**Figure 3.2.12.** Comparison of two values of the extent parameter. The first value (+'s) is calculated from measurements assuming that measured  $\text{NO}_x$  represents true  $\text{NO}_x$ . The second value (circles) is calculated assuming that measured  $\text{NO}_x$  represents  $\text{NO}_y$ . From Blanchard, 2001.

### 3.3 CONSTRAINED STEADY STATE AND OTHER ANALYSES BASED ON AMBIENT VOC AND NO<sub>x</sub>

#### 3.3.1. Summary information

- *Constrained steady state (CSS)* refers to a series of calculations, based on ambient VOC and NO<sub>x</sub>, that seeks to identify how the instantaneous rate of ozone production varies in response to changed NO<sub>x</sub> and VOC. In addition to these calculations, simple formulas have been developed to determine the sensitivity of instantaneous ozone production to NO<sub>x</sub> and VOC based on measured NO<sub>x</sub> and VOC.
- Because measured NO<sub>x</sub> and VOC are closely related to emission inventories, methods that would use measurements to evaluate inventories are also included here.
- Two similar forms of constrained steady state calculations have been used: the Observation-based Model by Cardelino and Chameides (1995, 2000) and the constrained steady state model developed by Kleinman et al. (1997, 2000). These both consist of 0-d calculations driven by ambient NO<sub>x</sub> and VOC measurements.
- Tonnesen and Dennis (2000a) and Kirchner et al. (2001) both derived simple formulas that relate NO<sub>x</sub>-VOC sensitivity of instantaneous ozone production to the ratio of reactivity-weighted VOC to NO<sub>x</sub>. Kleinman et al. (1997, 2000) developed a somewhat more complicated formula in terms of VOC, NO<sub>x</sub>, and sources of odd hydrogen radicals.
- No reliable way has been developed to determine the NO<sub>x</sub>-VOC sensitivity of ozone concentrations based on measured NO<sub>x</sub> and VOC. However, average O<sub>3</sub>-NO<sub>x</sub>-VOC sensitivity in Eulerian AQMs is broadly similar to the sum of calculated instantaneous NO<sub>x</sub>-VOC sensitivity rates.
- Accuracy of VOC measurements is a major concern for CSS and all other methods that rely on measured VOC. Measurements of highly reactive VOC are especially uncertain.
- CSS calculations must be based on measurements that include all directly emitted VOC. If some directly emitted species are omitted from the measurements, their concentrations must be estimated based on estimated ratios relative to measured species. Complete omission of unmeasured species would bias the CSS calculation.
- Additional uncertainties of these methods include the likely variation of short-lived VOC with altitude and the possibility that individual measurements are affected by on-site emissions. Methods such as CSS effectively assume that surface measurements are representative of the entire convective mixed layer, in which ozone is formed.

- CSS calculations by themselves do not include methods for identifying errors or uncertainties. These sources of error can often be identified if the CSS calculation is combined with a more direct analysis of measurements, focusing on measured correlations among VOC.
- Because measured VOC and  $\text{NO}_x$  are closely related to emission inventories, it may be useful to use these measurements as a basis for evaluating and modifying emission inventories in addition to (or instead of) calculating  $\text{NO}_x$ -VOC sensitivity directly. Methods for evaluating emission inventories from measurements include (i) analysis of species correlations and (ii) inverse modeling using standard 3-d air quality models.

### 3.3.2. Conclusions and recommendations

- Three alternative approaches involving ambient  $\text{NO}_x$  and VOC are feasible for use in evaluating ozone chemistry: (i) a full CSS calculation from ambient data; (ii) a simple rule-of-thumb for instantaneous  $\text{NO}_x$ -VOC sensitivity, such as the ratio of reactivity-weighted VOC to  $\text{NO}_x$ , and (iii) evaluation and modification of emission inventories based on ambient measurements.
- A full CSS calculation (such as the model developed by Cardelino and Chameides) could easily be developed and made available to regulators. CSS calculations are much easier to use than Eulerian AQMs, and evaluation of measured VOC and  $\text{NO}_x$  with a CSS calculation would be no more difficult than a direct analysis of the data without the CSS calculation.
- In contrast with other methods, it is likely that a reliable, simple rule can be developed that identifies instantaneous  $\text{NO}_x$ -VOC chemistry in terms of reactivity-weighted  $\text{NO}_x$  and VOC. It is also fairly certain that ambient VOC and  $\text{NO}_x$  are directly related to  $\text{O}_3$ - $\text{NO}_x$ -VOC sensitivity.
- CSS calculations and associated rules for interpreting measured VOC and  $\text{NO}_x$  are potentially useful for analyzing seasonal trends in apparent  $\text{O}_3$ - $\text{NO}_x$ -VOC sensitivity and to identify differences between individual events and locations.
- No formal method has been developed for using CSS approaches in combination with standard 3-d air quality modeling. CSS model results might be used to confirm or deny the general conclusions of an air quality model. Formal methods of comparison between CSS calculations and AQMs might be developed. However it may be more useful to use measured VOC and  $\text{NO}_x$  as a basis for evaluating and modifying emission inventories in AQMs.

- Analyses based on measured  $\text{NO}_x$  and VOC should include comparisons that would evaluate measurement accuracy. CSS calculations are unreliable unless a complete set of measurements of primary VOC is available, including accurate measurement of highly reactive VOC.

### 3.3.3. Constrained steady state models

Constrained steady state models consist of 0-d calculations of photochemical processes, often with little or no time component. These calculations are widely used to investigate the concentrations of short-lived radical species such as OH and  $\text{HO}_2$  (e.g. McKeen et al., 1997; Tan et al., 2001). In a constrained steady-state calculation the long-lived species are all derived from measured concentrations or from assumptions about ambient conditions. The short-lived species are then calculated with the assumption that they are in steady state. In addition, calculations of this type often use measured photolytic rate constants if these measurements are available. Dynamics, including possible dilution through vertical mixing and horizontal advection, are not included.

The CSS calculations are generally not useful unless measurements include a relatively complete set of directly emitted VOC. Intermediate organics might be estimated as part of the calculation (see next paragraph). Directly emitted species must be set as part of the initial conditions of the calculation.

CSS calculations must make assumptions about the concentrations of unmeasured organics, usually including aldehydes and other reaction products of directly emitted hydrocarbons, and potentially short-lived organic nitrates such as PAN. In the CSS model used by Kleinman et al. (1997, 2000, 2001), PAN and relatively short-lived intermediate organics (e.g. methylvinyl ketone) were generally assumed to be at steady state.

The observation-based model developed by Cardelino and Chameides consisted of a similar 0-d calculations with a more sophisticated method for establishing concentrations of intermediate VOC. Their model consisted of 0-d calculations that were performed for full day rather than for a fixed point in time as done by Kleinman et al. The calculations represented a convective mixed layer that increased with height (entraining air from aloft) as the day progressed. Pseudo-emission terms were added to insure that all measured species were constrained to remain at measured values. Unmeasured species (aldehydes, PAN) were allowed to accumulate throughout the time period of the calculation based on photochemical production and removal. A dilution factor was also applied to the unmeasured species to represent the growth of the convective mixed layer. No dilution due to horizontal transport was included.

Cardelino and Chameides also modified the CB-IV chemistry in their calculation so that directly emitted VOC and secondary reaction products were not lumped into a single species. Species categories in the CB-IV mechanism that included both primary and secondary species (e.g. ALD2, which is used to represent both secondary aldehydes and directly emitted alkenes) were separated into two species.

Kleinman et al. and Cardelino and Chameides both calculated the production rate of ozone and used the calculated production rate to make predictions about NO<sub>x</sub>-VOC sensitivity. In both cases the calculation was repeated with reduced NO<sub>x</sub> and reduced VOC. Changes in ozone production rates were recorded in a form adopted from the Relative Incremental Reactivity (RIR) format (Carter, 1995):

$$RIR = \frac{\Delta P_{O_3}/P_{O_3}}{\Delta S/S} \quad (3.3.1)$$

where  $\Delta P_{O_3}$  represents the difference between the ozone production rate ( $P_{O_3}$ ) in the initial calculation and the ozone production rate in a calculation with concentrations of a precursor S (either NO<sub>x</sub> or VOC) changed by an amount  $\Delta S$ . Kleinman calculated ozone production and precursor sensitivity at individual time periods. Cardelino and Chameides summed the calculated production and precursor sensitivity over a 12-hour time period. The sum used by Cardelino and Chameides effectively gives greater weight to NO<sub>x</sub>-VOC sensitivity at times and places with higher rates of ozone production.

The CSS calculations do not generate any model predictions that can be evaluated in comparison with measurements. In effect, measurements only provide input to the calculations. Summed ozone production in the calculations cannot be directly compared to measured O<sub>3</sub>. However, Kleinman's results also established a relation between instantaneous NO<sub>x</sub>-VOC chemistry and concentrations of odd hydrogen radicals, which might be evaluated against ambient measurements (see Section 3.3.4).

#### **3.3.4. Short formulas for NO<sub>x</sub>-VOC sensitivity.**

Tonnesen and Dennis (2000a) and Kirchner et al. (2001) independently derived a simplified formulas for determining the sensitivity of ozone production rates to precursor emissions. Tonnesen and Dennis used a 3-d simulation for the northeastern U.S. (using RADM) as the basis for evaluating instantaneous ozone production. They used simulations with changed NO<sub>x</sub> and VOC emissions to identify the change in the ozone production rate

associated with changed emissions. These changes were then correlated with possible indices for the sensitivity of ozone production rates (see Figure 3.3.1).

Tonnesen and Dennis derived several formulas that correlate with the  $\text{NO}_x$ -VOC sensitivity of instantaneous production, including the ratio of rates of production of  $\text{H}_2\text{O}_2$  and  $\text{HNO}_3$ . The ratios most likely to be useful for regulatory purposes were: (i)  $\text{O}_3/\text{NO}_x$ ; and (ii) a ratio based on  $r\text{VOC}/\text{NO}_x$ . The exact ratio used by Tonnesen and Dennis was:

$$I(\text{HC}, \text{NO}_2) = \frac{\alpha \beta k_m[\text{HC}]_m}{\alpha \beta k_m[\text{HC}]_m + k_a[\text{NO}_2]} \quad (3.3.2)$$

where  $\alpha$  (=1.3) represents an adjustment factor to account for unmeasured VOC. A simple ratio of reactivity-weighted VOC to  $\text{NO}_2$  is related to their formula by

$$\frac{r\text{VOC}}{r\text{NO}_2} = \frac{I(\text{HC}, \text{NO}_2)}{1 - \alpha I(\text{HC}, \text{NO}_2)} \quad (3.3.3)$$

Tonnesen and Dennis found that VOC-sensitive instantaneous chemistry corresponds to  $I(\text{HC}, \text{NO}_2)$  less than 0.8 and  $\text{NO}_x$ -sensitive chemistry corresponds to  $I(\text{HC}, \text{NO}_2)$  greater than 0.85. These are equivalent to  $r\text{VOC}/r\text{NO}_2$  less than 4 and greater than 5.7. Kirchner et al. (2001) gave approximately the same values, expressed as  $r\text{NO}_2/r\text{VOC}$ , using the RACM mechanism (Stockwell et al., 1997).

These results have not been tested elsewhere, but some form of this formula might provide a convenient basis for interpreting measured VOC and  $\text{NO}_x$ . Use of the ratio  $r\text{VOC}/\text{NO}_x$  might also be compared with formulas based on analysis of ozone formation potential (e.g. Carter et al., 1994, 1995).

Kleinman et al. (1997, 2000, 2001) devised a more complicated formula. Kleinman et al. found that the  $\text{NO}_x$ -VOC sensitivity of instantaneous ozone production was consistently correlated with the parameter  $L_N/Q$ , which related the loss rate for  $\text{NO}_x$  ( $L_N$ ) to the rate of production of primary odd hydrogen radicals ( $Q$ ). They found that  $\text{NO}_x$ -sensitive chemistry was always associated with  $L_N/Q$  below 0.5 and that VOC-sensitive chemistry was always associated with  $L_N/Q$  above 0.5. The same relation between instantaneous  $\text{NO}_x$ -VOC sensitivity and  $L_N/Q$  was found in constrained steady state calculations based on measurements in Nashville, New York and Phoenix. Kleinman et al. also found that the division between instantaneous  $\text{NO}_x$  benefits versus disbenefits occurred when

$L_N/Q$  was equal to 0.67. These results were similar to the photochemical analysis associated with  $NO_x$ -VOC indicators (Section 3.10). Kleinman et al. developed a formula for the  $NO_x$ -VOC sensitivity of instantaneous ozone production, as a function of  $L_N/Q$ . More recently, Kleinman et al. (2001) proposed that the same  $L_N/Q$  could be calculated directly from measurements of ambient  $NO$ ,  $NO_2$ , VOC, and the parameter  $Q$ . They proposed that  $Q$  could be determined from measured  $O_3$ , HCHO and photolytic rate constants.

The Kleinman formula was calculated based on a single photochemical mechanism (RADM), but there is a good chance that the formula will be universal. Unlike the simpler  $rVOC/NO_x$  ratio, the  $L_N/Q$  formula accounts for variations with sunlight and has been used in model calculations at different times of day. The correlation between calculated  $NO_x$ -VOC sensitivity and  $L_N/Q$  is also much stronger than between  $rVOC/NO_x$  (see Figure 3.3.2). The major limitation of the  $L_N/Q$  formula is that it requires measurements that may not be available. The parameter  $Q$  requires measured HCHO. In addition, locations with high alkenes (e.g. Houston) may have  $Q$  influenced by other organics. Kleinman's correlation is especially useful for research, because directly measured OH and  $HO_2$  might be used directly to evaluate the  $L_N/Q$  formula (Thornton et al., 2002).

In terms of  $rVOC$  and  $NO_x$ , Kleinman's formula can be approximated as:  $\frac{rVOC^2 Q}{NO_x^4}$ . This contrasts with the simpler ratio  $rVOC/NO_x$ , which was used by Tonnesen and Dennis (2000a), Kirchner et al. (2001) and Chameides et al. (1992).

The exact formula proposed by Kleinman is as follows:

$$\frac{L_N}{Q} = 0.5 \left( \frac{rVOC}{NO_x} + \sqrt{\left(\frac{rVOC}{NO_x}\right)^2 + 4 \frac{rVOC^2 Q}{NO_x^4}} \right) \quad (3.3.3a)$$

$$\frac{rVOC}{NO_x} = \frac{k_1 [NO_2] k_3 [NO]}{k_2 [VOC]} + \frac{1}{2Q k_{eff}} \quad (3.3.3b)$$

where  $k_1$  represents the reaction rate of OH with  $NO_2$ ,  $k_2$  represents the reaction rate of individual VOC with OH (summed over all VOC),  $k_3$  represents the reaction rate of  $HO_2$  with  $NO$ ,  $\frac{1}{2Q k_{eff}}$  is the ratio of  $HO_2$  to  $HO_2+RO_2$ , and  $k_{eff}$  is the combined rate constant for  $HO_2+HO_2$  and  $HO_2+RO_2$ .

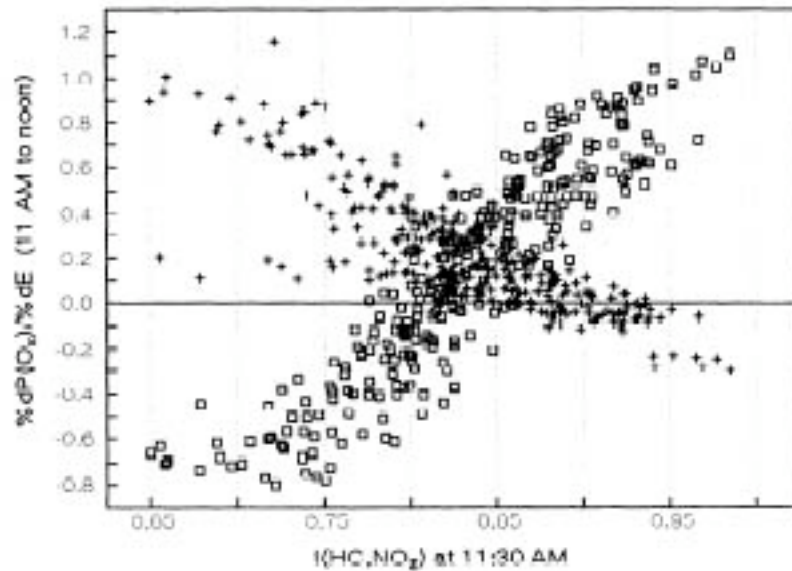


**Figure 3.3.1.** Predicted change in the rate of ozone production in response to a percent change in VOC (+'s) or in  $\text{NO}_x$  (squares), plotted versus an index that is a function of reactivity-weighted VOC and  $\text{NO}_2$  ( $I(\text{HC}, \text{NO}_2)$ , Equation 3.3.2). The change in ozone production is represented as percent relative to percent change in  $\text{NO}_x$  or VOC. Results are for RADM simulations of New York (Tonnesen et al., 2000a).

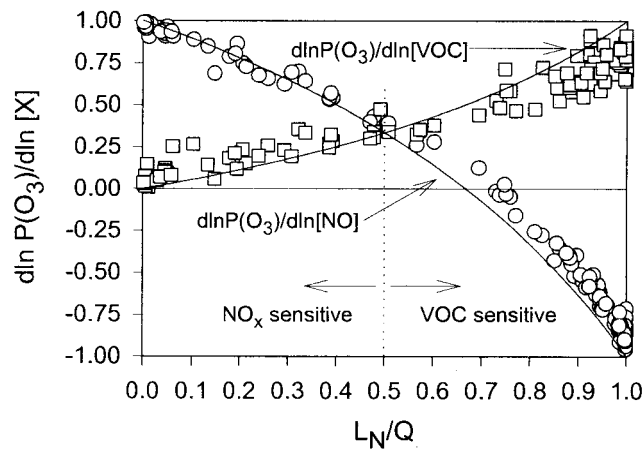


**Figure 3.3.2.** Predicted sensitivity of the instantaneous ozone production rate to changes in NO and VOC, based on calculations with the constrained steady state (CSS) model driven by measurements from the 1998 DOE field campaign in Phoenix. Sensitivity is reported as the percent change in ozone production relative to the percent change in NO or VOC ( $d\ln P(\text{O}_3)/d\ln[\text{NO}]$  and  $d\ln P(\text{O}_3)/d\ln[\text{VOC}]$ ) and is shown as a function of the ratio of photochemical removal of  $\text{NO}_x$  to the radical source ( $L_N/Q$ , defined in Section 3.3.4). The squares show results of the CSS calculation. The lines show results of the analytic formula (Equation 3.3.3).

### 3.3.5. Integrating from instantaneous ozone production to ozone concentrations

A major limitation of the CSS calculations is that they only give  $\text{NO}_x$ -VOC sensitivity associated with the instantaneous rate of ozone production. They do not provide direct information about how ozone concentrations depend on  $\text{NO}_x$  and VOC. The  $\text{NO}_x$ -VOC dependence of ozone concentrations depends on photochemical production over time periods of several hours, and sometimes over several days, and involves transport from distant locations. The  $\text{NO}_x$ -VOC dependence of ozone at an individual site is often very different from that which would be predicted from the instantaneous photochemistry at the site.

Cardelino and Chameides (1995) compared results of their CSS model with results of an Eulerian AQM for a single episode in Atlanta. They used VOC and  $\text{NO}_x$  concentrations from the AQM as pseudo-observations to drive the CSS calculation, thus producing an equivalent CSS calculation for an AQM that was in perfect agreement with ambient measurements. They examined  $\text{NO}_x$ -VOC sensitivity predictions from the AQM for (i) peak  $\text{O}_3$ , (ii) locations with  $\text{O}_3$  greater than 120 ppb; and (iii) locations with  $\text{O}_3$  greater than 100 ppb. This was compared with the  $\text{NO}_x$ -VOC sensitivity found for the 12-hour summation of instantaneous  $\text{PO}_3$  from the CSS calculations. They found that  $\text{NO}_x$ -VOC sensitivity for peak  $\text{O}_3$  in the AQM was comparable to the 12-hour summation based on pseudo-observations at a single downtown location, and that  $\text{NO}_x$ -VOC sensitivity for  $\text{O}_3$  above 100 ppb and above 120 ppb in the AQM was comparable to the 12-hour summation based on the downtown location and four suburban locations within 20 km of downtown. These results suggest a broad correlation between CSS calculations and  $\text{O}_3$ - $\text{NO}_x$ -VOC sensitivity, but they do not prove that the same relation would hold in all locations or during events with different meteorology.

In a case study of the New York metropolitan area, Kleinman et al. (2000) found that CSS calculations in the entire metropolitan area were consistent with VOC-sensitive chemistry. Because the calculations included measurements that extended from near downtown out to the downwind region with the highest  $\text{O}_3$ , they concluded that the evidence was consistent with VOC-sensitive ozone concentrations. This conclusion was also consistent with observed  $\text{O}_3$  and  $\text{NO}_y$ , interpreted as an indicator ratio.

Kirchner et al. (2001) investigated the use of reactivity-weighted  $\text{VOC}/\text{NO}_x$  as evidence for  $\text{O}_3$ - $\text{NO}_x$ -VOC sensitivity in Eulerian AQM simulations for Athens and the Swiss plateau. They introduced tracers in their model representing low (VOC-sensitive)  $r\text{VOC}/\text{NO}_x$  and high ( $\text{NO}_x$ -sensitive)  $r\text{VOC}/\text{NO}_x$  at 8 am, and compared the

distribution of these tracers with the impact of reduced VOC and  $\text{NO}_x$  in their model. The VOC and  $\text{NO}_x$  reductions were applied just for a one-hour period (8-9 am) to avoid complications that would be caused by varying chemistry along the transport path. They found that predicted sensitivity to the reduced  $\text{NO}_x$  and VOC was strongly correlated with the amount of  $\text{NO}_x$ -sensitive and VOC-sensitive tracer at each model location. The correlation between  $\text{NO}_x$ -VOC sensitivity and the tracers was stronger than the correlation with the indicator ratio  $\text{O}_3/\text{NO}_z$  and comparable to the correlation with the ratio  $\text{H}_2\text{O}_2/\text{HNO}_3$ . It is unclear whether the same results would be found for emission reductions applied throughout the day.

The evidence suggests that CSS calculations and  $\text{rVOC}/\text{NO}_x$  are likely to be correlated with  $\text{O}_3$ - $\text{NO}_x$ -VOC sensitivity in general, but it is not certain whether this correlation is universal. The possibility of varying results for different locations and for different events are comparable to the possibility of varying results associated with indicator ratios.

### **3.3.6. Accuracy and completeness of $\text{NO}_x$ and VOC measurements**

Questions of accuracy have been raised about measurements of both VOC and  $\text{NO}_x$ , especially associated with the PAMs network.

In order to provide meaningful results, CSS calculations and other related methods require measurements that include all directly emitted VOC. Secondary VOC can be incorporated into the calculation as described in Section 3.3.3. If unmeasured primary species are omitted, then the resulting calculation will have VOC reactivity that is lower than probable ambient conditions and will constantly give biased  $\text{NO}_x$ -VOC predictions. Biogenic VOC are especially important in this context. Highly reactive anthropogenic VOC are also important. The issue of reactive VOC was highlighted by the recent Texas Air Quality Study, in which it appeared that fast-reacting alkenes had a major impact on ozone formation.

Unmeasured anthropogenic VOC can be estimated by using ratios between individual VOC species that were established from previous data sets. Parrish et al. (2000) reported that correlations among individual VOC often suggest that these species are present in similar ratios throughout the U.S. This is especially true among closely related species (e.g. individual alkenes or individual aromatics). Parrish et al. (2000, 1998) report observed ratios for many of these species.

Parrish et al. found that individual measurements of alkenes, especially in the PAMS network, are subject to considerable uncertainty. They found that the distribution of species in PAMS measurements frequently showed a pattern that was comparable to that of fresh auto emissions, without any sign of photochemical aging. This might be due to the impact of on-site emissions at many PAMS sites, or it might be due to general uncertainties associated with measured alkenes. Parrish et al. (1998) reported an intercomparison among 33 measured ensembles of speciated VOC, and found that mean values were within 4% of a reference measurement. However, the individual measured average VOC concentrations had biases ranging from 45% low to 85% high. Comparisons among individual measurements of alkenes, aromatics and isoprene showed scatter of +/-38%, +/-47% and +/-80% respectively. In addition, Parrish et al. (1998) reported evidence of systematic biases in many measurement sets, including the PAMS network.

For practical purposes, the uncertainties cited by Parrish et al. (1998) would not prevent use of measurements to derive meaningful information about the ozone formation process. However, measured VOC could not be used reliably if the measurements show systematic biases that would cause underestimates or overestimates in summed VOC or in VOC reactivity.

Cardelino and Chameides (2000) also reported that measured NO in the PAMS network often is not of sufficient accuracy for use in their CSS calculations. They found that in case studies in Houston, Washington DC, and New York City, measured NO during the afternoon (often the time of maximum ozone production) was often below the detection limit of the instruments (1-3 ppb). This prevented them from deriving valid information about NO<sub>x</sub>-VOC sensitivity in these locations. Suggested improvements to the PAMS network that might solve this problem were suggested by McClenny (2001).

Parrish et al. (1998, 2000) recommended a series of internal consistency tests for ambient VOC measurements. Many of these tests are also associated with methods to evaluate emission inventories from ambient measurements. These are described in Section 3.3.7.

### **3.3.7. Methods for evaluating emission inventories from measurements**

If CSS models are to be used for regulatory purposes, it is necessary to develop methods to use CSS results to evaluate Eulerian AQMs that are often used to establish policy. No such methods have been developed. Some methods for the direct use of measured VOC and NO<sub>x</sub> to evaluate AQMs are suggested in Section 4. However, the

most direct use of measured VOC and  $\text{NO}_x$  in the context of AQMs is to evaluate emission inventories. These inventories represent the single largest uncertainty in AQMs. Evaluation and modification of emission inventories with ambient measurements would accomplish many of the goals of CSS modeling.

Two types of methods are available for evaluating emission inventories: direct evaluation based on measured correlation between species; and inverse modeling with AQMs. Inverse modeling is discussed below (Section 3.3.8).

Direct evaluation of emission inventories is based on a correlations between individual anthropogenic species that have closely related emission sources and/or chemistry, and can therefore be expected to be correlated in ambient measurements. These correlations can be used directly to derive emission ratios or they may be compared with predictions from AQMs. Many of these correlations are associated with tests of measured VOC ensembles for internal consistency, as proposed by Parrish et al. (1998, 2000).

Species correlations as a basis for estimating emissions have been investigated in Boulder, CO (Parrish et al., 1991, Goldan et al., 1995, 1997), Nashville, TN (Goldan et al., 2001), Los Angeles (Lurmann and Main, 1992), and at rural sites in the eastern U.S. (Buhr et al., 1992, 1995).

Parrish et al. (1998) reported that many closely related species show similar patterns of correlation in measurements across the U.S. These include measurements of individual species within the alkane, alkene or aromatic families that have similar lifetimes (e.g. ethene versus propene, toluene versus ethylbenzene, etc.). Ratios among these species are closely associated with emission ratios (see Figure 3.3.3). These measured ratios can be compared with the ratios in urban emission inventories or with ratios associated with specific sources (e.g. automobiles) (Jobson et al., manuscript in preparation).

Some of the major uncertainties in emission inventories are associated with ratios of emissions among different families of VOC (or between VOC and  $\text{NO}_x$ ) that also have different atmospheric lifetimes. In this case, correlation between species is expected show scatter between two limiting cases: a case in which the concentrations reflect the emissions ratio among the species; and a case in which concentrations represent the ratio of photochemical loss rates. This may still be used to evaluate estimated emission rates, as illustrated in Figure 3.3.4. In correlations between a relatively short-lived species and a relatively long-lived species, there is often a clearly defined maximum for the correlation between species. This maximum ratio (see Figure 3.3.4) can be interpreted as

the ratio of direct emissions of the short lived species relative to the longer lived species. Lower ratios would represent photochemically processed air in which the short-lived species has been removed more rapidly.

Information based on correlations between species with different lifetimes is much more uncertain than information derived from species with similar lifetimes, as in Figure 3.3.3.

Complete recommendations for evaluation of measured VOC are described in Parrish et al. (1998, 2000).

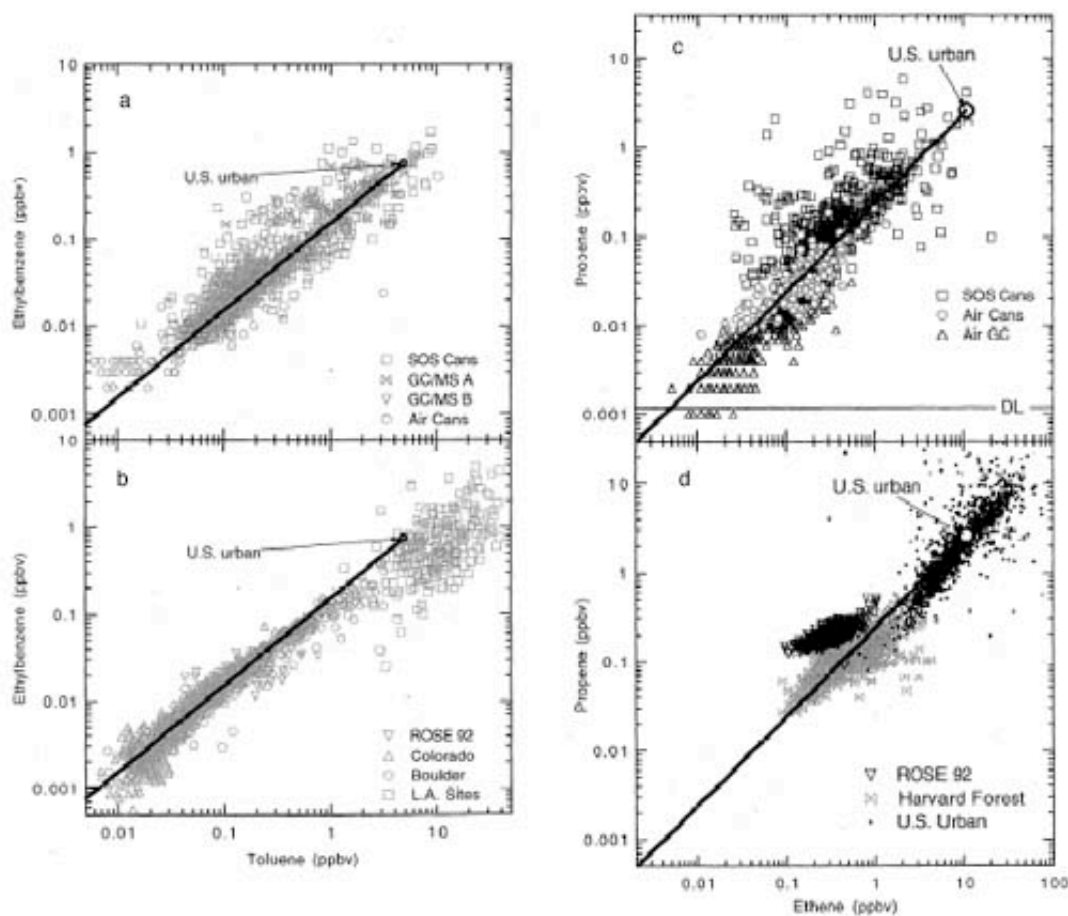


**Figure 3.3.3.** Measured correlations among VOC with similar lifetimes (in ppb). Measurements show toluene versus ethylbenzene (a and b) and ethene versus propene (c and d). The measurements include data from the Southern Oxidant Study/Middle Tennessee Ozone Study (a and c) and from field campaigns in Rose, AL, Harvard, MA and Boulder, CO (b and d). The open circle represents median measured values from 39 cities in the U.S., and the solid line represents a constant ratio equal to the urban median. From Parrish et al. (1998).

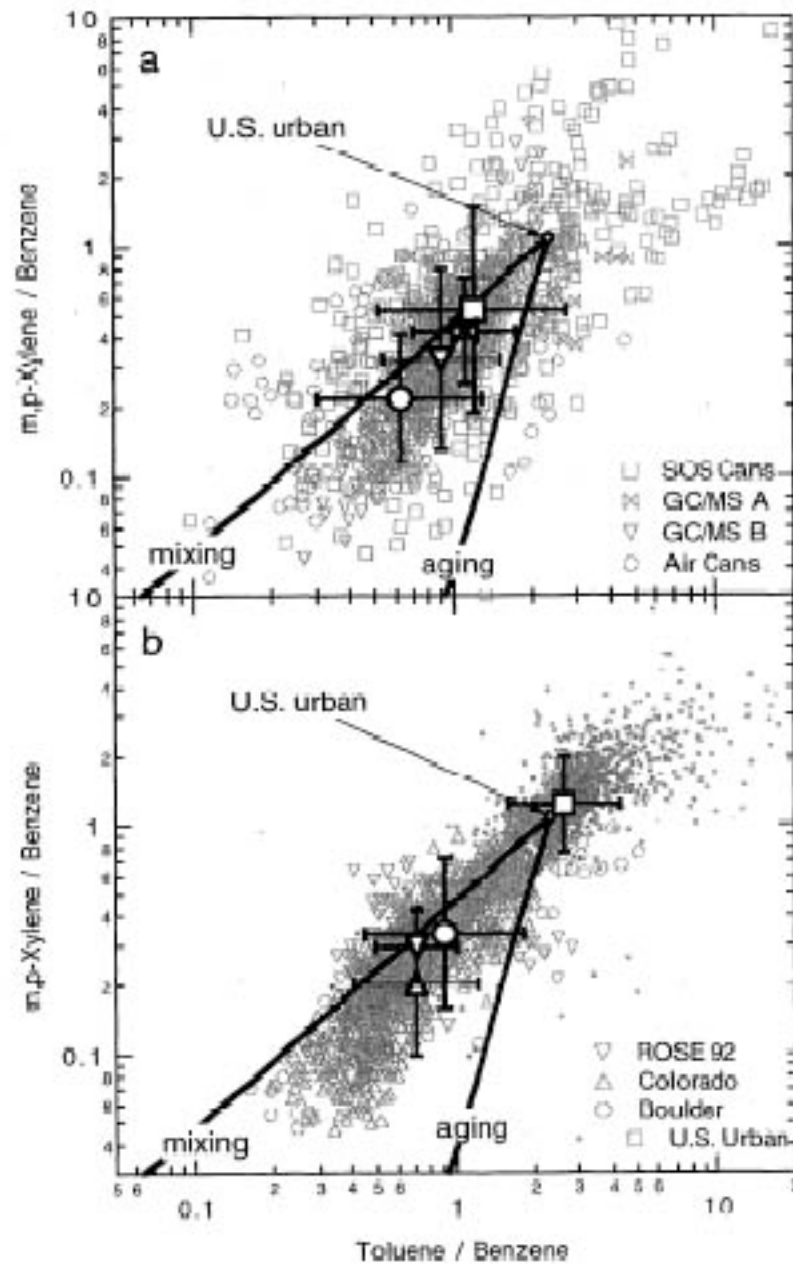


**Figure 3.3.4.** Measured correlations among VOC with different lifetimes (in ppb). Measurements show the ratio of m and p xylene to benzene versus the ratio of toluene to benzene. The measurements include data from the Southern Oxidant Study/Middle Tennessee Ozone Study (a) and from field campaigns in Rose, AL, and Boulder, CO (b). The open square represents median measured values from 39 cities in the U.S. The solid lines represent (i) a constant ratio equal to the urban median; and (ii) a ratio that would be expected from photochemical aging of initial concentrations equal to the urban median. From Parrish et al. (1998).

### **3.3.8. Inverse modeling**

Inverse modeling (M. Chang et al., 1996, 1997; Mendoza-Dominguez and Russell, 2000, 2001; Gilliland and Abbitt, 2001) is a method that adjusts emission estimates in air quality models based on a set of ambient measurements. The method begins with a standard scenario for an air quality model and makes modifications to the emission field in order to bring the model into agreement with a set of measurements. The process uses model calculations with small changes in emissions to estimate the relation between emissions and concentrations at each measurement site. Iterative changes are made in emission fields until a satisfactory simulation is developed.

Application of inverse modeling techniques is based on the assumption that discrepancies between models and measured values are entirely due to emissions (rather than to horizontal wind fields, rates of vertical dispersion or photochemical removal). This assumption can lead to especially bad results in cases where measurements at individual sites are heavily influenced by transport patterns that may not be represented perfectly in the model. These situations can lead to anomalous results, e.g. derived negative emission rates or emission rates increased by factors of 10 or more. Mendoza-Dominguez and Russell developed constraints that would prevent anomalous results in these cases.

Mendoza-Dominguez and Russell (2002) applied this technique to ambient measurements of VOC and particulates in Atlanta, and were able to show that ambient VOC was consistent with emissions approximately twice as high as inventory values. Ambient concentrations of biogenic VOC and several other species appeared consistent with emission inventories. M.E. Chang et al. (1996) found that inverse modeling generated estimates for isoprene emissions up to 10 times higher than inventory estimates, possibly numerical instability in their calculations.

Inverse modeling requires a much greater effort than the other techniques reported here, but offers a significant advantage: it generates an AQM scenario that includes a relatively complete representation of transport (often omitted in OBM) along with good agreement with measured primary VOC and  $\text{NO}_x$ . This allows analyses of the relation between air pollutants and specific emission sources and investigation of specific control strategies, which can only be analyzed with an AQM.

### **3.3.9. Other uncertainties**

In order to be valid for use in observation-based analysis, measured VOC and  $\text{NO}_x$  must be representative of the environment in which ozone production occurs. Surface ozone concentrations during periods of high  $\text{O}_3$  are

generally influenced by photochemical production throughout the convective mixed layer, which typically extends to 1000 m. elevation or higher. Errors may occur if VOC and  $\text{NO}_x$  are measured at surface sites if surface concentrations differ from average conditions throughout the mixed layer.

Differences between surface concentrations and conditions in the mixed layer are most likely for short-lived species. The characteristic time for mixing in the convective layer is 15-60 minutes, and longer-lived species can be expected to be well mixed. Variation with height is especially likely for isoprene. Andronache et al. found that isoprene concentrations decreases by a factor of 2 between measurements at 10 m. and measurements at 200 m., even during the daytime (see Figure 3.3.5). In addition, individual measurements of isoprene (especially in urban areas) sometimes show variations with height of a factor of 5. These differences are based on measurements well above a forest canopy. Surface measurements at urban or suburban sites with trees nearby may show larger impacts.

Comparisons between measured VOC and AQMs (for example, as used in emissions modeling) are also sensitivity to the rate of near-surface vertical mixing in the AQMs. Models generally predict variations in species concentrations between the surface layer and aloft, especially for isoprene. If the model vertical distribution differs from the ambient distribution, then the inverse modeling technique may generate erroneous emission adjustments. Comparisons between model vertical distributions and measured distributions need to be done to insure that comparisons between model and measured values near the surface are not distorted by vertical mixing. This is especially true for isoprene.

Measurements at urban or suburban sites may also be affected by on site emission of  $\text{NO}_x$  and VOC, and consequently may differ from the ambient conditions associated with ozone formation. As described above, Parrish et al. (2001) found that measurements at PAMS sites had VOC distributions that were typical of fresh auto emissions and did not show evidence of photochemical aging. This occurred at both urban and suburban sites, including locations that were significantly removed from major emission sources other than local traffic.

The inverse modeling reported by Mendoza-Dominguez and Russell (2002) provides an example of possible errors. Mendoza-Dominguez and Russell reported a case study in which emission rates for both  $\text{NO}_x$  and most anthropogenic VOC were apparently underestimated by 30%-50% in comparison with emission rates derived from measurements. In this situation it may be unclear whether the consistent underestimate should be attributed to the

emission inventory, to dispersion rates in the model, or to the impact of on-site emissions at measurement sites.

Measurement-based evidence is more certain when the measurements suggest that ratios between simultaneously emitted species (especially between individual VOC and  $\text{NO}_x$ ) differ from inventory values.

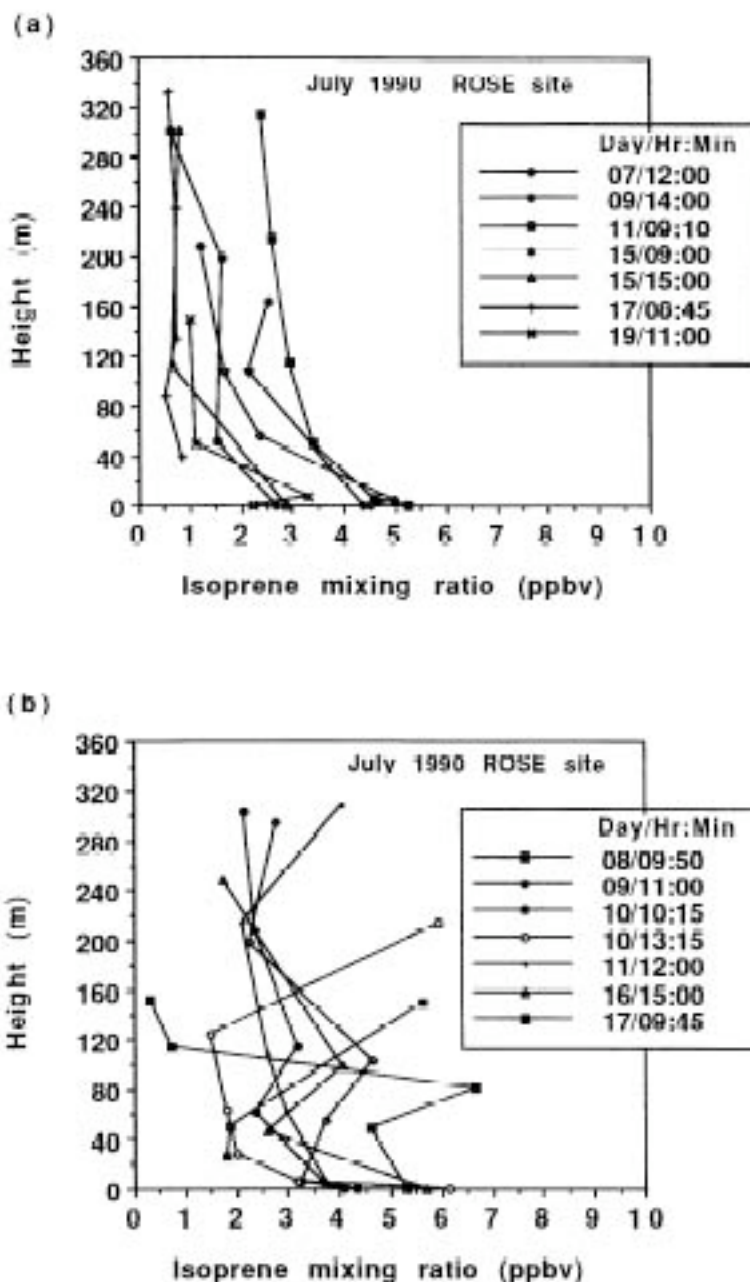


**Figure 3.3.5.** Vertical profiles of isoprene measured during the daytime above a forested site at Rose, AL during July, 1990. Individual profiles were classified as (a) simple or (b) complex patterns. From Andronache et al., 1994.

#### ***SECTION 4. PRACTICAL IMPLEMENTATION OF OBSERVATION-BASED METHODS***

This section discusses the initial development of possible protocols for use of observation-based methods in a regulatory context. Detailed descriptions of procedures are given for two methods: NO<sub>x</sub>-VOC indicators and constrained steady state analyses based on ambient NO<sub>x</sub> and VOC. A separate description is not given for smog production algorithms. These algorithms would include many of the same procedures described in association with NO<sub>x</sub>-VOC indicators, but with a different index for interpreting results in terms of NO<sub>x</sub>-VOC sensitivity.

Especially in the case of constrained steady state and associated analysis of measured NO<sub>x</sub> and VOC, the recommended protocols are tentative and not presented in great detail. Specific procedures will need to be worked out and modified based on experience as the methods are used in a regulatory context. As of this writing, applications of OBMs (except for the smog production algorithms) have been associated with major research efforts. Standardized formats and methods for identifying errors will need to be developed as experience with regulatory applications accumulates.

Implementation of each OBM requires three stages: (i) analysis of measured data for quality assurance and to insure that the measurements are consistent with the requirements of the OBM; (ii) interpretation of results from measured data in terms of NO<sub>x</sub>-VOC sensitivity; and (iii) methods for using the OBM to evaluate and modify results of 3-d air quality models. There also needs to be a standard form for short output that can be easily understood and interpreted in a regulatory context.

**Results from combined OBMs and AQMs:** NO<sub>x</sub>-VOC indicators and CSS calculations are largely complementary, in that they derive information from different measurements (secondary reactive nitrogen for indicators, primary NO<sub>x</sub> and VOC for CSS). Because they use different measurements, results from one method can either confirm or contradict results from the other.

Similarly, NO<sub>x</sub>-VOC indicators and methods adapted from CSS calculations can both be used to evaluate results of an AQM. Results from an AQM that are in agreement both with measured NO<sub>x</sub>-VOC indicators and with the measured VOC and NO<sub>x</sub> associated with CSS should be viewed as very reliable.

NO<sub>x</sub>-VOC indicators and smog production algorithms use similar measurements (O<sub>3</sub> and reactive nitrogen) but give different interpretations. If one of these two methods is used, the choice should be based on which one is believed to be accurate. Smog production algorithms might be used as a complementary method along with CSS.

**What to do when models and measurements disagree:** Development of control strategies for reducing ozone in regulatory applications is almost always done based on results of 3-d Eulerian models. A likely major use of OBMs is to evaluate the accuracy of these models and suggest changes that would improve model performance. In many cases the OBM may validate the predictions of air quality model applications. Some procedure needs to be developed for cases in which significant disagreement is found between AQMs and the results of an OBM or between AQMs and measurements associated with an OBM.

In the most common circumstance, results of measurements associated with an OBM may suggest that emission rates in an air quality model are erroneous and that better agreement with measurements can be obtained in a scenario of the AQM with modified emissions. In cases where both measured NO<sub>x</sub> and VOC and measured NO<sub>x</sub>-VOC indicator ratios show better agreement with a model scenario that uses modified emissions, the modified version might be viewed as more likely to be correct than the original.

## 4.1 NO<sub>x</sub>- VOC INDICATORS

### 4.1.1. Required measurements

The method requires measurements of O<sub>3</sub> and either NO<sub>y</sub> or HNO<sub>3</sub>. In addition, measurements of NO<sub>x</sub> and aerosol NO<sub>3</sub><sup>-</sup> (if not included in the NO<sub>y</sub> measurement) are useful.

The measurements need to be made over a network broad enough to include most of the locations with elevated O<sub>3</sub>, including the locations likely to have the highest O<sub>3</sub> in the region. If not otherwise included, it is also useful to include at least one urban site and one rural site that is likely to represent regional background conditions. Only afternoon measurements (12-6pm) would be used as part of the indicator analysis.

Measurements must avoid two common errors. Measured NO<sub>y</sub> sometimes fails to include HNO<sub>3</sub> because HNO<sub>3</sub> is lost along the measurement inlet tube (Parrish et al., 2000; McClenny et al., 2000). NO<sub>x</sub> measurements made with commercially available chemilluminescence often include some organic nitrates and some (but not all) HNO<sub>3</sub> in addition to NO<sub>x</sub> (Winer et al., 1974, Logan, 1989). Either of these errors would invalidate the measurement for

use in association with the indicator method. McClenny (2000) gave recommendations for modification of the PAMS network to insure quality.

Measured  $\text{H}_2\text{O}_2$  and/or total peroxides would also be very useful, but these are unlikely to be available.

#### 4.1.2. Quality assurance of measurements

Measured  $\text{NO}_y$  should be investigated for two purposes: (i) to insure that  $\text{HNO}_3$  is included in the measurement; and (ii) to insure that ambient conditions are appropriate for use of the indicator method. These can both be done by examining correlations of  $\text{O}_3$  versus  $\text{NO}_z$  (derived from measured  $\text{NO}_y$  and  $\text{NO}_x$ ) and comparing to previously measured  $\text{O}_3$  versus  $\text{NO}_y$ ,  $\text{O}_3$  versus  $\text{NO}_z$ , and  $\text{O}_3$  versus organic nitrates. Figures 3.1.9, 3.1.10 and 3.1.14 show measured correlations that can be used for evaluating measurements used as part of regulatory studies.

Measurements should also be compared with predicted  $\text{O}_3$  versus  $\text{NO}_y$ ,  $\text{O}_3$  versus  $\text{NO}_z$ , and  $\text{O}_3$  versus organic nitrates from models (see Figures 3.1.7 and 3.1.13). Comparison with these model correlations are important because the criteria for  $\text{NO}_x$ -sensitive and VOC-sensitive indicator ratios were based on models with the specific correlation patterns shown in the figures. If measurements are not consistent with these model correlations the indicator ratios may not be valid.

In these figures, the correlation between  $\text{O}_3$  and  $\text{NO}_y$  and between  $\text{O}_3$  and  $\text{NO}_z$  is expected to show significant scatter. However the approximate maximum values of  $\text{O}_3$  for a given  $\text{NO}_y$  or  $\text{NO}_z$  should correspond with the well-defined maximum in the model correlation (Figure 3.1.7). As described elsewhere, a specific correlation between  $\text{O}_3$  and  $\text{NO}_y$ , between  $\text{O}_3$  and  $\text{NO}_z$ , and between  $\text{O}_3$  and  $\text{HNO}_3$  is predicted during  $\text{NO}_x$ -sensitive conditions, and this correlation represents the maximum  $\text{O}_3$  for the given  $\text{NO}_y$ ,  $\text{NO}_z$  or  $\text{HNO}_3$  (or, alternatively, the minimum  $\text{NO}_y$ ,  $\text{NO}_z$  or  $\text{HNO}_3$  for a given  $\text{O}_3$ ). The measured correlation should be consistent with this pattern.

These should be compared with measured correlations for the afternoon hours (1pm-5pm local time). Following Trainer et al. (1993) it might be useful to sort the measured data by photochemical age (interpreted based on  $\text{NO}_x/\text{NO}_y$ ) and investigate separately the measurements that represent photochemically aged conditions (defined as  $\text{NO}_x/\text{NO}_y < 0.3$ ). This restricted data set is likely to show a stronger correlation with  $\text{O}_3$  and will eliminate periods (e.g. with clouds or rain) that are less likely to be of interest.

Measured correlations between  $\text{O}_3$  and  $\text{NO}_y$ , etc. should be accumulated for (i) each individual measurement site, with data for the full season or full duration of the available data set; and (ii) the entire ensemble of

measurements on each individual day of interest. Investigation of the seasonal correlation from individual measurement sites is proposed as a method for identifying measurement sites with consistent errors. Correlations for individual days will be used to interpret conditions for the given day.

For purposes of evaluation, measured  $O_3$  should be binned by  $NO_y$ ,  $NO_z$ , or  $HNO_3$  (i.e.  $O_3$  associated with  $NO_y$  between 1 and 2 ppb, between 2 and 3 ppb, etc.) The upper 25<sup>th</sup> percentile values of the ozone distribution should be used as a test parameter, for values of  $NO_y$  and  $NO_z$  below 15 and for values of  $HNO_3$  below 10. This value should be compared with the  $O_3$  for  $NO_x$ -sensitive conditions in Figure 3.1.7.

Measurement ensembles should be rejected for use as  $NO_x$ -VOC indicators if the ozone values for given  $NO_y$  identified in this way are consistently higher than the model values by 25% or more. Measured  $O_3$  equal to or below the model  $NO_x$ -sensitive values is acceptable.

Situations with higher measured  $O_3$  for given  $NO_y$  have four possible causes: (i)  $HNO_3$  may have been lost in the measurement apparatus and not included in  $NO_y$ ; (ii)  $HNO_3$  may have been removed due to rapid deposition, for example, during rain events; (iii) model photochemistry may not represent the rate of ozone production per  $NO_x$  correctly in  $NO_x$ -sensitive environments; or (iv) the measurement may have been affected by upwind conditions with unusually high  $O_3$  and low  $NO_y$  (possibly due to upwind deposition of  $HNO_3$ ). In each of the first two cases the indicator method cannot be used because the component of the measurement with the  $NO_x$ -VOC signal (the  $HNO_3$ ) has been lost. In the third case, the erroneous model chemistry would invalidate the use of indicator ratios. In the fourth case it might still be possible to use indicator ratios, using background values that reflect the high  $O_3$  and low  $NO_y$  upwind, but this use of indicator ratios would be speculative.

By contrast, when measured correlations between  $O_3$  and  $NO_y$ , etc. are consistent with the range of values in models, then variations in  $O_3/NO_y$  can be interpreted as an indicator for  $NO_x$ -VOC sensitivity.

#### **4.1.3. Interpretation of measured results**

Following quality assurance, measurements may be interpreted in two ways. Values of the indicator ratios  $(O_3 - O_{3b}) / (NO_y - NO_{yb})$ , etc may be used directly and identified as being associated with  $NO_x$ -sensitive, VOC-sensitive or mixed sensitivity. Alternatively, the measured correlation of  $O_3$  versus  $NO_y$  may be superimposed over the model correlation for locations of mixed sensitivity. Measurements close to the mixed values would be

identified as having mixed sensitivity, while  $O_3/NO_y$  ratios significantly above or below this correlation would be viewed as representing  $NO_x$ -sensitive or VOC-sensitive conditions, respectively.

Figure 4.1.1 illustrates this interpretation for the measured data from Nashville (July 13, 1995) reported by Sillman et al., 1998. As shown in the figure, the relatively low  $O_3$  in the vicinity of Nashville would be consistent with  $NO_x$ -sensitive conditions, while the high  $O_3$  towards the center of the city is close to model values representing mixed sensitivity.

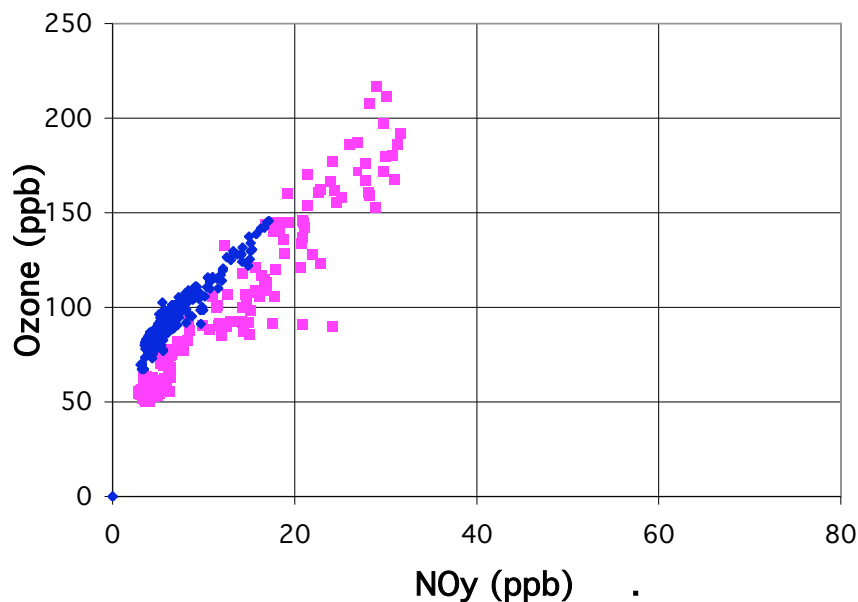


**Figure 4.1.1.** Measured  $O_3$  versus  $NO_y$  at Nashville on July 13, 1995 (blue dots), compared with  $O_3$  versus  $NO_y$  from models at locations representing the transition from  $NO_y$ -sensitive to VOC-sensitive conditions. Interpreted as  $NO_x$ -VOC indicators, measured  $O_3$  versus  $NO_y$  higher than the transition values would represent  $NO_x$ -sensitive conditions.

#### 4.1.4. Evaluation of air quality models

Use of measured  $O_3$  and reactive nitrogen to evaluate air quality models is probably the most promising use of the indicator concept. Use of indicator ratios by themselves to diagnose  $O_3$ - $NO_x$ -VOC sensitivity gives cause for

doubt because it is not certain whether the correlation between indicator ratios and  $\text{NO}_x$ -VOC sensitivity is universally valid. Use of measured species to evaluate model scenarios should remain valid even if the correlation between indicators and  $\text{NO}_x$ -VOC sensitivity is less than perfect.

An evaluation of models using measured reactive nitrogen should include the following steps:

**Adjustment of model boundary values:** When air quality models are used to evaluate conditions in individual metropolitan areas, they often include adjustments to  $\text{O}_3$  along the model boundary in order to reflect transport into the area. Typically, concentrations of  $\text{HNO}_3$  and organic nitrates are set to zero along the model boundary. This can be the cause of poor performance for indicator ratios (see Section 3.1.5) but it can also cause disagreement between model and measured correlations among ozone and reactive nitrogen. Measurements, e.g. Trainer et al., 1993, show that elevated  $\text{O}_3$  is also associated with elevated reactive nitrogen.

To correct this problem, model boundary conditions for PAN and  $\text{HNO}_3$  should be added based on the assumed  $\text{O}_3$ . PAN and  $\text{HNO}_3$  at the boundary should be set based on the correlations between  $\text{O}_3$  and  $\text{HNO}_3$  and between  $\text{O}_3$  and organic nitrates shown in Figures 3.1.7 and 3.1.12.

**Direct comparison between model and measured correlations:** The model and measured correlation between  $\text{O}_3$  and  $\text{NO}_y$ , etc. for the afternoon hours should be compared directly as shown in Figure 3.1.9.

Model values for this comparison should be taken from locations corresponding to the array of measurement sites. It is also useful to compare the measured correlation to model values for the entire domain, as a way of identifying varied conditions at sites not included in the measurements.

**Model versus measurement statistics:** A formal comparison would use the following statistics for comparison between models and measurements:

- (i)  $\text{O}_3$ ,  $\text{NO}_y$  and  $\text{O}_3/\text{NO}_y$  ratio (or equivalent with  $\text{NO}_z$  and  $\text{HNO}_3$ ) for all model values of  $\text{O}_3$  within 10 ppb of the model maximum, and for all measured values of  $\text{O}_3$  within 10 ppb of the measured maximum. Measurements should be within 25% of model values.
- (ii)  $\text{O}_3$ ,  $\text{NO}_y$  and  $\text{O}_3/\text{NO}_y$  ratio (or equivalent with  $\text{NO}_z$  and  $\text{HNO}_3$ ) for all model values of  $\text{O}_3$  above 80 ppb, and for all measured values of  $\text{O}_3$  above 80 ppb. Specific statistics for this comparison should be developed, (e.g. number of hours with  $\text{O}_3/\text{NO}_y$  at certain values).

- (iii) The range of  $O_3$  associated with specified intervals of  $NO_y$  in models and measurements, for relatively low  $NO_y$ : (e.g. 3-4 ppb, 5-6 ppb, 7-8 ppb). Model  $O_3$  for these intervals should be within 25% of measured values. (The equivalent can be done with  $NO_z$  or  $HNO_3$ .)

The comparison between model and measured values at low  $NO_y$  is intended not to evaluate the model, but rather to evaluate the validity of drawing inferences from the comparison between model and measured values at higher  $NO_y$ . Model values at low  $NO_y$  are almost always suggestive of  $NO_x$  sensitive chemistry and show a relatively narrow correlation between  $O_3$  and  $NO_y$ . When a disagreement appears between models and measurements for  $NO_y$  in this range of values, it suggests an error (either in the model or in measurements) that cannot be attributed to  $NO_x$ -VOC sensitivity. Figure 3.1.11 illustrates this type of situation. In this case, results of the other model-measurement comparisons should be discounted.

In addition to the model-measurement analysis, it is also useful to investigate whether the predicted relation between model  $O_3$ - $NO_x$ -VOC sensitivity and indicator ratios remains valid for the simulated case. This can be done by comparing results between a model base case and scenarios with reduced  $NO_x$  and VOC and generating plots equivalent to Figure 3.1.2 and 3.1.7.

**When models and measurements disagree:** Disagreements between models and measurements should be regarded as serious in cases where the model and measurements show good agreement for low  $O_3$  but show a significant disagreement for  $O_3/NO_y$ ,  $O_3/NO_z$  or  $O_3/HNO_3$  in the vicinity of peak  $O_3$ . These erroneous patterns suggest that the model predictions for  $O_3$ - $NO_x$ -VOC sensitivity are biased.

In developing alternative model scenarios, the ratio  $(O_3-O_{3b})/(NO_y-NO_{yb})$  and similar ratios can be interpreted as surrogates for the ratio of reactivity-weighted VOC to  $NO_x$  ( $rVOC/NO_x$ ) in the emission inventory. An alternative scenario might be generated by increasing or decreasing VOC throughout the emission inventory in proportion to the discrepancy for  $(O_3-O_{3b})/(NO_y-NO_{yb})$  associated with peak  $O_3$ . Discrepancies between model and measured  $NO_x$  might be addressed in two ways: either by adjusting  $NO_x$  emissions or by adjusting dispersion rates (e.g. the height of the afternoon convective mixed layer) to change peak  $NO_y$ .

The resulting modified scenario should have different  $O_3$ - $NO_x$ -VOC sensitivity relative to the model base case and should also show better agreement with measured  $O_3$  and reactive nitrogen. The changed  $NO_x$ -VOC

predictions should be interpreted as a measure of the level of uncertainty in those predictions. The modified scenario might also be tested against observed VOC and  $\text{NO}_x$  if such measurements are available.

#### 4.1.5. Summary of proposed regulatory procedure

1. Quality assurance: Plot measured  $\text{O}_3$  versus  $\text{NO}_y$  (and, if available,  $\text{O}_3$  versus  $\text{NO}_z$  and  $\text{O}_3$  versus  $\text{HNO}_3$ ) for the hours 1-5pm in comparison with the model correlation for  $\text{NO}_x$ -sensitive locations only in 3.1.7. Measured ensembles are judged as valid for the indicator method if  $\text{O}_3/\text{NO}_y$  values are equal to or lower than the model correlation for  $\text{NO}_x$ -sensitive locations.
2. Numerical quality assurance: Identify median and 75<sup>th</sup> percentile values of  $\text{O}_3$  associated with low ranges of  $\text{NO}_y$  (2-4 ppb, 4-6 ppb, 6-8 ppb) and compare with model values for  $\text{NO}_x$ -sensitive locations in Figure 3.1.7. Measured 75<sup>th</sup> percentile  $\text{O}_3$  should be no more than 25% higher than model  $\text{O}_3$  for the given range of  $\text{NO}_y$ .
3.  $\text{NO}_x$ -VOC evaluation: Plot measured  $\text{O}_3$  versus  $\text{NO}_y$ , etc. for the hours 1-5pm in comparison with the model correlation for locations with mixed sensitivity in Figure 3.1.7. Measured values higher than the mixed-sensitivity values are interpreted as representing  $\text{NO}_x$ -sensitive conditions and model values lower than the mixed-sensitivity values are interpreted as representing VOC-sensitive conditions.
4.  $\text{NO}_x$ -VOC numerical evaluation: Identify measured  $\text{O}_3/\text{NO}_y$  or  $(\text{O}_3-\text{O}_{3b})/(\text{NO}_y-\text{NO}_{yb})$ , etc. for peak  $\text{O}_3$  (1-5 pm only) during each event of interest, and identify the range of measured values for  $\text{O}_3$  greater than 85 ppb, in comparison with the ratio values identified in Section 3.1.1. as representing the transition value for  $\text{NO}_x$ -sensitive versus VOC-sensitive photochemistry.
5. Evaluation of air quality model: Plot model  $\text{O}_3$  versus  $\text{NO}_y$  (1-5 pm) for the ensemble of locations corresponding to measured values, in comparison of measurements. Identify model ratios as in Step 4 and compare with measured values. A satisfactory model should have ratios within 25% of measured values. (A similar test can be done using model values for the full domain.)

## 4.2 CONSTRAINED STEADY STATE WITH MEASURED $\text{NO}_x$ AND VOC

### 4.2.1. Required measurements

The method requires speciated VOC measurements, including a reasonably complete representation of directly emitted VOC, and measured  $\text{NO}_x$ . These must include the major biogenic species (isoprene). Secondary species

(aldehydes, biogenic reaction products) may be useful, but these are not necessary. Measured photolysis rates are also useful but not necessary.

It is critical that the measured VOC and  $\text{NO}_x$  are acceptable in terms of accuracy, and that any biases (e.g. missing VOC species) are accounted for in the analysis. The existing PAMS network may need to be improved to correct previously identified errors, as described in Parrish et al. (1998) and Cardelino and Chameides (2001) (see Section 3.3.6).

#### **4.2.2. Quality assurance of measurements**

Quality assurance of measured data sets can be established by examining correlations between individual VOC species, between individual VOC and  $\text{NO}_x$ , and between  $\text{NO}_x$  and  $\text{NO}_y$ . These correlations can be used to establish (i) emission ratios between individual species; and (ii) analysis of apparent photochemical aging between species. The same correlations would also be used in the analysis of measurements for content, especially with regard to model-measurement comparisons.

Exact procedures for quality assurance, interpretation of VOC measurements and derivation of emission ratios among species need to be established. A complete analysis might consist of the following:

- Display of correlations among individual VOC within each of three major families (alkanes, alkenes and aromatics) relative to a reference species in each family (propane, propene and either benzene or toluene), following the forms of Figure 3.3.4. These displays should be used to establish apparent emission ratios among species. As shown in Figure 3.3.4, the line representing the maximum ratio of a short-lived to a long-lived species represents the apparent emissions ratio.
- Display of correlations of representative VOC from each family relative to a single reference species (propane), in order to identify emission ratios.
- Comparison of the above results for early morning (6-9am) and midday/afternoon (11-5pm) to identify differences related to photochemical aging.
- Comparison of derived emission ratios among species with prior measurements that represent typical emission ratios among species in the U.S., with emission ratios from inventories for the metropolitan area, and with emission ratios associated with automobile exhaust. (The latter is intended to identify

measurement that may be dominated by fresh auto emissions.) Table 4.2.1 provides a summary of prior measurements.

- Display of the correlation between isoprene and a representative anthropogenic VOC (e.g. propane) during midday and early afternoon (12-3pm), which corresponds to the time of peak isoprene, and display of the isoprene diurnal profile.
- If  $\text{NO}_y$  is available, the correlations between  $\text{NO}_x$  and  $\text{NO}_y$ , between  $\text{O}_3$  and  $\text{NO}_x$  and between  $\text{O}_3$  and  $\text{NO}_z$  should be displayed, in order to establish whether measured  $\text{NO}_x$  can be regarded as true  $\text{NO}_x$  or whether it also includes PAN. Correlations of  $\text{O}_3$  versus  $\text{NO}_x$  and  $\text{O}_3$  versus  $\text{NO}_z$  can be compared with patterns from models or with research-grade measurements (see Section 4.1.1)

This may be well beyond the scope of regulatory analysis. However, a reasonable short summary might be done by deriving emission ratios for the major VOC reactivity classes, based on measured correlations, and comparing these ratios with inventory values. When emission ratios derived from measurements differ substantially from the expected emission rates, a judgement would need to be made whether the results represent true ambient conditions, measurement errors, or the impact of direct emissions (typically, auto exhaust) at the measurement site.

A separate analysis should identify VOC species that appear to be missing from the measurements, and adjust the total measured VOC to account for the missing species.

Quality assurance for biogenic species is more difficult because no correlation is expected between biogenic VOC and anthropogenic species. The correlation between the two major biogenic VOC (isoprene and  $\alpha$ -pinene) might be used for quality assurance, but deviations from expected values are more likely due to the minor species ( $\beta$ -pinene) rather than to isoprene. The results for isoprene can be interpreted only in comparison with predicted correlations and diurnal profiles from 3-d models. Individual judgment will be necessary to decide whether discrepancies reflect errors in emission inventories rather than model dispersion rates or measurement error.

**Table 4.2.1****Measured concentrations of hydrocarbons**

Median concentrations are shown of the 48 most abundant ambient air hydrocarbons in 39 U.S. cities. Reported by Parrish et al. (1998) from Seila et al. (1989).

Rank	Compound	ppbC	Rank	Compound	ppbC
1	i-pentane	45.3	25	n-heptane	4.7
2	n-butane	40.3	26	2,3-dimethylbutane	3.8
3	toluene	33.8	27	c-2-pentene	3.6
4	propane	23.5	28	1,2,3-trimethylbenzene	3.4
5	ethane	23.3	29	methylcyclohexane	3.4
6	n-pentane	22.0	30	n-decane	3.3
7	ethene	21.4	31	1,3,5-trimethylbenzene	3.0
8	m&p-xylene	18.1	32	C11 aromatic	3.0
9	2-methylpentane	14.9	33	t-2-pentene	2.9
10	i-butane	14.8	34	o-ethyltoluene	2.9
11	acetylene	12.9	35	p-ethyltoluene	2.8
12	benzene	12.6	36	C10 aromatic	2.8
13	n-hexane, 2-ethyl-1-butene	11.0	37	n-octane	2.6
14	3-methylpentane	10.7	38	2-methyl-1-butene	2.6
15	1,2,4-trimethylbenzene	10.6	39	1,2-dimethyl-3-ethylbenzene	2.5
16	propene	7.7	40	t-2-butene	2.5
17	2-methylhexane	7.3	41	2,3,4-trimethylpentane	2.5
18	o-xylene	7.2	42	2-methylheptane	2.5
19	2,2,4-trimethylpentane	6.8	43	1,4-diethylbenzene	2.4
20	methylcyclopentane	6.4	44	3-methylheptane	2.2
21	3-methylhexane	5.9	45	n-nonane	2.2
22	2-methylpropene, 1-butene	5.9	46	cyclohexane	2.2
23	ethylbenzene	5.9	47	2,4-dimethylpentane	2.2
24	m-ethyltoluene	5.3	48	cyclopentane	2.1

**4.2.3. Interpretation of measured results**

Interpretation of measured VOC and NO<sub>x</sub> includes two components: (i) application and interpretation of results from constrained steady state calculations; and (ii) derivation of emission rates based on measured correlations among VOC and NO<sub>x</sub>.

**Results of constrained steady-state calculations:** Three different methods have been used to display results from constrained steady-state calculations. Cardelino and Chameides (1995) simply reported the summed impact of reduced NO<sub>x</sub> and reduced VOC on ozone production, where ozone production was summed over 12 hours on a single day, and included summed values for several measurement sites that represented conditions for a given

metropolitan area. Tonnesen and Dennis (2000a) presented graphs that showed the predicted change in ozone production due to changed  $\text{NO}_x$  and VOC at each individual hour and each location, plotted against a proposed indicator for instantaneous chemistry based on reactivity-weighted VOC and  $\text{NO}_x$ . Kleinman et al. (1997, 2000, 2001) also showed the predicted change in ozone production rates at individual times and locations, plotted against the parameter  $L_N/Q$  which explained  $\text{NO}_x$ -VOC chemistry. Kleinman et al. compared patterns for different locations, which often had different  $\text{NO}_x$ -VOC sensitivity but the same relation between  $\text{NO}_x$ -VOC sensitivity and the parameter  $L_N/Q$ . The results from Kleinman et al. were the only results based on measurements. The results shown by Cardelino and Chameides (1995) were based on pseudo-data derived from a 3-d air quality model. Similarly, the results from Tonnesen and Dennis (2000a) represented predictions from an AQM.

For regulatory purposes it is useful to show how the predicted sensitivity to  $\text{NO}_x$  and VOC is related to the rate of ozone production ( $\text{PO}_3$ ) and how it varies with geography.  $\text{NO}_x$ -VOC sensitivity is most important during periods of high ozone production. This is accomplished in part by summing  $\text{PO}_3$  over extended time periods and by representing the impact of reduced  $\text{NO}_x$  and reduced VOC based on the summed impact over time, as done by Cardelino and Chameides (1995).

The following display is suggested: diurnal sums of the impact of reduced  $\text{NO}_x$  and VOC, plotted against the equivalent sum of  $\text{PO}_3$ , from measurements collected over a season, and separate sums for different geographical locations within a metropolitan area. The summed impact of reduced  $\text{NO}_x$  and VOC on ozone production, as used by Cardelino and Chameides (1995), provides a convenient single-number summation. The summed ratio of reactivity-weighted VOC to  $\text{NO}_x$  ( $r\text{VOC}/\text{NO}_x$ ) summed over the midday hours associated with maximum ozone production (10am-4pm) also provides a useful summary of measurements, because this ratio is closely associated with  $\text{NO}_x$ -VOC sensitivity. This sum must be done for midday rather than morning, because midday values include the impact of biogenic VOC and because midday values represent conditions at the time of maximum ozone production.

The relative impact of anthropogenic versus biogenic VOC is also of interest to the regulatory community. This can be represented by displaying the ratio of biogenic to anthropogenic VOC, expressed either as ratio of reactivity-weighted sums or a ratio of ozone formation potentials (Carter, 1994, 1995), plotted versus  $\text{PO}_3$ . A single-number summation can be developed by calculating the weighted sums of biogenic and anthropogenic VOC, weighted both

by reactivity (or by ozone formation potentials) and by the calculated rate of ozone production at the time of the observation.

**Derived emission rates:** The other major result of this analysis consists of inferred emission rates for anthropogenic VOC and  $\text{NO}_x$  in comparison with emission inventories. The correlations between measured VOC species, suggested as part of quality assurance (Section 4.2.2) also provide an effective way of displaying results of the analysis that have implications for the regulatory process. Derived emission rates and ratios provide single-number summations of these results.

#### **4.2.4. Evaluation of air quality models**

Constrained steady state calculations and associated  $\text{NO}_x$  and VOC measurements can be used to evaluate air quality models in two ways: direct comparisons between model and measured values or between values derived from AQMs and from constrained steady state calculations; and evaluation of emission inventories.

In both cases, adjustment of AQMs to improve agreement with measured values will require changes in emission rates. The measured  $\text{NO}_x$  and VOC are controlled largely by these rates.

**Comparison between model and measured values:** Evaluation of an AQM using results of constrained steady state calculation can be done most efficiently by deriving predicted species concentrations from the AQM that correspond to the times and locations of available measurements. These model values can then be regarded as pseudo-data and used to drive the equivalent CSS calculation. Assuming that CSS uses the same photochemical mechanism as the AQM, comparison between CSS results based measurements and CSS results based on AQM species concentrations provides an estimate of the impact of model-measurement differences on  $\text{NO}_x$ -VOC predictions.

The summed impact of reduced  $\text{NO}_x$  and VOC on ozone production at the measurement sites, used by Cardelino and Chameides (1995) as a single-number summation of results from the CSS calculation, also provides a convenient summation of the extent of agreement between the AQM and measured  $\text{NO}_x$  and VOC.

A direct comparison between model and measured values for the ratio  $r\text{VOC}/\text{NO}_x$  (including both morning and midday values) is also a useful way to summarize model performance and bias with regard to measured  $\text{NO}_x$  and VOC.

The ratio of summed biogenic and anthropogenic VOC concentrations, each weighted by reactivity and by rate of ozone production coincident with the measurement (or with pseudo-data from the AQM) provides a simple estimate of impact of biogenic VOC in the AQM in comparison with measurements.

***Evaluation of emission inventories:*** Model emission inventories can be adjusted in two ways. Ratios of emission inventories derived from the graphical display of measurements can be used to adjust emission rates throughout a metropolitan area, by adjusting emission rates throughout by a constant factor. Separate adjustment factors may be applied for geographical subregions with different emissions characteristics, based on results at different measurement sites. An alternative method is to use inverse modeling procedures (Mendoza-Dominguez and Russell, 2000, 2001, 2002).

It is also useful to display the predicted values of correlations between individual VOC, as described in Section 4.2.2, in comparison with measured values. Comparisons between predicted correlations from AQMs and measured values will clearly identify the extent of agreement or disagreement.

As described in Section 4.2.2, emission rates for biogenic species cannot be derived directly from correlations among measured species. Evaluation of biogenic emission rates is possible through model-measurement comparisons for (i) diurnal concentration profiles, and (ii) averaged midday and afternoon concentrations (11am-3pm) for equivalent model and measured locations. The midday and afternoon period is recommended as the time period associated both with maximum photochemical activity and maximum impact of biogenic species.

#### **4.2.5. Summary of proposed regulatory procedure**

1. Derive emission rates of all major anthropogenic VOC based on measured correlations between individual VOC. Compare the derived emission rates with rates from emission inventories used in air quality models. The comparison should be expressed as reactivity-weighted sums of VOC species associated with major VOC categories, and as reactivity-weighted sums of all anthropogenic VOC. The measurement-based emission rates are derived from species correlations between each VOC and a reference VOC (propane), and between propane and  $\text{NO}_y$  in order to derive ratios for  $r\text{VOC}/r\text{NO}_x$ . Suggested numerical procedure: identify a sequence of intervals for the measured values of the reference VOC (propane); identify near-maximum (90<sup>th</sup> percentile) measured value other VOC species

for each interval value of the (slower-reacting) reference VOC; and interpret the slope between near-maximum values and reference value as the ratio of emissions.

2. Quality assurance: Compare derived emission rates with emission rates from inventories. In cases of major discrepancies, a judgment must be made whether the measured value or inventory value is correct. In cases where species appear to be missing from measurements, the measurements should be supplemented with inferred concentrations of missing VOC.
3.  $\text{NO}_x$ -VOC evaluation: either
  - (i) Calculate ozone production based on measurements (including adjustment from #2) using the constrained steady state model, and plot ozone production ( $P_{\text{O}_3}$ ) versus calculated impact of reduced  $\text{NO}_x$  and reduced VOC; or
  - (ii) Plot reactivity-weighted VOC (rVOC) versus  $\text{NO}_x$  ( $r\text{NO}_x$ ) at measurement sites associated with urban and regional ozone production, averaged over the hours of maximum ozone production (10am-4pm). The rVOC versus  $\text{NO}_x$  can be interpreted in comparison with the values of  $r\text{VOC}/r\text{NO}_x$  associated with  $\text{NO}_x$ -sensitive and VOC-sensitive instantaneous chemistry (Section 3.3.4).

$\text{NO}_x$ -VOC numerical evaluation. High and low measured  $r\text{VOC}/r\text{NO}_x$  shows the approximate extent of  $\text{NO}_x$ -sensitive and VOC-sensitive photochemical production in the region.
4. Numerical  $\text{NO}_x$ -VOC evaluation: either
  - (i) Report the summed  $P_{\text{O}_3}$  and summed change in  $P_{\text{O}_3}$  associated with either reduced  $\text{NO}_x$  or VOC using the constrained steady state model, following the procedures recommended by Cardelino and Chameides (1995) (see Section 3.3.3) for an individual event; or
  - (ii) Report the average  $r\text{VOC}/r\text{NO}_x$  for the event, based on summed rVOC and  $r\text{NO}_x$  summed individually over the hours of maximum ozone production (10am-4pm) at measurement sites associated with urban and regional ozone production. Approximate  $\text{NO}_x$ -VOC sensitivity is inferred based on the correlation between sensitivity and  $r\text{VOC}/r\text{NO}_x$  from Section 3.3.4.
5. Evaluation of air quality model: Repeat steps #3 and #4 using VOC and  $\text{NO}_x$  concentrations from air quality model scenarios in place of measurements. The difference between results from models and measurements gives an indication of possible bias in  $\text{NO}_x$ -VOC predictions from models. Differences

between emission rates inferred from models and rates from emission inventories (step #1) also provides an evaluation of possible bias in model scenarios.

## ***SECTION 5. RECOMMENDATIONS FOR FURTHER RESEARCH***

The research topics discussed below address two broad issues:

- Research designed to evaluate the accuracy of a proposed OBM
- Research designed to develop standard procedures for using an OBM to derive results useful in a regulatory context. This also includes work to establish measurement networks with sufficient accuracy.

### **5.1. NO<sub>x</sub>-VOC indicators**

These recommendations are also useful in connection with smog production algorithms.

1. Expansion of the PAMS network to include NO<sub>y</sub> measurements of sufficient accuracy, based on recommendations from McClenny et al. (2000).
2. Evaluation of correlations between O<sub>3</sub> and individual reactive nitrogen species (PAN, HNO<sub>3</sub>, and other organic nitrates) in comparison with predictions of AQMs using various photochemical mechanisms. This should lead to an understanding concerning the relative amount of HNO<sub>3</sub> and organic nitrates predicted by the various photochemical mechanisms (including SAPRC 99, as the mechanism with the most complete speciation, and CB-IV, as the mechanism most commonly used in regulatory applications).
3. Development of a data base of correlations between O<sub>3</sub> and NO<sub>y</sub>, O<sub>3</sub> and NO<sub>z</sub>, O<sub>3</sub> and HNO<sub>3</sub> and O<sub>3</sub> versus PAN from research-grade measurements, preferably from measurements that have been published in scientific literature. This should include identification of different patterns in locations with different probable NO<sub>x</sub>-VOC sensitivity. Research-grade measurements of these species have been made in Nashville, New York, Philadelphia, Houston and Los Angeles. These measurements should be compared and reported in a way that can be used for evaluating the accuracy of measurements used during regulatory studies.

4. Development of an equivalent data base of correlations between  $O_3$  and reactive nitrogen from PAMS and other networks used in regulatory studies, and evaluation in comparison with research-grade measurements.
5. Comparison of proposed indicator ratios ( $O_3/NO_y$ ,  $O_3/NO_z$ ,  $O_3/HNO_3$ ) and related ratios ( $O_3/PAN$ ) in identical calculations using different photochemical mechanisms. This should also include comparisons of ratios of production rates for ozone and  $NO_z$ , ozone and  $HNO_3$ , etc. for different amounts of VOC,  $NO_x$  and for different VOC species.
6. Evaluation of photochemical mechanisms in comparison with smog chamber experiments that include specific transitions between  $NO_x$ -sensitive and VOC-sensitive conditions. Experiments associated with the smog production algorithms are especially useful in this regard. Measured values of proposed indicator ratios in these experiments should be compared with values in equivalent photochemical calculations.

## **5.2. Constrained steady state/measured $NO_x$ and VOC**

1. The quality of measured  $NO_x$  and VOC at PAMS measurement sites may need to be upgraded to correct problems cited by Parrish et al. (2000) and Cardelino and Chameides (2000).
2. A software package should be developed for evaluating measured VOC and  $NO_x$  from the PAMS network, in close association with established protocols for reporting of PAMS data. This package should display a standard set of correlations among individual VOC and derive emissions ratios among VOC, following procedures used by Goldan et al. (1995) and Parrish et al. (1998, 2000). The package should include display of these derived emission ratios in comparison with U.S. averages and in comparison with fresh auto exhaust. Other standard tests for quality assurance could be included. The same software package can include the constrained steady state calculation for clear-sky conditions and display standard output.
3. Associated with the above recommendation, a series of standard tests for quality assurance of measured VOC, standard methods for display of results from measurements pertaining to anthropogenic and biogenic VOC inventories, and standard methods for reporting and interpreting results of constrained steady state calculations need to be developed.

4. The representation of the vertical distribution of directly emitted VOC in the current generation of air quality models needs to be investigated. This is especially important for highly reactive species (e.g. isoprene) during typical daytime conditions with rapid convective mixing. The rate of dispersion out of the surface layer in AQMs may have a significant impact on model species concentrations. Model vertical profiles of isoprene can be compared with measured profiles reported by Andronache et al. (1994) and Guenther et al. (1996a, 1996b). For other species, vertical profiles in regions with high direct emission rates need to be measured.

## SECTION 6. REFERENCES

- Andronache, C., W. L. Chameides, M. O. Rodgers, J. E. Martinez, P. Zimmerman, and J. Greenberg. Vertical distribution of isoprene in the lower boundary layer of the rural and urban southern United States. *J. Geophys. Res.*, 99,16989-17000, 1994.
- Blanchard, C. L., and D. Fairley. Spatial mapping of VOC and NO<sub>x</sub>-limitation of ozone formation in central California. *Atmos. Environ.* 2001, In press.
- Blanchard, C. L. Spatial Mapping of VOC and NO<sub>x</sub> Limitation of Ozone Formation in Six Areas. 92nd Annual Meeting of the Air and Waste Management Association, Orlando, Florida. June 24-28, 2001; paper no.. 21, session no. AB-2c.
- Blanchard, C. L., and T. Stoeckenius, Ozone response to precursor controls: comparison of data analysis methods with the predictions of photochemical air quality simulation models. *Atmos. Environ.*, 35, 1203-1216, 2001.
- Blanchard, C. L., Ozone process insights from field experiments- Part III: Extent of reaction and ozone formation. *Atmos. Environ.* 2000, 34: 2035-2043.
- Blanchard, C. L., F. W. Lurmann, P. M. Roth, H. E. Jeffries, and M. Korc, The use of ambient data to corroborate analyses of ozone control strategies, *Atmos. Environ.*, 33, 369-381, 1999.
- Blanchard, C. L., P. T. Roberts, L. R. Chinkin, and P. M. Roth. Application of smog production (SP) algorithms to the TNRCC COAST data. 86th Annual Meeting of the Air and Waste Management Association, San Antonio, Texas. 1995; paper 95\_TP15P.04.
- Blanchard, C. L., Spatial Mapping of VOC and NO<sub>x</sub> Limitation of Ozone Formation in Six Areas. 92nd Annual Meeting of the Air and Waste Management Association, Orlando, Florida. June 24-28, 2001; paper no. 21, session no. AB-2c.
- Bowen, J. L. and I. Valiela, Historical changes to atmospheric nitrogen deposition to Cape Cod, Massachusetts, USA., *Atmos. Environ.*, 35, 1039-1051, 2001.
- Buhr, M., D Parrish, J. Elliot, J. Holloway, J. Carpenter, P. Goldan, W. Kuster, M. Trainer, S. Montzka, S. McKeen, and F. C. Fehsenfeld, Evaluation of ozone precursor source types using principal component analysis of ambient air measurements in rural Alabama. *J. Geophys. Res.*, 100, 22853-22860, 1995.
- Buhr, M. P., M. Trainer, D. D. Parrish, R. E. Sievers, and F. C. Fehsenfeld, Assessment of pollutant emission inventories by principal component analysis of ambient air measurements, *Geophys. Res. Letters*, 19, 1009-1012, 1992.
- Butler, T. J., G. E. Likens and .B. J. B. Stunder, Regional-scale impacts of Phase I of the Clean Air Act Amendments in the USA: the relation between emissions and concentrations, both wet and dry, *Atmos. Environ.*, 35, 6, 1015-1028, 2001.
- Cardelino, C. and W. L. Chameides. An observation-based model for analyzing ozone-precursor relationships in the urban atmosphere. *J. Air Waste Manage. Assoc.*, 45, 161-180, 1995.
- Cardelino, C. A. and W. L. Chameides, The application of data from photochemical assessment monitoring stations to the observation-based model, *Atmos. Environ.*, 34, 2325-2332, 2000.

- Carroll, M.A., D. R. Hastie, B. A. Rdley, M. O. Rodgers, A. L. Torres, D. D. Davis, J. D. Bradshaw, S. T. Sandholm, H. I. Schiff, D. R. Karecki, G. W. Harris, G. I. Mackay, G. L. Gregory, E. P. Condon, M. Trainer, G. Hubler, D. D. Montzka S. Madronich, D. L. Albritton, H. B. Singh, S. M. Beck, M. C. Shipham, and A. S. Bachmeier, Aircraft measurements of NO<sub>x</sub> over the eastern Pacific and continental United States and implications for ozone production. *J. Geophys. Res.*, 95, 10199-10204 1990.
- Chin, M., D. J. Jacob, J. W. Munger, D. D. Parrish and B. G. Doddridge, Relationship of ozone and carbon monoxide over North America. *J. Geophys. Res.*, 99, 14565-14573, 1994.
- Carter, W. P. L. Development of ozone reactivity scales for volatile organic compounds, *J. Air Waste Manage. Assoc.*, 44, 881-899, 1994.
- Carter, W. P. L., Computer modeling of environmental chamber studies of maximum incremental reactivities of volatile organic compounds, *Atmos. Environ.*, 29-18, p. 2513, 1995.
- Chameides, W. L., F. Fehsenfeld, M. O. Rodgers, C. Cardellino, J. Martinez, D. Parrish, W. Lonneman, D. R. Lawson, R. A. Rasmussen, P. Zimmerman, J. Greenberg, P. Middleton, and T. Wang, Ozone precursor relationships in the ambient atmosphere. *J. Geophys. Res.*, 97, 6037-6056, 1992.
- Chang, M. E., D. E. Hartley, C. Cardelino, D. Hass-Laursen, and W. L. Chang, On using inverse methods for resolving emissions with large spatial inhomogeneities, *J. Geophys. Res.*, 102, 16023-16036, 1997.
- Chang, M. E., C. Cardelino, d. Hartley, and W. L. Chang, Inverse modeling of biogenic emissions, *Geophys. Res., Lett.*, 3, 3007, 1996.
- Chang, T. Y., D. P. Chock, B. I. Nance, and S. L. Winkler. A photochemical extent parameter to aid ozone air quality management. *Atmos. Environ.*, 31, 2787-2794, 1997.
- Chang, T. Y. and M. Suzio: "Assessing Ozone-Precursor Relationships Based on Smog Production Model and Ambient Data." *J. Air & Waste Manage. Assoc.* 45, 20-28 (1995).
- Chang, T. Y. and M. Suzio: "A Smog Production Model and An Assessment of Ozone Control Strategies." Proceedings of the 1994 AWMA Conference on Tropospheric Ozone: Critical Issues in the Regulatory Process. Air and Waste Management Association, Pittsburgh, PA 15222, pp. 550-561 (1996).
- Cheng, M-D., P. K. Hopke, and Y. Zeng, A receptor-oriented methodology for determining source regions of particulate sulfate observed at Dorset, Ontario, *J. Geophys. Res.*, 98, 16839-16849, 1993.
- Chin, M., D. J. Jacob, J. W. Munger, D. D. Parrish and B. G. Doddridge, Relationship of ozone and carbon monoxide over North America. *J. Geophys. Res.*, 99, 14565-14573, 1994.
- Chock, D. P., T. Y. Chang, S. L. Winkler, and B. I. Nance, The impact of an 8 h ozone air quality standard on ROG and NO<sub>x</sub> controls in Southern California. *Atmos. Environ.*, 33, 2471-2486, 1999.
- Clark, T. L. and T. R. Karl, Application of prognostic meteorological variables to forecasts of daily maximum one-hour ozone concentrations in the northeastern United States, *J. Appl. Meteo.*, 21, 1662-1671, 1982.
- Collins, W. J., D. S. Stevenson, C. E. Johnson, and R. G. Derwent, The European regional ozone distribution and its links with the global scale for the years 1992 and 2015, *Atmos. Environ.*, 34, 255-267, 2000.
- Daum, P. H., L. Kleinman, D. G. Imre, L. J. Nunnermacker, Y.-N. Lee, S. R. Springston, and L. Newman, Analysis of the processing of Nashville urban emissions on July 3 and July 18, 1995, *J. Geophys. Res.*, 105, 9155-9164, 2000.

- Dommen, J. A. S. H. Prevot, A. M. Hering, T. Staffelbach, G. L. Kok, and R. D. Schillawski, Photochemical production and the aging of an urban air mass. *J. Geophys. Res.*, 104, 5493-5506, 1999.
- Fenger, J., Urban air quality. *Atmos. Environ.*, 33, 4877-4900, 1999.
- Fiore, A. M., D. J. Jacob, J. A. Logan, and J. H. Yin, Long-term trends in ground level ozone over the contiguous United States, 1980-1995. *J. Geophys. Res.*, 103, 1471-1480, 1998.
- Fiore, A. M., D. J. Jacob, I. Bey, Y. M. Yantoska, B. D. Field, A. C. Fusco, and J. G. Wilkensen, Background ozone over the United States in summer: origin, trend, and contribution to pollution episodes. *J. Geophys. Res.*, in press, 2002 (available at <http://www-as.harvard.edu/chemistry/trop/recentpapers.html>).
- Fujita, E. M., B. E. Croes, C. L. Bennett, D. R. Lawson, F. W. Lurmann and H. H. Main, Comparison of emission and ambient concentration ratios of CO, NO<sub>x</sub>, and NMOG in California's south coast air basin. *J. Air Waste Mgmt. Assoc.*, 42:264-276 1992.
- Geron, C. D., A. B. Guenther, and T. E. Pierce. An improved model for estimating emissions of volatile organic compounds from forests in the eastern United States. *J. Geophys. Res.*, 99, 12773-12791, 1994.
- Gery, M. W. G. Z. Whitten, J. P. Killus and M. C. Dodge. A photochemical kinetics mechanism for urban and regional computer modeling. *J. Geophys. Res.*, 94, 12925-12956, 1989.
- Gillani, N. V. and J. E. Pleim. Sub-grid-scale features of anthropogenic emissions of NO<sub>x</sub> and VOC in the context of regional Eulerian models. *Atmos. Environ.*, 30, 2043-2059, 1996.
- Gilliland, A., and P. Abbitt, A sensitivity study of the discrete Kalman filter (DKF) to initial condition discrepancies, *J. Geophys. Res.*, 106, 17939-17952, 2001.
- Goldan, P. D., M. Trainer, W. C. Kuster, D. D. Parrish, J. Carpenter, J. M. Roberts, J. E. Yee, and F. C. Fehsenfeld. Measurements of hydrocarbons, oxygenated hydrocarbons, carbon monoxide and nitrogen oxides in an urban basin in Colorado: implications for emissions inventories. *J. Geophys. Res.*, 100, 22771-22785, 1995.
- Goldan, P. D., W. C. Kuster, and F. C. Fehsenfeld, Non-methane hydrocarbon measurements during the tropospheric OH photochemistry experiment, *J. Geophys. Res.*, 102, 6315-6324, 1997.
- Goldan, P. D., D. D. Parrish, W. C. Kuster, M. Trainer, S. A. McKeen, J. Holloway, B. T. Jobson, D. T. Sueper, and F. C. Fehsenfeld, Airborne measurements of isoprene, CO and anthropogenic hydrocarbons and their implications, *J. Geophys. Res.*, in press, 2001.
- Goldstein, A. H., and G. W. Schade, Quantifying biogenic and anthropogenic contributions to acetone mixing ratios in a rural environment, *Atmos. Environ.*, 34, 4997-5006, 2000.
- Guenther, A., P. Zimmerman, L. Klinger, J. Greenberg, C. Ennis, K. Davis, W. Pollock, H. Westberg, G. Allwine, and C. Geron, Estimates of regional natural volatile organic compound fluxes from enclosure and ambient measurements. *J. Geophys. Res.*, 101, 1345-1359, 1996a.
- Guenther, A., W. Baugh, K. Davis, G. Hampton, P. Harley, L. Klinger, L. Vierling, P. Zimmerman, E. Allwine, S. Dilts, B. Lamb, H. Westberg, D. Baldocchi, C. Geron, and T. Pierce, Isoprene fluxes measured by enclosure, relaxed eddy accumulation, surface layer gradient, mixed layer gradient, and mixed layer mass balance techniques. *J. Geophys. Res.*, 101, 18555-18567, 1996b.
- Hammer, M.-U., B. Vogel, and H. Vogel, Findings on H<sub>2</sub>O<sub>2</sub>/HNO<sub>3</sub> as an Indicator of Ozone Sensitivity in Baden-Württemberg, Berlin-Brandenburg, and the Po Valley Based on Numerical Simulations, *J. Geophys. Res.*, in press, 2001.

- Harley, R. A., R. F. Sawyer, J. B. Milford, Updated photochemical modeling for California's South Coast air basin: comparison of chemical mechanisms and motor vehicle emission inventories. *Enviro. Sci. Tech.*, 31, 2829-2839.
- Henry, R. C., C. W. Lewis, P. K. Hopke, and H. W. Williamson, Review of receptor modeling fundamentals, *Atmos. Environ.*, 18, 1507-1515, 1984.
- Hess, G. D., F. Carnovale, M. E. Cope, and G. M. Johnson, The evaluation of some photochemical smog reaction mechanisms-I. Temperature and initial composition effects. *Atmos. Environ.*, 26A, 625-641, 1992.
- Hess, G. D., F. Carnovale, M. E. Cope, and G. M. Johnson, The evaluation of some photochemical smog reaction mechanisms-II. Initial addition of alkanes and alkenes. *Atmos. Environ.*, 26A, 642-650, 1992.
- Hess, G. D., F. Carnovale, M. E. Cope, and G. M. Johnson, The evaluation of some photochemical smog reaction mechanisms-III. Dilution and emissions effects. *Atmos. Environ.*, 26A, 651-658, 1992.
- Hirsch, A. I., J. W. Munger, D. J. Jacob, L. W. Horowitz, and A. H. Goldstein, Seasonal variation of the ozone production efficiency per unit  $\text{NO}_x$  at Harvard Forest, Massachusetts. *J. Geophys. Res.*, 101, 12659-12666, 1996.
- Hopke, P. K., *Receptor Modeling in Environmental Chemistry*, John Wiley, New York, New York, 1985.
- Jacob, D. J., B. G. Heikes, R. R. Dickerson, R. S. Artz and W. C. Keene. Evidence for a seasonal transition from  $\text{NO}_x$ - to hydrocarbon-limited ozone production at Shenandoah National Park, Virginia. *J. Geophys. Res.*, 100, 9315-9324, 1995.
- Jacob, D.J., J.A. Logan, and P.P. Murti., Effect of Rising Asian Emissions on Surface Ozone in the United States, *Geophys. Res. Lett.*, 26, 2175-2178, 1999.
- Jacobson, M. Z., R. Lu, R. P. Turco, and O. P. Toon, Development and application of a new air pollution modeling system-Part I: Gas-phase simulations. *Atmos. Environ.*, 30, 1939-1963, 1996.
- Jaegle, L., D.J. Jacob, W.H. Brune, D. Tan, I. Faloon, A.J. Weinheimer, B.A. Ridley, T.L. Campos, and G.W. Sachse, Sources of HOx and production of ozone in the upper troposphere over the United States, *Geophys. Res. Lett.*, 25, 1705-1708, 1998.
- Johnson, G. M., A simple model for predicting the ozone concentration of ambient air. Proc. Eighth Inter. Clean Air Confer., Melbourne, Australia, May 2, 1984, p. 715-731.
- Johnson, G. M. and S. M. Quigley, A universal monitor for photochemical smog, paper 89-29.8, Air and Waste Management Association 82<sup>nd</sup> Annual Meeting and Exhibition, Anaheim, CA, June 25-30, 1989,
- Johnson, G. M., S. M. Quigley, and J. G. Smith. Management of photochemical smog using the AIRTRAK approach. 10th International Conference of the Clean Air Society of Australia and New Zealand, Auckland, New Zealand, March, 1990, p. 209-214.
- Kim, B. M. and R. C. Henry, Application of SAFER model to the Los Angeles PM10 data, *Atmos. Environ.*, 34, 1747-1759, 2000.
- Kirchner, F., F. Jeaneret, A. Clappier, B. Kruger, H. van den Bergh, and B. Calpini, Total VOC reactivity in the planetary boundary layer 2. A new indicator for determining the sensitivity of the ozone production to VOC and  $\text{NO}_x$ , *J. Geophys. Res.*, 106, 3095-3110, 2001.

- Kleinman, L. H., P. H. Daum, Y-N. Lee, L. J. Nunnermacker, S. R. Springston, J. Weinstein-Lloyd, and Jochen Rudolph, Sensitivity of ozone production rate to ozone precursors, *Geophys. Res. Lett.*, 28, 2903-2906, 2001.
- Kleinman, L. I., P. H. Daum, Y-N. Lee, L. J. Nunnermacker, S. R. Springston, J. Weinstein-Lloyd, P. Hyde, P. Doskey, J. Rudolf, J. Fast and C. Berkowitz, Photochemical age determinations in the Phoenix metropolitan area. *J. Geophys. Res.*, 10.1029/2002JD002621, 2003.
- Kleinman, L. I., P. H. Daum, D. G. Imre, J. H. Lee, Y-N. Lee, L. J. Nunnermacker, S. R. Springston, J. Weinstein-Lloyd, and L. Newman, Ozone production in the New York City urban plume, *J. Geophys. Res.*, 105, 14495-14511, 2000.
- Kleinman, L. I., Ozone process insights from field experiments – part II; observation-based analysis for ozone production. *Atmos. Environ.*, 34, 2023-2034, 2000.
- Kleinman, L. I., P. H. Daum, J. H. Lee, Y-N. Lee, L. J. Nunnermacker, S. R. Springston, L. Newman, J. Weinstein-Lloyd and S. Sillman. Dependence of ozone production on NO and hydrocarbons in the troposphere. *Geophys. Res. Lett.*, 24, 2299-2302, 1997.
- Kleinman, L. I., Low and high-NO<sub>x</sub> tropospheric photochemistry. *J. Geophys. Res.*, 99, 16831-16838, 1994.
- Kubler, J., H. van den Bergh, and A. G. Russell, Long-term trends of primary and secondary pollutant concentrations in Switzerland and their response to emission controls and economic changes, *Atmos. Environ.*, 35, 1351-1363, 2001.
- Lefohn, A.S., D.S. Shadwick, S.D. Ziman, The Difficult Challenge of Attaining EPA's new Ozone Standard, *Environ. Sci. & Technol.*, 276A-282A, 1998.
- Li, Q., *et al.*, Transatlantic Transport of Pollution and its Effects on Surface Ozone in Europe and North America, *J. Geophys. Res.*, in press, 2002 (available at <http://www-as.harvard.edu/chemistry/trop/recentpapers.html>).
- Lin, C., and J. B. Milford, Decay-adjusted chemical mass balance receptor modeling for volatile organic compounds, *Atmos Environ.*, 28, 3261-3276, 1994.
- Lin, X., M. Trainer, and S. C. Liu, On the nonlinearity of tropospheric ozone, *J. Geophys Res.*, 93, 15879-15888, 1988.
- Liu, S. C., M. Trainer, F. C. Fehsenfeld, D. D. Parrish, E. J. Williams, D. W. Fahey, G. Hubler, and P. C. Murphy, Ozone production in the rural troposphere and the implications for regional and global ozone distributions. *J. Geophys. Res.*, 92, 4191-4207, 1987.
- Logan, J. A., Ozone in rural areas of the United States, *J. Geophys. Res.*, 94, 8511-8532, 1989.
- Lu, C-H. and J. S. Chang. On the indicator-based approach to assess ozone sensitivities and emissions features. *J. Geophys. Res.*, 103, 3453-3462, 1998.
- Luke, W. T., T. B. Watson, K. J. Olszyna, R. Lauren Gunter, R. T. McMillen, D. L. Wellman, and S. W. Wilkison, Comparison of airborne and surface trace gas measurements during the Southern Oxidant Study, *J. Geophys. Res.*, 103, 22317-22337, 1998.
- Lurmann, F. W., and H. H. Main, Analysis of the ambient VOC data collected in the Southern California Air Quality Study, Sonoma Technology, Inc., Santa Rosa, CA, 1992.

- Lurmann, F. W., Lloyd, A. C., and Atkinson, R. A chemical mechanism for use in long-range transport/acid deposition computer modeling. *J. Geophys. Res.* 91, 10905-10936, 1986.
- Martilli, A., A. Neftel, G. Favaro, F. Kirchner, S. Sillman, and A. Clappier, Simulation of the ozone formation in the northern part of the Po Valley with the TVM-CTM. *J. Geophys. Res.*, in press, 2001.
- McClenny, W. A. ed, Recommended Methods for Ambient Air Monitoring of NO, NO<sub>2</sub>, NO<sub>y</sub>, and Individual NO<sub>x</sub> Species, EPA/600/R-01/005, September, 2000.
- McKeen and S. C Liu, Hydrocarbon ratios and the photochemical history of air masses, *Geophys. Res. Letters*, 20, 2363-2366, 1993.
- McKeen, S. A., S. C. Liu, E.-Y. Hsie, X. Lin, J. D. Bradshaw, s. Smyth, G. L. Gregory, and D. R. Blake, 1996. Hydrocarbon ratios during PEM-WEST A: A model perspective. *J. Geophys. Res.*, 101, 2087-2109.
- McKeen, S. A., G. Mount, F. Eisele, E. Williams, J. Harder, Pl Goldan, W. Kuster, S. C. Liu, K. Baumann, D. Tanner, A. Fried, S. Sewell, C. Cantrell, and R. Shetter, Photochemical modeling of hydroxyl and its relationship to other species during the Tropospheric OH Photochemistry Experiment. *J. Geophys. Res.*, 102, 6467-6493, 1997.
- Mendoza-Dominguez, A., J. W. Boylan, Y-J. Yang and A. G. Russell, Efficient sensitivity analysis of an air quality model for primary and secondary aerosol source impact quantification, submitted to *J. Geophys. Res.*, 2002.
- Mendoza-Dominguez, A., and A. G. Russell, Estimation of emission adjustments from the application of four-dimensional data assimilation to photochemical air quality modeling, *Atmospheric Environment*, 35, 2879-2894, 2001.
- Mendoza-Dominguez and Russell, Iterative Inverse Modeling and Direct Sensitivity Analysis of a Photochemical Air Quality Model, *Environ. Sci. Technol.*, 3, 4974-4981, 2000.
- Milford, J., D. Gao, S. Sillman, P. Blossey, and A. G. Russell. Total reactive nitrogen (NO<sub>y</sub>) as an indicator for the sensitivity of ozone to NO<sub>x</sub> and hydrocarbons. *J. Geophys. Res.* , 99, 3533-3542, 1994.
- Milford, J., A. G. Russell, and G. J. McRae, A new approach to photochemical pollution control: implications of spatial patterns in pollutant responses to reductions in nitrogen oxides and reactive organic gas emissions. *Environ. Sci. Tech.* **23**, 1290-1301, 1989.
- NARSTO. An Assessment of Tropospheric Ozone Pollution: A North American Perspective. The NARSTO Synthesis Team, July, 2000.
- National Research Council (NRC), Committee on Tropospheric Ozone Formation and Measurement. *Rethinking the Ozone Problem in Urban and Regional Air Pollution*, National Academy Press, 1991.
- Olszyna, K. J., E. M. Bailey, R. Simonaitis, and J. F. Meagher. O<sub>3</sub> and NO<sub>y</sub> relationships at a rural site. *J. Geophys. Res.*, 99, 14557-14563, 1994.
- Olszyna, K. J., W. J. Parkhurst, and J. F. Meagher, Air chemistry during the 1995 SOS/Nashville intensive determined from level 2 network, *J. Geophys. Res.*, 103, 31143-31153, 1998.
- Oreskes, N., K. Shrader-Frechette, and K. Beliz, Verification, validation, and confirmation of numerical models in the earth sciences, *Science*, 263, 641-646, 1994.

- Parrish, D. D., M. Trainer, M. P. Buhr, B. A. Watkins, and F. C. Fehsenfeld. Carbon monoxide concentrations and their relation to concentrations of total reactive oxidized nitrogen at two rural U.S. sites. *J. Geophys. Res.*, 96, 9309-9320, 1991.
- Parrish, D. D., et al., Internal consistency tests for evaluation of measurements of anthropogenic hydrocarbons in the troposphere, *J. Geophys. Res.*, 103, 22,339-22,359, 1998.
- Parrish, D.D., and F.C. Fehsenfeld, Methods for gas-phase measurements of ozone, ozone precursors and aerosol precursors, *Atmos. Environ.*, 34, 1921-1957, 2000.
- Paulson, S. E. and J. H. Seinfeld. Development and evaluation of a photooxidation mechanism for isoprene. *J. Geophys. Res.*, 97, 20703-20715, 1992.
- Paulson, S. E. and J. J. Orlando, The reaction of ozone with alkenes: An important source of HO<sub>x</sub> in the boundary layer, *Geophys. Res. Lett.*, 23, 3727-3730, 1996.
- Pierce, T., C. Geron, L. Bender, R. Dennis, G. Tonnesen, and A. Guenther, Influence of increased isoprene emissions on regional ozone modeling, *J. Geophys. Res.*, 103, 25611-25630, 1998.
- Prevot, A. S. H., J. Staehelin, G. L. Kok, R. D. Schillawski, B. Neiningner, T. Staffelbach, A. Neftel, H. Wernli, and J. Dommen, The Milan photooxidant plume. *J. Geophys. Res.*, 102, 23375-23388, 1997.
- Reynolds, S., H. Michaels, P. Roth, T. W. Tesche, D. McNally, L. Gardner, and G. Yarwood, Alternative base cases in photochemical modeling: their construction, role, and value. *Atmos. Environ.*, 30, 12, 1977-1988, 1996.
- Ridley, B. A., S. Madronich, R. B. Chatfield, J. G. Walega, R. E. Shetter, M. A. Carroll, and D. D. Montzka, Measurements and model simulations of the photostationary state during the Mauna Loa Observatory Photochemistry Experiment: Implications for radical concentrations and ozone production and loss rates. *J. Geophys. Res.*, 97, 10375-10388, 1992.
- Roberts, J. M., J. Williams, K. Baumann, M. P. Buhr, P. D. Goldan, J. Holloway, G. Hubler, W. C. Kuster, S. A. McKeen, T.B. Ryerson, M. Trainer, E. J. Williams, F. C. Fehsenfeld, S. B. Bertman, G. Nouaime, C. Seaver, G. Grodzinsky, M. Rodgers, and V. L. Young, Measurements of PAN, PPN, and MPAN made during the 1994 and 1995 Nashville Intensives of the Southern Oxidant Study: Implications for regional ozone production from biogenic hydrocarbons. *J. Geophys. Res.*, 103, 22473-22490, 1998.
- Roselle, S. J. and K. L. Schere. Modeled response of photochemical oxidants to systematic reductions in anthropogenic volatile organic compound and NO<sub>x</sub> emissions. *J. Geophys. Res.*, 100, 22929-22941, 1995.
- Ryerson, T. B., M. B. Buhr, G. Frost, P. D. Goldan, J. S. Holloway, G. Hubler, B. T. Jobson, W. C. Kuster, S. A. McKeen, D. D. Parrish, J. M. Roberts, D. T. Sueper, M. Trainer, J. Williams, and F. C. Fehsenfeld, Emissions lifetimes and ozone formation in power plant plumes. *J. Geophys. Res.*, 103, 22569-22584, 1998.
- Ryerson, T. B., M. Trainer, J. S. Holloway, D. D. Parrish, L. G. Huey, D. T. Sueper, G. J. Frost, S. G. Donnelly, S. Schauffler, E. Atlas, W.C. Kuster, P. D. Goldan, G. Hubler, J. F. Meagher, and F. C. Fehsenfeld, Observations of ozone formation in power plant plumes and implications for ozone control strategies, *Science*, **292**, 719-722, 2001.
- Seila, R. L., W. A. Lonneman, and S. A. Meeks, *Project Summary* □ *Determination of C<sub>2</sub> to C<sub>12</sub> Ambient Air Hydrocarbons in 39 U.S. Cities, from 1984 through 1986, EOA Rep., EPA/600/S3-89/058*, Environ. Pot. Agency, Washington, D.C., 1989.

- Sillman, S. The use of  $\text{NO}_y$ ,  $\text{H}_2\text{O}_2$  and  $\text{HNO}_3$  as indicators for  $\text{O}_3$ - $\text{NO}_x$ -ROG sensitivity in urban locations. *J. Geophys. Res.*, 100, 14175-14188, 1995.
- Sillman, S., K. Al-Wali, F. J. Marsik, P. Nowatski, P. J. Samson, M. O. Rodgers, L. J. Garland, J. E. Martinez, C. Stoneking, R. E. Imhoff, J-H. Lee, J. B. Weinstein-Lloyd, L. Newman and V. Aneja. Photochemistry of ozone formation in Atlanta, GA: models and measurements. *Atmos. Environ.*, 29, 3055-3066, 1995.
- Sillman, S., D. He, C. Cardelino and R. E. Imhoff. The use of photochemical indicators to evaluate ozone- $\text{NO}_x$ -hydrocarbon sensitivity: Case studies from Atlanta, New York and Los Angeles. *J. Air Waste Manage. Assoc.*, 47, 642-652, September, 1997.
- Sillman, S., D. He, M. Pippin, P. Daum, L. Kleinman, J. H. Lee and J. Weinstein-Lloyd. Model correlations for ozone, reactive nitrogen and peroxides for Nashville in comparison with measurements: implications for VOC- $\text{NO}_x$  sensitivity. *J. Geophys. Res.* 103, 22629-22644, 1998.
- Sillman, S. The method of photochemical indicators as a basis for analyzing  $\text{O}_3$ - $\text{NO}_x$ -hydrocarbon sensitivity. NARSTO reviews of tropospheric ozone, available at <http://www.cgenv.com/Narsto/critrev.papers.html>, 2000.
- Sillman, S., M. T. Odman, and A. G. Russell, Comment on "On the indicator-based approach to assess ozone sensitivities and emissions features" by C-H. Lu and J. S. Chang, *J. Geophys. Res.*, 106, D18, 20,941, 2001.
- Sillman, S., Comment on 'The Impact of An 8-hour Ozone Air Quality Standard on VOC and  $\text{NO}_x$  Controls in Southern California' by Chock, et al., *Atmos. Environ.* 35, 3370-3371, 2001.
- Sillman, S., and D. He, Some theoretical results concerning  $\text{O}_3$ - $\text{NO}_x$ -VOC chemistry and  $\text{NO}_x$ -VOC indicators, *J. Geophys. Res.*, 107, 10.1029/2001JD001123, 2002.
- Sillman, S., R. Vautard, L. Menut, and D. Kley,  $\text{O}_3$ - $\text{NO}_x$ -VOC sensitivity and  $\text{NO}_x$ -VOC indicators in Paris: results from models and ESQUIF measurements, *J. Geophys. Res.*, in press, 2003.
- Sosa, G., J. West, F. San Martini, L. T. Molina and M. J. Molina, "Air Quality Modeling and Data Analysis for Ozone and Particulates in Mexico City." MIT Integrated Program on Urban, Regional and Global Air Pollution Report No. 15, 76 pages, October 2000, available from <http://eaps.mit.edu/megacities/index.html>.
- Staffelbach, T., A. Neftel, A. Blatter, A. Gut, M. Fahrni, J. Stahelin A. Prevot, A. Hering, M. Lehning, B. Neininger, M. Baumie, G. L. Ko, J. Dommen, M. Hutterli and M. Anclin. Photochemical oxidant formation over southern Switzerland, part I: Results from summer, 1994. *J. Geophys. Res.*, 102, 23345-23362, 1997.
- Stockwell, W. R., F. Kirchner and M. Kuhn. A new mechanism for regional atmospheric chemistry modeling. *J. Geophys. Res.*, 102, 25847-25879, 1997.
- Stockwell, W. R., P. Middleton, J. S. Chang, and X. Tang. The second generation Regional Acid Deposition Model chemical mechanism for regional air quality modeling, *J. Geophys. Res.*, 95, 16343-16367, 1990.
- Tan, D., I. Faloon, W. H. Brune, P. Shepson, T. L. Couch, A. L. Sumner, T. Thornberry, M. A. Carroll, E. Apel, D. Riemer, and W. Stockwell,  $\text{HO}_x$  budgets in a deciduous forest: Results from the PROPHET summer 1998 campaign, *J. Geophys. Res.*, 106, 24407-24428, 2001. Thielman, A., A. S. H. Prevot, F. C.; Gruebler, and J. Staelhelin, Empirical ozone isopleths as a tool to identify ozone production regimes, *Geophys. Res. Lett.*, 28, 2369-2372, 2001a.
- Thielman, A., A. S. H. Prevot, and J. Staelhelin, Sensitivity of ozone production derived from field measurements in the Italian Po Basin, *J. Geophys. Res.*, in press, 2001b.

- Thornton, J. A., P. A. Wooldridge, R. C. Cohen, M. Martinez, H. Harder, W. H. Brune, E. J. Williams, F. C. Fehsenfeld, S. R. Hall, R. E. Shetter, B. P. Wert, and A. Fried, Observations of ozone production rates as a function of  $\text{NO}_x$  abundances and  $\text{HO}_x$  production rates in the Nashville urban plume, *J. Geophys. Res.*, in press, 2002.
- Tonnesen, G. S. and R. L. Dennis, Analysis of radical propagation efficiency to assess ozone sensitivity to hydrocarbons and  $\text{NO}_x$ . Part 1: Local indicators of odd oxygen production sensitivity, *J. Geophys. Res.*, 105, 9213-9225, 2000a.
- Tonnesen, G. S., and R. L. Dennis, Analysis of radical propagation efficiency to assess ozone sensitivity to hydrocarbons and  $\text{NO}_x$ . Part 2: Long-lived species as indicators of ozone concentration sensitivity, *J. Geophys. Res.*, 105, 9227-9241, 2000b.
- Trainer, M., D. d. Parrish, P. d. Golday, J. Roberts, and F. C. Fehsenfeld, Review of observation-based analysis of the regional factors influencing ozone concentrations, *Atmos. Environ.*, 34, 2045-2061, 2000.
- Trainer, M., D. D. Parrish, M. P. Buhr, R. B. Norton, F. C. Fehsenfeld, K. G. Anlauf, J. W. Bottenheim, Y.Z. Tang, H.A. Wiebe, J.M. Roberts, R.L. Tanner, L. Newman, V.C. Bowersox, J.M. Maughner, K.J. Olszyna, M.O. Rodgers, T. Wang, H. Berresheim, and K. Demerjian. Correlation of ozone with  $\text{NO}_y$  in photochemically aged air. *J. Geophys. Res.*, 98, 2917-2926, 1993.
- Vogel, B., N., Riemer, H. Vogel, F. Fiedler, Findings on  $\text{NO}_y$  as an indicator for ozone sensitivity based on different numerical simulations, *J. Geophys. Res.*, 3605-3620, 1999.
- Watson, J. G., J. C. Chow, and E. M. Fujita, Review of volatile organic compound source apportionment by chemical mass balance, *Atmos. Environ.*, 35, 1567-1584, 2001.
- West, J. J., G. Sosa, F. San Martini, M. J. Molina, and L. T. Molina (2000) Air quality modeling and data analysis for ozone and particulates in Mexico City, MIT-IPURGAP Report No. 15, 76 pages, Oct. 2000.
- Wild, O., and H. Akimoto, Intercontinental transport of ozone and its precursors in a three-dimensional global CTM, *J. Geophys. Res.*, 106, 27,729-27,744, 2001.
- Williams, E. J., K. Baumann, J. M. Roberts, S. B. Bertman, R. B. Norton, F.C. Fehsenfeld, S. R. Springston, L. J. Nunnermacker, L. Newman, K. Olszyna, J. Meagher, B. Hartsell, E. Edgerton, J. R. Pearson, and M. O. Rodgers, Intercomparison of ground-based  $\text{NO}_y$  measurement techniques, *J. Geophys. Res.*, 103, 22261-22280, 1998.
- Winer, A. M., J. W. Peters, J. P. Smith, and J. N. Pitts, Jr. Response of commercial chemiluminescent  $\text{NO-NO}_2$  analyzers to other nitrogen-containing compounds. *Environ. Sci. Technol.* 1974, 8:1118-1121.
- Winkler, S. L. and D.P. Chock: "Reply on Comment on 'The Impact of An 8-hour Ozone Air Quality Standard on VOC and  $\text{NO}_x$  Controls in Southern California' by Chock, et al." *Atmos. Environ.* 35, 3371-3372 (2001).
- Yienger, J.J., *et al.*, The episodic nature of air pollution transport from Asia to North America, *J. Geophys. Res.*, 105, 26,931-26,945, 2000.

## ***APPENDIX: ADDITIONAL RESULTS FOR NO<sub>x</sub>-VOC INDICATORS***

This section includes (i) a statistical representation of indicator values associated with NO<sub>x</sub>-sensitive and VOC-sensitive locations in individual photochemical models; and (ii) complete graphical representation of material from Section 3.1.1.

**Numerical summary of indicator results:** Sillman (1995) and Sillman et al. (1998) developed the following as a convenient method to summarize information contained in indicator NO<sub>x</sub>-VOC sensitivity graphs (see Figure 3.1.1 and 3.1.2).

The summary information consists of the following: The distribution of indicator values is identified for (i) all locations with NO<sub>x</sub>-sensitive conditions in an individual model scenario; and (ii) all locations with VOC-sensitive conditions for the scenario. The distribution of NO<sub>x</sub>-sensitive and VOC-sensitive indicator values is then summarized by identifying (i) the 5<sup>th</sup>-percentile value; (ii) the median (50<sup>th</sup> percentile) value; and (iii) the 95<sup>th</sup>-percentile value.

Model results that show a strong separation of between NO<sub>x</sub>-sensitive and VOC-sensitive values have the following characteristics: median values associated with NO<sub>x</sub>-sensitive and VOC-sensitive conditions differ from each other by at least a factor of 2; and the 95<sup>th</sup> percentile value for VOC-sensitive conditions is typically equal to or lower than the 5<sup>th</sup> percentile value associated with NO<sub>x</sub>-sensitive conditions. These 95<sup>th</sup> and 5<sup>th</sup> percentile values are interpreted as the transition value for NO<sub>x</sub>-sensitive versus VOC-sensitive conditions.

By contrast, when model scenarios have significant overlap between NO<sub>x</sub>-sensitive and VOC-sensitive indicator values, then the 5<sup>th</sup>-percentile value for NO<sub>x</sub>-sensitive conditions is often as low or lower than the 50<sup>th</sup>-percentile value for VOC-sensitive conditions and/or the 95<sup>th</sup> percentile VOC-sensitive value is as high or higher than the 50<sup>th</sup> percentile value for NO<sub>x</sub>-sensitive conditions.

As is required for NO<sub>x</sub>-VOC indicators, NO<sub>x</sub>-VOC sensitivity is defined based on conditions as the same time and place as the model indicator value. Indicator values are not correlated to NO<sub>x</sub>-VOC sensitivity at different times of day, or at different locations. Results shown here are based on the definition of “NO<sub>x</sub>-sensitive” and “VOC-sensitive” given in Section 3.1.10.

**Table A-1****Distribution of indicator values for NO<sub>x</sub>- and VOC-sensitive locations in 3-d simulations**

The table shows 5th, 50th percentile and 95th percentile indicator values (with percentile ordering by indicator value) for VOC-sensitive locations and NO<sub>x</sub>-sensitive locations as defined in the text. The terms  $\Delta\text{O}_3$ ,  $\Delta\text{NO}_y$ ,  $\Delta\text{NO}_z$  and  $\Delta\Delta\text{NO}_3$  represent the difference between values at specified locations and background values. In some cases results are shown separately for (a) the full model domain and (b) an urban sub-domain. In these cases NO<sub>x</sub>-VOC sensitivity is defined relative to changed emissions within the model subdomain and background values are determined relative to the same subdomain. Models are described in Table 3-1. From Sillman and He (2002).

---

Indicator	VOC-sensitive locations			NO <sub>x</sub> -sensitive locations		
	5th percentile	50th percentile	95th percentile	5th percentile	50th percentile	95th percentile
$\Delta\text{O}_3/\Delta\text{NO}_y$ :						
Nashville, full domain	0.4	2.9	3.6	3.4	4.7	5.3
Nashville, high deposition*	0.3	3.5	4.3	4.6	6.7	7.7
Nashville, urban sub-domain	1.0	2.5	3.6	4.2	5.6	12.4
Northeast, full domain	2.8	4.0	4.8	5.7	7.7	9.0
Northeast, urban sub-domain	1.8	3.8	5.0	5.0	6.5	7.2
Lake Michigan	2.4	3.4	4.3	3.5	6.2	7.6
Atlanta	1.6	2.8	4.5	4.5	6.9	11.1
San Joaquin (Sillman)	0.6	2.8	4.9	4.4	7.5	11.4
San Joaquin (Lu and Chang)	1.3	3.2	4.2	3.6	8.4	32.4
Los Angeles (Godowitch)	0.9	2.3	4.6	5.2	7.9	11.9
Los Angeles (Chock)	0.6	3.7	6.0	3.5	8.6	13.7

---

Table A-1 (continued)

Indicator	VOC-sensitive locations			NO <sub>x</sub> -sensitive locations		
	5th percentile	50th percentile	95th percentile	5th percentile	50th percentile	95th percentile
<b>□O<sub>3</sub>/□NO<sub>z</sub>:</b>						
Nashville, full domain	1.2	3.6	5.0	3.8	5.3	6.1
Nashville, high deposition*	1.6	4.8	6.6	5.3	8.1	9.1
Nashville, urban sub-domain	1.9	4.0	5.0	5.1	7.1	15.4
Northeast, full domain	4.7	5.0	5.6	6.7	8.5	9.9
Northeast, urban sub-domain	2.8	4.4	5.4	5.7	7.4	8.3
Lake Michigan	3.0	4.0	5.2	5.7	7.3	8.5
Atlanta	3.6	4.5	5.9	6.1	9.2	14.6
San Joaquin (Sillman)	2.4	6.1	8.1	6.0	9.9	15.2
San Joaquin (Lu and Chang)	3.5	6.4	6.6	5.0	11.6	31.4
Los Angeles (Godowitch)	3.0	4.5	6.3	6.2	9.0	15.6
Los Angeles (Chock)	4.2	6.7	10.0	8.3	10.9	16.6
<b>□O<sub>3</sub>/□HNO<sub>3</sub>:</b>						
Nashville, full domain	1.4	4.2	6.5	4.6	6.7	8.2
Nashville, high deposition*	1.8	5.9	9.4	7.1	11.5	14.1
Nashville, urban sub-domain	2.2	5.1	7.9	8.0	12.8	40.3
Northeast, full domain	7.3	8.4	10.7	11.0	15.6	23.9
Northeast, urban sub-domain	4.9	8.4	11.4	13.1	27.3	235.7
Lake Michigan	3.6	4.8	7.6	8.8	12.5	18.2
Atlanta	4.1	5.3	7.3	7.3	13.1	20.5
San Joaquin (Sillman)	2.7	7.4	11.0	9.4	14.7	29.6
Los Angeles (Godowitch)	3.5	5.5	8.9	9.1	14.6	31.2
Los Angeles (Chock)	6.2	10.1	25.3	13.1	18.3	42.4
<b>O<sub>3</sub>/NO<sub>y</sub>:</b>						
Nashville	2.2	3.6	5.6	7.1	10.8	13.
Nashville, high dep.*	2.6	5.3	7.2	8.7	13.9	17.
Northeast corridor	5.0	5.4	6.5	8.2	12.7	18.
Lake Michigan	3.5	5.2	6.6	7.2	11.7	16.
Atlanta	3.6	5.1	7.2	8.1	14.3	27.
Los Angeles (Godowitch)	1.4	3.2	6.0	7.2	10.4	20.
Los Angeles (Chock)	1.0	5.4	9.1	5.9	18.	24.
San Joaquin (Sillman)	3.0	7.3	11.6	15.	26.	56.
San Joaquin (Chang)	5.4	7.7	12.3	12.5	22.	52.

Table A-1 (continued)

Indicator	VOC-sensitive locations			NO <sub>x</sub> -sensitive locations		
	5th percentile	50th percentile	95th percentile	5th percentile	50th percentile	95th percentile
<b>O<sub>3</sub>/NO<sub>2</sub>:</b>						
Nashville	5.3	6.3	7.3	8.4	12.4	13.
Nashville, high dep.*	7.0	8.8	9.9	10.5	16.8	20.
Northeast corridor	6.7	7.1	7.7	9.7	14.4	20.
Lake Michigan	4.5	5.8	8.1	11.2	15.3	18.
Atlanta	7.1	8.6	10.0	11.9	17.7	33.
Los Angeles (Godowitch)	4.6	6.2	8.4	8.7	12.0	25.
Los Angeles (Chock)	6.2	10.	15	14.	23.	31.
San Joaquin (Sillman)	11.	16.	19.	21.	35.	73.
San Joaquin (Chang)	14.	16.	20.	17.	32.	68.
<b>O<sub>3</sub>/HNO<sub>3</sub>:</b>						
Nashville	6.	8.	9.	12.	19.	21.
Nashville, high dep.*	8.	11.	14.	15.	25.	29.
Northeast corridor	10.	11.	16.	17.	27.	42.
Lake Michigan	5.	7.	11.	16.	28.	39.
Atlanta	8.	10.	13.	15.	25.	54.
Los Angeles (Godowitch)	5.	8.	12.	13.	19.	50.
Los Angeles (Chock)	9.	15.	40.	23.	39.	80.
San Joaquin (Sillman)	14.	20.	28.	27.	54.	155.
<b>H<sub>2</sub>O<sub>2</sub>//HNO<sub>3</sub>:</b>						
Nashville	0.11	0.18	0.23	0.30	0.64	0.82
Nashville, high dep.*	0.09	0.15	0.21	0.26	0.55	0.70
Northeast corridor	0.22	0.33	0.40	0.68	1.58	3.1
Lake Michigan	0.03	0.13	0.24	0.37	1.15	1.8
<b>(H<sub>2</sub>O<sub>2</sub>+ROOH)/HNO<sub>3</sub>:</b>						
Nashville	0.18	0.23	0.31	0.39	0.73	1.01
Nashville, high dep.*	0.22	0.28	0.37	0.54	1.14	1.48
Northeast corridor	0.22	0.39	0.54	0.93	2.0	4.3
Lake Michigan	0.06	0.20	0.32	0.49	1.6	2.6
Atlanta**	0.17	0.27	0.55	0.55	1.44	4.5
Los Angeles (Godowitch)**	0.06	0.22	0.41	0.40	0.87	2.8
Los Angeles (Chock)**	0.12	0.33	1.8	0.80	2.2	4.4
San Joaquin (Sillman)**	0.24	0.38	0.56	1.0	2.7	8.7
San Joaquin (Chang)**	0.17	0.23	0.52	0.72	1.8	6.3

Table A-1 (concluded)

Indicator	VOC-sensitive locations			NO <sub>x</sub> -sensitive locations		
	5th percentile	50th percentile	95th percentile	5th percentile	50th percentile	95th percentile
<b>H<sub>2</sub>O<sub>2</sub>/NO<sub>z</sub>:</b>						
Nashville	0.12	0.15	0.19	0.21	0.41	0.45
Nashville, high dep.*	0.10	0.13	0.17	0.18	0.37	0.41
Northeast corridor	0.14	0.20	0.21	0.36	0.80	1.4
Lake Michigan	0.03	0.10	0.19	0.27	0.60	0.87
<b>(H<sub>2</sub>O<sub>2</sub>+ROOH)/NO<sub>z</sub>:</b>						
Nashville	0.13	0.20	0.27	0.29	0.59	0.85
Nashville, high dep.*	0.15	0.22	0.30	0.35	0.79	1.08
Northeast corridor	0.14	0.24	0.28	0.49	1.10	1.91
Lake Michigan	0.05	0.15	0.26	0.35	0.81	1.22
Atlanta**	0.14	0.23	0.44	0.42	1.04	2.8
Los Angeles (Godowitch)**	0.05	0.17	0.33	0.26	0.55	1.4
<b>H<sub>2</sub>O<sub>2</sub>/NO<sub>y</sub>:</b>						
Nashville	0.05	0.09	0.12	0.17	0.36	0.42
Nashville, high dep.*	0.04	0.07	0.10	0.14	0.32	0.40
Northeast corridor	0.11	0.14	0.17	0.30	0.68	1.3
Lake Michigan	0.02	0.09	0.16	0.22	0.43	0.78
<b>(H<sub>2</sub>O<sub>2</sub>+ROOH)/NO<sub>y</sub>:</b>						
Nashville	0.08	0.12	0.18	0.24	0.52	0.98
Nashville, high dep.*	0.08	0.12	0.17	0.28	0.68	1.15
Northeast corridor	0.11	0.19	0.22	0.38	0.9	1.72
Lake Michigan	0.04	0.12	0.25	0.28	0.58	1.09
Atlanta**	0.10	0.12	0.19	0.29	0.83	2.2
Los Angeles (Godowitch)**	0.02	0.08	0.19	0.22	0.47	1.2

\* The Nashville high deposition scenario has dry deposition rates of 5 cm<sup>2</sup> s<sup>-1</sup> for H<sub>2</sub>O<sub>2</sub> and HNO<sub>3</sub>, as opposed to 2.5 cm<sup>2</sup> s<sup>-1</sup> in the standard scenario.

\*\* In models with CB-4 chemistry, "H<sub>2</sub>O<sub>2</sub>" is interpreted as a surrogate for the sum of H<sub>2</sub>O<sub>2</sub> and organic peroxides.